Modelling the Environmental Impacts of Suspended Mussel (*Mytilus edulis* L.) Farming

Jon Chamberlain

A thesis submitted in partial fulfilment of the requirements of Napier University for the degree of Doctor of Philosophy.

This research programme was carried out in collaboration with Fisheries Research Services, Marine Laboratory, Aberdeen and Dunstaffnage Marine Laboratory, Oban.

June 2002

NAPIER UNIVERSITY

EDINBURGH

PAGE

NUMBERING

AS ORIGINAL

ABSTRACT

The potential impacts of marine aquaculture operations on the environment are reviewed. The reported effects of suspended mussel farms on the benthic environment are examined and the potential impacts discussed. A framework to assess the impacts of suspended mussel farms is presented.

The use of simulation models to predict the impact of fish farm wastes on the benthic environment is discussed and the mathematical theory supporting such models is presented. The applicability of these models to mussel farming is discussed and the data required to undertake such modelling identified.

The effect of increased sedimentation on the macrobenthic community, physical structure and biogeochemistry of the surficial sediment around three suspended mussel farms are examined. At one site, the benthic community was subjected to bulk sedimentation, organic enrichment and reduced macrobenthic infaunal diversity. Elevated levels of organic carbon were recorded close to the farm. At the remaining two sites, benthic impacts were less clear and not demonstrably due to the mussel farms.

The settling velocity of mussel faeces and pseudofaeces was required to enable modelling of particles ejected from the farm sites. An experiment was devised to measure this parameter. The settling velocity of mussel faeces (~ 0.5 cms^{-1}) was less than pseudofaeces (~1 cms^{-1}). Differences in these settling velocities were attributed to the organic content and particle size of the excreted matter.

The particle tracking model DEPOMOD (Cromey *et al.*, 2000a) was used as a platform from which to develop a simulation model predicting the benthic impact of suspended mussel farms. Parameters within the model were modified to be represent a mussel farming scenario. Data from the three sites surveyed were applied to the model. Although the model results compared favourably with the field data, the model tended to overestimate the benthic impact as measured by the Infaunal Trophic Index.

The results of the model are discussed and improvements and further experiments are identified.

ACKNOWLEDGEMENTS

Many people have provided me with assistance, guidance and support during the time it has taken me to complete this PhD - a list to rival the size of this volume could be produced to acknowledge and thank everyone.

I am indebted to my supervisors Professor Paul Read, Dr Teresa Fernandes, Dr Ian Davies and Dr Thom Nickell. Without their expert guidance, encouragement and constructive criticism throughout the course of this study this would not have been possible.

The support and assistance offered by the mussel farm operators in UK and Ireland was invaluable and crucial to the progress of the project.

I am grateful for the support afforded to me from all the technical and administrative staff within the department at Napier. Special thanks are due to Jill Sales for her assistance with statistical analyses, Peter Gibson for help with faunal identification, John Kinross for providing technical advice and equipment and Karen Miller for her help from MARAQUA.

I am thankful to the directors and staff of Dunstaffnage Marine Laboratory, Oban and FRS Laboratory, Aberdeen for their assistance, use of laboratory space and equipment. I am particularly grateful to the NERC Diving Centre for logistical support, Chris Cromey for his advice on DEPOMOD, Phil Gillibrand for modelling guidance, Fiona Berry for her assistance with sample analysis and the staff at the FRS Fish Behaviour Unit for help with the settling velocity experiment. The assistance of the staff at the Aquaculture Development Centre and the Coastal Resources Centre at University College Cork was essential for the Ireland fieldwork to be successful. Additionally, I am grateful to Jason Hall-Spencer for his support and assistance when it was really necessary!

I am forever grateful to my parents for their continued support and encouragement over the years. Thanks to Helly for believing, the 'Beach Boys and Girls' of C6 for the entertaining and lighter side of life, Fen for her critical and informative views on mussel faeces, Catrina for her patience and understanding, and the staff and friends at S.E.P.A., Dingwall for their encouragement and support.

Finally, but by no means lastly, I would like to say a big thanks to all of the friends I have made and the people I have met during this Ph.D., you have all been an inspiration.

Thankyou

CONTENTS

1 Introduction

1.1 Fish farming

The environmental consequences of mariculture operations have been a matter of concern for as long as the modern aquaculture industry has existed. Ever since the initial development of commercial marine cage fish farming operations in Scotland in the late 1960's there have been misgivings over the possible short and long-term effects of the industry. The seminal review by Gowen *et al.* (1988) "Investigations into Benthic Enrichment, Hypernutrification and Eutrophication associated with Mariculture in Scottish Coastal Waters" included a summary of the research carried out to that date and laid the foundations for future research directions. Since then, there have been many studies into different aspects of the industry. Some of these projects have been as a direct result of this review, whilst others have come about in response to changes in husbandry practices, and the steadily increasing scale of operations within the marine cage fish farming industry. The main areas of environmental concern in Scotland have been:

1. Nutrient release and enrichment, and the potential for alteration of phytoplankton production
2. Impact of solid organic waste settling on the sea bed
3. The effects of harmful substances (e.g. antifoulants) and medicines on non-target organisms
4. The effects of escaped fish on wild stocks
5. The effects of sea lice infestations and diseases (to a lesser extent) from salmon farms on local wild salmonid stocks

There are now some broader issues emerging, associated with the long term sustainability of the industry. The diets of farmed species are currently heavily reliant on fish meal and fish oil. These are obtained primarily from industrial fisheries, with additional material being provided from the processing of farmed fish for human consumption. This has lead to criticism over the potential impacts, e.g. increased

exploitation rates, on the sustainability of fisheries and over the possible consequences for wider marine ecosystems that are dependent on these stocks. Concern has also been expressed over the concentrations of persistent organic contaminants (e.g. polychlorinated biphenyls, DDTs, and dioxins) found in farmed fish. These are derived from contaminants present in the fish oils that make up part of their diets and are thus concentrated in the farmed fish.

1.2 Mussel farming

In comparison to marine cage fish farming, shellfish cultivation is often considered relatively benign, particularly as artificial feeds and medicines are generally not used. The culture of marine bivalve molluscs in Scotland has increased markedly over the past decade, but remains rather small in comparison to the salmon cultivation industry. Commercial cultivation of edible mussels (*Mytilus edulis*, L.) and similar species has been developed in many parts of the world (Mason and Drinkwater, 1981).

Consumed throughout history, the mussel was much appreciated by the Romans, as shown by the quantity of shells often found in coastal archaeological excavations. According to legend, the origin of the mussel cultivation and the 'Mytiliculture', is attributed to an Irishman who was shipwrecked in the Bay of Aiguillon, France, in 1235. Patrick Walton, who had fled his native soil under questionable circumstances, was the sole survivor of the disaster. In a vain attempt to snare sea birds and catch fish for food, he suspended a net between two poles on the lower foreshore. Over time, he noticed that mussels became attached to the net and poles when it was submerged at high tide and that they tasted far superior to those that he found between the rocks. However, this story is controversial because it is possible that the mussel cultivation had already existed since the 10th or 11th century. For example, a mussel farm was documented in 1136 as being located in Esnandes and owned by the abbey of Saint Jean d'Angely, showing an early commercial interest.

A number of different growing and cultivation techniques have been developed around the world and are used within the mussel production industries. The dredging of wild mussels (Drinkwater, 1987) is at the boundary between wild fisheries and

cultivation. These mussels are harvested rather than farmed, although in areas such as the Wadden Sea, some management of bottom grown mussels does occur. This could be considered comparable to the ranching of stock, for example small mussels may be gathered and relocated in controlled densities in areas where accelerated growth will occur.

'True' farming techniques include an intertidal technique known as 'Bouchot' culture. Juvenile mussels are collected on ropes which are subsequently wound round poles in intertidal areas (Drinkwater, 1987). However, the most common method of mussel culture in Scotland and Ireland is the use of 'droppers', made of ropes or straps, that are suspended vertically in the water column, upon which mussels settle and grow (Gowen *et al.*, 1988). These droppers are hung from rafts, or floating or submerged longlines supported by floats, in areas where there is an abundant primary production to support growth of the mussels.

Table 1.1 : Shellfish production in Scotland for 1999 - 2001 (FRS, 2002)

Year	Pacific oysters (000s)	Native oysters (000s)	King Scallop (000s)	Queen Scallop (000s)	Mussels (tonnes)
1990	1441	1	68	1310	462
1991	2300	122	316	1529	462
1992	2560	194	489	1538	923
1993	2594	119	176	788	708
1994	2104	142	199	956	716
1995	1973	182	300	1147	882
1996	2781	96	302	1271	1072
1997	2787	11	223	1207	1307
1998	2857	87	343	3676	1355
1999	2895	142	127	2842	1400
2000	3088	51	323	2084	2003
2001	3483	103	236	1182	2988

There has been a general increase in mussel production in Scotland over the past decade. Production figures for the period 1990 – 1999 showed a 200 % increase in the size of the industry over this period. However, the most recent data available shows a massive increase in production with the output from the industry doubling over the period 2000-2001 (FRS, 2002) (Table 1.1). This is possibly due to the large number of new sites that have recently been leased in the Shetland Isles.

The most recently available data (2001) show that there were fluctuations in the prices of farmed mussels throughout the year. However, the estimated value at first sale was between £800 - £1300 per tonne. The approximate value of the mussel production in 1999 was thus £2.39 - 3.88 million. Mussels were the most valuable sector of the shellfish cultivation industry, making up between 50-75% of the total first sale value (FRS, 2002).

In the absence of the environmental effects arising from feed and medicines use, and sea lice infections as witnessed in fish farming, the main mechanisms for environmental effects from shellfish farming are linked to changes in the rates of nutrient cycling in the water column. These have the potential to lead to such effects as increased nutrient loading of the water and its possible feedback to primary production processes, or reductions in the food available to natural filter feeders present in the area of the farm. Secondly, there may be effects on the surficial sediment under and surrounding the farm sites. This could be in the form of smothering the benthos with organically enriched particles, leading to increased stress on the benthic community.

Grant (1996) drew comparisons between bivalve cultivation and other types of farming, in that it is analogous to the agriculture of grazers, the energetic basis of mussel farming being the conversion of primary production (largely micro-algal) into mollusc tissue. The culture environment may therefore be partitioned into two components:

1) the production, loss and redistribution of micro-algae and other food sources (i.e. the dynamics of the food supply); and

2) the processing and conversion of food into bivalve tissue, mediated by the physiological energetics of the cultured species.

An understanding of the mechanisms by which food is provided to, and converted by, the cultured species is fundamental to the integration of aquaculture within the wider ecosystem. Various studies have been able to relate field growth of bivalves to a number of critical environmental factors, an extensive discussion of which is provided in Smaal and Heral (1998). However temporal changes in these relationships are often great and the causality of the relationships is still a matter for discussion (Grant, 1996).

1.3 Organic Enrichment

As with all ecosystems, organic matter is vital to the functioning of coastal environments (McLusky, 1990), as the basis for detrital food chains. A small quantity of organic matter, well dispersed, can be readily utilised within the ecosystem to enhance levels of biological production. The quantity of organic matter required to cause an adverse effect on the surrounding area will be site specific and dependant upon a large range of parameters. However, the nature of the changes that occur to the benthic systems will be broadly similar at all locations, on both the physico-chemical character and biological components of the benthos. All bivalves generate faecal and pseudofaecal organic particulate material (biodeposits). Considerably quantities of this material can be generated at culture sites, where many thousands of bivalves are suspended in the water column. Grentz *et al.* (1991) estimated that approximately 600 kg of particulate biodeposits (faeces and pseudofaeces) could be generated for each tonne of production (measured as wet weight) over a growing cycle.

1.3.1 Physico-chemical alterations.

The majority of coastal marine sediments have an oxic layer overlying an anoxic layer. The presence and extent of the former depends on the balance between the consumption and supply of oxygen within the surficial layers (Findlay and Watling, 1997). Oxygen availability within sediments in shallow water marine environments is

affected by a variety of mechanisms – which include molecular diffusion, bioturbation, current flow and wave-generated advection. The oxygen consumption in sediment arises from faunal respiration, bacterial oxygen consumption and the oxygen used in the chemical oxidation of reduced compounds in the sediment. When organic inputs to the sea can be utilised aerobically, the rate of decomposition of organic matter is influenced by a number of other factors, including utilisation by benthic macrofauna, decomposition by heterotrophic bacteria and chemical oxidation to carbon dioxide and water.

Investigations provide evidence of increased overall oxygen consumption with increasing organic loading (Hansen *et al.*, 1990). One of the first effects of organic enrichment on the sediment biogeochemistry is the depletion of oxygen in the surficial layers as a result of increased bacterial activity in the degradation of organic matter (Cornel and Whoriskey, 1993).

When the demand for oxygen exceeds the supply, the sediment becomes anoxic and major changes occur in the sediment chemistry and consequently the ecology of the benthic infauna. In the absence of oxygen, lower energy anaerobic bacterial processes dominate the degradation of organic matter. The oxidation-reduction (redox) conditions in the sediment depend on the degree of organic enrichment and can be assessed by measurement of the electro-potential (expressed in mV) of the sediment (Zobell, 1946). As redox conditions decrease, microbiological activity in the sediment switches from aerobic oxidation, producing carbon dioxide and water, to the anaerobic bacterial degradation of organic matter using nitrate and sulphate as oxygen sources, leading to the formation of compounds such as methane, hydrogen sulphide and ammonia as described in Table 1.2.

The characteristic black colour of these reduced sediments arises from the formation of iron sulphides, through the reaction of hydrogen sulphide (released during sulphate reduction) with labile iron (Jorgensen, 1982; Morris, 1983). The processes of nitrification and denitrification, by which bacteria oxidise ammonia to nitrite and nitrate, and reduce nitrate to nitrogen gas respectively, become inhibited as nitrate levels increase and may cease to function as a mechanism for removal of organic

nitrogen (Kaspar *et al.*, 1988). However, the general absence of nitrate in the sulphate reduction zone of marine sediments suggests that nitrate can be fully utilised. This process, the development of biogeochemical zones in marine sediments, is found in other areas of organic enrichment, such as the sediment surrounding pulp mill effluents (Pearson and Rosenberg, 1978) and sewage sludge dumping grounds (Pearson, 1987). It is often reported along with the development of mats of distinctive white sulphide oxidising bacterial communities (*Beggiatoa* sp.). In extreme cases (low turbulence and high organic input), the water overlying the sediment may also become anoxic (Tsutsumi and Kikuchi, 1983). During periods of peak organic input, this bacterial mat may disappear and sulphide can be oxidised directly in the water column.

Table 1.2 : Microbial metabolism of organic matter, represented as carbohydrate units (modified from Froelich *et al.*, 1979)

Aerobic	Oxic	$CH_2O + O_2 \rightarrow CO_2 + H_2O$
Anaerobic	Denitrification	$5CH_2O + 4NO_3^- + 4H^+ \rightarrow 5CO_2 + 2N_2 + 7H_2O$
	Manganese reduction	$CH_2O + 2MnO_2 + 3CO_2 + H_2O \rightarrow 2Mn_2^+ + 4HCO_3^-$
	Iron Reduction	$CH_2O + 4Fe(OH)_3 + 7CO_2 \rightarrow 4Fe^{2+} + 8HCO_3^- + 3H_2O$
	Sulphate reduction	$2CH_2O + SO_4^{2-} \rightarrow H_2S + 2HCO_3^-$
	Methano-genesis	$2CH_2O \rightarrow CO_2 + CH_4$

Gas has been observed being released from sediments in fish farming areas under conditions of heavy organic matter deposition on the sediments (Black *et al.*, 1995). Hansen *et al.* (1990) noted a general relationship between the quantity of waste on the seabed beneath a fish farm and the quantity of gas released. This process, known as "out-gassing", occurs when methane from methanogenic bacteria entrains hydrogen sulphide whilst bubbling from the sediment. This gas was analysed by Samuelson *et al.* (1988) who reported that it was composed of 68 – 89% methane, 10 – 30% carbon dioxide and 1 – 2% hydrogen sulphide. These compounds, which are produced during

decomposition of organic material, were reported to be released in proportion to the increasing thickness of the accumulated matter.

1.3.2 Biological alterations.

Alteration of macrofaunal community structure by organic enrichment has been a keystone of benthic environmental studies (Findlay *et al.*, 1995), since the seminal review of Pearson and Rosenberg (1978). The development of low oxygen, even anoxic, conditions leads to the extinction of normal macrofauna and its replacement by annelid worms, especially oligochaetes. However, even such worms may be excluded from areas of greatest organic enrichment.

The general trend is towards a poor, or even depleted, benthic community in the vicinity of sources of organic enrichment. Further away, a more diverse community will persist, with a greater diversity and less pollutant-tolerant species. In some instances, it may be possible to measure a zone of bio-stimulation, where the benthic community structure is more enhanced (higher abundance, increased species diversity and biomass) than under 'normal' conditions. This is due to slight stimulation of the biological activity on the basis of a higher organic pool, but without the oxygen concentration decreasing to critical levels resulting in reducing (anaerobic) conditions in the sediment. Outwith this region, the biomass, species diversity and abundance normally approach levels which are typical for that location (Gowen and Bradbury, 1987; Brown *et al.*, 1987; Ritz *et al.*, 1989; Nature Conservancy Council, 1990; Weston, 1990; Pearson and Black, 2001).

Brown *et al.* (1987) were able to determine relationships comparable to those reported by Pearson and Rosenberg (1978) for use with salmon aquaculture sites and defined four phases or levels of impact associated with net-pens off the Scottish coast. These levels of impact are equivalent to "reference", "transitional", "peak of opportunists" and "azoic" communities, as defined by Pearson and Rosenberg (1978). Azoic sediments are those devoid of macrofauna. The communities defined as "transitional" and "peak of opportunist" are typified by higher diversity and increased numbers of individuals, respectively. Inherent to both of these approaches is an underlying

assumption of stability and similarity – samples taken from similar sediments will yield similar descriptions of benthic community structure "health" relatively independent of sampling time and location (Brown *et al.*, 1987).

When attempting to analyse alterations in the benthic infauna using biological diversity indices such as Shannon-Wiener and Simpson (Shannon and Weaver, 1949), clear evidence of disturbance is rare as significant community changes are normally only detected in close proximity to the source of enrichment (Brown *et al.*, 1987). To overcome this difficulty, multivariate statistical/discriminatory techniques, such as those presented by Warwick and Clarke (1991) and discussed in Chapter 3, are used to elucidate trends in the community composition. Another method that may be used in concert with multivariate techniques involves the sorting of species into different pollution-tolerant groups prior to analyses. One such method is the calculation of the Infaunal Trophic Index (Word, 1978), which classifies species into trophic feeding groups. This particular technique is discussed in more detail in Chapter 3.

In sediments very severely affected by a high input of organic matter, the surrounding area becomes azoic and completely devoid of benthic fauna (Pearson and Rosenberg, 1978). Weston (1990) reported that in areas surrounding a fish farm, up to 90% of the benthic macro- and megafaunal species previously present were eliminated. These components of the benthic community play a vital role in controlling the oxidising conditions of the sediments. Macrofaunal and megafaunal bioturbation considerably influences the biological, physical and chemical nature of the sediments (Aller, 1978; Aller, 1982; Rhoads and Boyer, 1982). Hansen *et al.* (1990) estimated that, on an annual basis, approximately 40 – 50% of organic matter from marine fish farms was degraded in the presence of bioturbating macrofauna, compared to 11 – 15% when these were absent. Thus, in the absence of bioturbation by macrofauna and megafauna, aerobic sedimentary processes are restricted to the top few millimetres (i.e. the sediment-water column interface). In such areas, the impoverished macrofaunal community is likely to be dominated by opportunistic polychaetes such as *Capitella capitata*, which are indicative of enriched sediments (Pearson and Rosenberg, 1978). These polychaetes can tolerate anoxia and high sulphide levels by

maintaining contact with oxygenated sea water above the sediment, thus resisting sulphide toxicity.

The reduced diversity of fauna under fish farms has been reported by several authors (e.g. Brown *et al.*, 1987; Hansen *et al.*, 1992; Pereira, 1997). Macrofauna appears to be absent generally when the accumulated layer of waste exceeds 10 cm. This may be attributed to the loose consistency of the sediment (i.e. lack of suitable substrate, as the accumulated layer is extremely flocculent causing difficulty in defining the true sediment/water interface) together with decreasing oxygen concentration and increasing sulphide concentration in the pore water. Reduced bioturbation lowers the rate of oxygen supply to the sub-surface layers of the sediment, and carbon mineralisation becomes anaerobic.

1.4 The physical environment of the shellfish cultivation industry

The UK shellfish farming industry is concentrated in Scotland and in estuaries on the south coast of England. Pockets of development occur elsewhere, such as in the Menai Straits, Wales. A brief examination of the potential impacts of shellfish farming was presented by Kaiser *et al.* (1998) and Kaiser (2001). These reports primarily concentrate on intertidal shellfish farming operation - the most common method for bivalve cultivation in England and Wales. Suspended mussel farming is almost entirely based in Scotland where the geomorphology of the West coast is ideal for siting farms. Deep water inlets (sea lochs) provide sufficient depth of water to allow the farms to be positioned close to the shore and shelter. Ideally, farm sites have sufficient depth of water for the cultivation lines to be suspended in the water column without the risk of the ends of the lines 'dragging' on the seabed which gives opportunity for predators (e.g. starfish, crabs) to attach themselves to the lines and attack the stock. The farming areas are generally far from significant sources of pollution, with water temperatures ranging from 5 – 15 °C. Additionally, protection from wave and wind action is beneficial to prevent loss of mussels through physical disturbance and falling off the lines.

Ironically, these ideal physical conditions may compound the potential environmental problems arising from biodeposits. The flushing rates of sea lochs vary enormously (Edwards and Sharples, 1985), however the presence of sills may restrict water movement and reduce tidal flushing. Generally, currents in sea lochs (apart from close to sill areas) are predominantly wind driven and weak, reducing the dispersion of excretory products from the farm sites. In such areas, there is potential for accumulation of biodeposits on the sea bed. Very little, if any, resuspension of sedimentary material will occur in depositional basins where shellfish farming is likely to be situated, which may result in the development of an organically enriched benthic environment.

Grant (1996) points out that many of the husbandry practices used in the mussel cultivation industry, including the selection of farm sites, have been developed on very practical bases, i.e. ease of road and boat access, property availability, protection from wave exposure and adequate water depth. Very little attention, in terms of management practices at farm sites, has been directed towards the actual physiology and growth of the bivalves (the product) and the potential effect on the surrounding environment. This is in spite of the fact that there have been numerous studies of natural populations of bivalves in the field, including studies of their physiological ecology in both laboratory and field situations. Much of this insight gained into the forcing mechanisms behind growth of bivalves in natural populations has not been used widely in planning or manipulation of culture sites in the UK (Grant, 1996).

1.5 Mussel physiology

Mussels filter seawater and extract suspended particles, the seston, which is a combination of living and non-living material. Most of the energy is derived from the phytoplankton component of the seston (Bayne, 1976). Seawater is drawn into the shell and passed through the gills where food particles become attached to a layer of mucus. Suitable food is 'actively' selected and carried into the mucus mouth while the rest of the material is bound with mucus, discarded and ejected from the shell (Bayne, 1976). This discarded material is known as the pseudofaeces. Once the retained food has passed through the digestive system, the remaining fraction is

voided as 'true' faeces. Additional excretory products include ammonium and phosphate, which can be utilised by micro-organisms, mainly phytoplankton. Extensive reviews of bivalve filter feeding mechanisms are given by Jorgensen (1990) and in the literature produced following the TROPHEE workshop (see Bayne, 1998).

The supply of particulate food to cultured populations affects bivalve feeding physiology in several ways, largely mediated through current flow and particle concentration (i.e. total seston). Grant (1996) suggested that three of these variables may be combined to calculate flux of food as a measure of supply.

$$Flow \times Concentration \times \%\ Particulate\ Organic\ Material\ (POM) = Supply$$

This value has an intuitive appeal because it may be compared to population consumption in the same units. However, Grant (1996) warns that particle flux has not proven to be a sufficient predictor of food supplies, probably because more complex components of this flux (e.g. the concentrations necessary to produce feeding responses) influence behaviour, and those responses are not necessarily in the same direction. For example, a turbid suspension of phytoplankton and silt delivered at a low flow rate could produce a relatively large flux of organic matter, but be of limited nutritional benefit due to feeding inhibition.

Jaramillo *et al.* (1992) described the filter feeding process as the mussels removing fine particles from the water column, repackaging them and returning them to the water as faecal (and pseudofaecal) pellets. These pellets settle onto the benthos in a process known as biodeposition (Haven and Morales-Alomo, 1966). The settling velocity of the faecal pellets is greater than that of the original fine particles composing the pellets (Simpson, 1982). Thus, through feeding and excretion of bivalves, phytoplankton and fine particles settle out in areas where the hydrographic processes would not normally allow this to occur.

Despite the majority of faecal material being consumed by epifauna living on or around the mussels, there remains a high deposition of organically rich deposits to the benthos (Tenore *et al*, 1982) that contribute to physico-chemical and biological

changes to the bottom sediment (Jaramillo *et al.*, 1992). The impact of particulate waste from fish farms is a critical factor influencing the holding capacity of individual farm sites. Although the parallel regulatory framework for shellfish farming is less developed, benthic impact is recognised as a consequence of mussel farming. It is likely that future regulation will require a more thorough assessment of the environmental impacts of shellfish farming. Modelling will be central to this.

1.6 Impacts of suspended mussel culture

1.6.1 Water column effects

Loo and Rosenberg (1983) estimated that 80% of food ingested by mussels was assimilated, with the remaining 20% being voided as faeces. Similarly, Rodhouse *et al.* (1985) calculated that approximately 20% of the carbon and nitrogen filtered from the water in the form of phytoplankton were released back into the water column.

Dahlback and Gunnarson (1981) estimated that the sedimentation rate under a mussel farm on the Swedish coast was three times greater than at a control site. Similarly, Kautsky and Evans (1987), in the Baltic, calculated that biodeposition comprised 24% of the annual sediment load, peaking during October to December. Hatcher *et al.* (1994) reported that sedimentation rates were always significantly higher, by at least a factor of two, under mussel lines compared with their reference site and that rates were low in winter and high in late summer and autumn. Neiland (1999) did not record the sedimentation rates at a site in Bantry Bay, Ireland, but high percentages of silt were recorded at the site suggesting an increased flux of material to the benthos.

Jaramillo *et al.* (1982) examined mussel biodeposition in the Quelle River Estuary, Southern Chile, calculating that biodeposition rates were at a maximum during the summer and mid-autumn. However, these peak biodeposition rates appeared to follow the temporal variability in temperature and salinity in the water column, rather than the peak periods of food concentration as reported by Tenore and Dunstan (1973 a&b).

Mussel cultures, through the sheer biomass of active filter feeders, have the potential to significantly lower the oxygen and phytoplankton concentrations as evidenced by lower growth rates on the downstream sides of the rafts (Odum, 1974). Production figures from suspended culture can be misleading, as they do not represent the true production per unit area of water body. The culture units are situated such that the stock is exposed to, and can therefore filter, a large volume of water, and the food which supports the growth is actually derived from primary production over a much larger portion of the water body than is covered by the farm itself. Indeed, as indicated above, if the density of cultures is great enough, they may compete for food with natural populations of filter feeders.

1.6.2 Benthic Effects

The effects of biodeposits from suspended mussel culture on the surrounding benthic environment have been addressed in a number of studies (e.g. Tenore *et al.*, 1982; Kaspar *et al.*, 1985; Baudinet *et al.*, 1990; Hargrave *et al.*; 1994, Grant *et al.*, 1995; Stenton-Dozey *et al.*, 1999). The reported effects of these biodeposits on the physico-chemical and biological structure of the surrounding surficial sediments were generally similar in all studies, although the extent and degree of impact differed considerably between locations.

Heavy sedimentation of mussel biodeposits has been reported to produce accumulations of faeces and pseudofaeces beneath the farms, effectively increasing organic enrichment and altering macrofaunal communities (Mattson and Linden, 1983; Kaspar *et al.*, 1985; Tenore *et al.*, 1985). Sedimentation rates up to three times greater than at reference sites have been reported (Dahlback and Gunnarson, 1981). Grenz (1989) suggested that average mussel biodeposit production in suspended culture could attain very high values, up to 345 kg m^{-2} y^{-1}. This increased sedimentation rate may select for benthic species more adaptable to low oxygen levels or to the instability of finer textured, high organic sediment (Tenore *et al.*, 1982). Jaramillo *et al.* (1992) and Grant *et al.* (1995) did not record such increases and Baudinet *et al.* (1990) concluded that mussel culture had little impact at their study

site. Grenz *et al.* (1990) reported that deposition of bloom phytoplankton confounded the effects of mussel biodeposition on sediment organic matter.

Macrofaunal abundance is commonly reduced in areas surrounding suspended mussel farms (Tenore *et al.*, 1982; Mattson and Linden, 1983; Jaramillo *et al.*, 1992; Grant *et al.*, 1995) with concomitant decreases in infaunal diversity and increased populations of opportunistic species (Mattson and Linden, 1983). The changes in the benthic fauna were attributed to increased sedimentation and organic enrichment from faeces produced by the mussels (Tenore *et al.*, 1982, 1985; Mattson and Linden, 1983; Kaspar *et al.*, 1985; Neiland, 1999). Tenore *et al.* (1982, 1985) also suggested that the increased sedimentation rate may select for benthic species that are more adaptable to low O_2 levels and/or to the instability of finer textured, high organic sediment.

Mattson and Linden (1983) reported that anaerobic sediment and opportunistic polychaetes were localised in a zone 5 - 20 m around the mussel culture. A year and a half after the mussels had been harvested, only a limited recovery of the benthic macrofauna was recorded. However, at the site examined by Grant *et al.* (1995), a diverse and active benthic community was recorded persisting beneath the farm, with a general similarity in species composition between farm and reference sites. They concluded the impacts on the benthos caused by the mussel lines were minimal.

Phaeophytin levels, measured by Kautsky and Evans (1987), were found to be several times higher in sediment under mussel cultures compared to sediment from outside the culture area. They suggested that this was due to high sedimentation of algal decay products possibly through conversion of chlorophyll a to phaeophytin during grazing by the mussels.

Grant *et al.* (1995) found that their study site did not display classic eutrophication responses, such as hypoxic conditions and suphidic sediments, and that the faunal biomass below the farm at times surpassed that at their reference site.

Dahlback and Gunnarson (1981) recorded a build-up of sediment rich in organic material and sulphide under a mussel culture. Increased sedimentation can also occur

as a result of the baffling effect caused by the suspended mussels impeding the flow of water around the culture sites (Odum, 1974). Sulphate reduction to H_2S was found to be stimulated in the sediment compared to a reference site, but since the site was small they did not consider that there was a risk of anoxic conditions developing in the water or the H_2S reaching the mussels. Nevertheless, both of these features were regarded as likely problems for larger operations.

These studies have drawn similar conclusions on the nature of the effects of mussel farms on the benthic environment, but reveal conflicting results on the extent and degree of impact and how this affects the surrounding environment.

1.7 Aims of the project

The environmental impact of marine cage fish farming has now been well described, and this has allowed the development of mathematical models through which the development of the industry can managed, and its environmental impacts controlled. The fundamental knowledge that would enable the same to be done for the mussel farming industry in Scotland does not exist. The aim of this project was:

To develop mathematical models of the impact on the seabed of suspended culture of mussels (*Mytilus edulis*).

In order to achieve this aim, a series of objectives were addressed:

- To describe the benthic impacts of mussel farming at sites typical of those used in Scotland and Ireland.;

- to development a conceptual framework of the impacts of mussel farming and their causes and to assess the suitability of existing models of the dispersion and effects of waste from fish farms for application to mussel farms;

- to develop and validate a management model of the effects of suspended mussel cultivation on the seabed in sheltered coastal waters,

In addressing the above objectives, a review was carried out of the available mathematical models of dispersion of particulate waste from aquaculture units (Chapter 2). On the basis of an assessment of the suitability of the models for adaptation to mussel farming based upon this review, a field programme was designed (Chapter 3) to obtain coherent data sets describing the impact of mussel farming in three distinct locations (Chapter 4). The results of these field surveys are discussed in Chapter 5. The review in Chapter 2 identified the need for information on the settling velocity characteristics of mussels faeces and pseudofaeces. The lack of this information is remedied by a series of laboratory experiments described in Chapter 6. The model selected for further development in Chapter 2 is described in detail in Chapter 7, together with the modifications necessary for its application to mussel farming. The model outputs are compared to field data from the three field locations, and the wider usefulness of the model is discussed in Chapter 8.

2 Introduction to modelling the benthic effects of mariculture

2.1 Applications of environmental modelling to aquaculture

2.1.1 Environmental Impact Assessment

The use of Environmental Impact Assessments in the planning and management of coastal projects is increasingly being required of potential developers. Following recent European Union legislation, the UK implemented the Environmental Impact Assessment (Fish Farming in Marine Waters) Regulations 1999. Under these Regulations, marine cage fish farm developments that meet or exceed certain criteria involving size, location and sensitivity of the environment, are subject to an EIA during the planning stage of the development. In preparing Environmental Impact Statements, developers are increasingly turning towards modelling techniques to predict the likely environmental consequences of their proposals.

The importance of modelling to the regulation of aquaculture is increasingly recognized by regulators as an essential part of the management process (Ervik *et al.* 1997; SEPA, 1998; Henderson *et al.*, 2001; Cromey *et al.*, 2002b). Models that predict the potential benthic impacts of mariculture operations can also be used in the planning phase of aquaculture developments to assess the appropriate size of farms, and thereby influence considerations of the economic viability of individual farms.

Simulation models can be important tools in the management of sites, both for predicting impact and as an aid in the design of monitoring programmes. With respect to wastes from aquaculture operations, there are three aspects that can be modelled: the quantities of material generated, dispersion after release or discharge and possible biological effects. The prediction of the biological consequences of a particular development, requires the application of sound ecological knowledge linked to the modelling outputs, as it is frequently not possible to undertake the number and complexity of field studies that would be required to cover all qualifying situations.

Mathematical models applied to mariculture may be empirical or mechanistic. The

former are based on statistical relationships between variables derived by observation, and are generally non-esoteric and do not necessarily require a great deal of scientific understanding of the underlying principles (Silvert, 1994). Mechanistic models attempt to describe the relationships between causes and effects with the expectation that all the variables included in the model may have significance within the natural system, and under the assumption that all significant variables are included. Sensitivity analysis is a valuable tool in determining how uncertainties in different parameter values contribute to the overall performance of a model. Silvert and Cromey (2000) recommend that it should be used planning the allocation of effort to different aspects of the modelling process. Complex ecosystem models are typically mechanistic and generally developed in relation to large-scale or multiple developments. With increasing levels of model sophistication, the amount of data required to parameterise and validate such models increases, and can potentially involve very high costs. Where complex ecosystem models have been used to manage water bodies supporting aquaculture operations, it is clearly appropriate to include aquaculture as an additional user of the system. This will involve both the demand by aquaculture operations for certain levels of environmental quality, and the inclusion of the farms as sources of dissolved and particulate wastes.

In most instances, however, given the relatively low risk of large-scale ecological change presented by shellfish mariculture wastes in Europe and N America (with the occasional marked exception, such as mollusc cultivation in the rias of north western Spain), there is little justification for the use of complex ecosystem models except in areas where there is likely to be large scale development. For these reasons, it has been suggested that complex ecosystem models are more appropriate for research rather than for use as management tools (GESAMP, 1991; 1996).

However, the need for relatively simple management models remains, and these are in routine use in some countries, such as Scotland, to assist in the regulation of marine cage fish farming developments. The use of these models does not preclude the need for field observations and data, which are essential to initialise the models and validate predictions. Validation must be regarded as an integral part of using a model as a predictive tool. In addition, all model predictions will have an associated error in

the output. The acceptability of this error, which should be determined on a site specific basis with regard to the perceived risk to the environment, should always be taken into account when management decisions are made on model outputs.

2.1.2 Sedimentation modelling

Of all the ecological effects of coastal aquaculture, probably the most frequently reported and best characterised are effects on the benthic environment. Benthic impact is also a central element in the monitoring and regulation of marine cage fish farms in Scotland and Norway, and is becoming increasingly so in Ireland. However, because benthic impacts are generally confined to a small area extending no more than a few tens of metres from the edges of the cages, they do not provide a useful measure of maximum intensity of aquaculture operations within an inlet. Benthic impacts amenable to modelling are limiting on a smaller scale than this (Silvert, 1992). The holding or carrying capacity of an inlet, which is a measure of the intensity of aquaculture operations that can be supported without detriment to either the farmed species themselves or to the environment, generally depends on effects that occur on a larger spatial scale (Silvert, 1992).

Sedimentation models have been developed in order to predict the magnitude and spatial extent of the deposition of particulate matter from fish farms. These models typically attempt to predict the trajectory of particles of waste (excess feed pellets and/or faecal matter) as they pass through the water column and impact upon the benthos (Hevia *et al.*, 1996). The critical physical parameters in these models are the hydrographic regime and the settling velocities of the wastes (Figure 2.1). Current speed and direction are generally parameterised by multiple measurements collected at regular (e.g. hourly) intervals (Gowen *et al.*, 1989; Cromey *et al.*, 2000a). Settling velocities of feed and faeces may either be assigned single mean values (Gowen *et al.*, 1989) or, more realistically, should be treated as a probability distribution with defined mean and standard deviation (Hagino, 1977).

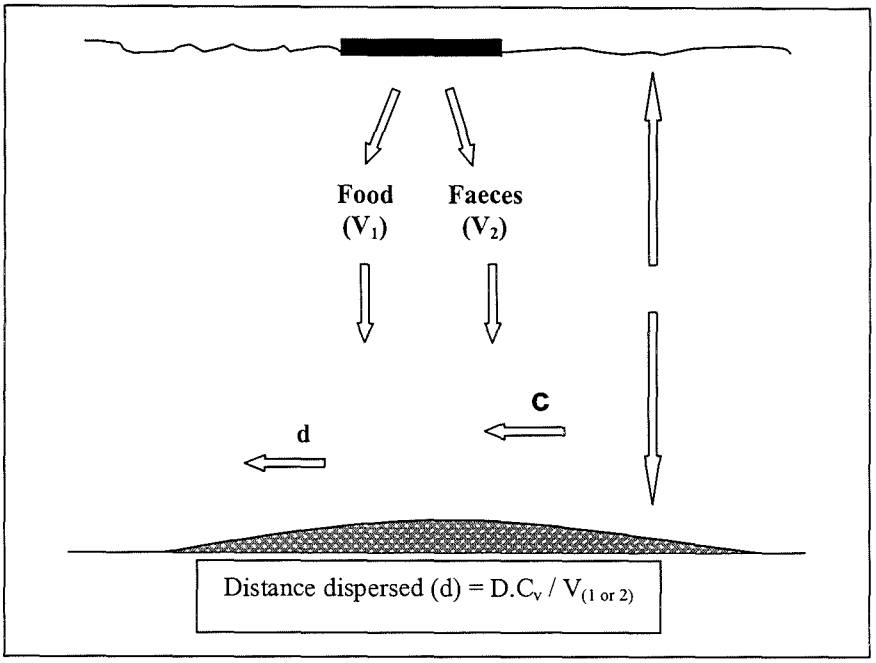

Figure 2.1 : A diagram illustrating the principle upon which simple, benthic deposition models are based. Where D is the depth of water beneath the cages, C, the current velocity and v_1 and v_2 are the settling velocities of uneaten food and faecal waste respectively (From Gowen *et al.*, 1989).

Existing models vary in their degree of complexity and inherent assumptions (Gowen *et al.*, 1994), but the output from the models is generally in the form of a contour diagram illustrating particulate matter deposition rate with reference to the location of the source of input (in this case the farm site). In most cases, existing sedimentation models consider only the trajectory of a settling particle through the water column and therefore are designed for low-energy environments. Clear limitations to such models are that they do not address resuspension and any subsequent particle transport. In high-energy coastal environments, there may be regular or episodic resuspension of sediments, and some caution should be used in applying sedimentation models that do not take potential resuspension into account to these locations.

Most of the existing sedimentation models are primarily based upon physical processes and make no predictions about the ecological consequences of a given loading of waste onto the sea bed because of the highly site specific nature of such effects. However, there have been a number of models developed recently that include established linkages between predicted loading and biological response (e.g. changes in population densities, species numbers, functional response of the

community). Findlay and Watling (1994) have taken some initial steps in this direction by relating carbon loading with sea-bed oxygen consumption and CO_2 production, but work remains to be done before sedimentation modelling can be used to quantify the loading that would maintain a given ecological state. The particle tracking model DEPOMOD (Cromey *et al.*, 2000 a&b, 2002 a&b) includes validated semi-empirical quantitative relationships between predicted solids accumulation (g m^{-2} yr^{-1}) and observed Infaunal Trophic Index (ITI) (WRc, 1992), and total abundance within Envelopes of Acceptable Precision.

Modelling of sedimentation in the marine environment has, to date, concentrated on sewer outfalls, pulpmill effluents and marine cage fish farms. These processes are readily amenable to sedimentation modelling as the quantity and nature of material being discharged can be calculated and regulated. By contrast, virtually no attention in this area has been applied to shellfish farming because it has been seen as relatively benign and therefore not a priority target for modelling development. However, there is increasing commercial interest in shellfish farming, often in areas which have traditionally been involved in fish farming. As discussed previously, intensive bivalve farming produces quantities of particulate waste from the concentration of organic and inorganic particles within the surrounding sea water. It is possible that the fate of these particulate wastes from suspended bivalve (e.g. mussels, oysters) culture could also be modelled using the same techniques as have been applied to cage fish farms.

Silvert (1994) suggests that there are five main potential areas of application for sedimentation models with respect to aquaculture operations:

1. Site selection: For any production level, establish the deposition rate of particulate wastes around the farm for assessment in relation to established environmental quality standards.
2. Defining site limitations: Establish the maximum production attainable at a site, given a maximum permissible loading of particulate matter to the sea bed, or similar criteria.
3. Determining responsibility: Organic material is introduced into aquatic environments by a variety of natural and anthropogenic sources. If adverse

ecological consequences of enrichment are observed, a sedimentation model could be used to determine the relative contribution from each major source.

4. Optimising production: Organically-enriched sediment can have adverse effects on growth, health and survival of the cultured species through mechanisms such as reduction in dissolved oxygen concentrations, production of hydrogen sulphide, persistence of antibiotic residues or in serving as a reservoir for pathogenic micro-organisms. Sedimentation models can be used as a tool to aid in the development of strategies to control enrichment at locations where enrichment has a deleterious effect on production.
5. Design and implementation of monitoring programmes: The magnitude of the predicted carbon loadings can be used to establish an appropriate intensity of monitoring (i.e. how frequently, number of variables measured). Model predictions of prevailing particle trajectories could be used to establish the locations of sampling sites required to identify areas of greatest predicted impact, or to test field conditions against permit conditions. For example, model results might be used to predict the extent of the benthic mixing zone. Some regulatory authorities have policies that accept degradation within a specified area around a given farm. Models can be used to direct monitoring efforts to the perimeter of the mixing zone in order to verify compliance.

2.1.3 Nutrient release modelling

Another environmental concern over mariculture activities is the possibility of nutrient loadings from fish farms affecting primary production, leading to eutrophication or an increased risk of harmful algal blooms (Henderson and Davies, 2001). This is a difficult problem from the viewpoint of predicting how increased nutrients will affect the phytoplankton community, but the calculation of the nutrient changes is not overly difficult and is be described below.

Nutrient concentrations (C) within an inlet can be calculated by an uptake/clearance type of model:

$$dC / dt = N / U - FC \qquad \text{Eq. 2.1}$$

where N is the rate of nutrient input, U is the volume and F is the flushing rate. Such models treat nutrients as conservative substances. This model can represent the balance between input to the water column from a fish farm and the loss of material through both physical transport and degradation. An equation of this format holds for each effluent of interest. The nutrient input from fish farming can be calculated on the basis of models available which describe the flow and partitioning of nutrients through fish farms. In some areas there may also be inputs from other sources, for example from the processing of fish, forestry, agriculture, and domestic waste. A holistic assessment of nutrient inputs to an inlet and the consequential potential for nutrient enrichment needs to address all significant sources of nutrients and include an estimate of the overall diffuse inputs to the system. Inputs from aquaculture may be more easily estimated that some other sources because of parameterisation and knowledge of feed and excretion loads.

The other main element of the above model of potential nutrient enrichment is tidal flushing rate (see Edwards and Sharples (1985) for detailed description of this procedure). Tidal flushing is calculated as the volume of water equal to the tidal prism exchanged on each tidal cycle. The ratio of the tidal prism to the total volume of a water body gives an estimate of the amount of flushing per cycle. This calculation is normally an overestimate of the tidal flushing rate because of incomplete mixing both within and outside the water body. Many inlets, particularly those in which the salt water enters beneath a lens of fresh water, are not efficiently flushed by tidal action. If the farms are located in brackish water that simply floats up and down on top of the tidal salt water, there may be virtually no dispersion from tidal flushing. Furthermore, even if the water within the inlet is well-mixed, there may be potential for the nutrient laden water that exits the inlet on the ebb tide to come back in on the next flood. In such circumstances, the tidal action is not fully efficient at removing nutrients from the inlet.

The tidal flushing rate can be corrected for these factors by taking into account two mixing terms, expressing the fraction of water which gets mixed both inside and outside the water body. At present there are few models that can be used to calculate these correction factors, and so estimates of tidal flushing must be viewed as overestimates unless there is good reason to believe that the mixing in both regions is close to complete.

2.1.4. Modelling of chemical releases

There is currently a great deal of activity in the area of modelling the environmental fate and effects of chemicals, such as medicines, used in fish farming. This type of modelling is involved in the authorisation of medicines and pesticides, and also in the regulation of their use. However, it is outside the scope of this thesis, as currently, such chemicals are not used in the culture of bivalves.

2.2 Aspects of the modelling of benthic impact of aquaculture

2.2.1 Sources of organic wastes

Silvert and Sowles (1996) provided a detailed discussion of some of the theoretical and practical difficulties associated with modelling benthic impact of fish farming. They identified two main sources of environmental disturbances associated with fish farming. These were excretion by fish themselves (coupled with the loss of feed not ingested by fish), and physical and biological disturbance associated with cage structures themselves.

The most detailed modelling work to date has been in relation to benthic impacts. This appears to be a consequence of two main factors. Firstly, benthic impacts are relatively easy to observe and describe, and secondly, many of the parameters needed to model benthic deposition are known and relatively easy to measure. Silvert and Sowles (1996) noted that particulate wastes include both wasted feed and fish faeces.

Larger particles settle on the bottom and can lead to severe benthic impacts, while finer particulates lead to increased turbidity in the vicinity of fish farms.

Faecal pellets vary greatly in composition and physical characteristics. For salmonids, the faeces tend to consist of mucoid strands rather than actual particles, which makes a large difference in their settling characteristics and probably affects their rate of degradation on the seabed (Chen *et al.*, 1999 a, b).

The influence of the general hydrographic characteristics of fish farm sites may be well recognised, and current regimes can be relatively easily measured by recording current meters. However, it is becoming apparent that the cage structures themselves can interfere with the current field for some distance around (and below) the cages. In addition to the influence of the physical presence of the cages, fouling organisms on these structures can significantly contribute to both the oxygen demand and nutrient removal.

2.2.2 Modelling the production and behaviour of particulate waste

Silvert and Sowles (1996) noted that part of the difficulty in modelling benthic impacts of aquaculture is the wide variation in the type of particulates produced by fish farms. One reasonable and useful simplifying assumption is that benthic impacts are due mostly to carbon loading, and that these impacts are proportional to the amount of carbon and are largely independent of the form in which the carbon reaches the benthos.

On this assumption, the production function for the particulate wastes can be represented by a distribution function $X(S)$ such that $X(S)dS$ is the amount of carbon with settling speed between S and $S + dS$. The total carbon production is then

$$X_{tot} = \int_0^\infty X(S)dS \qquad \text{Eq. 2.2}$$

Silvert and Sowles (1996) proposed the further assumption that the settling speeds are roughly constant during deposition. If this is so, then this description of the production of particulate carbon is sufficient to permit a detailed computation of the rates of carbon deposition on the seabed under and near the source fish cage.

The subsequent calculation of benthic deposition from *X(S)* is straightforward. Under conditions of uniform current *V* and depth *Z*, the time it takes for a particle of settling speed *S* to reach the bottom is

$$t = Z / S \qquad \text{Eq. 2.3}$$

and during this time interval the particle will be displaced by the amount:

$$D_Z(S) = Vt = VZ / S \qquad \text{Eq. 2.4}$$

Since distribution function *X(S)* is known, this equation can be integrated to calculate the distribution $D_Z(S)$, which gives the amount of carbon falling at speed *S* deposited at the point represented by the displacement vector $D_Z(S)$.

In most cases, the current *V* is variable, and carbon concentrations must be averaged over time. The resulting distribution can be thought of as representing a pile of deposited carbon under each point within the cage. Total deposition is obtained through a further averaging process, this time over all points within the cage (Silvert and Sowles, 1996).

Gowen *et al.* (1994) addressed a further significant complexity, in that currents are seldom uniform all the way from the bottom of the cage to the seabed - indeed they must decline to zero at the benthic boundary layer in addition to any larger scale shear in the water column. Gowen *et al.* (1994) noted that this could be accounted for through estimation of horizontal displacement as

$$D_Z(S) = \left[\int_0^Z V(z)dz \right] / S = V_{av} / S \qquad \text{Eq. 2.5}$$

where V_{av} is the depth-averaged value of V.

A further complication in passing from desk models to field application is that the water depth is rarely uniform, and therefore the current must be averaged over the full trajectory of a sinking particle. Gowen *et al.* (1994) present a rather involved computer algorithm for solving this problem, but conceptually the problem of variable depth is relatively easy to solve. Instead of starting at the surface and following the trajectory down until the particle reaches the bottom, the particle is started at the bottom and worked upwards to the surface. The advantage of this technique is that, if the trajectory calculations of the particle start at the surface, the depth at the point at which the particle reaches the bottom is not known until the entire trajectory has been calculated. However, if trajectory calculations of the particle starts from the bottom and backtracks to the surface, this depth is already known. Since the horizontal displacement $D_Z(S)$ is a known function of water depth, and for each point on the bottom the depth Z is known, the value of - $D_Z(S)$ identifies the point on the surface from which particles with settling speed S would originate. If this point falls within the farm structure, it can be assumed that deposition is occurring, and if it is not within the farm then deposition will not be occurring. Although the averaging over settling speed S and over time leads to quite complex mathematical expressions, the algorithm is computationally straightforward.

An alternative approach to this problem was developed by Silvert (1994), based on a set of simplifying assumptions about the distribution of settling speeds and which uses mean current velocities to estimate the horizontal dispersion of particles. A particle falling at speed, <S>, in current, <V>, falls at an angle, θ, from vertical given by

$$\tan\theta = \frac{<V>}{<S>} \qquad \text{Eq. 2.6}$$

thus, if the current is uniform, and if the depth of water is <Z>, then the particle falls at a horizontal distance

$$D = < Z > \tan\theta = \frac{< Z >< V >}{< S >} \qquad \text{Eq. 2.7}$$

from where it started. The result is that the footprint of the farm site, namely the region in which the particles fall, is displaced by this distance from directly under the cage. For all types of discharge, there will be a mix of particles that fall at different speeds, so for different types of particles, the points at which they hit the seabed are different. This will result in a superimposition of footprints, each corresponding to particles of different size and density, and thus different settling rates.

By assuming that the displacement is random, the approximate result

$$A' = \mathrm{A} + \pi\, \mathrm{D}^2 \qquad \text{Eq. 2.8}$$

expresses the area of deposition of particles, A', in terms of the area of the farm itself, A. If the farm structure is circular with radius R, the radius of the depositional area is given by

$$R' = \sqrt{(R^2 + D^2)} \qquad \text{Eq. 2.9}$$

and the area is

$$A' = \pi\,(R')^2 = \pi R^2 + \pi D^2 = A + \pi D^2 \qquad \text{Eq. 2.10}$$

This is not the exact result for other shapes of farm, but the coefficient is generally close enough to D to make this a useful approximation Silvert (1994). Although this is recognised as only approximate and involves a number of assumptions, in many practical management situations there is insufficient information for more exact reliable predictions to be calculated.

The calculation of the mean deposition rate in this approximation requires only that we know the output of particulates, X_{tot}, and the area over which they are deposited, A', giving a mean flux to this area of the bottom of X_{tot}/A'.

A more important consideration is that the current speed usually varies with depth, especially in fjordic systems, where current shear in the water column is a common factor. The depth averaged value of the current should be used in this case (Gowen *et al.*, 1994, Silvert and Sowles, 1996), but if the depth varies, this can be a complex quantity to calculate (Silvert and Cromey, 2001).

It is apparent that these calculations are very sensitive to the settling rates used (Silvert, 1994), and thus they are constrained both by the limited data available on settling rates of particulates under different feeding regimes and by the difficulty of identifying the proportions of different types of particulates present, and their decomposition rates (i.e. the function $X(S)$). It is also possible that the underlying conceptual models of waste production and subsequent deposition may not always represent the actual processes involved. For example, it has been suggested that faeces from salmon may not settle gradually in an unimpeded manner. Rather, faecal strands from salmonids may settle on, stick to, or become entangled with, the bottom of the cage and the predator net beneath and around the cage. When these nets are agitated during storm events and other periods of energetic water movement, the faecal matter may be shaken loose. Such episodic processes could certainly affect the deposition patterns of these particulates.

2.2.3 Accumulation of organic matter on the sea bed

Benthic deposition is the forcing function that leads to carbon accumulation on the bottom, but actual observable carbon loading in the sediment is the integrated result of several competing processes which both add and remove carbon; these include not only deposition, but also resuspension, bioturbation, bacterial decomposition and grazing. The scale of these processes will be affected by factors such as the fluctuation of near-bed current speeds, the degree of bed consolidation, biological

activity and the degree of 'stickiness' of freshly deposited material. Each of these processes is complex and difficult to model in detail, but the overall sum of these processes may be represented by an uptake-clearance model of the form

$$dC / dt = S - kC \qquad \text{Eq. 2.11}$$

where C is the accumulated carbon under the site, S is the depositional rate of particulates, and k is a constant that represents the combined lowest-order effects of removal and degradation processes. Under steady-state conditions, this equation would result in C increasing asymptotically to a maximum level given by S-k. Although this may seem unrealistic, since conditions of constant deposition results in the constant accumulation of buried carbon, if C is interpreted as being the 'biologically active' fraction of total carbon in the benthos, this equation may not be unreasonable.

Accumulated carbon is not itself directly harmful, but its utilization and degradation can have both beneficial and detrimental consequences to the environment. Some of the processes that act on benthic carbon can lead to favourable conditions encouraging the growth of commercially valuable benthic resources such as fish and crustaceans. However, heavier accumulations of organic carbon and other nutrients can result in high bacterial densities and an impoverished benthic environment. The use of models to determine the scale of effects on the benthic environment is fundamental to a coherent approach to the sustainability of mariculture.

2.2.4 Sedimentation modelling - Current state of the art

The most advanced model of the processes leading to, and the biological consequences of, the deposition on the sea bed of particulate waste from cage fish farms is the DEPOMOD model (Cromey *et al.*, 2000 a). DEPOMOD consists of a series of modules that address components of the processes involved. The main modules are:

- The Grid generation Module, which creates the site specific grid on which the model is based. This includes details of cage numbers and layout, site characteristics, etc
- The Particle Tracking Module, which takes amounts of waste, particle attributes and hydrographic data as input and models settling, advection, current shear and turbulence
- The Resuspension and Carbon Module, which models resuspension events and the degradation of organic matter on the seabed.
- The Benthic Module, which takes information on the rate of carbon accumulation from then preceding module and predicts the response of the benthic community to that input.

Details of the processes modelled by DEPOMOD are described in CHAPTER 7, together with the alterations necessary to adapt DEPOMOD to deal with the waste produced from suspended culture of mussels.

3 Field Studies of the Impact of Mussel Farming - Materials and Methods

3.1 Field sampling programme

3.1.1 Field Site Selection

A number of farms were selected for survey work to quantify the effects of mussel farms on the surrounding benthic environment. A preliminary desk study was undertaken of many farms on the coasts of west Scotland and south west Ireland to identify sites that were suitable for the project. Criteria for suitability were as follows:

- Encompassing a range of farm sizes and biomasses, and numbers of years in production;
- Located within sheltered sea areas of depositional nature, with soft muddy bottom type and relatively low current velocities, such that the biodeposits from the farm sites would not be dispersed beyond the near-field area around the farm;
- Within a depth of water of less than 30m, to allow *in situ* observations and sample collections using SCUBA. Depths of between 10 m and 20 m were ideal for this technique as this allowed sufficient underwater time to complete all tasks.

Three sites were selected, pertaining to large (150 tonnes, site B), medium (100 tonnes, site A) and small (20 – 25 tonnes, site S) biomass of mussels. At their request, agreements of confidentiality were made with the shellfish farmers who assisted with this study. The farmers allowed access to their farm sites for sampling, and provided production statistics and other required information. The agreements prevent the naming, or in other ways identifying, any of the operators or sites which were used in this study. The project greatly benefited from the information provided by the farmers as a result of the goodwill created.

3.1.2 Hydrographic Measurements

Arrays of electromagnetic current meters (S4, InterOcean Systems) were deployed close to the farm sites at the time of surveying. The S4 electromagnetic current meter measures the voltage resulting from the motion of a conductor (water flow velocity) through a magnetic field according to Faraday's law of electromagnetic induction. Simply stated, Faraday's law defines the voltage produced in a conductor as the product of the speed of the conductor (water flow velocity) times the magnitude of the magnetic field times the length of the conductor. In the case of the S4, the conductor length is the effective path between the sensing electrodes. A circular coil, internal to the S4, driven by a precisely alternating current, generates the magnetic field intensity. The use of an alternating magnetic field and synchronous detection techniques to measure the voltage at the sensing electrodes provides an extremely stable, low noise current movement. Two orthogonal pairs of electrodes and an internal flux gate compass provide the current vector.

The positioning of the current meters was defined so as to reflect the local current movements, while avoiding any 'self shading' effect of the mussel lines. The meters were moored from a single line at specific heights above the seabed (after Leftley and MacDougall, 1991). The current speed and direction around the farms were recorded for a minimum period of 15 days (equivalent to one spring-neap tidal cycle) after which the meters were recovered. The hydrographic records were downloaded from the meters and subsequently analysed.

3.1.3 Positioning of benthic sampling stations

The data from the current meters were analysed and the direction of major current flow through each farm was determined. Using this information, and also taking into account the predominant wind direction around the site, a transect line was established along predicted gradients of deposition of particulate produced by the mussel farms. Sampling stations were then located along this line at specific distances from the farm. These stations were representative of the area of distribution of the biodeposits. The

transect continued away from the site to the point where little or no impact could be discerned from *in situ* observations.

3.1.4 Sediment sample collection for biological and physico-chemical parameters

All sediment samples were collected by SCUBA divers using plastic core tubes (57 mm internal diameter (i.d.), 300 mm length at site S; 102mm i.d., 250mm length at sites A and B). These were gently pushed into the sediment by hand, taking care to preserve the sediment-water interface. All sediment cores collected were to a depth of 100 – 120 mm deep. Once the core tube had been pushed into the sediment, a tight fitting stopper was inserted in the top of the tube. A second stopper was then inserted in the bottom of the tube by sliding it down and under the core so that the core of sediment could be withdrawn from the surrounding environment undisturbed. The differences in the sizes of cores were due to the availability of equipment at the time of sampling. Both sizes were considered suitable for the type of samples being collected.

3.2. Description of mussel farm sampling sites

3.2.1 Site S

Site S was located in approximately 11 m of water in a sheltered embayment of a small enclosed sea loch. The raft was approximately 15 metres square and constructed of wooden struts mounted on enclosed polystyrene block floats (Figure 3.1). The farm had been in production for approximately three years at time of sampling and supported 20 - 25 tonnes of mussels in their second year of growth. The ropes were seeded with mussel spat collected from within the bay. The farm generally produced 15 – 18 tonnes of marketable size mussels (45- 50 mm length) every year, collected in a single harvest during summer. The seabed was flat, and showed little variation along the transect line. The maximum tidal range was 2.1 m (Admiralty tables). The mussels were cultured in the upper 8 m of the water column, on droppers suspended from a floatation raft. The general layout of the site is illustrated in Figure 3.2.

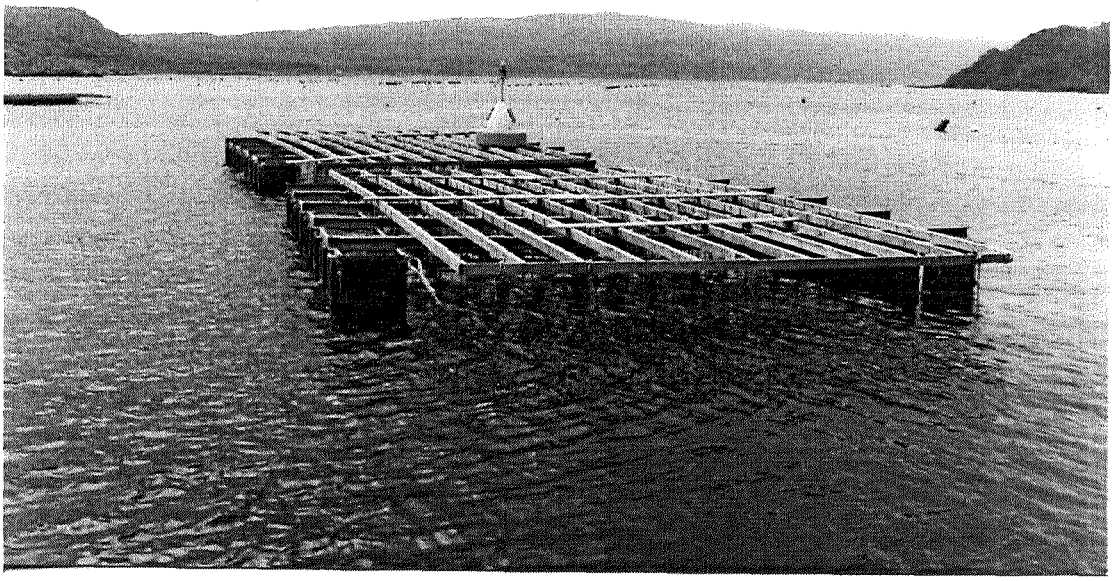

Figure 3.1	Photograph of the mussel raft at Site S

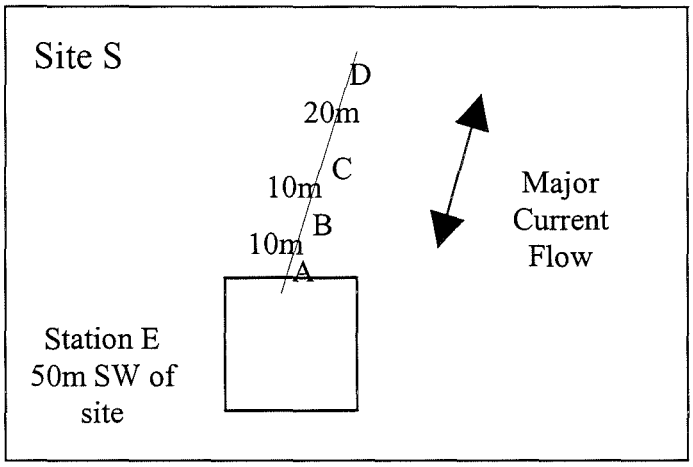

Figure 3.2	Schematic diagram of the mussel farm at Site S showing with direction of major current flow and location of sampling stations

3.2.1.1 Water current measurements

An array of three current meters was deployed 15 m to the east of the rafts in early July 1997. The meters were placed at 9 m (upper layer), 6 m (mid layer) and 3 m (bottom layer) above the seabed and the current speed and direction around the farm were recorded over a 19-day period between 11/7/97 and 30/7/97.

The current measurements (described in Results Chapter Section 4.1.1) indicated that the predominant (tidal) current flow was oscillatory along a north-easterly / south-westerly axis. A transect was defined in a north-easterly direction from beneath the edge of the farm and four sampling stations (SA, SB, SC and SD) were established along this line. Station SA was situated directly beneath the edge of the raft, station SB was at 10 m distance and station SC at 20 m distance from the edge of the farm. Station SD was situated at 40 m distance from the edge of the farm, at the end of the transect. An additional reference station (station SE) was also established 50 m south-west of the mussel raft in an area of similar depth and bottom type (mud) to that surrounding the culture site (Figure 3.2).

3.2.1.2 Benthic sampling

It was intended that 10 cores would be taken from each station for infaunal analysis. However, due to the constraints of diving, 10 cores were obtained from stations SA and SE, nine from station SB, five from station SC and four from station SD in July 1997. Samples were taken for sediment redox profiles and benthic macrofauna analysis. Replicate sediment samples (3) were also taken from each station for granulometry, carbon and nitrogen elemental analysis and sediment pore water analysis.

3.2.2 Site A

Site A was located in a large, well-flushed embayment, to the north of the shoreline. The farm had been in production for over 8 years and supported *circa.* 100 tonnes of mussels in their second year of growth. The ropes were seeded with mussel spat collected locally. The farm generally produced 70 – 75 tonnes of marketable size mussels (45 – 50 mm length) every year. The mussels were harvested throughout the

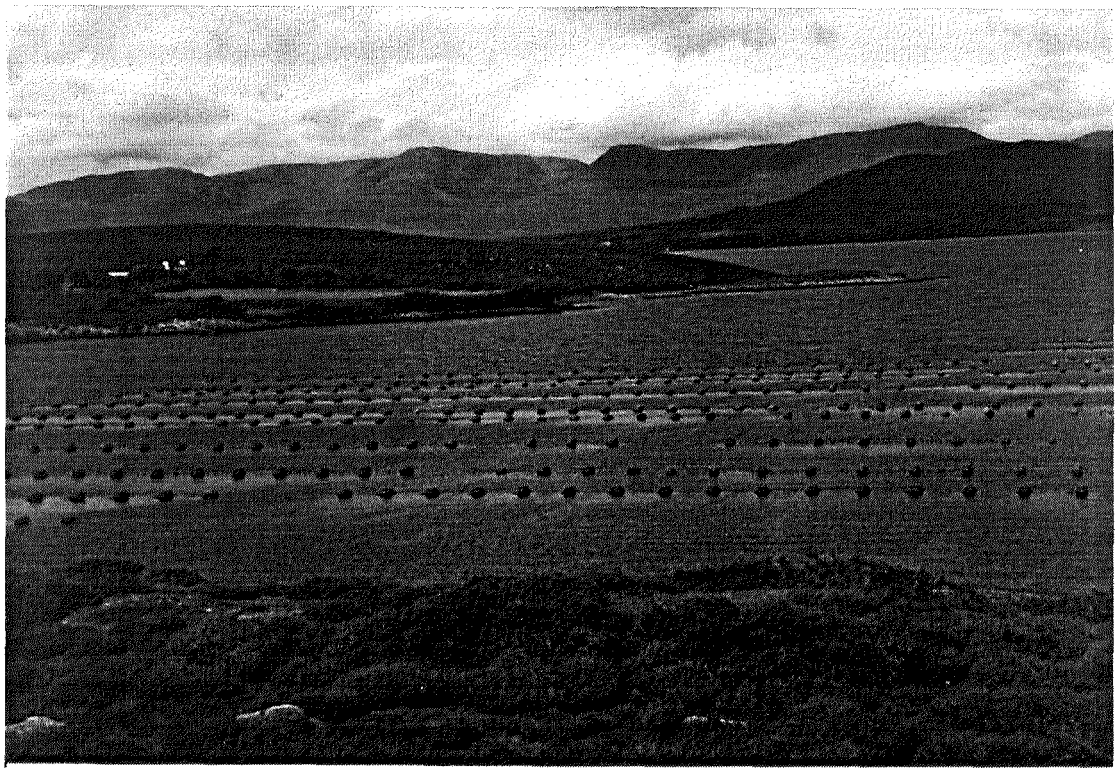

Figure 3.3	Photograph of the mussel raft at Site A

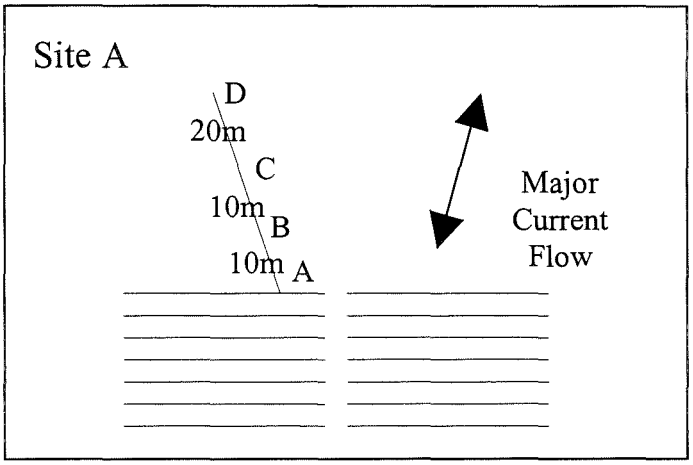

Figure 3.4	Schematic diagram of the mussel farm at Site A showing with direction of major current flow and location of sampling stations

year. The area was of flat bathymetry in a depth of 11 m with a maximum tidal range of 1.8 m (Admiralty tables). The farm was of the longline type, with mussels being grown in the upper 8 m of the water column on droppers from heavy surface longlines supported in the water column by large floatation drums (Figure 3.3). The longlines were orientated parallel to the shoreline, approximately 140 m long and arranged at 15 m intervals. The general layout of the site is illustrated in Figure 3.4

3.2.2.1 Water current measurements

Two current meters were deployed at this site, 20 m north of the edge of the farm at 8 m (upper layer) and 2 m (lower layer) above the seabed. The current speed and direction around the farm were recorded over a 15-day period between 06/07/98 and 21/7/98.

The current data (described in Results Chapter Section 4.2.1) indicated that the predominant (tidal) current flow was oscillatory along a north - north-easterly / south - south-westerly axis. The current speeds recorded at this site suggested that the gradient of deposition along the major current axis would extend outwith the immediate proximity of the farm site, making sampling by diver less practicable. Therefore a 'shorter' sampling transect was established at an acute angle to the major current flow axis, on a bearing of 345° (Figure 3.4).

3.2.2.2 Benthic sampling

Four sampling stations were established: station AA directly beneath the edge of the farm, station AB 10 m along the transect, station AC 20 m along the transect and station AD a total of 40 m away from the edge of the farm. It was considered, from *in situ* observations, that no effect from the farm would be observed beyond station AD.

Replicate sediment core samples were taken at each sampling station. These were for infaunal analysis (5 replicates), granulometry and carbon and nitrogen elemental analysis (3 replicates), sediment redox measurements (3 replicates) and sediment porewater analysis (3 replicates).

3.2.3 Site B

Site B was situated in the lee of an island approximately 70 m from the shore. The farm had been in production for over 13 years at time of sampling, and supported 150 tonnes of mussels, in all stages of growth. The ropes were seeded with mussel spat collected from within the bay. The farm generally produced in excess of 100 tones of marketable size mussels (45 – 50 mm length) per year that were continuously harvested. The area was of relatively flat bathymetry in 15 m of water with a maximum tidal range of 1.8 m (Admiralty tables). This farm was also of the long-line type, with mussels suspended on ropes in the upper 8 m of the water column. The lines were orientated parallel to the shoreline, approximately 175 m long and were arranged at 15 m intervals (Figure 3.5). The general layout of the site is illustrated in Figure 3.6

3.2.3.1 Water current measurements

Two current meters were deployed at this site, 20 m south of the edge of the farm at 8 m (upper layer) and 2 m (lower layer) above the seabed. The current speed and direction around the farm was recorded over a 14-day period .

The current data (described in Results Chapter Section 4.3.1) indicated the predominant (tidal) current flow was oscillatory along a north – northeasterly / south – southwesterly axis. A transect was defined in a south – southwesterly direction (bearing approximately 200°) from beneath the edge of the farm. Three sampling stations were established along this transect: station BA directly beneath the edge of the farm, station BB 10 m along the transect and station BC a further 20 m along the transect (Figure 3.6).

3.2.3.2 Benthic sampling

Replicate sediment core samples were taken at each sampling station. These were for infaunal analysis (5 replicates), granulometry and carbon and nitrogen elemental analysis (3 replicates), sediment redox measurements (3 replicates) and sediment porewater analysis (3 replicates).

Figure 3.5	Photograph of the mussel raft at Site B

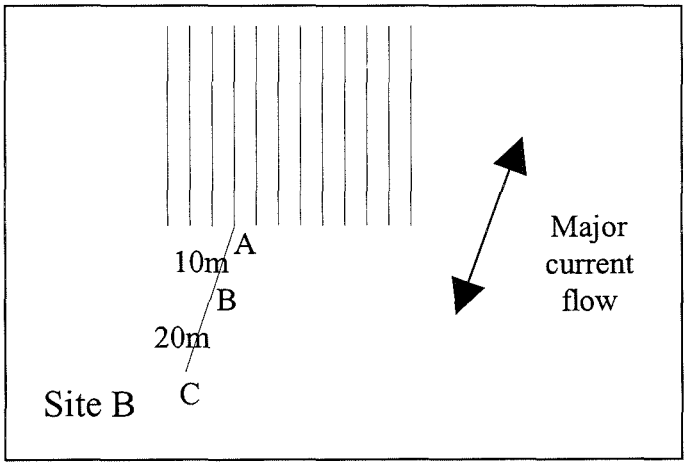

Figure 3.6	Schematic diagram of the mussel farm at Site B showing with direction of major current flow and location of sampling stations

3.3 Laboratory procedures and analyses

3.3.1 Sectioning of sediment cores

Cores for physico-chemical analysis were stored upright in incubation tanks overnight, with the top of the cores open for free water exchange with the collected bottom water. The tanks were maintained at constant temperature (~ 8 °C) and aerated *via* air pumps.

The cores were sliced into sections of differing lengths, depending upon the type of analysis to be undertaken. Sections were 3 cm long for infauna samples and 1 cm for the other analyses. Cores were sectioned using suitable sized rings (constructed from the material of the cores to match the diameter) as guides, and an aluminium slicer (100 x 100 x 0.5 mm, sharpened at one edge). To aid the extrusion and sectioning of the cores, a piston was carefully inserted into the bottom of the core tube, keeping the top of the core tightly sealed to prevent loss of the sample from the core tube. The arrangement was then secured in a suitable retort stand from where slicing was performed. The rings containing the required length sediment slices were removed from the core using the slicer and processed as described below.

3.3.2 Sediment analyses

3.3.2.1 Benthic macrofauna

Immediately upon retrieval at the surface (or shore), the sediment cores for faunal analysis were sliced into 3 sections, 3 cm in length from the surface layer, and fixed in buffered 10 % formal saline containing 0.1 % rose Bengal stain. Immediate slicing was undertaken to prevent migration of biota within the core. In the laboratory, samples were sieved through a mesh of 500 μm pore size and the retained fauna were stored in 70% Ethyl alcohol. The fauna was subsequently sorted, identified using standard keys and counted using a binocular microscope (See Appendix 2 for taxonomic references).

3.3.2.2 Redox potential

As soon as possible after the cores were retrieved on the shore, the redox potential was measured at 5 mm intervals (for the upper 20 mm) and 10 mm intervals thereafter, from the surface using a redox electrode (300 x 10 mm; Russell pH Ltd.), mounted in a Palmer stand, which was wound down into the sediment. The Eh (mV) profiles were measured using a waterproof pH-redox meter (Russell RL100).

Before, and after, each Eh profile was determined, the electrode was calibrated as described by Zobell (1946). A repeatable Eh reading of 250 ± 10 mV was required to confirm that the electrode was calibrated. A reading outwith this range required the probe to be recalibrated with clean fresh Zobell's solution (1.399 g potassium ferrocyanide, 1.089 g potassium ferricyanide and 1.456 g potassium chloride made up to 1 dm^3 in distilled water), or replaced with another probe. Distilled water was used to rinse the probe each time it was transferred between the Zobell's solution and the sediment core and *vice versa*. The measurements were corrected to the normalised hydrogen electrode by the addition of 198 mV to each reading as described by Pearson and Stanley (1979).

3.3.2.3 Granulometry

Three cores from each sampling station were sliced into 1 cm sections to a depth of 6 cm. The samples (~ 5 g) were stored in plastic sample bags and stored at -20 °C and subsequently freeze dried. Particle size of the dried sediment was determined using a Malvern Mastersizer/E (Malvern Instrument, Worcestershire, UK) with a 300 mm lens. Prior to analysis, a sample of sediment (1 - 2 g) was sieved through a 500μm mesh, mixed and ultrasonicated in the sample bath to remove entrapped air. The Mastersizer is a light-scattering based particle sizer comprised of an optical measurement and computer. The angle through which light is scattered by a particle is a function of the particle's size and shape, and this property is used to model the size distribution of the sample. From the computed results (PC running Mastersizer/E version 1.2a software) the particle size characteristics of the samples were determined for subsequent data analysis. Full procedural details are given in Appendix 1 (M840).

3.3.2.4 Organic carbon and nitrogen.

Three cores from each station were sliced into 1 cm sections to a depth of 6 cm. The samples (~ 1 - 2 g) were stored in plastic sample bags and stored at -20 °C until freeze dried. The samples were ground to a homogenous fine powder using a small ball mill (Appendix 1 SOP120). The samples were then stored in dry, airtight bags until analysis.

In order to measure the organic carbon content of the sediment samples, it was necessary to remove inorganic carbon (carbonates) by treatment of sediment samples with 15% hydrochloric acid (Appendix 1 SOP 170). The samples were then stored in a dessicator until analysed by elemental analyser.

Total organic carbon content of the samples was determined by Perkin-Elmer CHN Elemental Analyser model 2400 (Perkin-Elmer, Beaconsfield, Buck, U.K.). The silver cups containing the samples were introduced into the analyser and the weight percentage content of organic carbon, nitrogen and hydrogen was determined by standard techniques (Appendix 1 M860). The CHN analyser uses a combustion method to convert the sample elements to simple gases (CO_2, H_2O and N_2). The sample is first oxidised in a pure oxygen environment; the resulting gases are then reduced at exact conditions of pressure, temperature and volume. Finally, the product gases are separated. Then, under steady state conditions, the gases are measured as a function of thermal conductivity.

3.3.3. Pore water nutrient analyses

Three cores from each station were sliced into 1 cm sections to a depth of 6 cm, under nitrogen to maintain anoxic conditions. Each slice was transferred to a centrifuge tube (20 cm^3) and centrifuged (4000 g, 10 mins). The supernatant was decanted into a glass scintillation vial (17 cm^3) and filtered into a nylon vial (5 cm^3) via a glass fibre filter (0.45 um; 25 mm; Whatmann GF/F) held in a Sartorius filter assembly. This filter process ensured the removal of any remaining suspended solids in the supernatant. The samples were stored under nitrogen and frozen (-20°C) for subsequent analysis for nutrients.

Care was taken when handling and storing the nutrient samples to avoid contamination of low concentration nutrients. All preparatory and analytical laboratory-ware used was pre-washed in a solution of Decon 90 in distilled water (5%) for at least 6 hours, rinsed in double distilled water and washed for a further 6 hours in hydrochloric acid (10%) in distilled water and oven dried.

Concentrations of ammonia and reactive phosphate were determined in pore water samples by standard manual colourimetric methods, adapted slightly to allow for the low volumes of sample available, and the high concentrations of nutrients.

3.3.3.1 Ammonia

Ammonia was determined by an indophenol blue method. In the presence of a catalyst and excess chlorine, ammonia reacts with phenol to form indophenol blue. The intensity of the blue colour is proportional to the concentration of the ammonia, the absorbancies were measured at 630 nm (Appendix 1 M770).

3.3.3.2 Phosphate

Phosphate was determined by a classical single-solution molybdenum blue method. Ortho-phosphate forms a yellow complex with molybdate ions in strongly acid solutions. The phosphomolybdate complex is reduced in the presence of trivalent antimony by ascorbic acid to molybdenum blue. The intensity of the blue colour is proportional to the phosphate concentration and is determined by colourimetric measurements (Appendix 1 M870).

3.3.4 Quality Assurance

The measurements of particle size distribution, carbon and nitrogen concentrations, and nutrients in pore waters were all carried out under a Laboratory Quality System accredited by the United Kingdom Accreditation Service (UKAS). All methods had been fully validated in the laboratory prior to adoption as standard, and also through participation in series of national and international intercalibration exercises: for example, the ICES and QUASIMEME laboratory performance studies. All analyses were established as being under statistical control by participation in the laboratory

quality control procedures. At least one laboratory reference material (LRM) was analysed with each batch of samples and plotted on Shewart Control Charts. If the LRM was outwith two standard deviations of the continuous mean, the batch results were rejected and the samples were re-analysed.

3.3.5 Data Analyses

The physico-chemical data were checked for normality using Anderson-Darling test and homogeneity of variances by the Bartlett test. Data not conforming to either of these two were transformed using an appropriate transformation (Zar, 1984). Differences between the samples were assessed using a one-way ANOVA test with a Tukey pairwise comparison test using MINITAB (10.0). This analysis was carried out on all the physico-chemical results for each layer of the sediment, using a significance level of $p = 0.05$.

Variability in the benthic infaunal data between sampling stations was assessed using the following standard univariate measures of community structure: number of Species (S), number of Individuals (*N*), Shannon-Wiener diversity index (*H', log*$_2$) (Shannon and Weaver, 1949), Margalef's species richness index (*d*) and Pielou's Eveness Index (*J'*) (Pielou, 1966).

Univariate measures of community structure	
Number of Species	S
Number of Individuals	N
Shannon-Wiener Diversity Index where P_i is the proportion of the total count (or biomass etc) arising from the *i*th species	$H' = -\sum_i P_i(\log_2 p_i)$
Margalef's Species Richness Index	$d = (S-1)/\log_2 n$
Pielou's Eveness Index where $H'_{(max)}$ is the maximum diversity which could be achieved if all species were equally abundant (= log *S*)	$J' = H'_{(observed)} / H'_{(\max)}$

Univariate measures provide a useful means to summarise important attributes of benthic community structure, and have the advantage of being amenable to straightforward statistical testing. The primary variables S and N are unambiguous descriptors, while the derived variables H', d and J' (along with ratios of the primary variables), attempt to combine the attributes of species occurrence, and apportioning of individuals among those species, with varying degrees of sophistication.

The limitations attached to single-figure summaries of complex data are well recognised. For example, natural events such as a particularly successful recruitment, or excessive predation, may give rise to changes in diversity comparable with those occurring in response to some anthropogenic influences. Misinterpretation of the causes of such events can only be prevented by reference to the basic data. A further limitation of the use of univariate measures is that widely different communities can produce similar summary univariate values. Therefore, the use of univariate measures in assessments of anthropogenic effects should always be accompanied by complementary (e.g. multivariate) techniques to aid in expert interpretation of the underlying causes of any patterns in the data.

Multivariate analyses were carried out on the faunal data to assess (dis)similarities between community assemblages. All multivariate analyses were performed using the PRIMER (Plymouth Routines In Multivariate Ecological Research) package, version 4.0 (Warwick and Clarke, 1994). One important feature of the multivariate PRIMER programs is that they do not utilise any known structure among the samples, e.g. their division into replicates within groups. This is in contrast with Canonical Variate Analysis, for example, which deliberately seeks out ordination axes that, in a certain well-defined sense, best separate out the known groups (e.g. Mardia *et al.*, 1979). Dendrograms were produced by hierachical agglomerative clustering, with group average linking, from the Bray-Curtis similarity matrices. The Bray-Curtis index was chosen because of its ability to deal with matrices with a high proportion of zero data entries, i.e. it is not influenced by joint absences (Field *et al.*, 1982). The raw community data were square root transformed to downweight the influence of the more abundant species. This was chosen *a priori* as a compromise between 'no transformation' in which different community assemblages may result from variability

in the most common taxa, and a strong transformation such as 4^{th} root or log (x+1), in which rarer species have very strong influences on community (dis)similarities (Warwick and Clarke, 1994).

Non-metric Multi-Dimensional Scaling (or MDS) was carried out on the sample similarity matrix from which an ordination plot was produced. The MDS plot is arbitrarily scaled, located, rotated or inverted: it gives the positions of samples *relative* to each other. The relative distance between each of the sample positions on the plot reflects the relative similarity of sample species composition. Since the MDS ordination represents a multi-dimensional ordination in 2 dimensions, there will usually be some distortion or 'stress' between the ranked dissimilarities and corresponding distances in the plot. Each algorithm has an associated stress value, the influence of which on the reliability of ordination plots is discussed by Warwick and Clarke (1994). Since the algorithm is an iterative procedure, it is possible that it could converge on a 'local minimum' rather than a 'global minimum' of this stress function. Therefore, the procedure was repeated for different random starting configurations to confirm that these gave the same solution (with the lowest stress value) several times (Warwick and Clarke, 1994), i.e. increasing the number of starting points in the ordination plots increases the chance of producing the most optimum MDS plot. The final MDS ordination in each analysis was that with the lowest associated stress value out of nine iterations and at least 10 different random starting configurations.

Testing for significance between the different sampling station communities was performed using a one-way ANOSIM test (analysis of similarities) in which the null hypothesis (H_o) in each case was that there were no significant differences between the sampling stations. The ANOSIM test can be regarded as a non-parametric equivalent of the MANOVA test (e.g. Mardia *et al.*, 1979) in which few, if any, assumptions about the data are made. Benthic community data are usually far from normally distributed (Clarke, 1993) and, therefore, a non-parametric test is usually more suitable. However, no corrections are made for multiple pairwise testing (Warwick and Clarke, 1994), consequently, more emphasis should be placed on the value of R, the test statistic, rather than the p value. The test statistic R will always be between 0 and 1; if R = 1 all replicates within stations are more similar to each other

than any other replicates from different stations, while if $R = 0$ similarities between and within stations will be the same on average. As with standard univariate tests, it is possible for R to be significantly different from zero yet relatively small if there are many replicates for each site. The ANOSIM test is more reliable for indicating treatment differences than the MDS plot since it works on the full similarity matrix rather than the approximation to it in 2-dimensions (Warwick and Clarke, 1994).

Variability in the benthic infauna data between sampling stations was also assessed using the Infaunal Trophic Index (ITI) (Word, 1978, 1980; Mearns and Word, 1982), which parameterises the characteristics of the benthic macroinfaunal community in terms of feeding strategies.

It has been recognised for many years, and described in the classic publications by Pearson and Rosenberg (1978) that a series of sequential changes occurs in benthic communities in relation to increasing organic enrichment. Changes in biomass, species abundance and diversity are also accompanied by changes in feeding strategy from filter feeders to deposit feeders. It is this change in feeding strategy that is the basis of ITI. The use of the ITI was recommended by the Comprehensive Studies Task Team of GCSDM (CSTT, 1994) for use in assessment of the impact of sewage discharges on benthic infauna. Its utility was based on studies undertaken in California (Mearns and Word, 1982) and the index developed there by Word (1978) was adapted for use in UK conditions by WRc Plc (1992). It relies on the assessment of changes in the feeding (trophic) mode of the benthic organisms in an area subject to increasing organic enrichment.

Most of the following detailed description of the processes underlying the ITI has been taken from Word (1980).

The purpose of the ITI is to describe the feeding behaviour of bottom benthic communities in terms of a single understandable parameter. These animals fall into four groups: they are either suspension or deposit feeders that feed above, on or below the mud surface. The ITI was developed in California, USA and was first published by Word in 1978. Since then it has been adapted for use in UK waters (WRc, 1992)

but the principles remain the same. Invertebrates have been divided into four groups based on what type of food is eaten, where it is obtained and how it is obtained.

Trophic Group 1 - Suspension feeders

These animals feed on detritus and usually lack sediment grains in their gut contents. They obtain food from the water column. Suspension feeding organisms include those that actively pump water and suspended particles through a filtration apparatus and those that use highly developed feeding appendages to sieve particles from the water column with the aid of bottom currents. Passive suspension feeding is an additional suspension feeding technique that results in accumulations of detrital materials near the tubes of apparent surface detrital feeders. Typical examples of suspension feeders are: *Spio, Spiophanes, Sabella, Ampelisca, Corophium, Phaxas pellucidus, Mya arenia, Ophiothrix fragilis* and *Amphiura filiformis*.

Trophic Group 2 - Surface detritus feeders

Surface detrital feeders obtain the same types of food as suspension feeders but they usually obtain their food from the upper 0.5 cm of the sediment. Because their stomach contents do not reveal any major differences, behavioural observations serve as the only means of separating suspension feeders from surface detrital feeding animals. Two typical surface detrital feeding behaviours are used by members of several different phyla. First, there are those organisms that are relatively stationary. These animals have modified feeding appendages that search the surface of the sediment and then locate, capture and convey food items to the animal. The second type, mobile surface detrital feeders, move from one food item to the next rather than drawing it towards them. Typical examples of surface detritus feeders are: *Nephtys incisa, Levinsenia gracilis, Polydora,* Cirratulidae, Scalibregmatidae, *Photis, Mysella* and *Ophiura.*

Trophic Group 3 - Surface deposit feeders

Surface deposit feeders generally obtain their nourishment from the top few centimetres of the sediment and feed on encrusted mineral aggregates, deposit particles or biological remains. Particles are consistently > 100um. The two basic feeding strategies classified in this group are mobile surface deposit feeders and

stationary surface deposit feeders. Examples of surface deposit feeders are: *Anaitides, Goniada maculata, Nephtys hombergii, Scoloplos armiger, Nucula* and *Thyasira.*

Trophic Group 4 - Sub-surface deposit feeders

Sub-surface deposit feeders are generally mobile, deep burrowers that feed on deposited organic material. Their feeding behaviour is variable and these animals are adapted to live in sediment which is highly anaerobic. Examples of sub-surface deposit feeders are: *Ophryotrocha, Schistomeringos, Capitella capitata, Notomastus latericeus,* Oligochaeta and *Bittium.*

The ITI value (score) for each station was calculated using the following formula:

$$ITI = 100 - 33.3\left(\frac{0N_1 + 1N_2 + 2N_3 + 3N_4}{N_1 + N_2 + N_3 + N_4}\right)$$

where N_1 = abundance of trophic group 1 organisms

N_2 = abundance of trophic group 2 organisms

N_3 = abundance of trophic group 3 organisms

N_4 = abundance of trophic group 4 organisms

The resulting score defines the status of the benthic community. Benthic predictions are based on 0.1 m^2 grab sample size areas. Word (1979) described the following levels of benthic disturbance:

ITI	Description of community (general definition from sea loch data sets)
>50	little effect
20 - 50	enriched
<20	degraded

4. Field Studies of the Impact of Mussel Farming - Results

At each of the study sites data were collected concerning hydrography, sediment physico-chemical characteristics and benthic faunal communities. In this chapter, the data are presented for each of the three study sites, S, A and B.

4.1 Site S

4.1.1 Water Currents

Comprehensive analyses of the hydrographic data collected at Site S are presented in Appendix 3 - Site S. A summary of the hydrographic data at Site S is presented in Figure 4.1 (a and b) for the surface current data, Figure 4.2 (a and b) for the midwater current data and Figure 4.3 (a and b) for the bottom current data. The hydrographic measurements revealed the site to be very weakly flushed, with the mean current velocity to be approximately 0.01 m s^{-1} throughout the water column (Table 4.1).

Table 4.1 : Hydrographic characteristics at Site S.

	Surface	Middle	Bottom
Mean Current Velocity (cm s^{-1})	1.4	1.1	0.9
Residual Current Velocity (cm s^{-1})	0.6	0.5	0.1
Residual Current Direction (deg)	229	188	330

Surface currents were recorded in all directions, with a high proportion of the stronger current speeds being along a north-east/south-west axis. The highest velocities (and also the most abundant) were in the south/westerly direction (Figure 4.1 b). Current speeds at the surface attained a maximum of 0.07 m s^{-1} during periods at spring tide. The frequency histogram (Figure 4.1 a) illustrates the most frequent currents were < 0.03 m s^{-1} , with only 8.42% of the recordings exceeding this velocity. As suggested by the residual plot (Appendix 3 - Site S), the most frequent direction of flow was towards the south-east.

a)

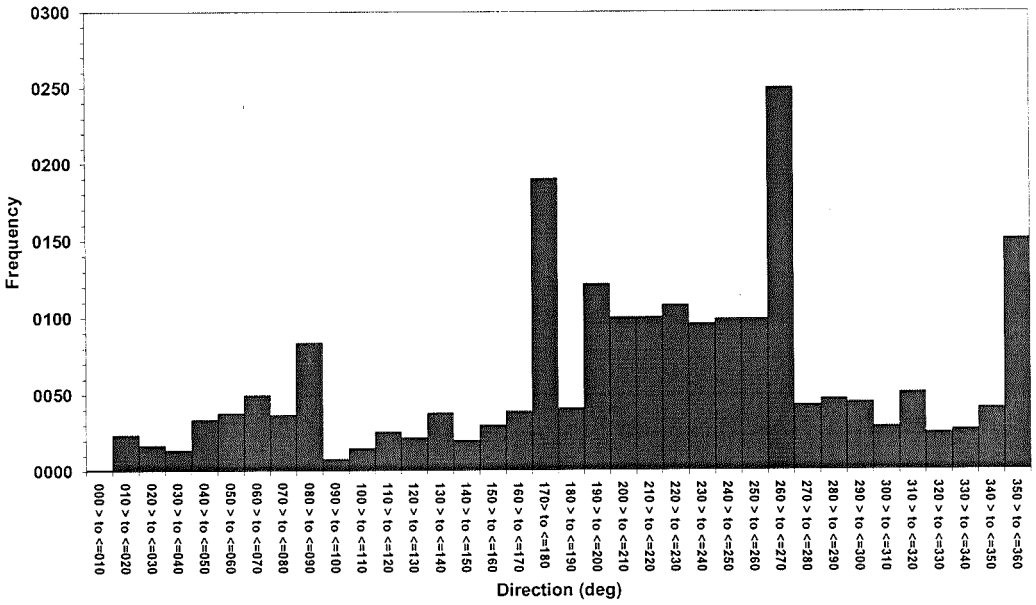

b)

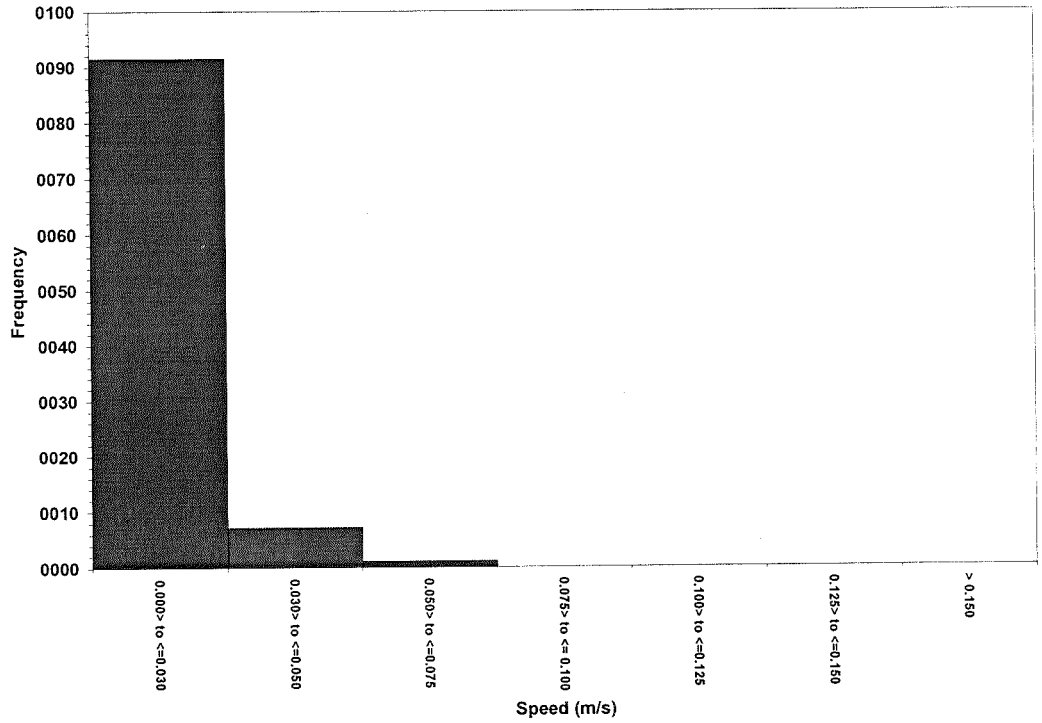

Figure 4.1 a and b Site S Surface current direction and velocity frequency histograms

a)

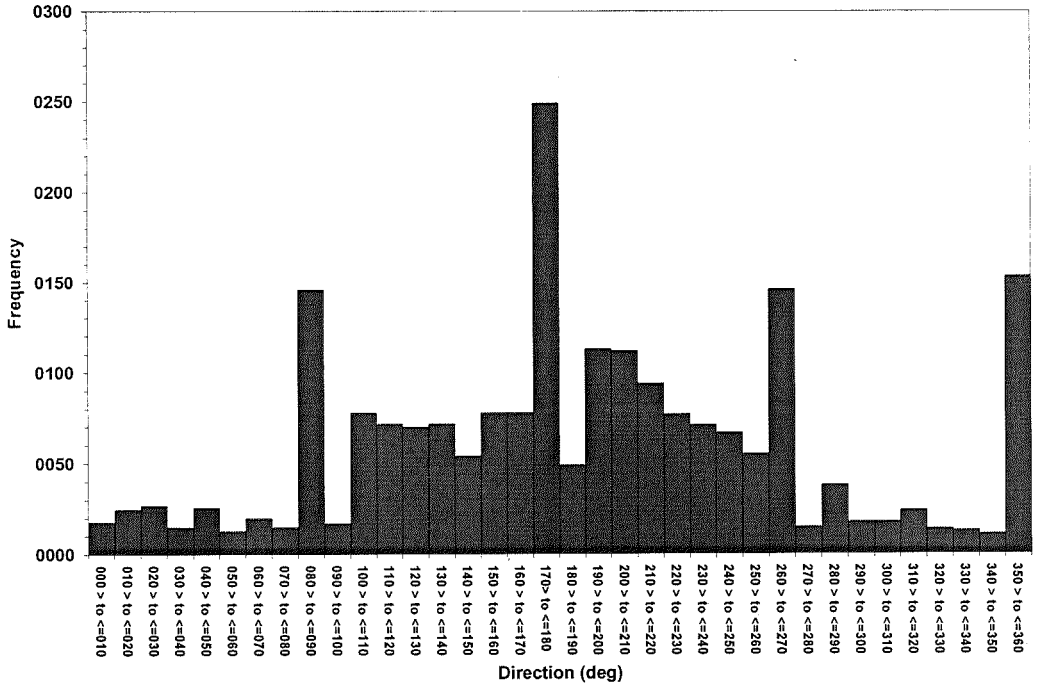

b)

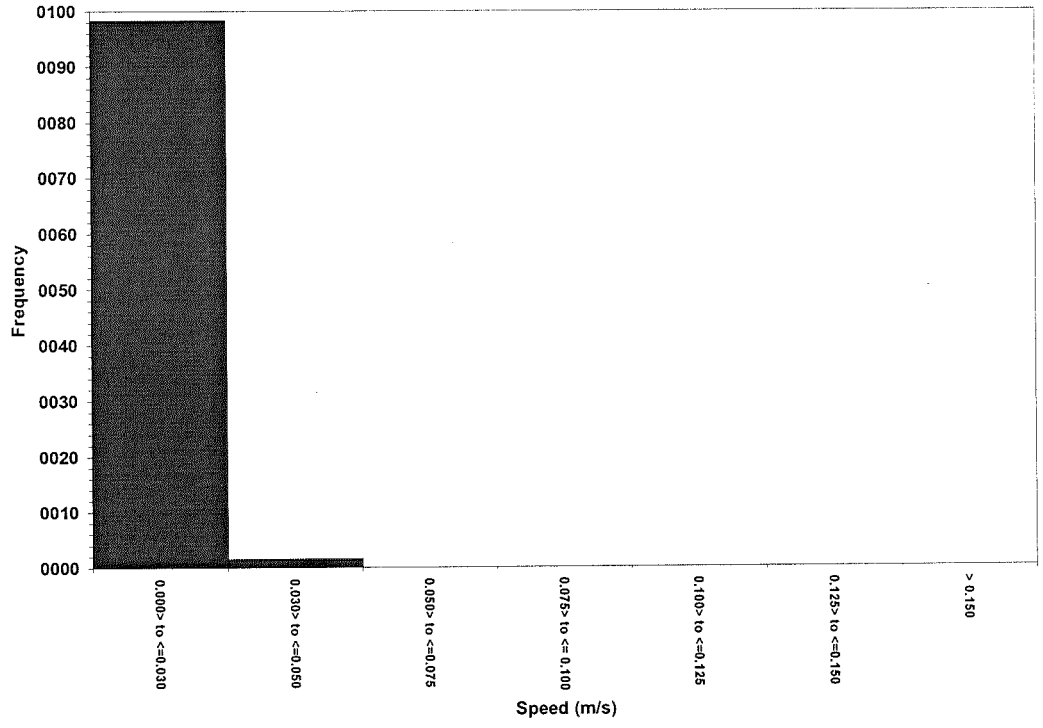

Figure 4.2 a and b Site S Midwater current direction and velocity frequency histograms

a)

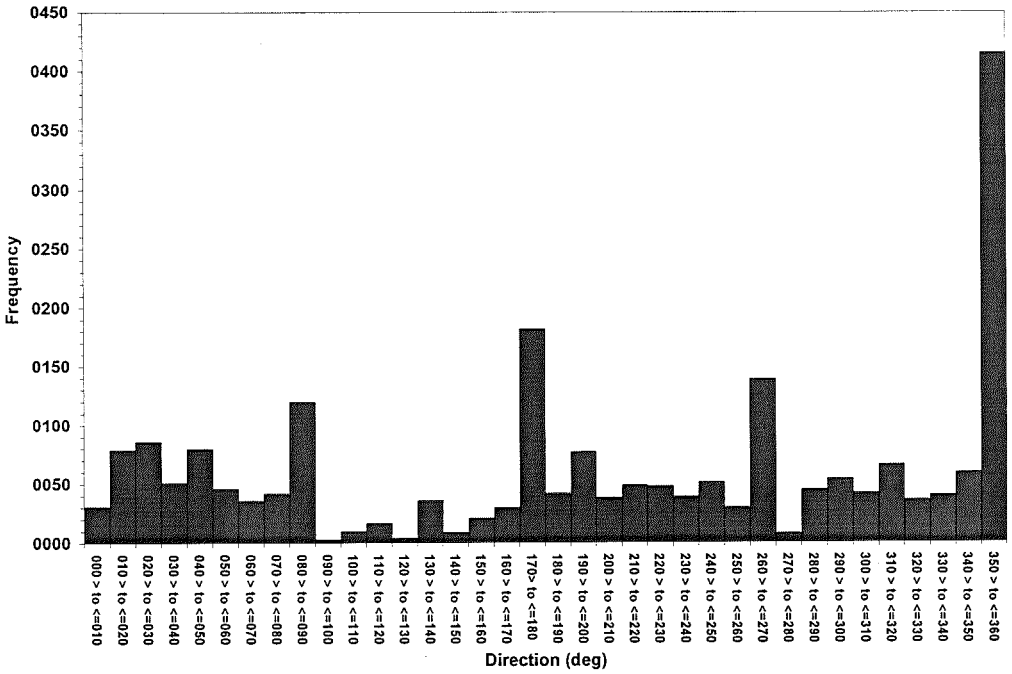

b)

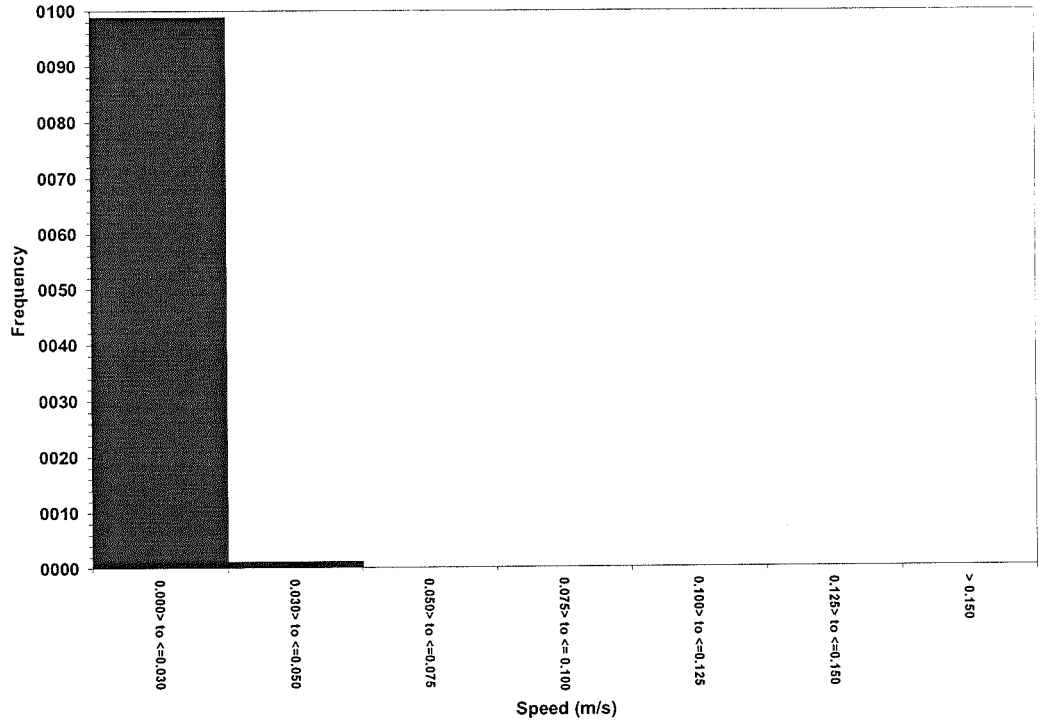

Figure 4.3 a and b Site S Bottom current direction and velocity frequency histograms

Current flows in mid-water were similar in direction to those found at the surface, with generally slower speeds (Table 4.1), and the residual current was also in a south-easterly direction (Appendix 3 - Site S). The current velocities varied between zero and 0.05 m s^{-1} - the majority of readings (98.43%) were < 0.03 m s^{-1}. There was little difference in current velocity and direction between spring and neap tide periods.

Currents velocities recorded at the seabed were <0.03 m s^{-1} for 98.84% of the deployment period. The scatterplots (Appendix 3 - Site S) and histograms (Figure 4.3 a and b) show that the most frequently recorded current direction at the seabed was to the north. This is also shown in the residual plot (Appendix 3 - Site S) indicating a general north-westerly direction. However, measurements were recorded in all directions and the currents were generally very weak.

4.1.2 Sediment Redox

The sediment redox potential remained positive throughout the sediment depth and varied marginally between each sampling station. A well developed redox potential discontinuity layer (RDL) occurred at approximately 0.5 cm below the sediment surface at stations A and B (Figures 4.4 (i) and (ii) respectively). The RDL was poorly defined at stations C, D and E (Figures 4.4 (iii), (iv) and (v) respectively) and occurred at a greater depth in the sediment. There was considerable variation in the recorded Eh values between the replicate samples.

The redox potential value of the surficial sediment was similar at each station at approximately +400 mV. Sediment Eh values were reduced with depth. However, there were no significant differences observed between the sampling stations at each sediment depth layer.

At sediment depths greater than 3 cm, the Eh value remained relatively constant at approximately +50 mV at all stations, with the exception of station D. There was high variability between the replicate cores at this station, which lead to fluctuations in the

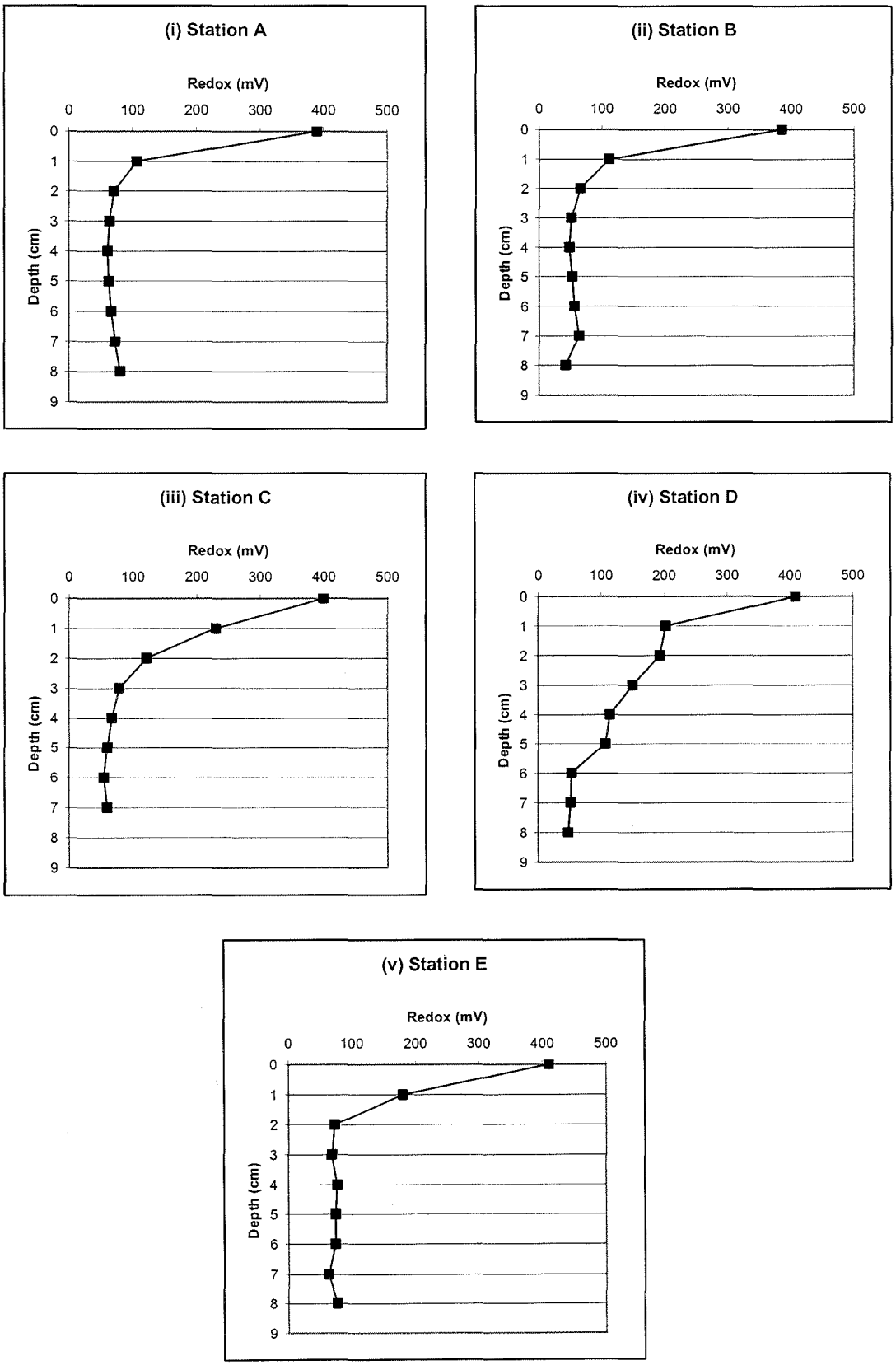

Figure 4.4 (i – v) Site S Redox potential (mV) with depth at each sampling station

mean redox value, and possibly accounted for the very poorly defined RDL at this station. The Eh value remained relatively constant at + 50 mV beyond the 6 cm sediment depth.

4.1.3 Granulometry

Particle size analyses described the sediment at this site as generally poorly sorted fine to medium silt, with a distribution that was symmetrical or finely skewed and meso- or leptokurtic. Throughout the site, the sediment characteristics varied only marginally between the sampling stations. The proportion of fine sediment (weight percentage of particles <63 μm) fluctuated between 85 % and 95 %. The median phi and sorting coefficient variables exhibited only slight variations with depth and between sample stations. The calculated variables and sediment descriptors for this site are presented in Appendix 3 - Site S

The proportion of fine sediment (< 63 μm) in the surficial (1 cm) layer increased between stations A and B, with a noticeable reduction at stations C and D (Figure 4.5, i – vi). The fine sediment content at sample station E was comparable to that observed at station A. The median phi variable (Figure 4.6, i – vi) followed this trend between stations with a maximum value recorded at station B and minimum at station D. The sorting coefficient values (Figure 4.7, i – vi) exhibited a similar but 'reciprocal' trend, due to the method of calculation of this variable, with a maximum value recorded at station D and minimum at station B.

Within the 2 cm layer, a general increase in the < 63 μm fraction was observed from station A to stations B and C, with a subsequent reduction in the fine sediment content at stations D and E (Figure 4.5 i – vi). Similar trends were observed in the median phi and sorting coefficient (reciprocal trend) variables (Figure 4.6 i – vi and 4.7 i – vi). Median phi values were significantly greater ($p = 0.05$) at station C compared with station E.

A similar trend was observed in the 3 cm layer, with slight increases in the < 63 μm fraction, median phi values, and decrease in sorting coefficient, between station A and B,

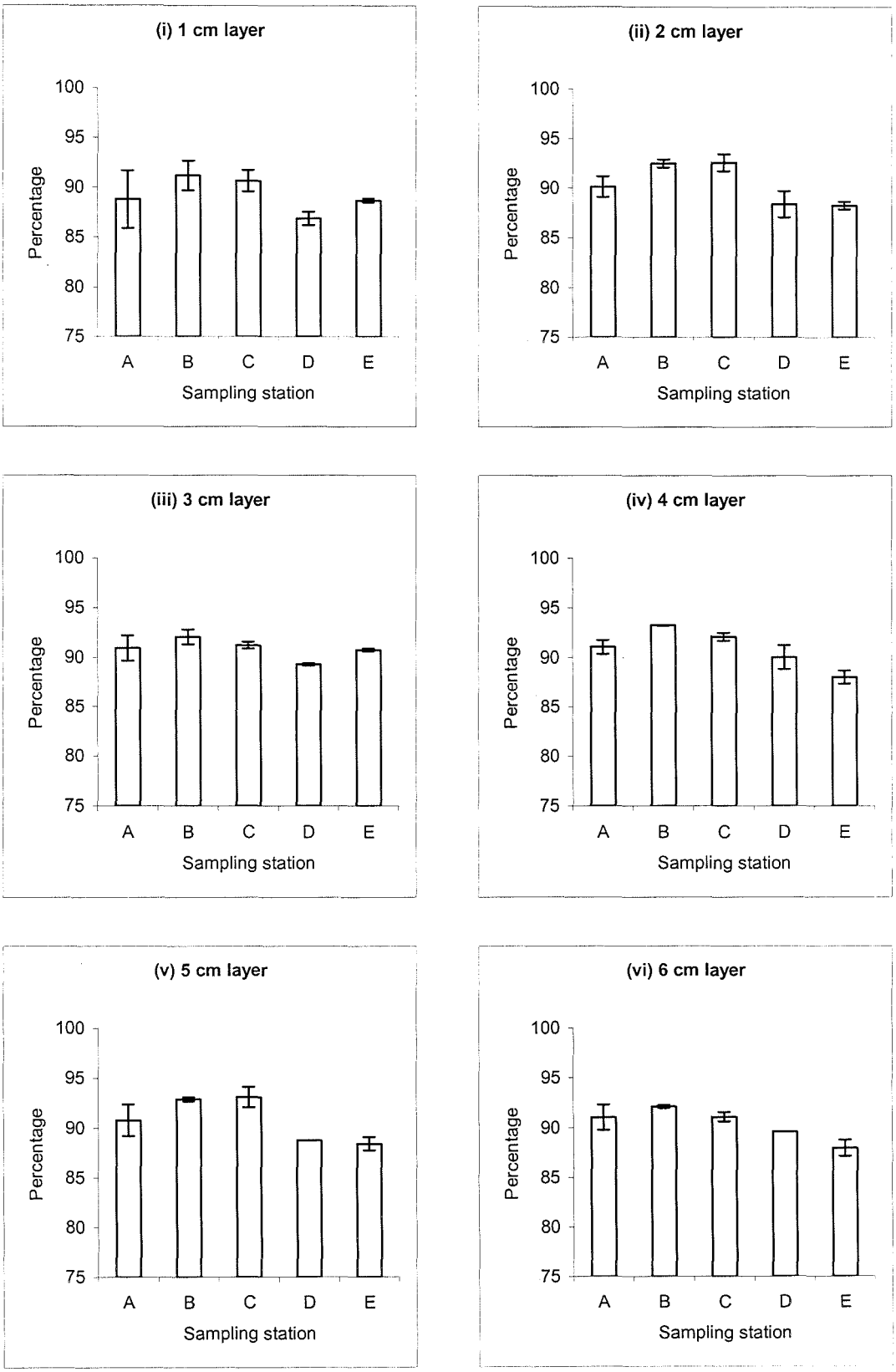

Figure 4.5 (i – vi) Site S: The percentage sediment < 63μm with depth at each sampling station

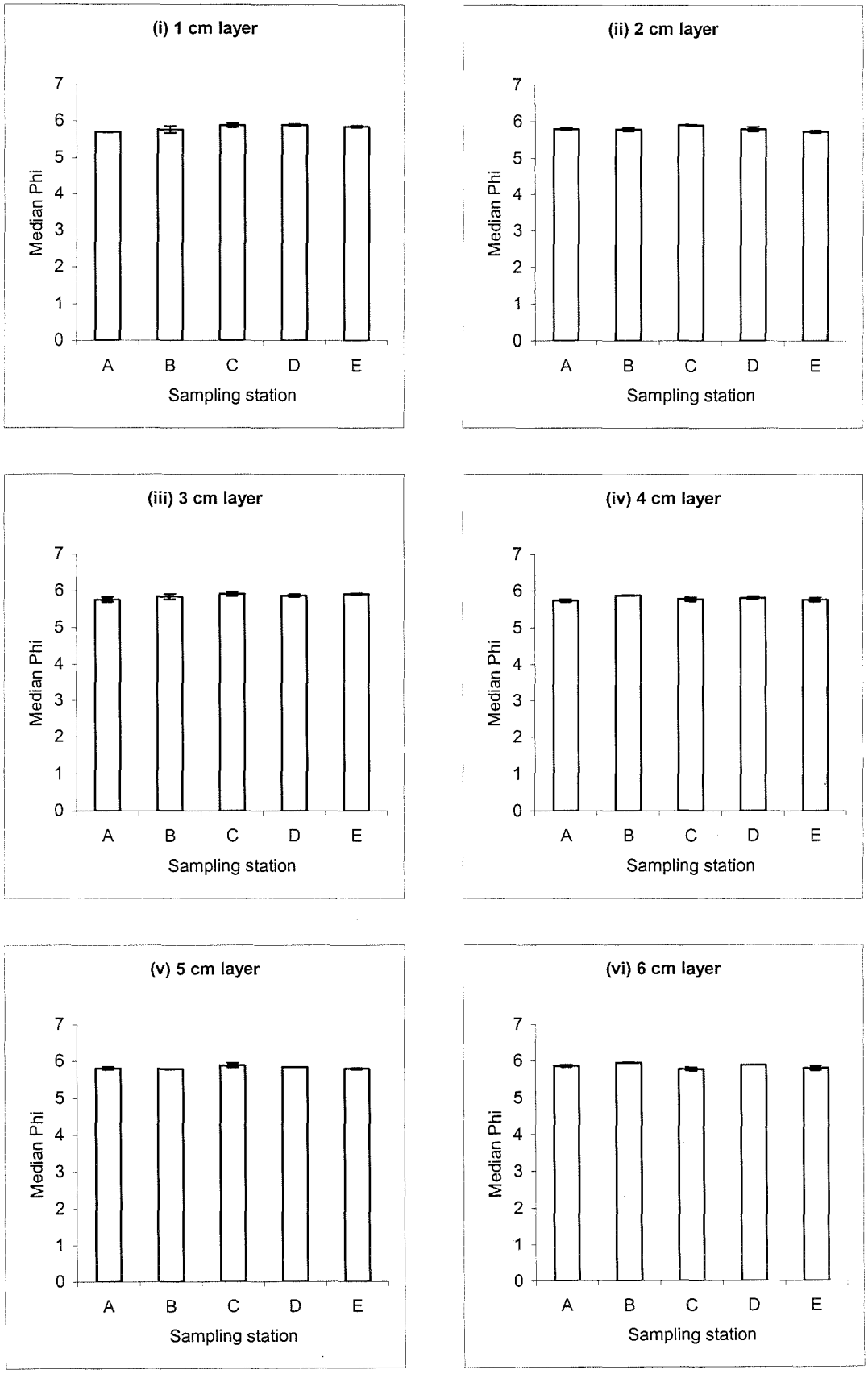

Figure 4.6 (i – vi) Site S: The sediment median phi value with depth at each sampling station

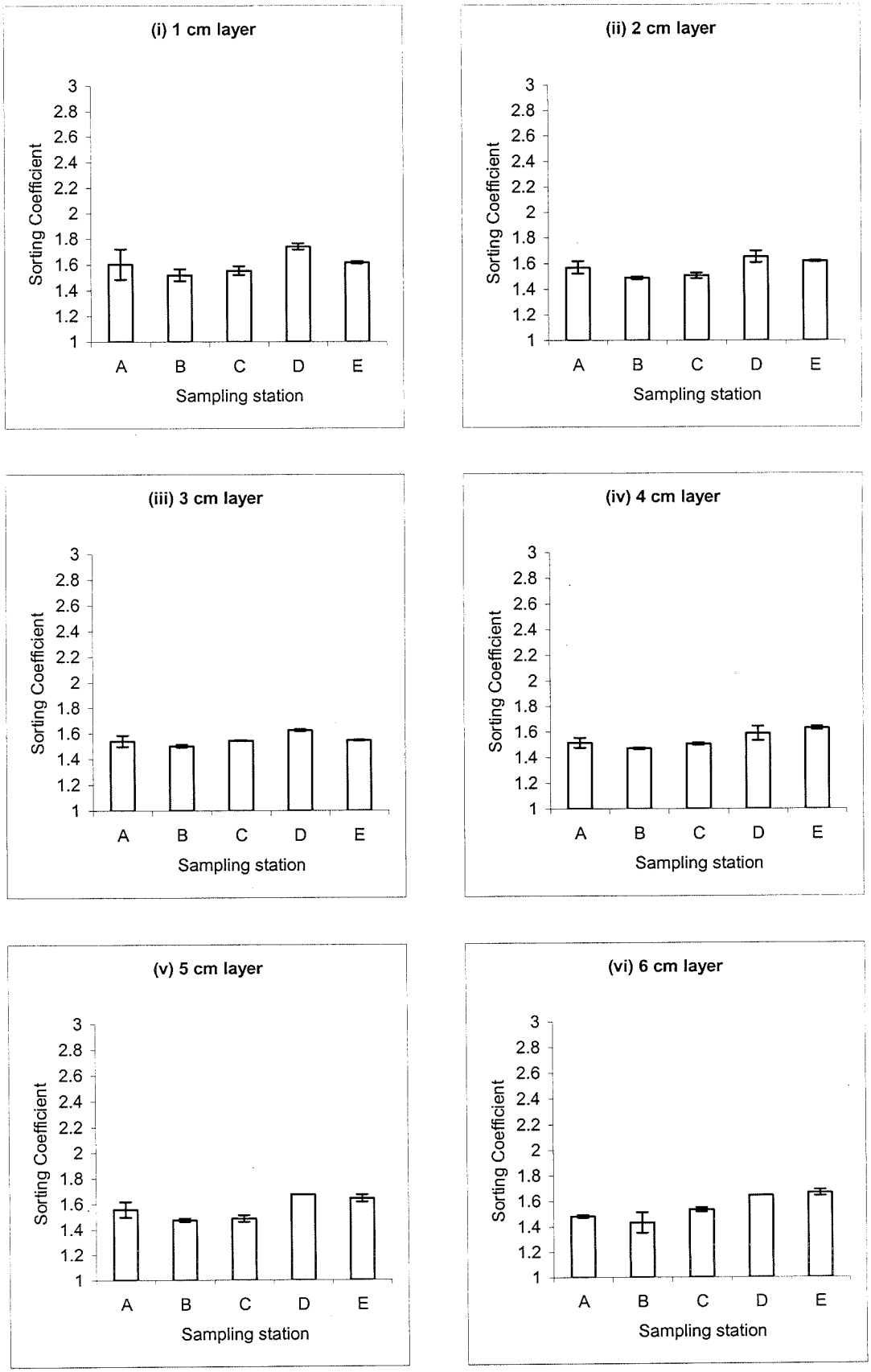

Figure 4.7 (i – vi) Site S: The sediment sorting coefficient value with depth at each sampling station

with subsequent decreases (increase for sorting coefficient) at stations C and D. The values at station E were comparable to those recorded at station A. Significant differences were not observed between stations for the < 63 μm fraction and median phi values (Figures 4.5 i - vi and 4.6 i – vi). However, the sorting coefficient value recorded at station B was significantly less than at station D (Figure 4.7 i – vi).

There was a significantly greater proportion of fine sediment at stations B and C than at station E at the 4 cm layer (Figure 4.5 i – vi). Comparable trends were observed between all measured variables at this depth and those of the sediment depth layers above with peaks in the proportion of sediment < 63 μm, median phi (Figure 4.6 i – vi) and sorting coefficient values (Figure 4.7 i – vi) occurring at station B.

Similar trends in the data were observed at the 5 cm and 6 cm layers, with the variables at a maximum (< 63 μm fraction, median phi value) or minimum (sorting coefficient) at the intermediate stations (B or C). However, significant differences were not observed between the stations at these sediment layer depths for the measured variables.

The data were also examined for differences in particle size within cores. There were no apparent trends in the data, indicating that the surficial layer was not different from the rest of the cores.

4.1.4 Sediment Carbon and Nitrogen

The distribution of the sediment organic carbon and nitrogen concentrations closely followed the trend observed in the < 63 μm fraction and median phi value in the particle size analysis as described in section (4.1.3). In general, particularly for the upper layers of sediment (1 – 3 cm), there was an increase in the concentration of both parameters from station A to B, followed by a marked decrease at stations C and D. The concentrations at station E were usually greater than those found at station D. Results for all carbon and nitrogen elemental analysis variables are presented in Appendix 3 - Site S.

The percentage organic carbon concentration in the surficial sediment (1 cm layer) fluctuated between a maximum at station B and minimum at station D. The concentration at stations A, B and C were significantly greater than at station D (Figure 4.8 i – vi). Similar trends were observed in the nitrogen concentration of the sediment, with the greatest concentration recorded at station B. The nitrogen concentration at station C was significantly greater than at station D (Figure 4.9 i – vi). There was a general (non–significant) decrease in the carbon/nitrogen ratio from station A to station E (Figure 4.10 i – vi).

Within the 2 cm layer, the organic carbon concentration was similar at stations A, B and C (all ~ 3.20 %). A marked decrease in concentration was observed at station D, where concentrations were significantly different to those recorded at stations A and C (Figure 4.8 i – vi). A similar trend was observed in the sediment nitrogen concentration (Figure 4.9 i – vi), however, no significant differences between the stations were observed. The carbon/nitrogen ratios at this sediment depth (Figure 4.10 i – vi) were significantly greater at stations A and B than at stations D and E. A general decrease in this parameter was observed with distance from the farm site.

Similar trends in organic carbon and nitrogen concentrations were observed at 3 cm sediment depth. A marked decrease in carbon concentration was observed at station D (Figure 4.8 i – vi). The sediment nitrogen concentrations (Figure 4.9 i – vi) fluctuated between station E (maximum) to an anomalous minimum at station B, however, significant differences were not recorded for this variable. The carbon – nitrogen ratios were significantly greater at station A than station D and also at station B than at stations D and E (Figure 4.10 i – vi).

The organic carbon and nitrogen concentration distribution trends recorded in the upper layers (1 – 3 cm) of the sediment were also observed throughout the sediment depth (4 – 6 cm layers). However, these trends became less distinct with depth and no significant differences were recorded between stations for these variables.

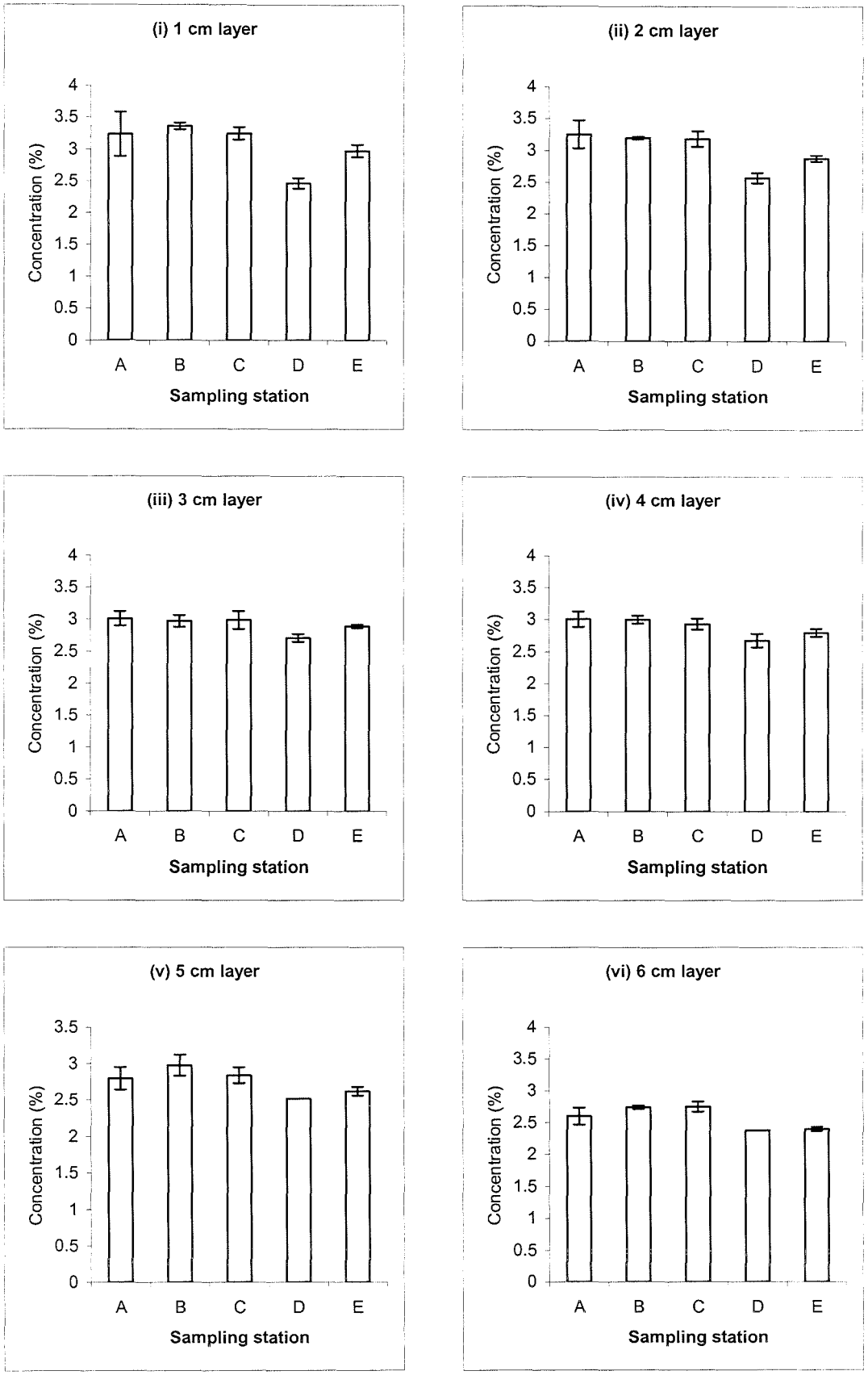

Figure 4.8 (i – vi) Site S: The percentage carbon content of the sediment with depth at each sampling station

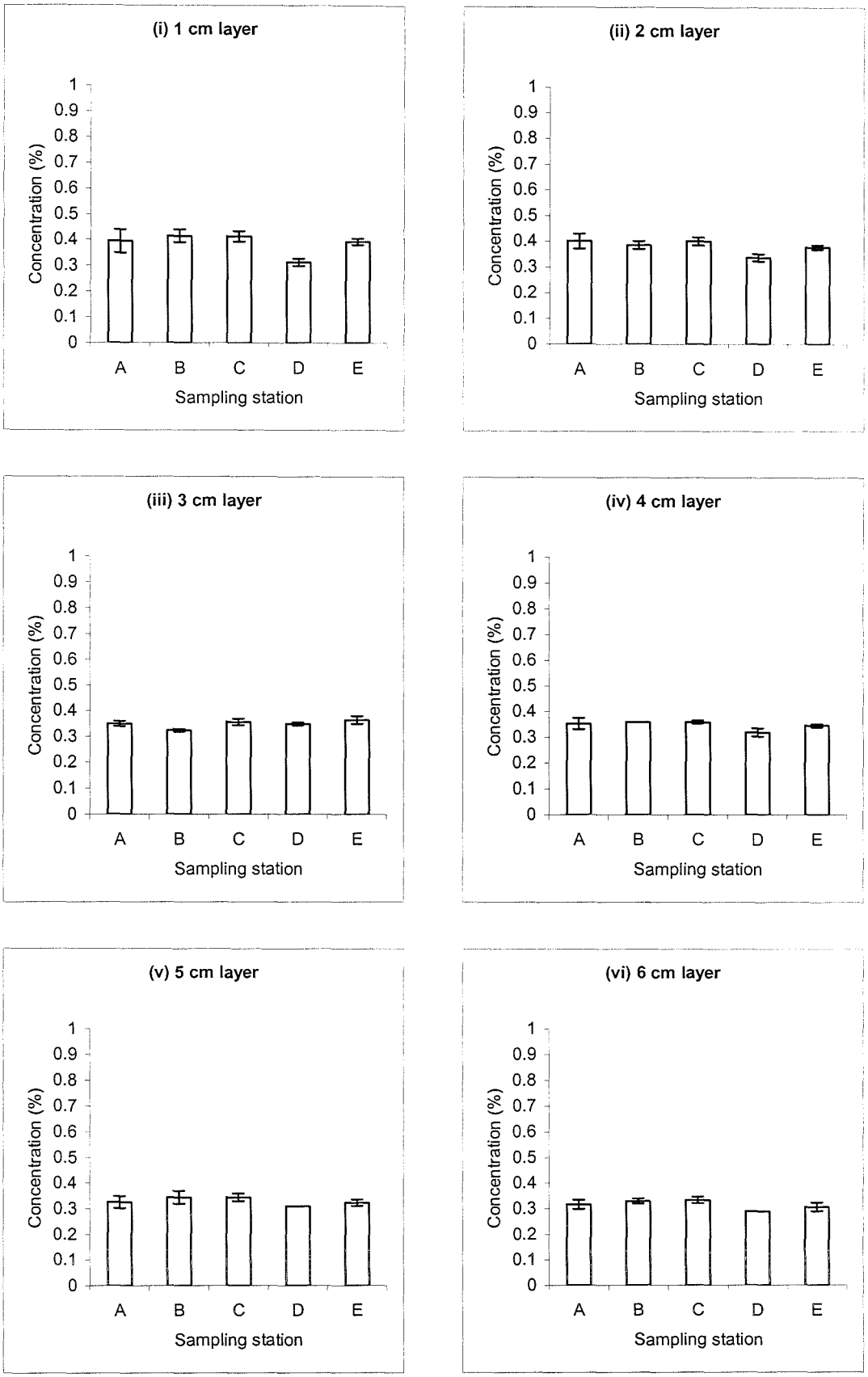

Figure 4.9 (i – vi) Site S: The percentage nitrogen content of the sediment with depth at each sampling station

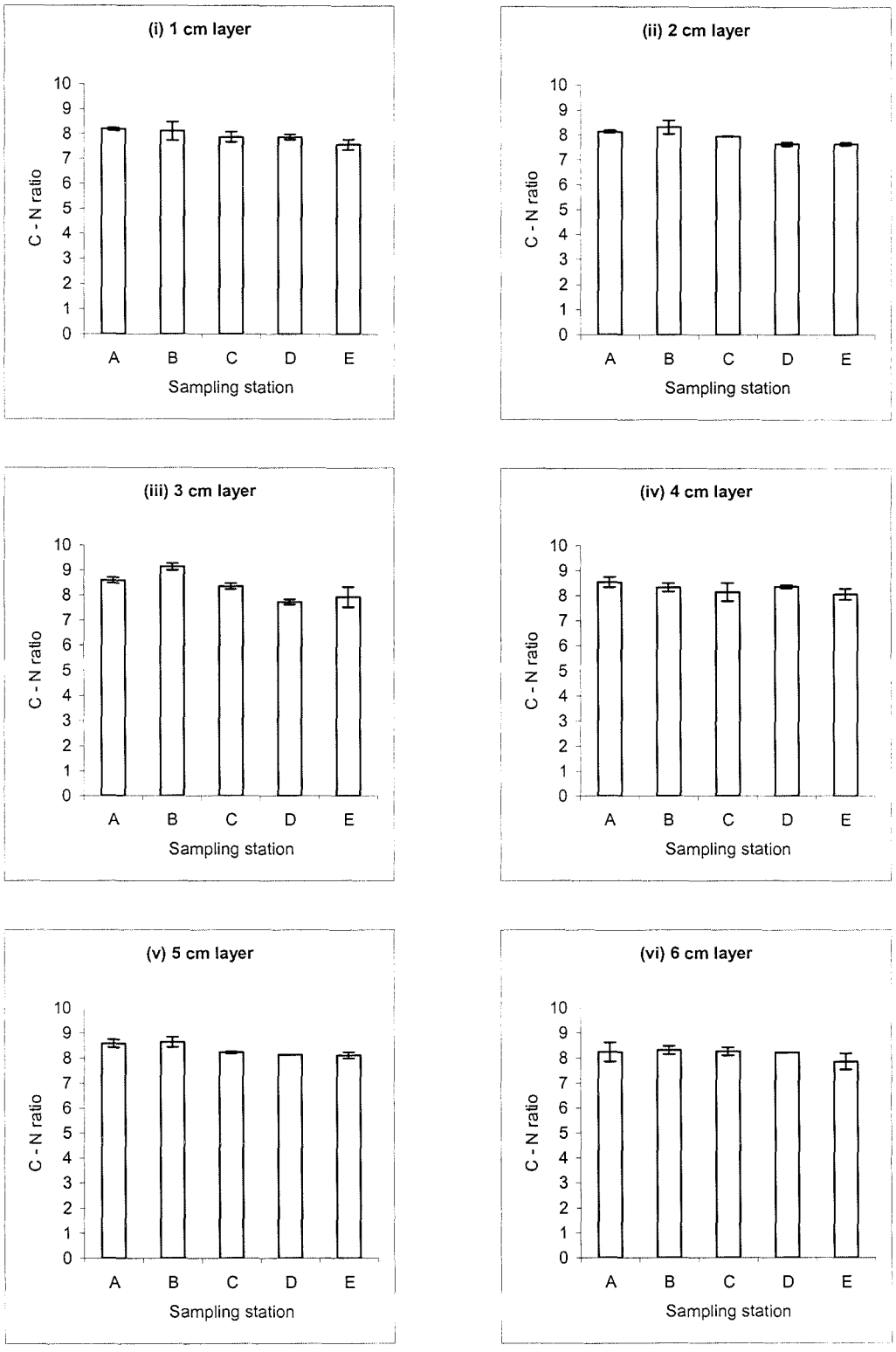

Figure 4.10 (i – vi) Site S Carbon to Nitrogen ratio with depth at each sampling station

4.1.5 Benthic Community Structure

A total of 44 species were identified at this site, comprising 932 individuals (complete species/abundance matrix is presented in Appendix 3 - Site S). The five most abundant species at each station are presented in Table 4.2 together with the percentage of the total number of individuals they represent.

Table 4.2 : Top five ranked species (abundance), numbers and percentage of total across stations at Site S.

		N	%			N	%
A	Nematode spp.	89	42.2	B	Nematode spp	72	37.7
	Tharyx killariensis	20	9.48		*Prionospio fallax*	49	25.7
	Prionospio fallax	20	9.48		*Sphaerosyllis erinaceus*	15	7.85
	Capitella capitata	13	6.16		*Tharyx killariensis*	10	5.24
	Ophryotrocha hartmanni	12	5.69		Bivalve (A) spp.	5	2.62
		Total	73.01			Total	79.11

C	Nematode spp	180	60.8	D	Nematode spp	42	36.8
	Prionospio fallax	33	11.1		*Prionospio fallax*	22	19.3
	Sphaerosyllis erinaceus	24	8.11		*Melinna palmata*	13	11.4
	Bivalve (B) spp.	17	5.74		Bivalve (B) spp	8	7.02
	Prionospio spp.	13	4.39		*Sphaerosyllis erinaceus*	6	5.26
		Total	90.14				79.78

		N	%
E	Nematode spp	32	26.7
	Prionospio fallax	31	25.8
	Bivalve (B) spp.	19	15.8
	Copepod spp.	17	14.2
	Bivalve (A) spp.	9	7.5
		Total	67.0

The dominant taxa were made up of nematode and the polychaetes *Prionospio fallax* [Soderstrom, 1920] and *Sphaerosyllis erinaceus* [Claparéde, 1863], both of which were ubiquitous. The bivalve *Abra alba* (W Wood, 1802) was present at stations C, D and E

but only one specimen was recovered from station B and none at station A. The polychaete *Tharyx killariensis* (Southern, 1914) was more abundant at stations A and B than those further away from the culture site. The macrofauna recorded at all sampling stations were typical of those associated with the similar soft, fine muddy sediment types.

4.1.5.1 Univariate Analysis of Community Structure

Similarities between the stations, in the number, type and distribution of animals recorded, were observed. Analysis of the indices derived from the species/abundance data matrix revealed no significant differences between the stations, as measured by the Shannon-Wiener index (*H'* $\log_2$), Margalef's species richness (d) and Pielou's evenness index (*J'*) (Table 4.3).

Table 4.3 : Univariate analysis of the benthic community structure at Site S.

Univariate measure/index	Sampling Station				
	A	B	C	D	E
Number of Individuals	211	191	296	114	120
Number of Species	24	26	18	21	11
H' $\log_2$	2.223	2.103	1.503	2.128	1.859
J'	0.6995	0.6455	0.52	0.699	0.7751
d	4.298	4.76	2.988	4.223	2.089

4.1.5.2 Multivariate Analysis of Community Structure

The complete species/abundance matrix was used for multivariate analyses (Appendix 3 - Site S). The dendrograms produced by hierarchical agglomerative clustering, together with the 2-dimensional ordination plots produced by non-metric MDS of the resulting community are presented in Figures 4.11 and 4.12. The stress value associated with this MDS ordination was '0.24'. Although there is no critical cut-off value for stress values above which a species matrix cannot be represented adequately in a 2-dimensional MDS plot, a low stress value is desirable. Warwick and Clarke (1994) suggest that stress values between 0.1 – 0.2 give 'only potentially useful 2-dimensional pictures'. Under these circumstances, they recommend that the MDS plot should be complemented with other techniques such as clustering. Therefore, the dendrogram (Figure 4.11) should be used to

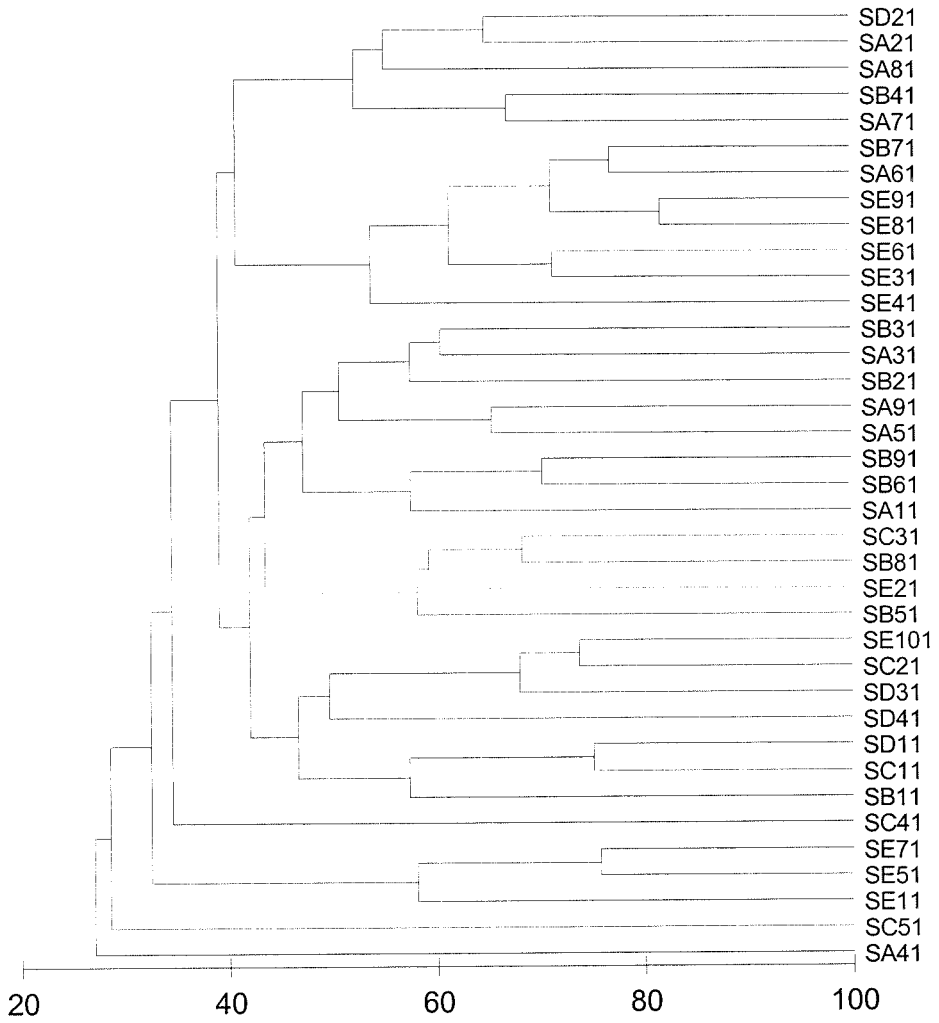

Figure 4.11 Dendrogram of all replicates at each station at Site S, using group-averaged clustering from Bray Curtis similarities on root-transformed abundances.

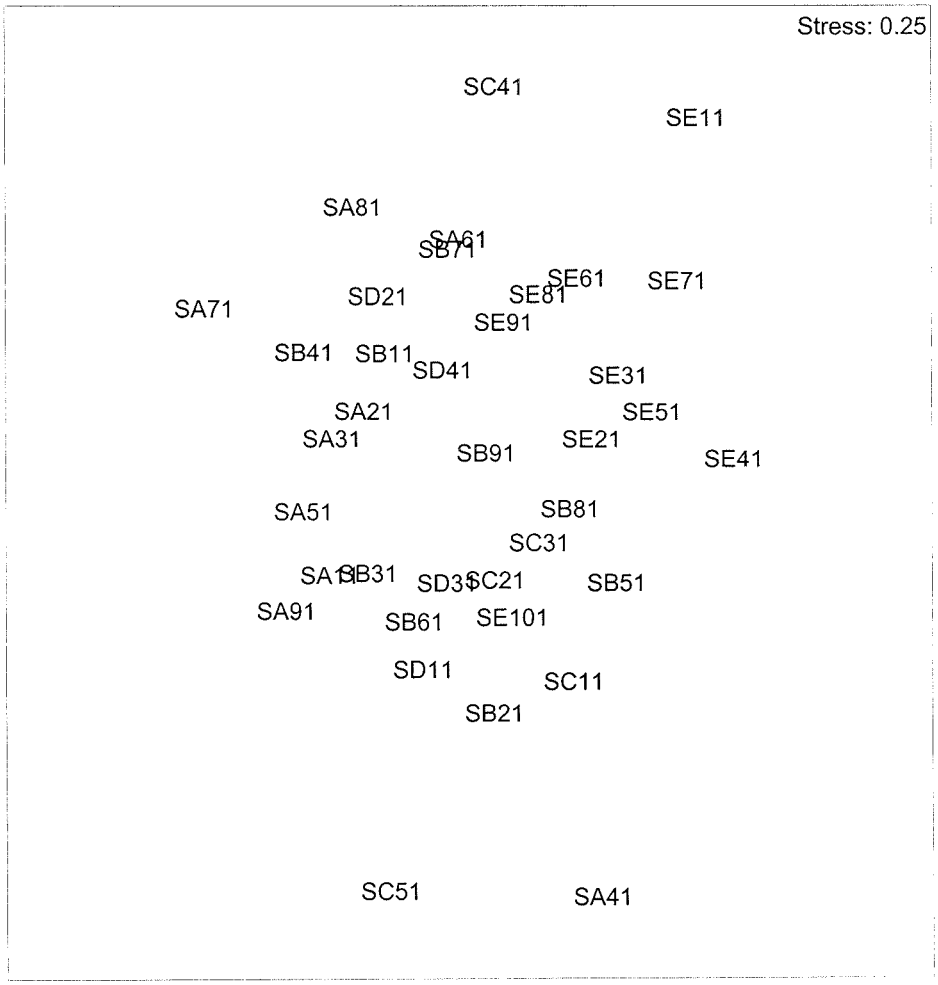

Figure 4.12 Two-dimensional ordination plot of all replicates at each station at Site S.

aid in the interpretation of the MDS plot. However, superimposition of the cluster groups at arbitrary levels from the dendrograms onto the ordination plots, as outlined by Warwick and Clarke (1994), was not performed since this tends to add discrete subdivisions onto a community continuum.

Using arbitrary cut-off values, the groups can possibly be separated into 'near farm' and 'away from farm' groups. Lines have been superimposed on the MDS plots indicating these groups, however, these plots suggest that there is very little difference between the benthic community structure with distance from the farm site. These were statistically analysed by One-way ANOSIM tests. Significant differences in the community structure between sampling stations were not observed.

4.1.5.3 Infaunal Trophic Index

A reduced species/abundance matrix was used for ITI analysis containing 843 individuals. This was because some of the species identified were not benthic polychaetes and therefore not included in the calculations. The ITI scores for each station are presented in Table 4.4.

Table 4.4 : Number of individuals in each of the trophic groups and the resultant ITI score at each station at Site S.

Number of individuals in trophic group:	Station				
	A	B	C	D	E
1	0	1	0	2	0
2	48	40	44	16	0
3	35	63	48	39	40
4	122	79	183	48	35
ITI	21.38	26.67	16.57	24.52	17.86

The ITI values calculated at this site ranged between 26.67 and 16.57. These values suggest that the whole area is stressed and that there is no difference in the benthic infaunal structure between the near farm sites and those at a greater distance. Consequently, there does not appear to be any measurable near field effect from the farm.

4.2 Site A

4.2.1 Water Currents

Comprehensive analyses of the hydrographic data collected at Site A are presented in Appendix 3 - Site A. A summary of the hydrographic data collected at Site A is presented in Figure 4.13 (a and b) for the surface current data and Figure 4.14 (a and b) for the bottom current data. The hydrographic measurements revealed the site to be poorly flushed, with the majority of current velocity measurements < 0.03 m s^{-1} (Table 4.5).

Table 4.5 : Hydrographic characteristics at Site A.

	Surface	Bottom
Mean Current Velocity (cm s^{-1})	3.11	3.14
Residual Current Velocity (cm s^{-1})	1.25	0.75
Residual Current Direction (deg)	52	277

Surface currents were recorded in all directions. A high proportion of stronger velocity recordings being observed along a north-east/south-west axis, with the strongest and greatest occurrence being in a north-easterly direction (Figure 4.13 b). Current speeds at the surface reached a maximum of 0.12 ms^{-1} at periods at spring tide. The frequency histogram (Figure 4.13 a) illustrates that a high proportion (55.53%) of flows were < 0.03 ms^{-1} and 28.6% were within the 0.03 – 0.05 ms^{-1} bin. As suggested by the residual plot (Appendix 3 - Site A), the most frequent direction of flow was towards the north-east.

Seabed currents were similar in velocity to the surface data (Figure 4.14 a and b). However, the majority of current direction measurements were to the south-west. 53.31% of the readings were between zero and 0.03 ms^{-1} and 25.87% within the 0.03 – 0.05 ms^{-1} bin. The maximum current velocity recorded was 0.11 ms^{-1}. The residual flow plot (Appendix 3 - Site A) shows a general bottom water movement towards the southwest.

a)

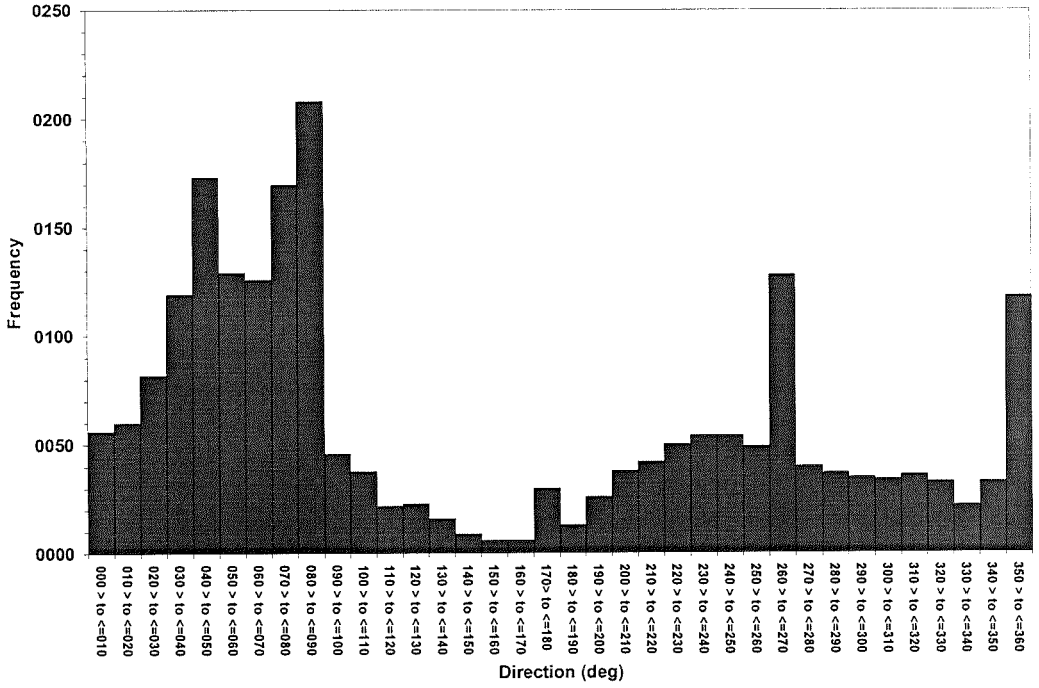

b)

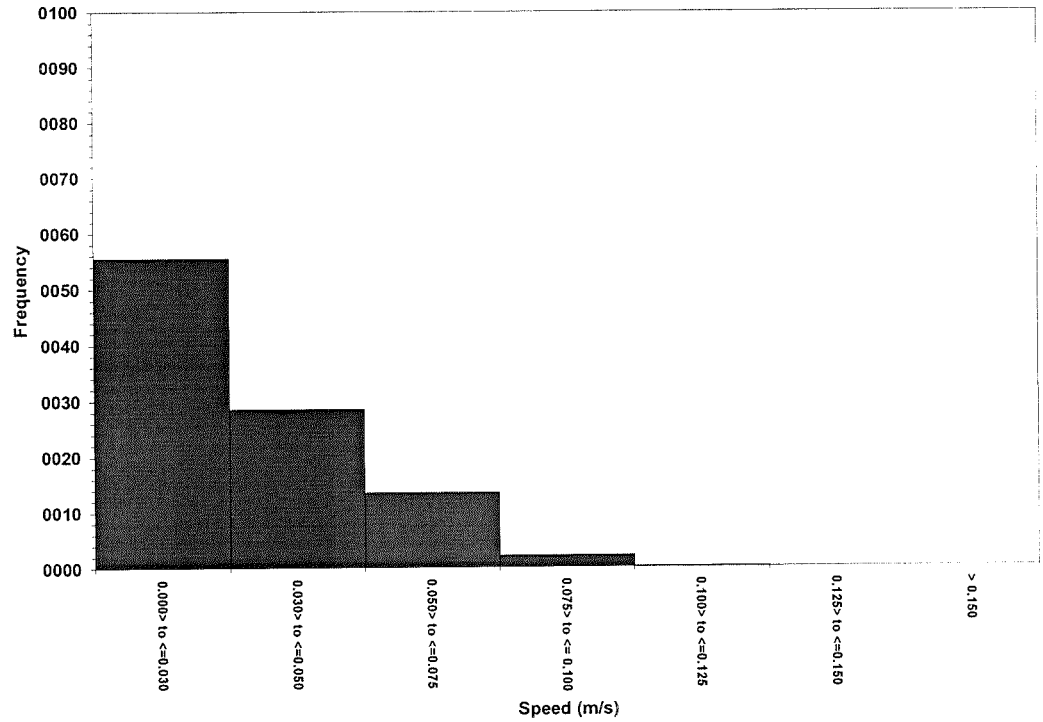

Figure 4.13 a and b Site A Surface current direction and velocity frequency histograms

a)

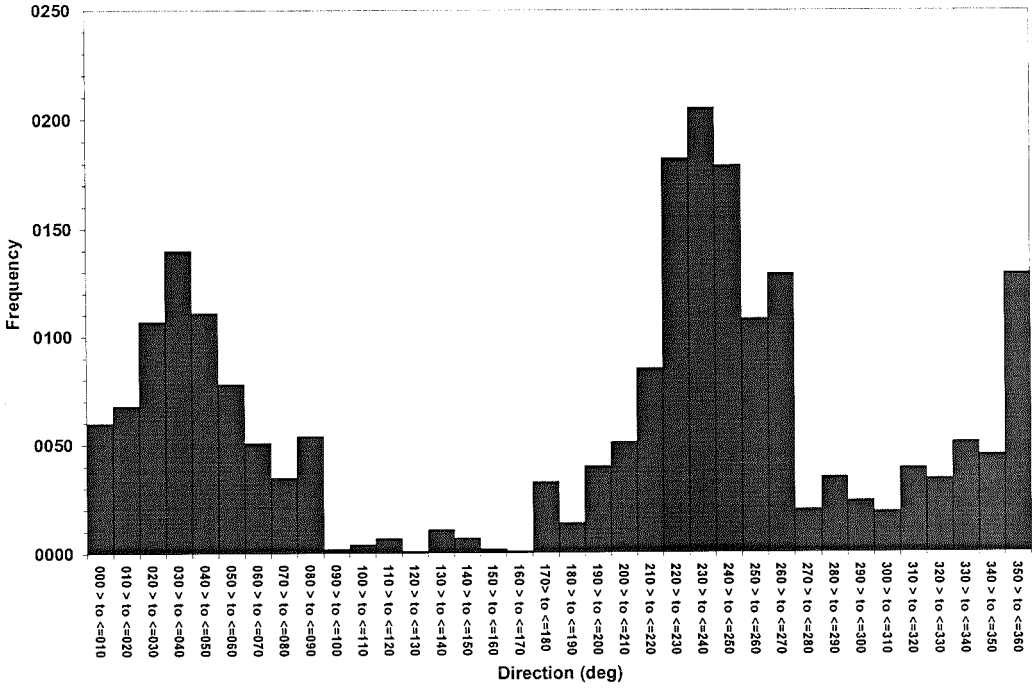

b)

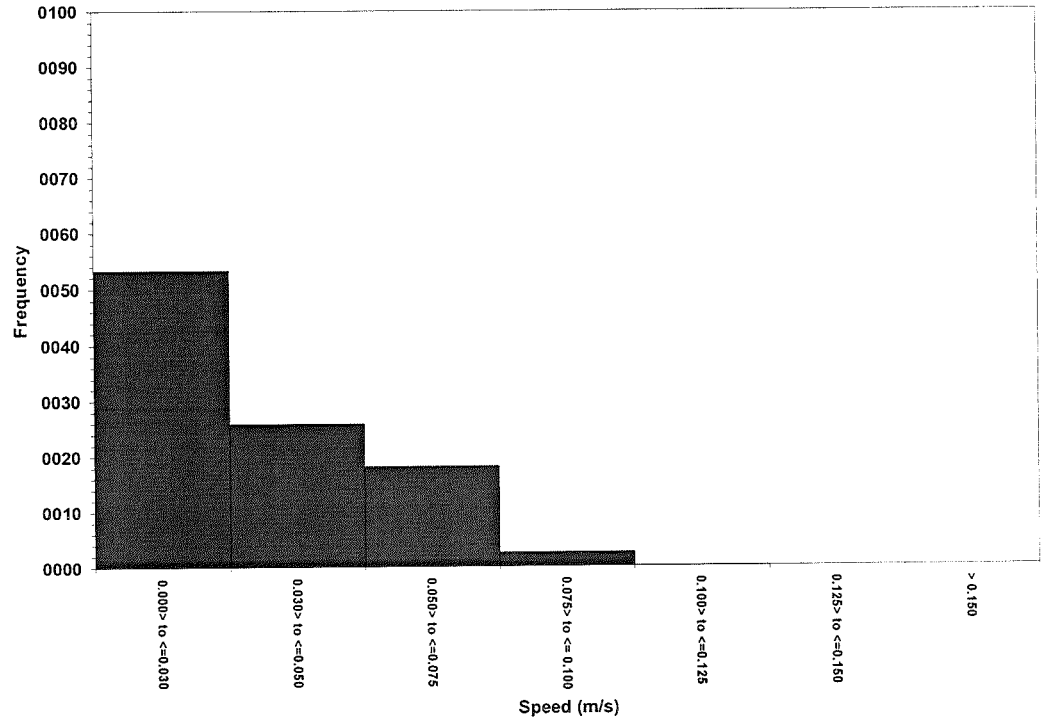

Figure 4.14 a and b Site A Bottom current direction and velocity frequency histograms

Overall, current movement at the site was predominantly tidally driven with a clear diurnal tidal cycle illustrated in the direction time series plot (Appendix 3 - Site A).

4.2.2 Sediment Redox

The sediment Eh values remained positive at each sampling station throughout the depths of sediment sampled (Figures 4.15 i – iv). The Eh profiles at stations B, C and D were clustered, suggesting little difference in the organic/particulate loading between the areas. Maximum Eh values were recorded at station A, closest to the farm site, both at the surface and throughout the sediment depth.

There was no distinct sediment RDL at any of the stations, with a gradual decrease in Eh over the surficial 2 cm layer at stations B, C and D and throughout the whole 6 cm sampling depth at station A. At all stations, the surficial layer Eh values were all in excess of +400 mV, whilst the minimum Eh value recorded was at the deepest sediment layer (6 cm) approximately + 100 mV.

In the 1 cm layer, there were distinct decreases in Eh values at stations B, C and D from the surface values. Such a decrease was not observed at station A where redox potentials remained in excess of +300 mV. At the 2 cm layer, stations B, C and D were at approximately +100 mV. Eh values at these stations did not vary significantly for the remaining core depth. Station A values gradually decreased with depth and was +100 mV at 5 cm and 6 cm layers.

4.2.3 Granulometry

Particle size analysis described the sediment at this site as generally poorly sorted medium to fine silt, with a distribution that was symmetrical or finely skewed and mesokurtic. The sediment was homogenous throughout the sediment depth at all stations sampled. Marginal fluctuations in the sediment characteristics were observed at this site; however, no significant differences between the stations were recorded for the measured variables.

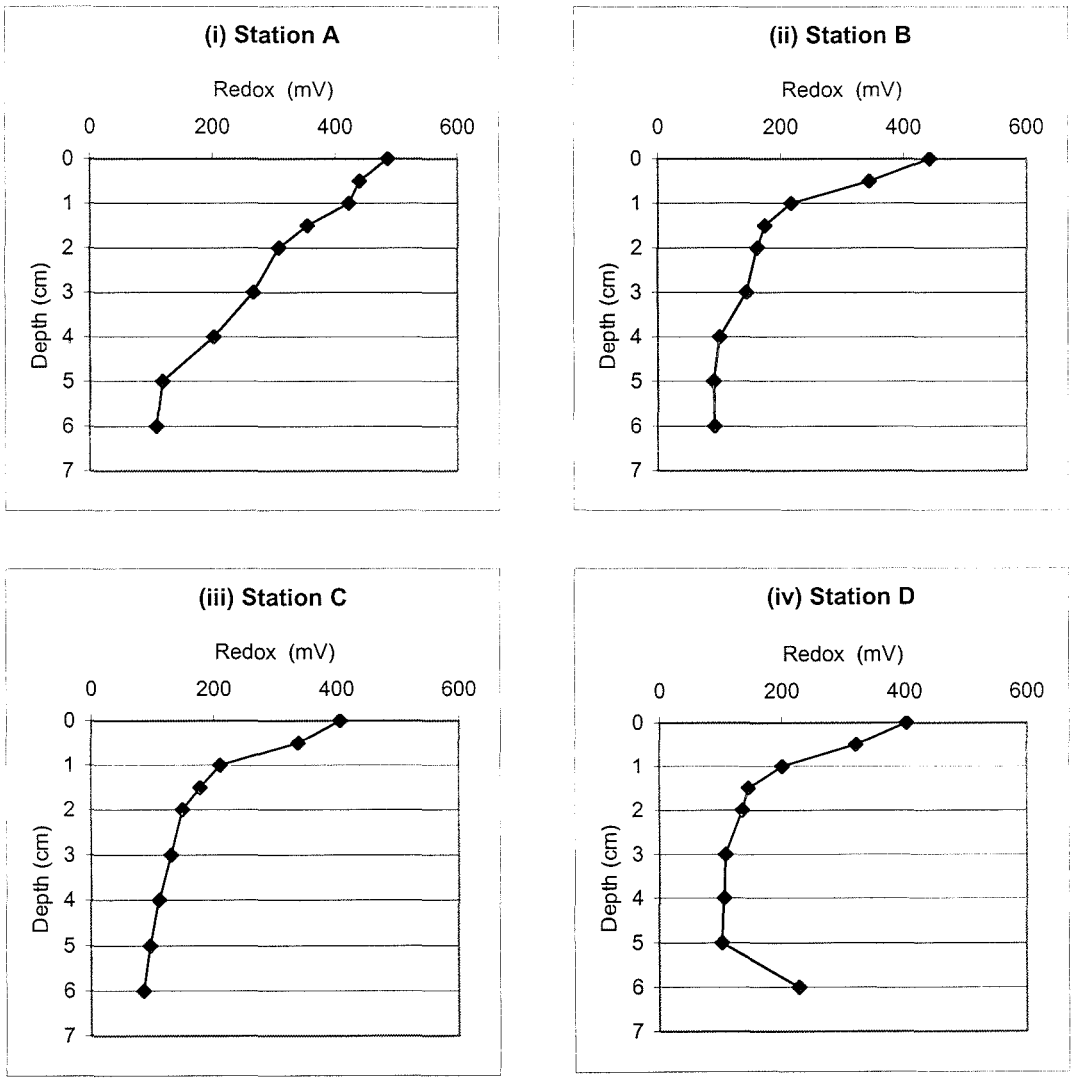

Figure 4.15 (i – iv) Site A Redox potential (mV) with depth at each sampling station

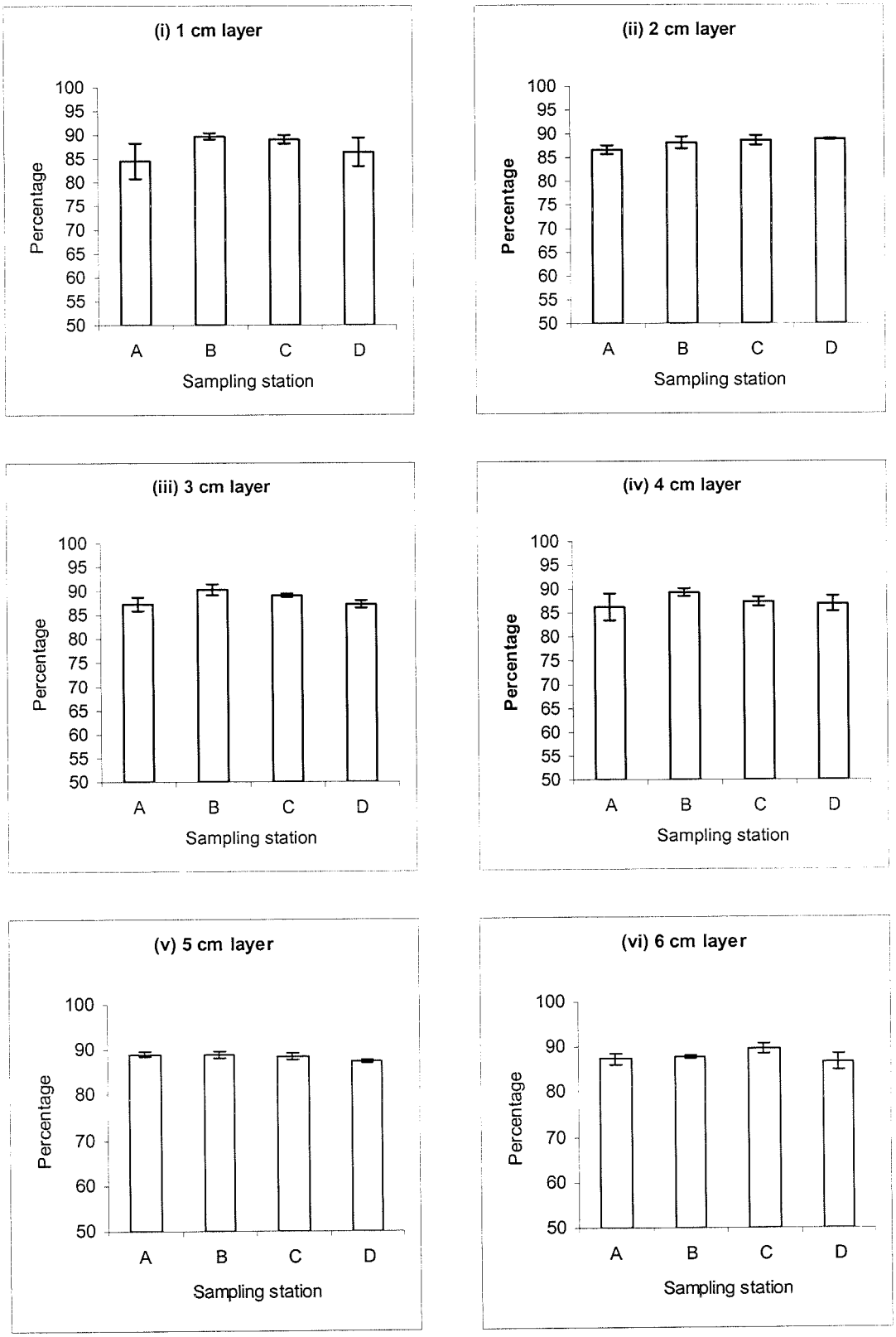

Figure 4.16 (i – vi) Site A: The percentage sediment < 63μm with depth at each sampling station

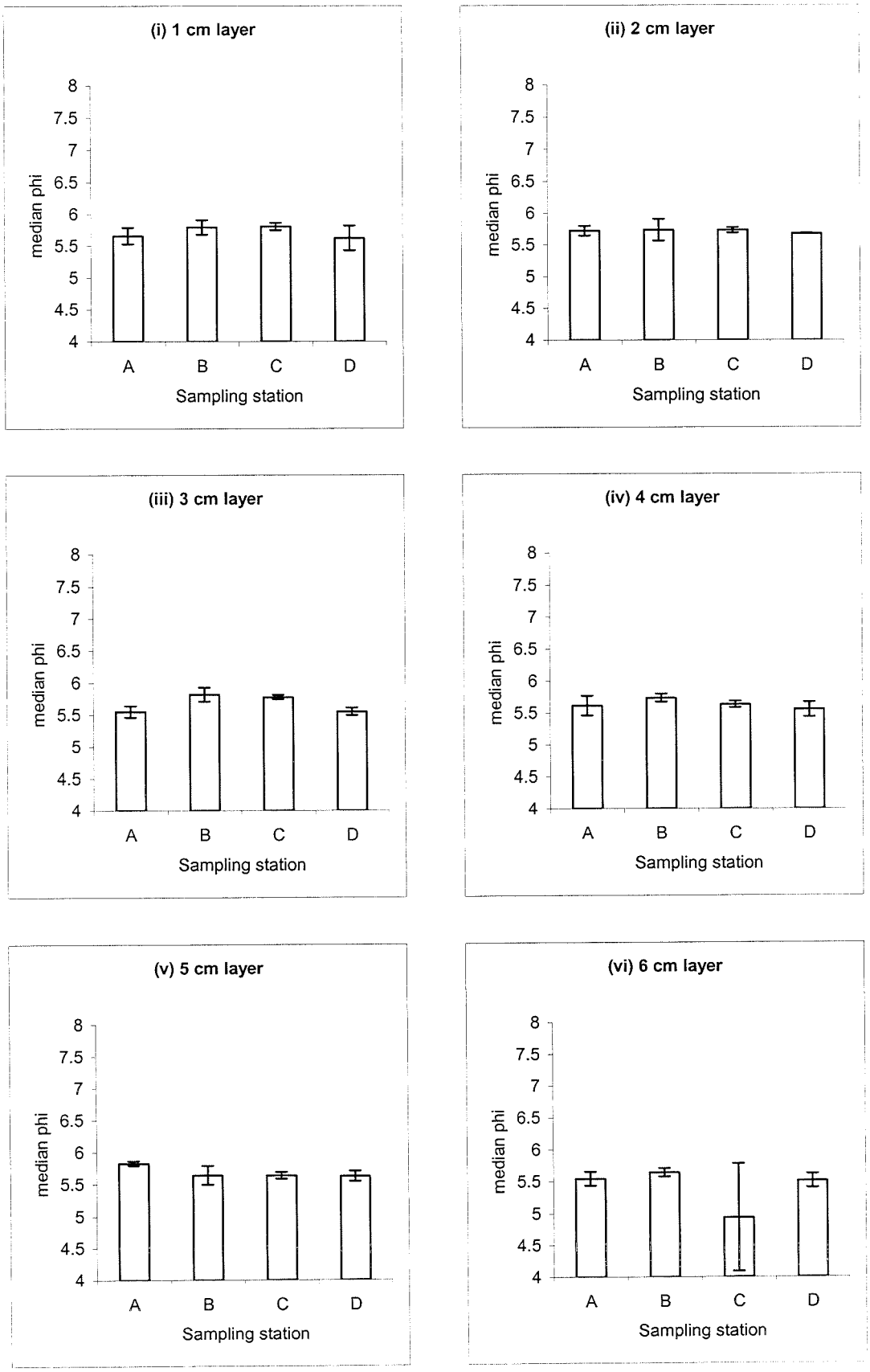

Figure 4.17 (i – vi) Site S: The sediment median phi value with depth at each sampling station

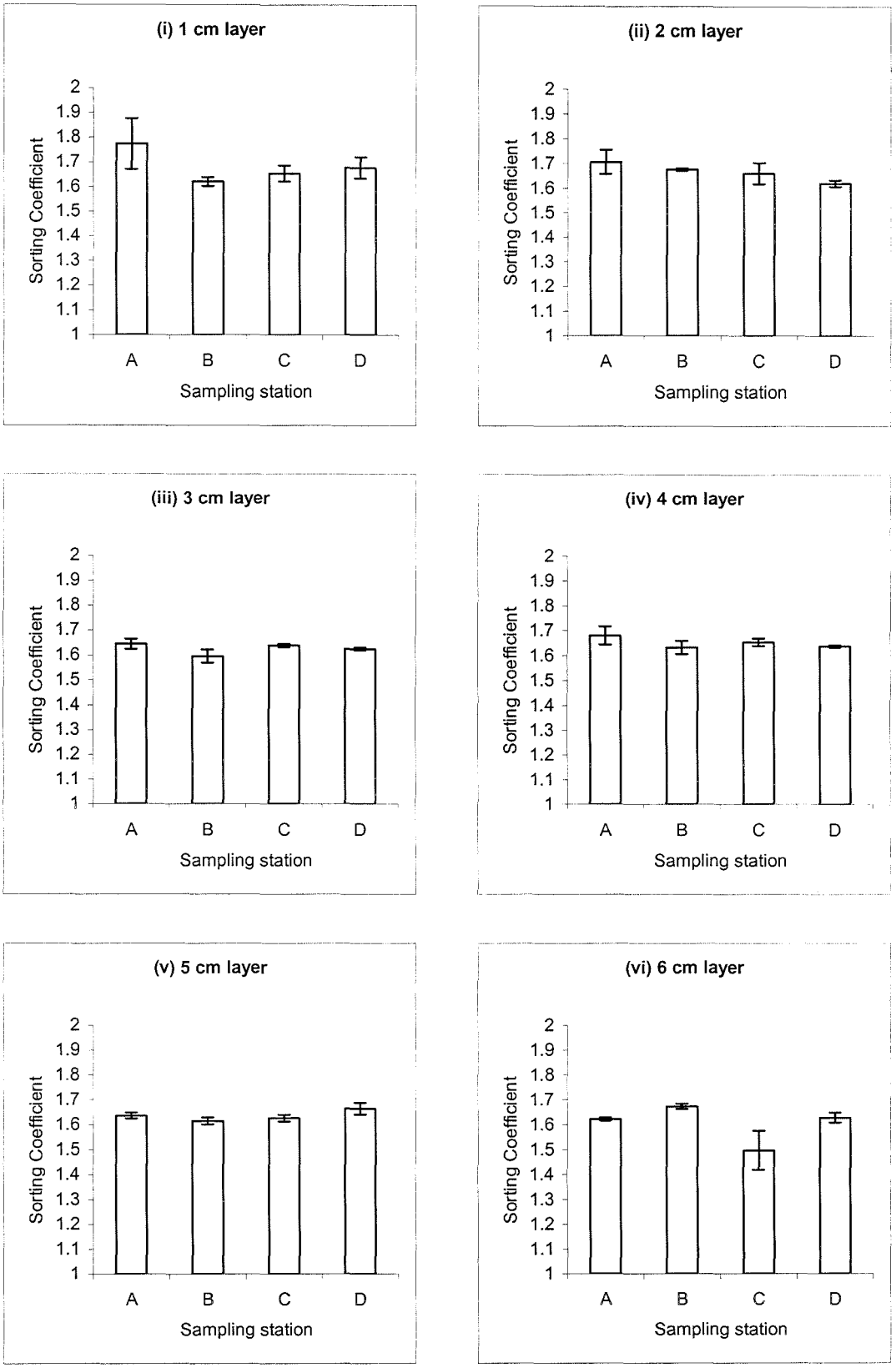

Figure 4.18 (i – vi) Site A: The sediment sorting coefficient value with depth at each sampling station

There was a tendency throughout the sediment depth for the <63 μm fractions and median phi values to be greater at stations B and C. This trend was not as noticeable for the sorting coefficient variables. There were no significant differences between the measurements of sediment variables for any of the layers (surficial 1cm to 6 cm depth) as described by percentage < 63 μm (Figure 4.16 i – vi), median phi value (Figure 4.17 i – vi) and sorting coefficient (Figure 4.18 i – vi). The calculated variables and sediment descriptors for this site are presented in Appendix 3 - Site A.

The percentage of fine sediment (< 63 μm) in the surficial layer (1 cm) ranged between 84.53% ± 3.72 at station A to 89.70% ± 0.64 at station B (Figure 4.16 i). The proportion of fines and the median phi values were elevated, and sorting coefficient depressed, at stations B and C compared to stations A and D.

Within the 2 cm layer, there was a marginal increase in the proportion of fine sediment from station A to station D (Figure 4.16 ii). This trend was not observed for the median phi values (Figure 4.17 ii) which remained constant (~ 5.70) at all stations. Slight decreases in the sorting coefficient values were observed with distance from the farm (Figure 4.18 ii).

At the 3 cm layer, the percentage < 63 μm fraction and median phi values were greatest at the intermediate stations (B and C) (Figures 4.16 and 4.17 iii). A reciprocal trend was observed in the sorting coefficient values (Figure 4.18 iii). Similarly, these trends in the sediment particle size characteristics were also observed at the deeper layers of the sediment, however significant differences between stations were not observed.

4.2.4 Sediment Carbon and Nitrogen

There was a general increase in the sediment organic carbon and nitrogen concentrations of the sediment, throughout the sediment depth, with distance from the farm site. There was no obvious trend in the carbon/nitrogen ratios throughout the sediment depth, with

the values fluctuating between replicates and stations. Results for all carbon and nitrogen elemental analysis at this site are presented in Appendix 3 - Site A.

In the surficial sediment (1 cm layer), there was an increase in both the organic carbon and nitrogen concentrations of the sediment from station A to station C (Figures 4.19 i and 4.20 i). This trend continued in the sediment nitrogen concentration for station D, but a decrease was observed in the organic carbon concentration. There was a general decrease in the carbon – nitrogen ratio (Figure 4.21 i) with distance from the farm. However no significant differences were observed between any of the stations for these variables.

Similarly, at the 2 cm layer, the sediment organic carbon and nitrogen concentrations of the sediment generally increased with distance from the farm site (Figures 4.19 ii and 4.20 ii). The carbon/nitrogen ratio (Figure 4.21 ii) was maximal at station A (7.61 ± 0.20) decreasing to around 7.00 at stations B, C and D.

A slight increase in sediment organic carbon concentration was observed at the 3 cm layer with distance from the farm. However, the sediment nitrogen concentration did not reveal any such trend with marginal fluctuations being recorded with distance from the farm site (Figures 4.19 iii and 4.20 iii). The carbon/nitrogen ratio increased from station A to C (Figure 4.21 iii), but significant differences were not recorded.

Within the 4 cm sediment depth, there was an increase in the organic carbon and nitrogen content with distance from the farm. The sediment nitrogen content was significantly different between station A and stations C and D. The carbon/nitrogen ratios remained approximately constant at all sample stations.

There were general increases in the organic carbon and nitrogen concentrations of the 5 cm and 6 cm (Figures 4.19 v-vi and 4.20 v-vi) sediment layers with distance from the farm. The organic carbon concentration at the 5 cm layer at station D was significantly greater than at stations A and B.

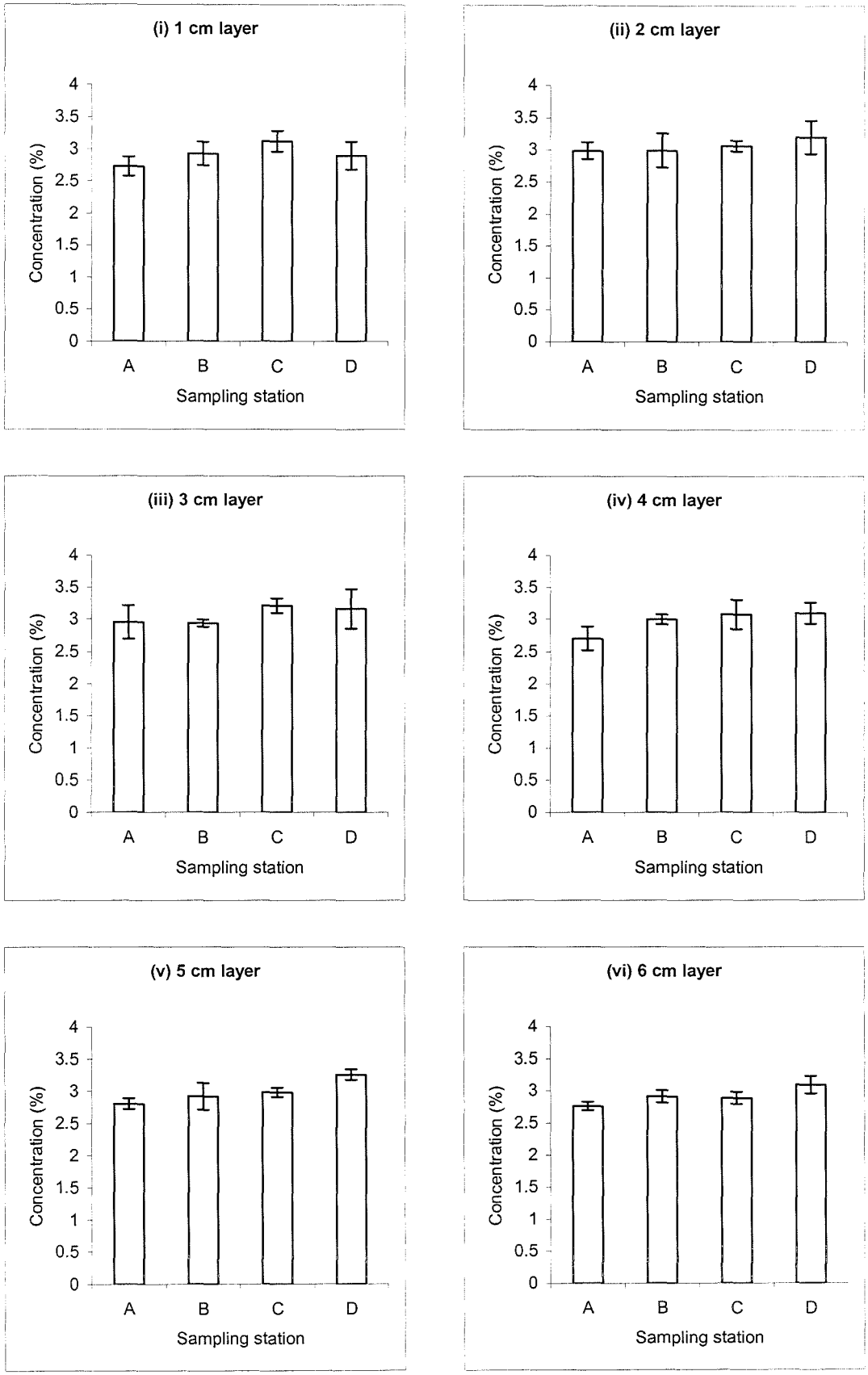

Figure 4.19 (i – vi) Site A: The percentage carbon content of the sediment with depth at each sampling station

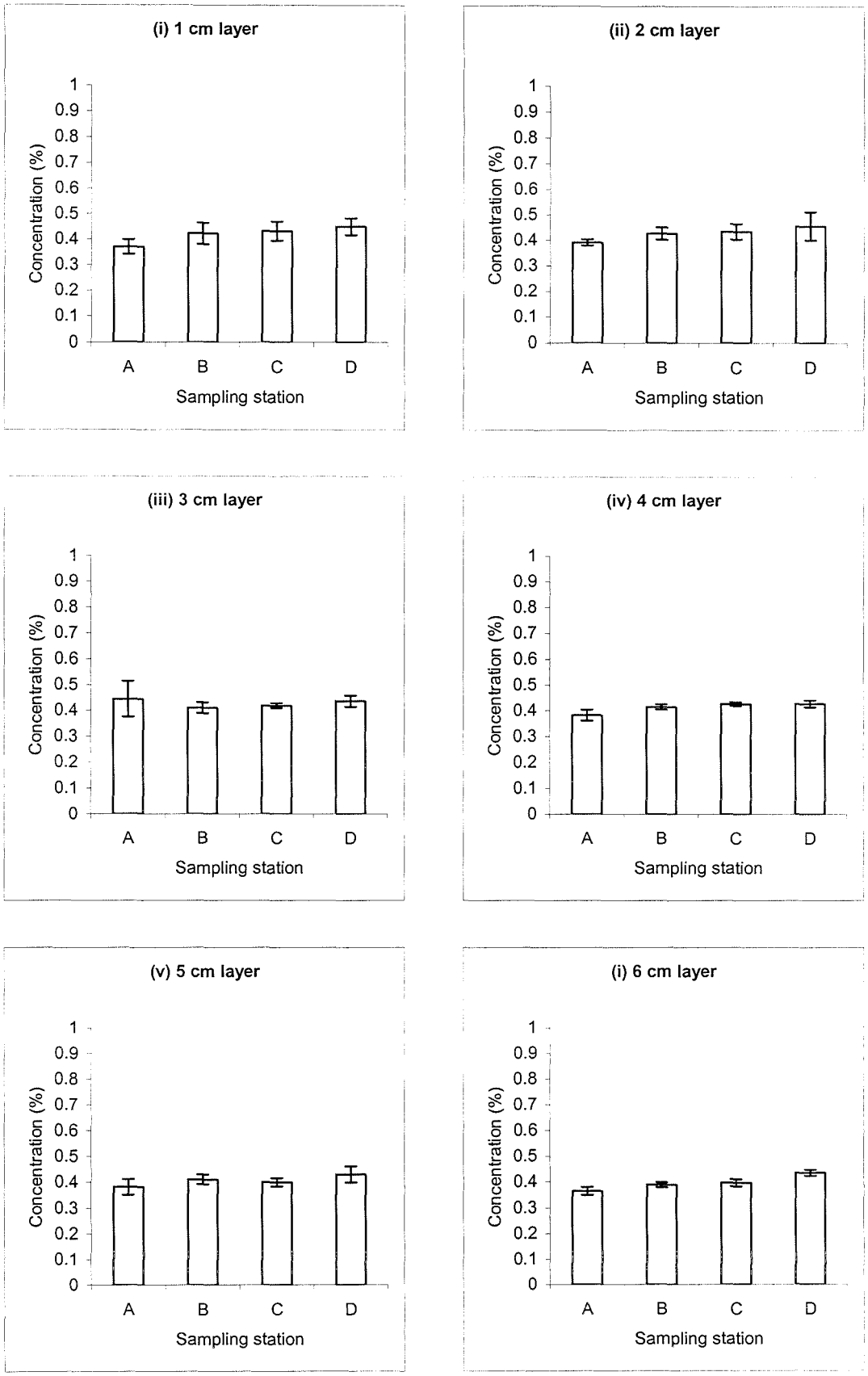

Figure 4.20 (i – vi) Site A: The percentage nitrogen content of the sediment with depth at each sampling station

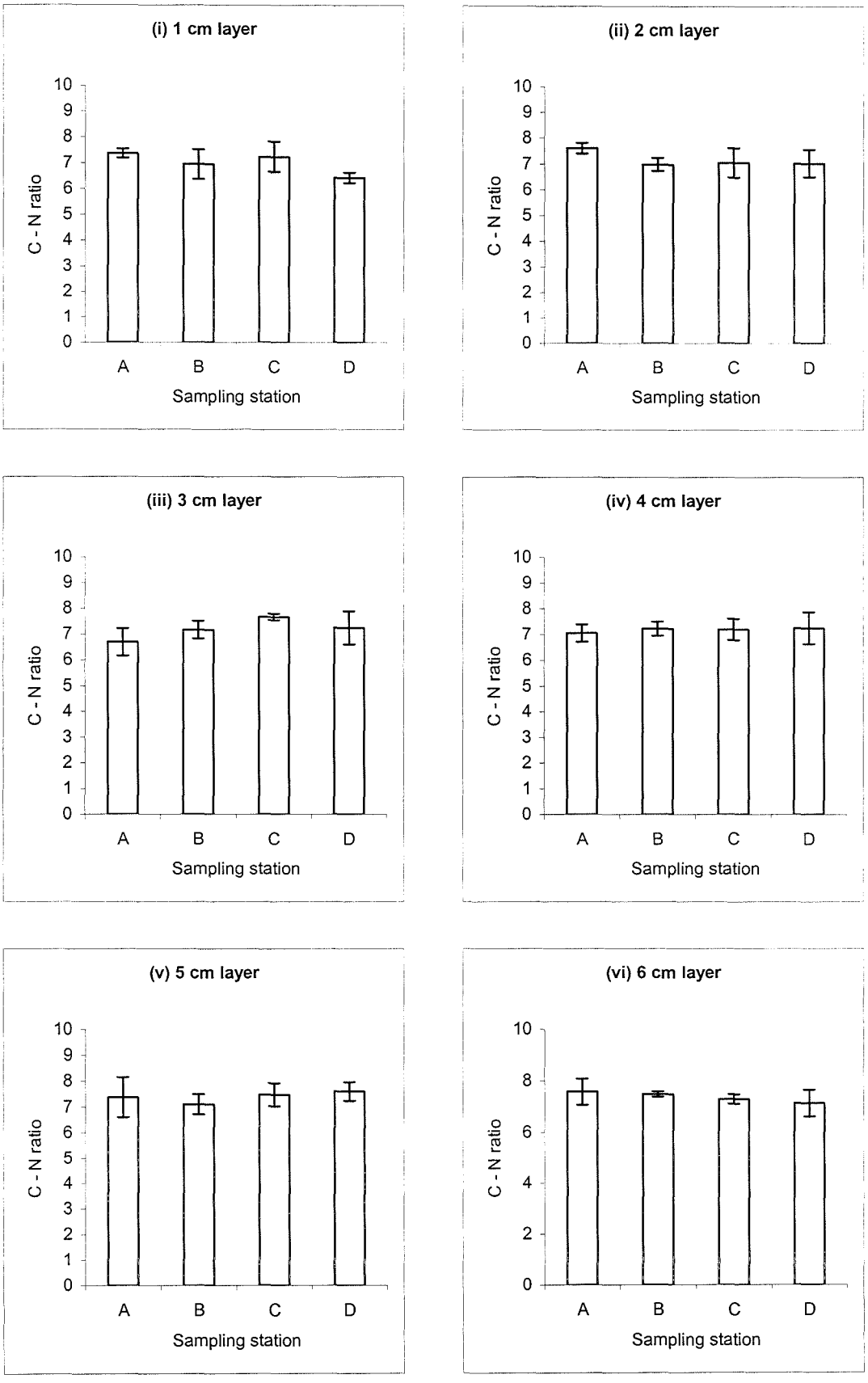

Figure 4.21 (i – vi) Site A Carbon to Nitrogen ratio with depth at each sampling station

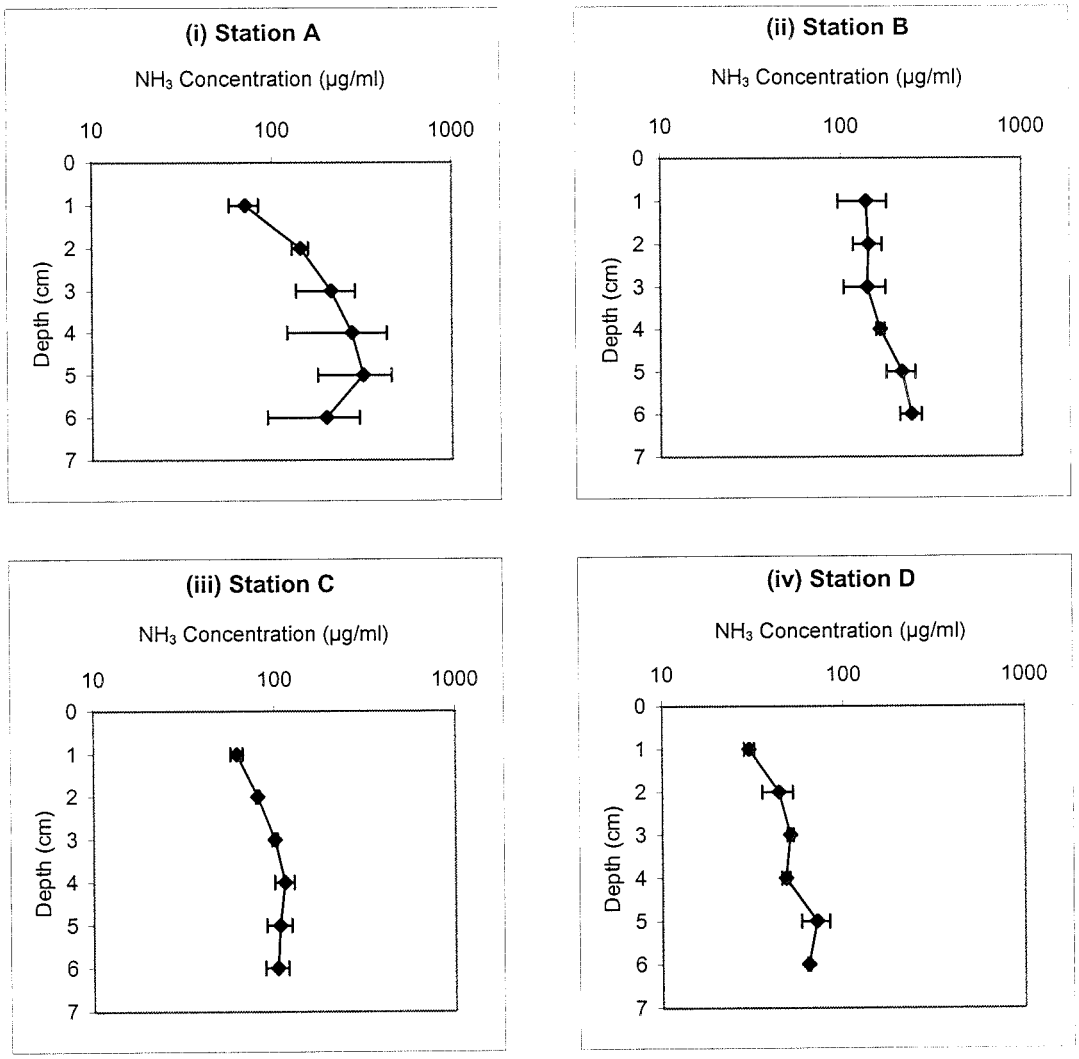

Figure 4.22 (i – iv) Site A – NH_3 concentration within the sediment with depth at each sampling station

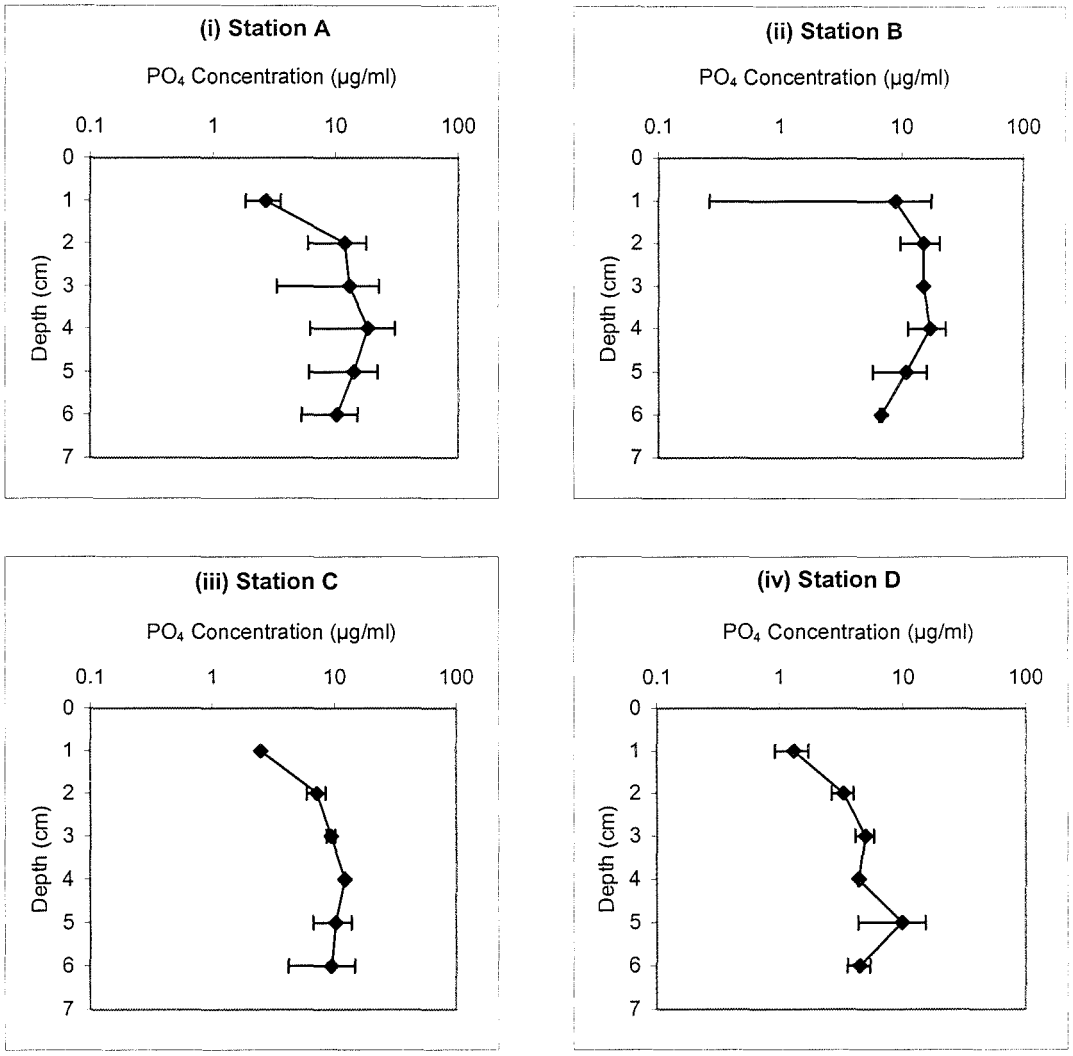

Figure 4.23 (i – iv) Site A – PO_4 concentration within the sediment with depth at each sampling station

Significant differences were observed in the organic carbon concentration at the 6 cm layer between station A and station D. In addition, the sediment nitrogen content was significantly different between stations A, B and C and station D and also between station A and station C. The carbon/nitrogen ratio remained approximately 7.3 for all stations at both these sediment depths.

4.2.5 Sediment Pore Water

There was a general increase in Ammonia and Phosphate concentration with depth at all the sampling stations (Figure 4.22 and 4.33; i - iv). There was high variability between replicates resulting in difficulty determining any significant differences between the stations.

Within the surficial layer, the concentration of ammonia ranged between 30 μgml^{-1} at station D to 137 μgml^{-1} at station B. Phosphate concentrations within this layer were similarly distributed with the minimum concentration being recorded at station D (1.32 μgml^{-1}) and maximum concentration at station B (8.90 μgml^{-1}).

There was an overall increase in concentrations of both variables at the 2 cm and 3 cm layers at all sampling stations. Peak concentrations were recorded at station A 5 cm layer for ammonia (320 μgml^{-1}) and station A 4 cm layer for phosphate (18.4 μgml^{-1}).

4.2.6 Benthic Community Structure

A total of 35 macrofaunal species were identified at this site, comprising 629 individuals (complete species/abundance matrix is presented in Appendix 3 - Site A). The five most abundant species at each station are presented in Table 4.6, together with the percentage of the total number of individuals they represent.

Species composition at this site was dominated by the polychaetes *Aphelochaeta marioni* (Saint-Joseph, 1984) and *Cirratulus cirratus* (O. F. Müller, 1776). These were

particularly abundant at the stations close to the farm sites and decreased in number with distance from the farm. The remaining community was typical of a soft-muddy bottom benthos, comprising deposit and surface feeding benthic macrofauna.

Table 4.6 : Top five ranked species (abundance), numbers and percentage of total across stations at Site A.

		N	%			N	%
A	*Aphelochaeta marioni*	81	32.2	B	Tanaidae spp.	27	21.2
	Cirratulus cirratus	28	11.1		*Podarkeopsis capensis*	16	12.6
	Podarkeopsis capensis	27	10.7		*Scoloplos armiger*	12	9.4
	Cossuridae spp.	23	9.1		*Aphelochaeta marioni*	12	9.4
	Prionospio falax	16	6.3		Gammaridae spp.	11	8.6
		Total	69.7			Total	61.4

C	Tanaidae spp.	19	15.0	D	Cossuridae spp	23	18.4
	Podarkeopsis capensis	18	14.2		Tanaidae spp	21	16.8
	Cossuridae spp.	14	11.1		*Ophryotrocha hartmanni*	9	7.2
	Protodorvillea kefersteini	12	9.5		*Protodorvillea kefersteini*	8	6.4
	Aphelochaeta marioni	11	8.7		*Scoloplos armiger*	8	6.4
		Total	58.7				55.2

4.2.6.1 Univariate Analysis of Community Structure

Similarities between the stations, in the number, type and distribution of animals recorded, were observed. Analysis of the indices derived from the species/abundance data matrix revealed no significant differences between the stations, as measured by the Shannon-Wiener index (H' $\log_e$), Margalef's species richness (d) and Pielou's evenness index (J') (Table 4.7). All values for Shannon-Wiener diversity index were between 2.3 and 2.7, implying little direct impact from the farm.

Table 4.7 : Univariate analysis of the benthic community structure at Site A.

Univariate measure/index	Sampling Station			
	A	B	C	D
Number of Individuals	251	127	126	125
Number of Species	23	19	23	21
H' $\log_e$	2.378	2.569	2.667	2.658
J'	0.7584	0.8727	0.8507	0.873
d	3.982	3.716	4.549	4.142

4.2.6.2 Multivariate Analysis of Community Structure

The complete species matrices were used for multivariate analyses (Appendix 3 - Site A). The dendograms produced by hierarchical agglomerative clustering, together with the 2-dimensional ordination plots produced by non-metric MDS of the resulting community are presented in Figures 4.24 and 4.25. The stress value associated with this MDS ordination was 0.21. Similarly to Site S, due to the high value of this stress value, the associated dendogram (Figure 4.24) should be used to aid in the analysis of the community structure and any differences that lie therein. There is an apparent trend in the MDS plot with distance from the farm site. A line has been superimposed onto the plot to indicate this. Generally, samples taken closer to the farm site are clustered at one side of the plot, whilst those samples further away are at the other side. However, because of the high stress value, it is unclear whether the observed changes along the transect are significant and can be attributed to the farm site. These were statistically analysed by One-way ANOSIM tests. Significant differences in the community structure between stations were not observed.

4.2.6.3 Infaunal Trophic Index

A reduced species/abundance matrix was used for ITI analysis containing 607 individuals. This was because some of the species identified were not benthic polychaetes and therefore not included in the calculations. The ITI scores for each station are presented in Table 4.8.

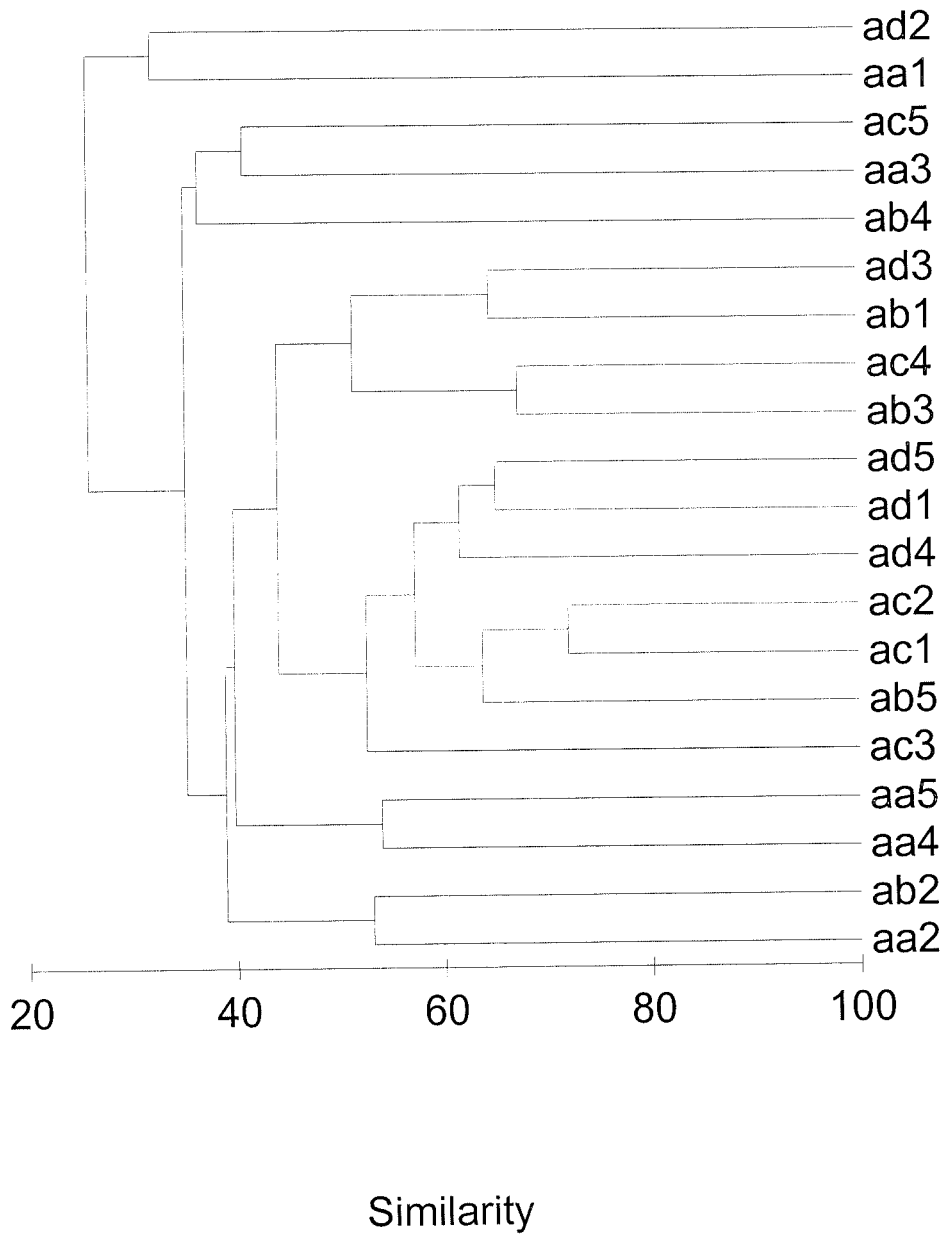

Figure 4.24 Dendrogram of all replicates at each station at Site A, using group-averaged clustering from Bray Curtis similarities on root-transformed abundances.

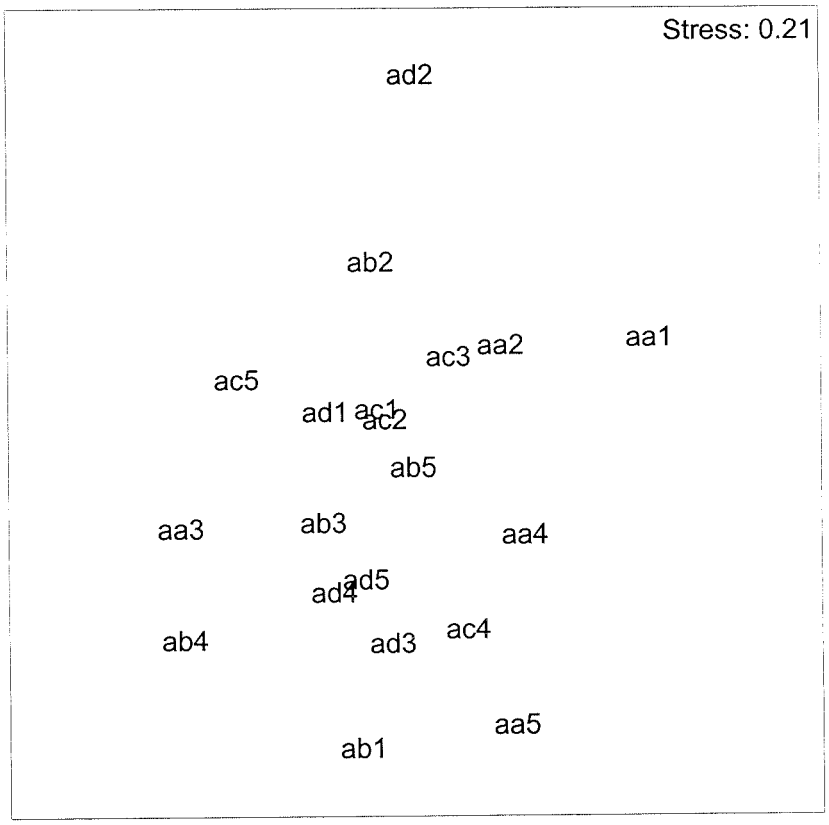

Figure 4.25 Two-dimensional ordination plot of all replicates at each station at Site A.

Table 4.8 : Number of individuals in each of the trophic groups and the resultant ITI score at each station at Site A.

	Station			
Trophic Group	A	B	C	D
1	0	0	0	0
2	182	69	71	67
3	52	33	30	25
4	13	17	19	29
ITI	56.18	47.95	47.83	43.86

Little difference is observed in the ITI scores between the sampling stations. Stations B, C and D are within the 'enriched' category and Station A is classed as 'little effect' according to Word (1979). However, the values are all clustered around the borderline between these two categories and consequently this distinction is not considered significant.

4.3 Site B

4.3.1 Water Currents

Comprehensive analyses of the hydrographic data collected at Site S are presented in Appendix 3 - Site B. A summary of the hydrographic data obtained from Site B is presented in Figure 4.26 (a and b) for the surface current data and Figure 4.27 (a and b) for the bottom current data. The hydrographic measurements revealed the site to be very weakly flushed, with the mean current velocity to be < 0.03 ms^{-1} throughout the water column (Table 4.9). Currents were generally parallel to the shore in a north/south direction.

Surface currents were recorded in all directions with a high proportion of stronger velocity recordings being made in along a north/south axis and greatest occurrence being in a

a)

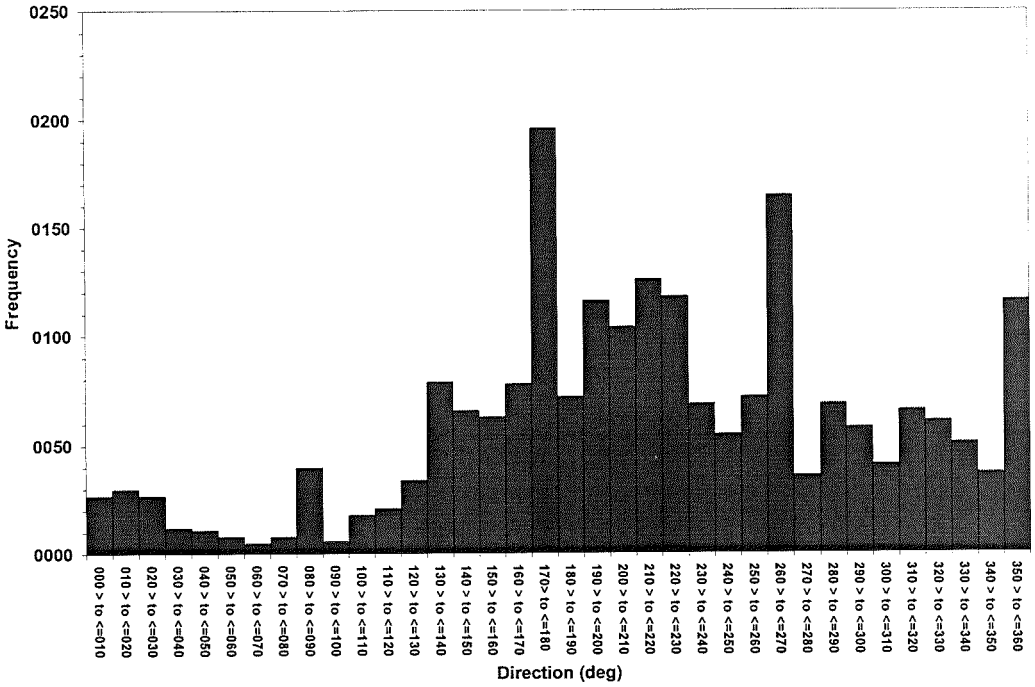

b)

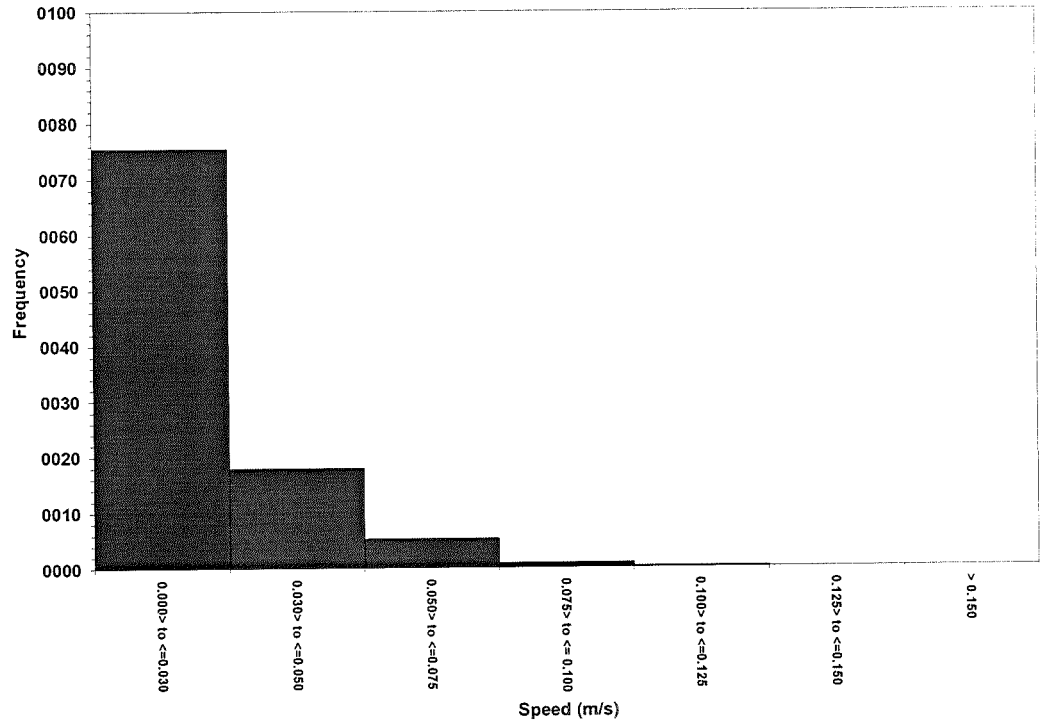

Figure 4.26 a and b Site B Surface current direction and velocity frequency histograms

a)

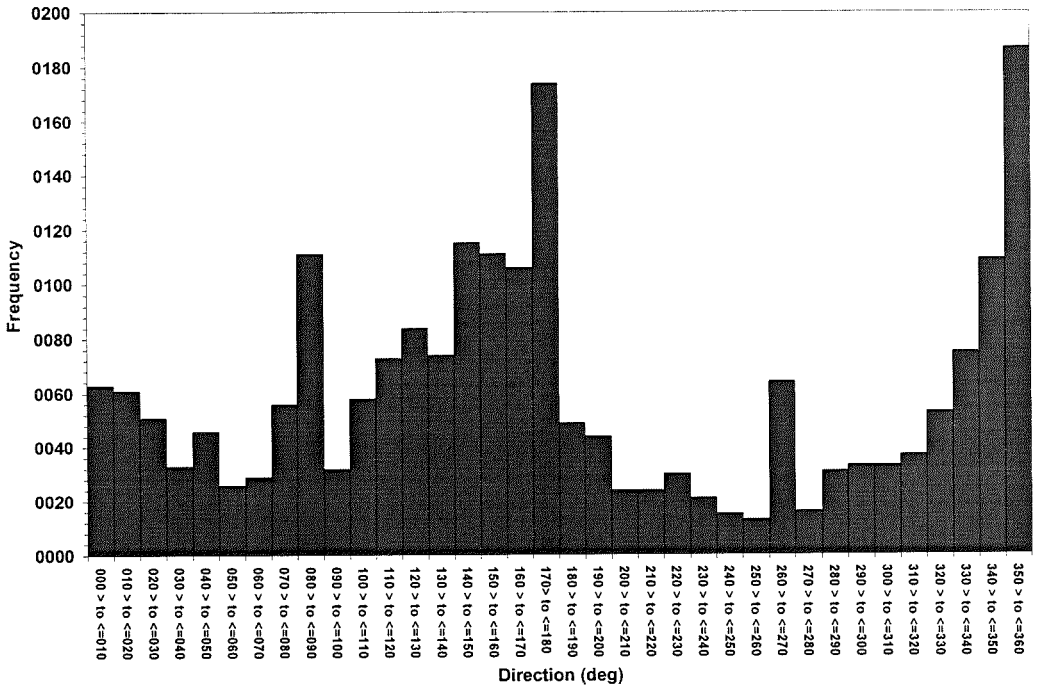

b)

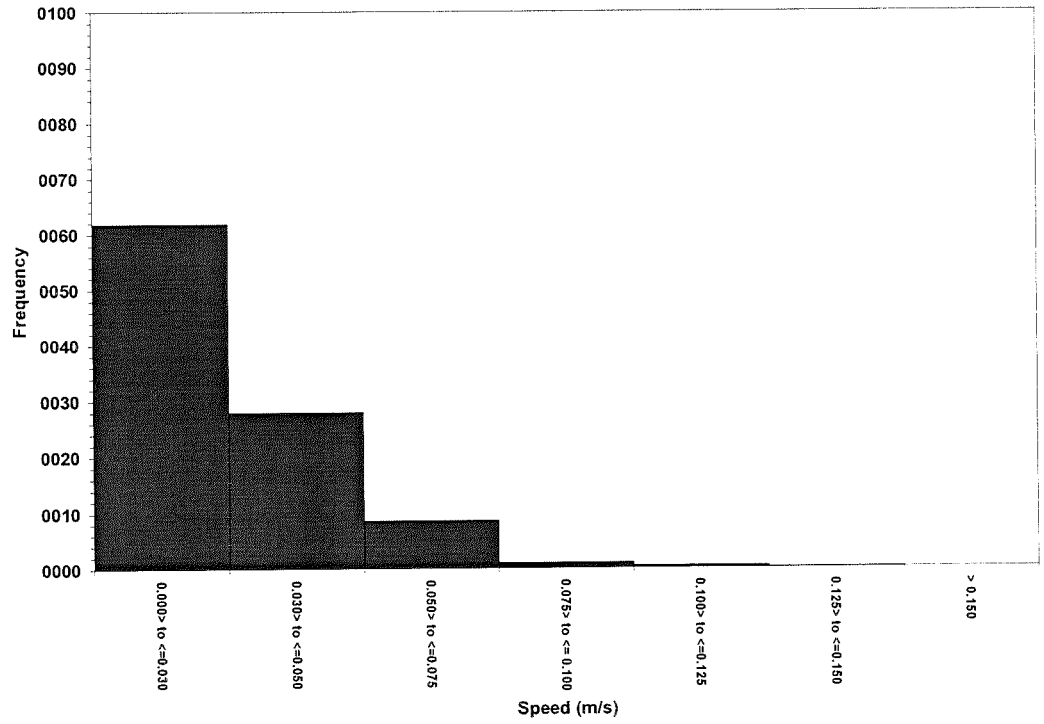

Figure 4.27 a and b Site B Bottom current direction and velocity frequency histograms

southerly direction (Figure 4.26 b). Current speeds reached a maximum of 0.12 ms^{-1} at periods during spring tide. The frequency histogram illustrates that the majority of current velocity measurements were <0.03 ms^{-1}, with 25% of the recordings exceeding this velocity (Figure 4.26 a). The residual plot (Appendix 3 - Site B) shows the general water movement to be towards the south-west.

Table 4.9 : Hydrographic characteristics at Site B.

	Surface	Bottom
Mean Current Velocity (cm s^{-1})	2.28	2.85
Residual Current Velocity (cm s^{-1})	0.76	0.40
Residual Current Direction (deg)	226	102

Seabed currents were similar with the majority of readings being made along a north/south axis. Current speeds attained a maximum of 0.13 ms^{-1} whilst 61.87% of the readings being <0.03 ms^{-1} (Figure 4.27 a and b). The residual plot (Appendix 3 - Site B) illustrates that the general water movement was towards the west. However, tidally driven currents to the north and south dominated the site.

4.3.2 Sediment Redox

Throughout the core depth, Eh values recorded at station A were consistently lower and more reducing, increasing with distance from the farm site (Figure 4.28 i - iii). A clearly defined RDL occurred at stations A and B in the upper 1 cm of sediment. This was not as apparent at station C, with a more gradual reduction in sediment redox potential with depth.

Eh values were positive at all stations in the surface layer, ranging from +100 mV (Station A) to +350 mV (Station C). Within the upper 1 cm layer of the sediment, sediment Eh became negative at stations A and B going down to −100 mV. These values were maintained for the remainder of the sediment profile. Redox at Station C was positive throughout the sediment depth, decreasing gradually with depth.

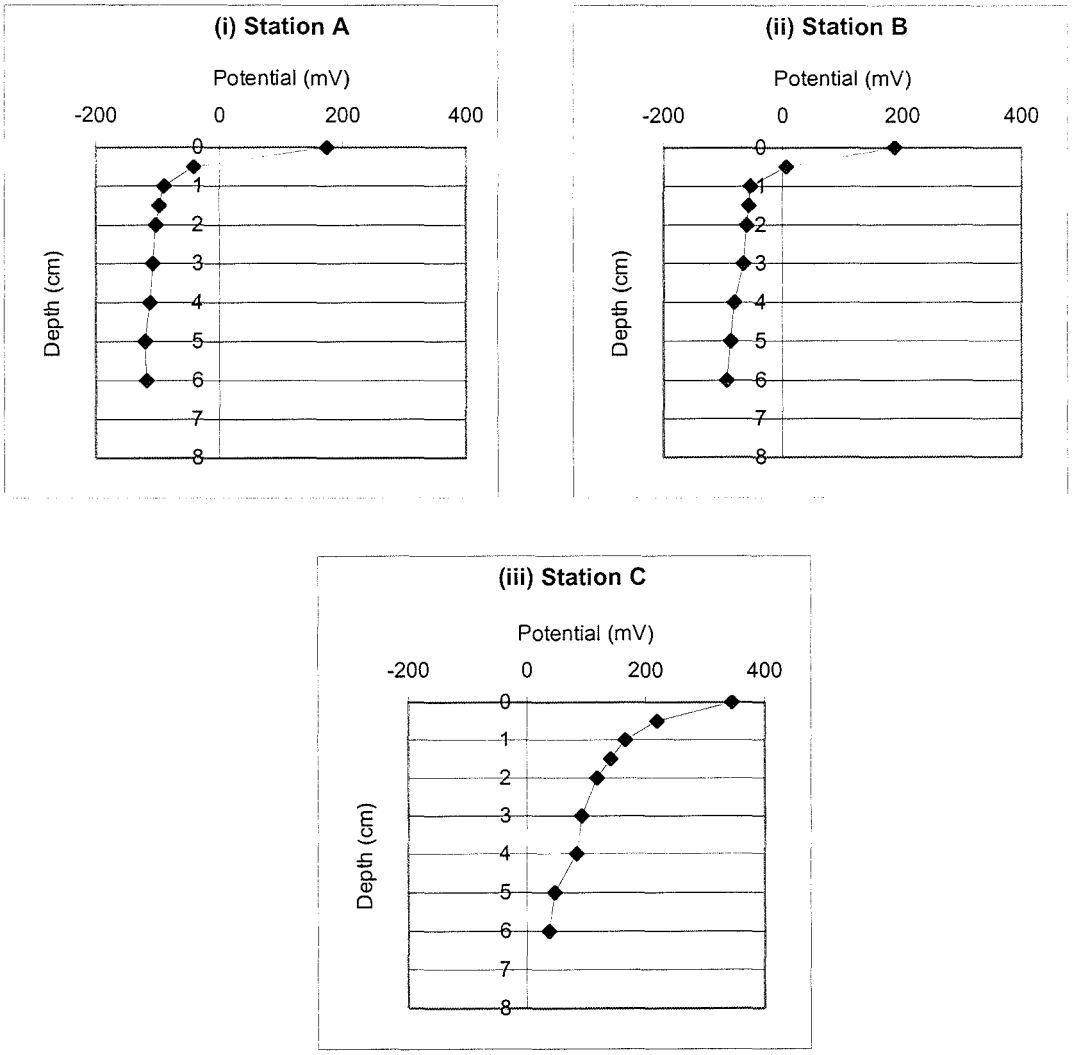

Figure 4.28 (i – iii) Site B Redox potential (mV) with depth at each sampling station

4.3.3 Granulometry

Particle size analysis revealed that each sampling station had a different sediment description. Station A was described as a poorly sorted fine to medium silt, with a symmetrical or fine to coarse skewed meso- or lepto-kurtic distribution. Station B was very poorly sorted medium/coarse silt with a symmetrically platy- or meso-kurtic distribution whereas station C was very poorly sorted coarse silt with a symmetrical or fine skewed platykurtic distribution. The calculated variables and sediment descriptors for this site are presented in Appendix 3 - Site B.

There were significant trends in the sediment characteristics of the surficial layer of sediment (1 cm layer). The proportion of fine sediment (< 63 μm) was significantly different between each station, the greatest value observed at station A, through station B to station C (Figure 4.29 i). This trend was also observed in the median phi value (Figure 4.30 i), which was significantly greater at stations A and B than at station C. The reciprocal but significant trend was also observed for sorting coefficient values (Figure 4.31 i) where station A was significantly lower than station C.

Similar trends were observed in the 2 cm sediment layer. The proportion of fine sediment (Figure 4.29 ii) was greatest at station A and decreasing with distance from the farm site. All the stations were significantly different to each other at this layer. The median phi values followed a similar trend, with significant differences being observed between stations A and station C (Figure 4.30 ii). There was a distinct, but non-significant, difference between station A and stations B and C within the sorting coefficient values (Figure 4.31 ii).

At the 3 cm layer this trend was again observed with significant differences being recorded between all stations in the fines fraction (Figure 4.29 iii) and sorting coefficient (Figure 4.31 iii). The median phi values were significantly greater at station A and B when compared to station C (Figure 4.30 iii).

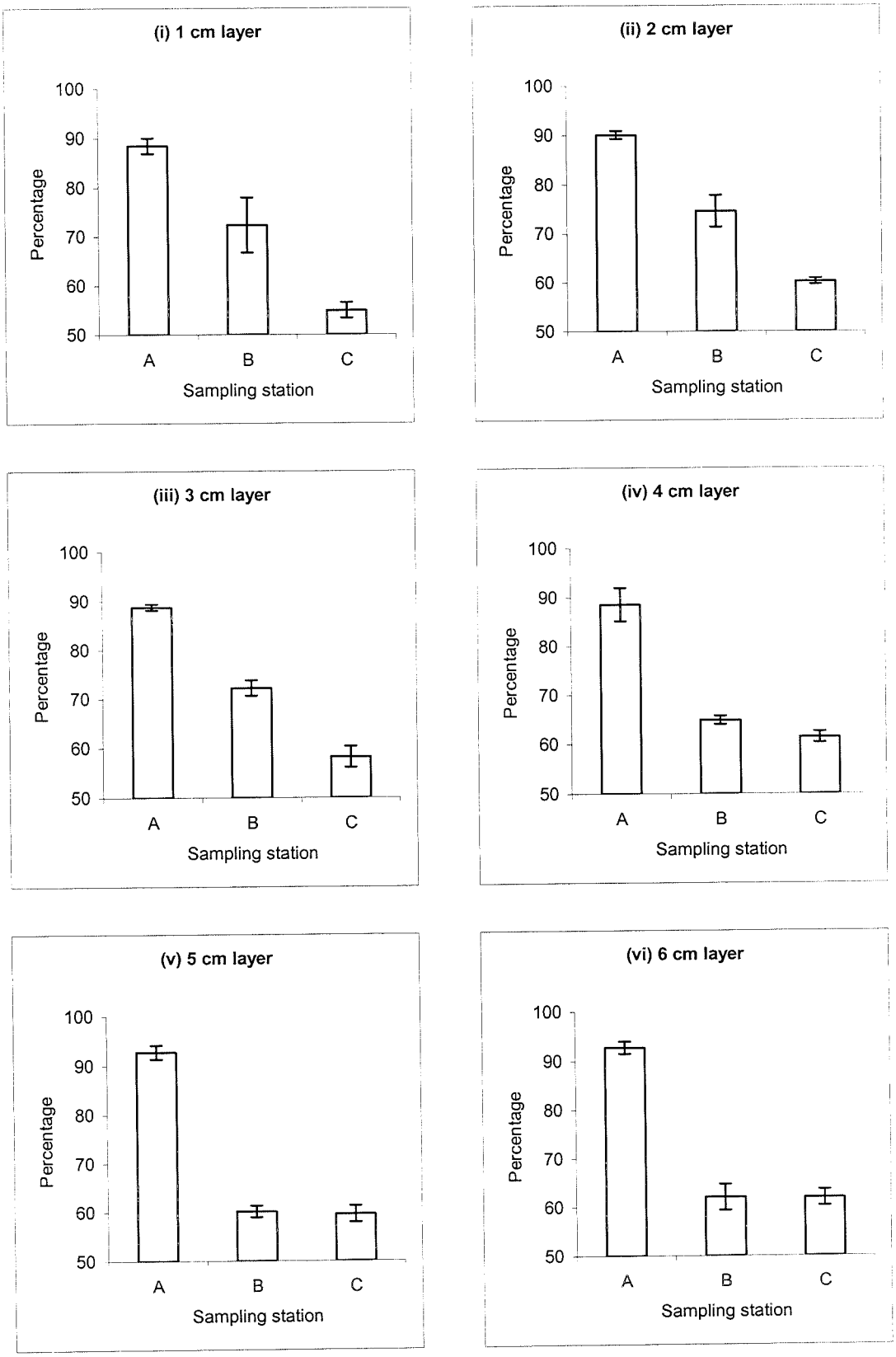

Figure 4.29 (i – vi) Site B: The percentage sediment < 63μm with depth at each sampling station

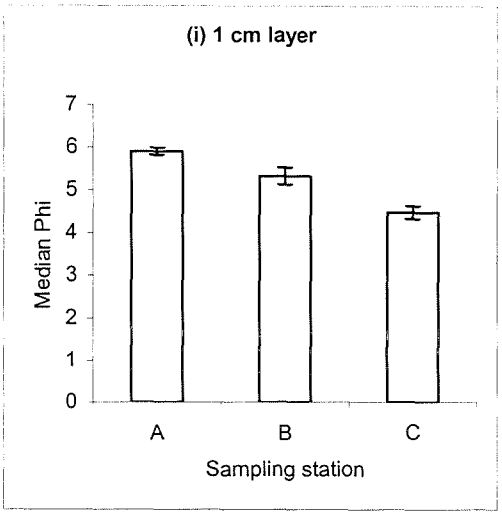

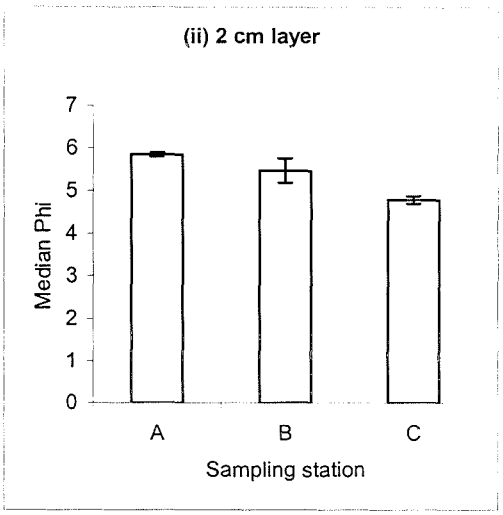

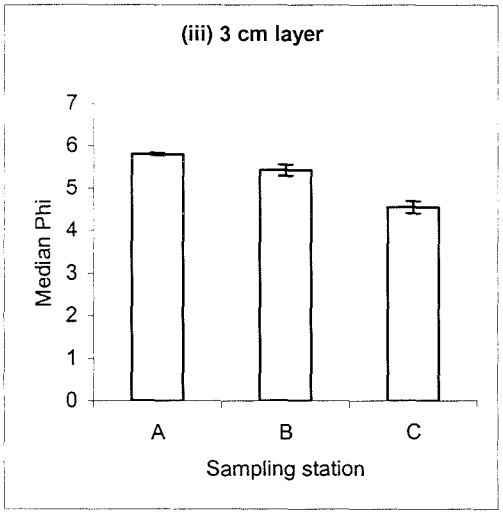

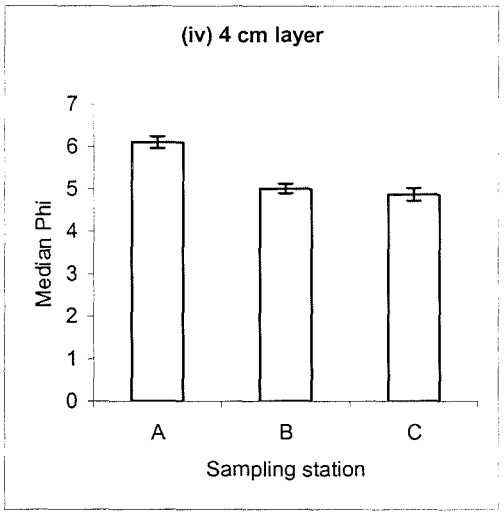

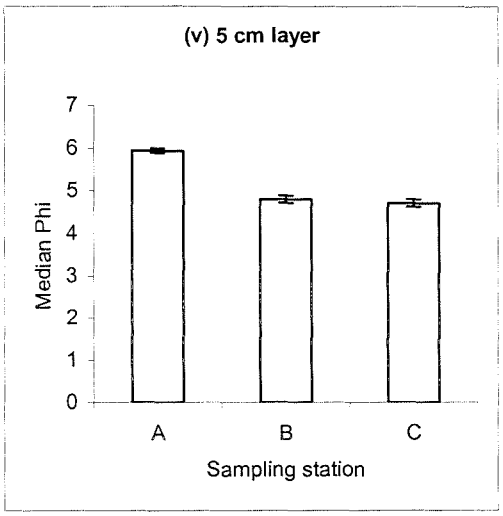

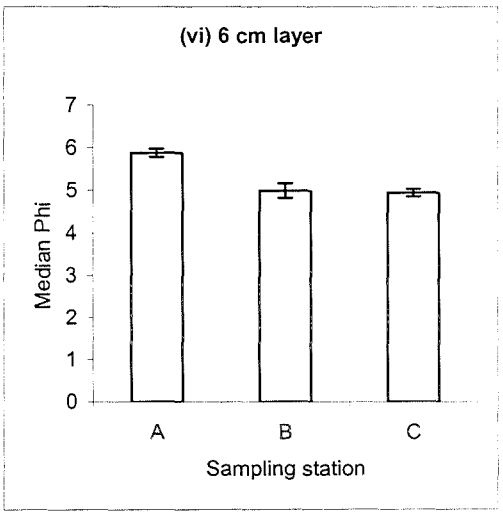

Figure 4.30 (i – vi) Site B: The sediment median phi value with depth at each sampling station

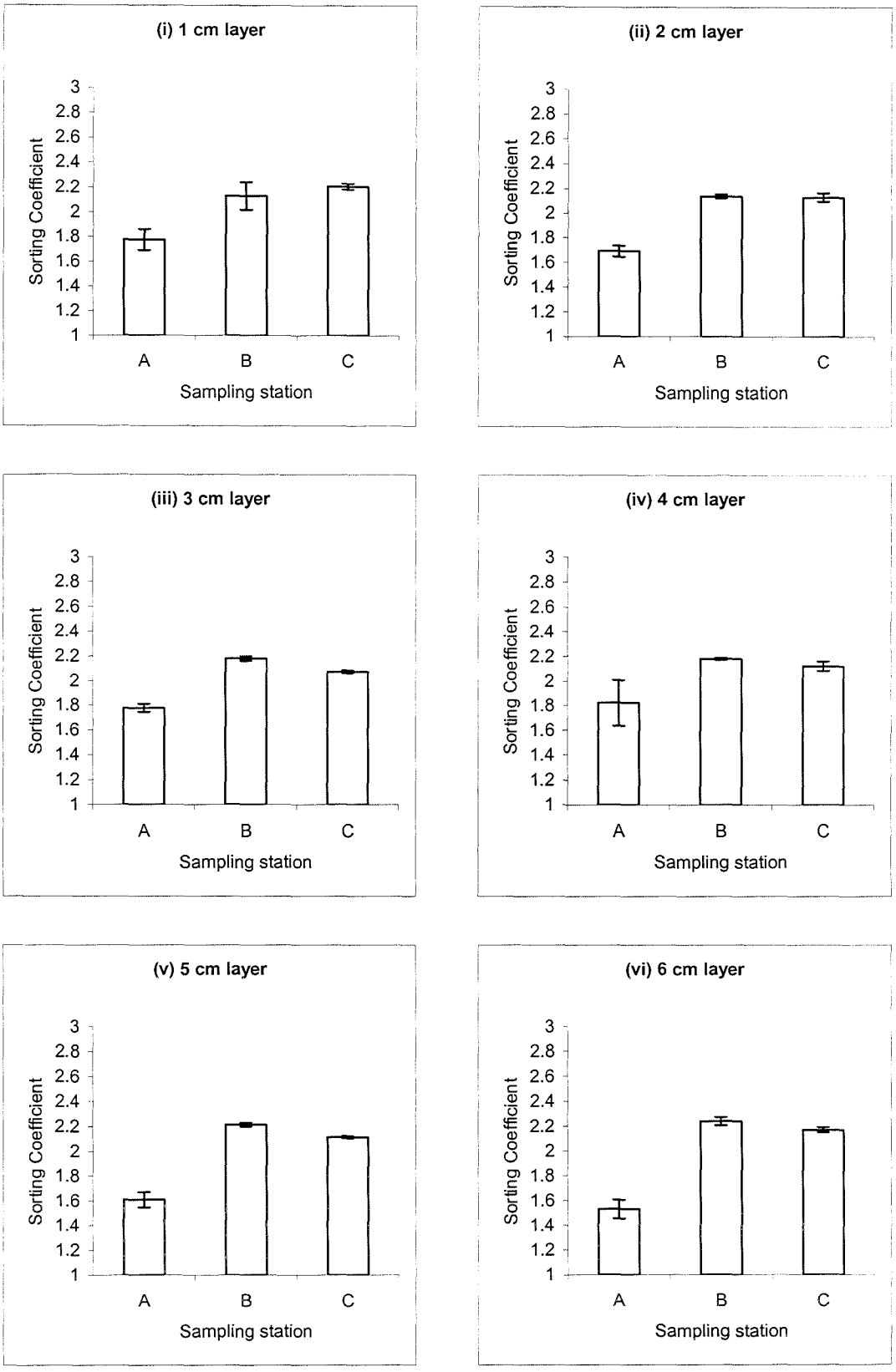

Figure 4.31 (i – vi) Site B: The sediment sorting coefficient value with depth at each sampling station

There was significantly greater proportion of < 63 μm at station A than at stations B and C at the 4 cm layer. Reciprocal trends were observed in the sorting coefficient values, however no significant differences were observed.

In the 5 cm layer, the median phi values at station A were significantly greater than those observed at stations B and C (Figure 4.30 v). Station A had a significantly greater proportion of fine sediment and lower sorting coefficient value than observed at stations B and C (Figures 4.29 v and 4.31 v).

This trend was repeated in the 6 cm layer, with station A significantly different to stations B and C for all the measured variables.

4.3.4 Sediment Carbon and Nitrogen

There was a general decrease in the organic carbon and nitrogen concentration, and an associated increase in carbon/nitrogen ratio in the sediment with distance from the farm site. Results for all carbon and nitrogen elemental analyses for this site are presented in Appendix 3 - Site B.

In the surficial layer (1 cm), the organic carbon content at station A was greater (non-significant) than station B, and significantly greater than station C (Figure 4.32 i). The nitrogen content of the sediment followed a similar pattern (Figure 4.33 i). The carbon/nitrogen ratio increased with distance from the far site, with values at station A and B being significantly less than those observed at station C (Figure 4.34 i).

The 2 cm sediment layer exhibited similar trends in organic carbon concentration, decreasing with distance from the farm site (Figure 4.32 ii). However, these differences were not sufficient to be significant. The nitrogen concentration and carbon-nitrogen ratio at this layer were significantly different between stations A and C (Figures 4.33 ii and 4.34 ii).

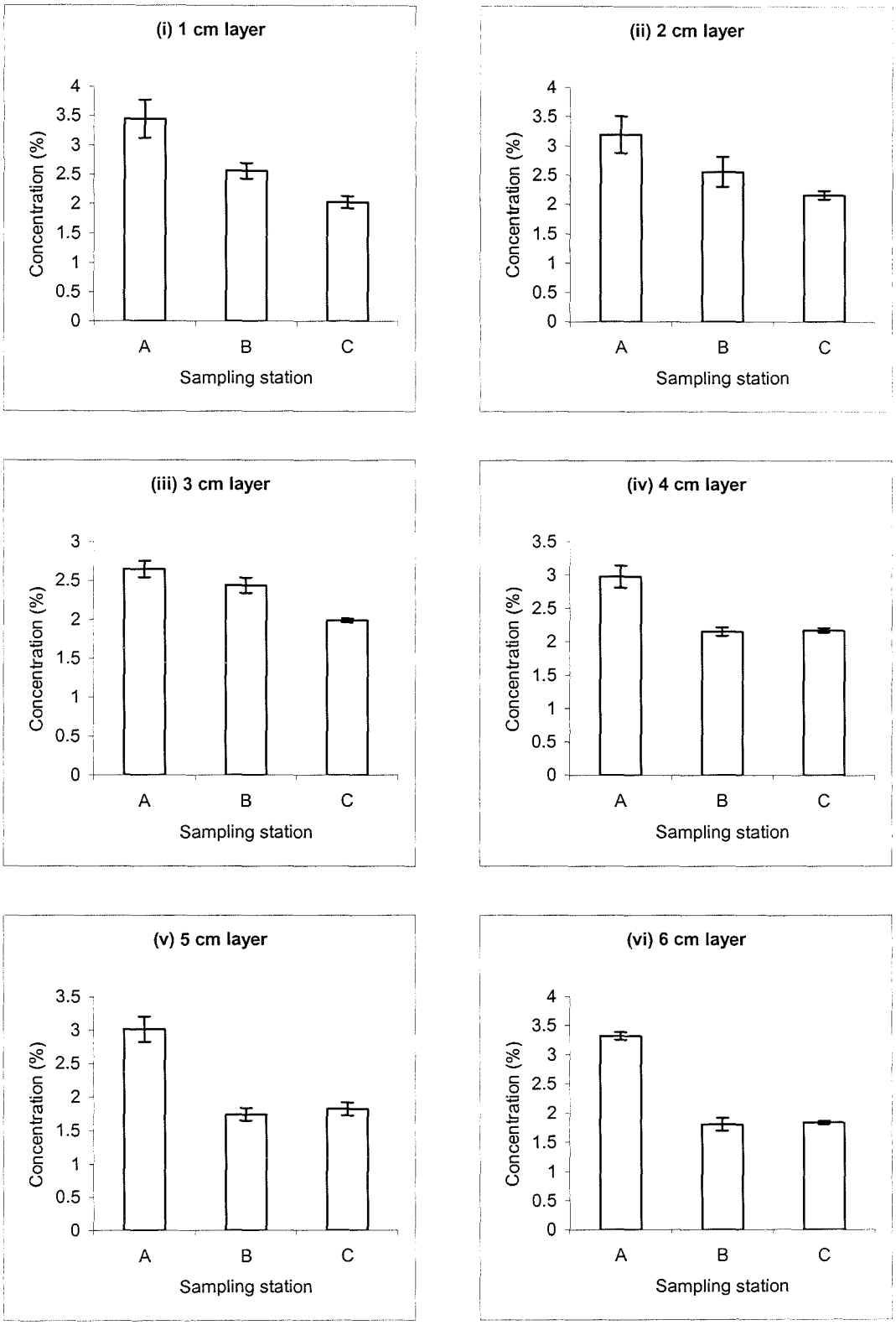

Figure 4.32 (i – vi) Site B: The percentage carbon content of the sediment with depth at each sampling station

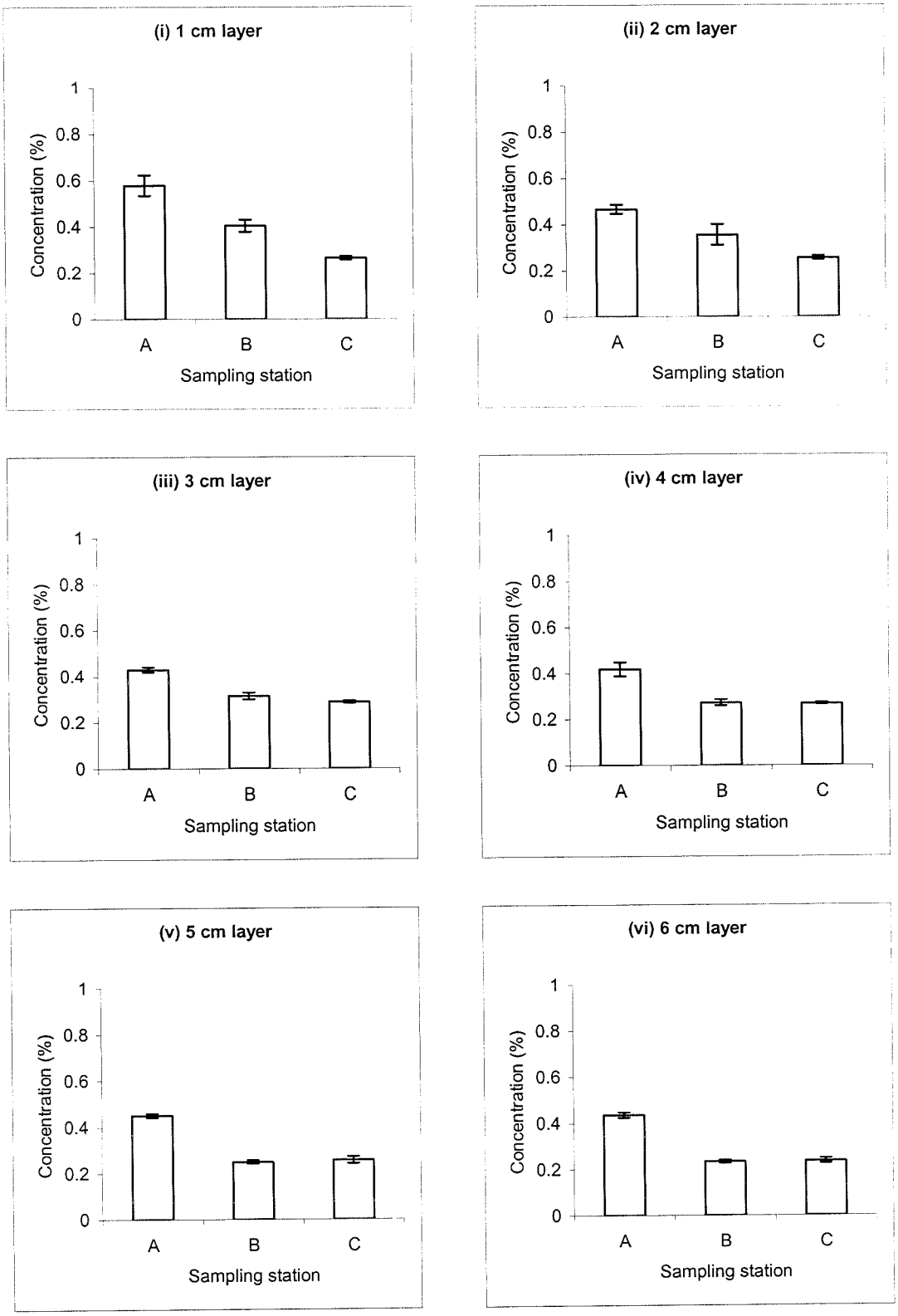

Figure 4.33 (i – vi) Site B: The percentage nitrogen content of the sediment with depth at each sampling station

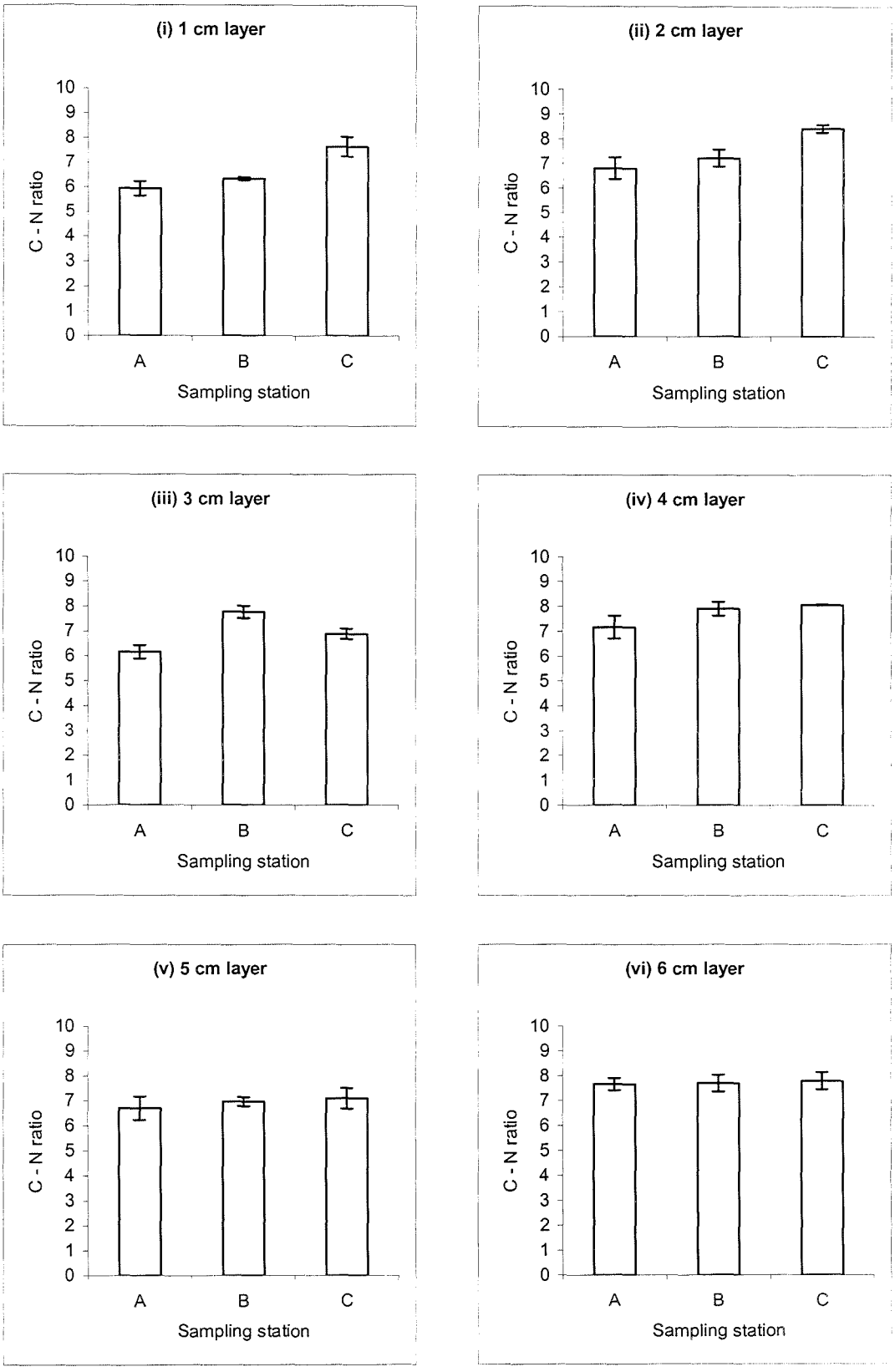

Figure 4.34 (i – vi) Site B Carbon to Nitrogen ratio with depth at each sampling station

There was a general decrease in the organic carbon and nitrogen content of the sediment at the 3 cm layer, the organic carbon concentration at stations A and B were significantly greater than at station C (Figure 4.32 iii). Station A was significantly greater than stations B and C for nitrogen concentration (Figure 4.33 iii). The carbon-nitrogen ratio was significantly less at station A compared to station B, however, significant differences were not observed at station C. This was due to the low organic carbon concentration recorded at station B.

At the 4 cm layer, both the organic carbon and nitrogen content of the sediment was significantly greater at station A than at stations B and C (Figures 4.32 iv and 4.33 iv). The carbon-nitrogen ratio increased with distance from the farm site (Figure 4.34 iv), however no significant differences between stations were observed.

Similar trends were observed in the 5 cm and 6 cm layers, with significantly greater concentrations being recorded at station A than stations B and C. The carbon-nitrogen ratio at both these layers increased with distance from the farm site with no significant differences recorded.

4.3.5 Sediment Pore Water

A general increase in Ammonia and Phosphate concentrations was observed with depth, apart from an anomalous result at Station A 2 cm layer (Figures 4.35 and 4.36, i - iii). This result does not fit the general trend of the data and is considered unrepresentative of the overall trend in the data.

Within the surficial layer, the concentration of ammonia was significantly different between station B and C (55 μgml^{-1} and 38 μgml^{-1} respectively) and Station A (1117 μgml^{-1}). Significant differences between all stations were observed for Phosphate concentration at this layer (A - 63.9 μgml^{-1}; B - 20.9 μgml^{-1}; C - 3.16 μgml^{-1}).

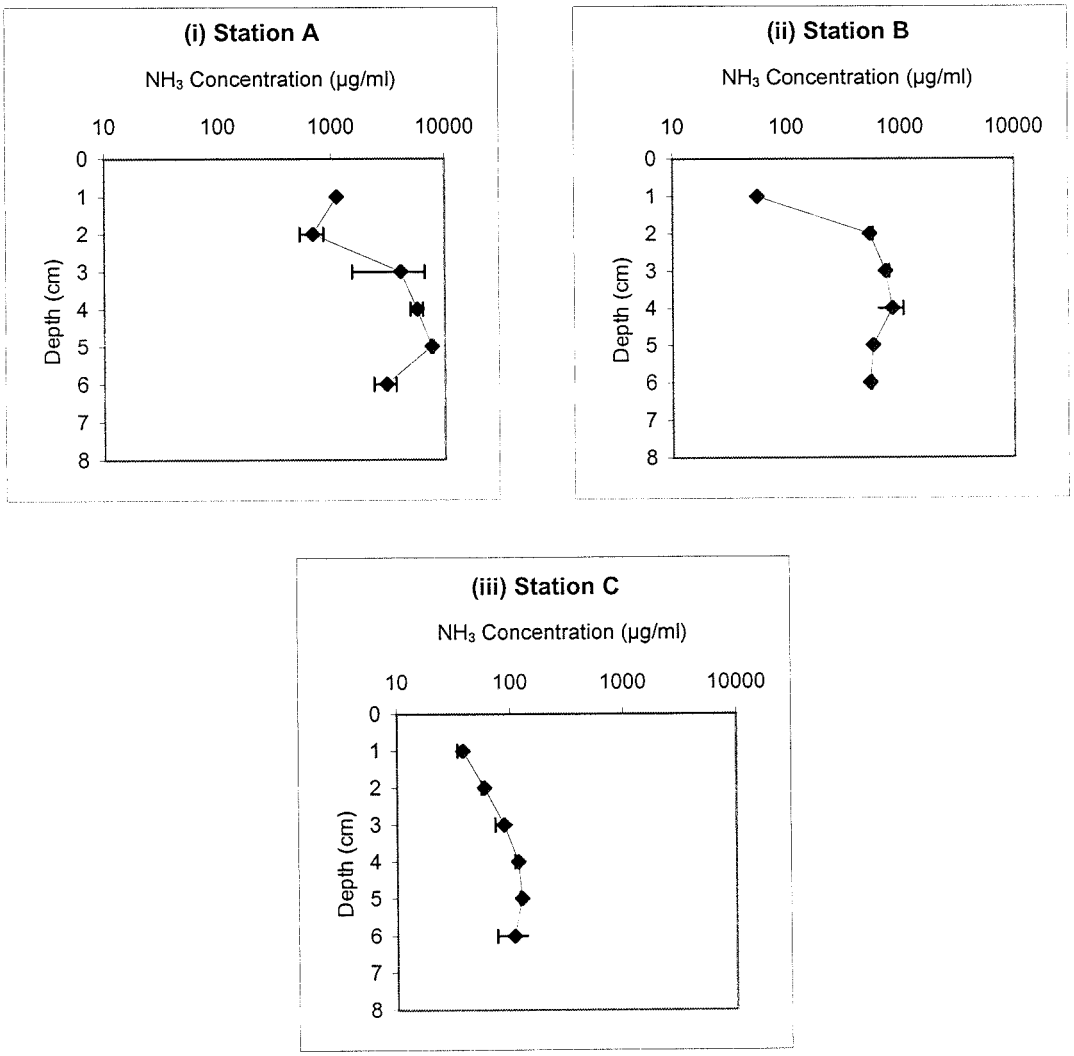

Figure 4.35 (i – iii) Site B – NH_3 concentration within the sediment with depth at each sampling station

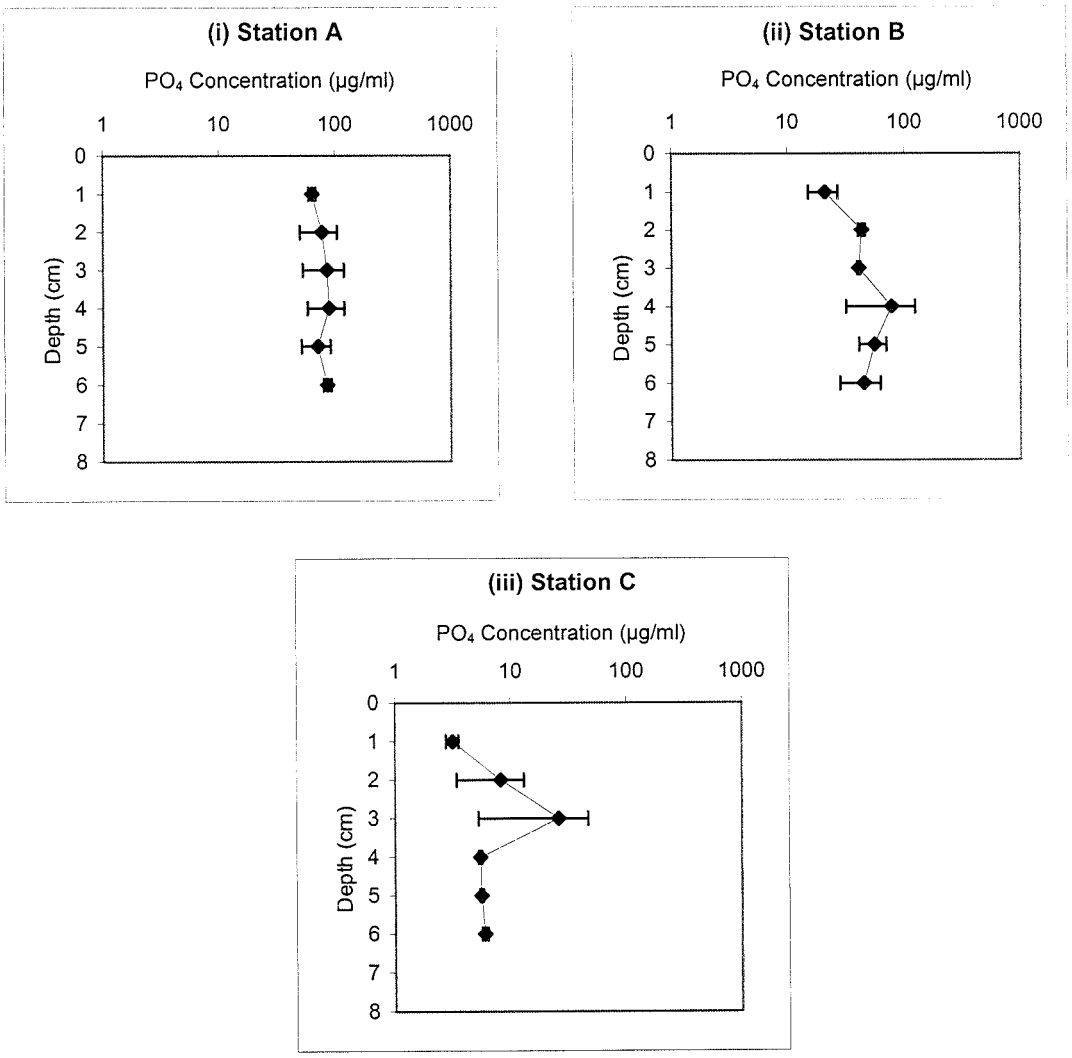

Figure 4.36 (i – iii) Site B – PO_4 concentration within the sediment with depth at each sampling station

Significant differences between all stations were recorded in concentration of ammonia at every layer from 3 cm to 6 cm. Peak concentrations of ammonia were recorded at station A at the 5 cm layer (7723 μgml^{-1}), station B at the 4 cm layer (849 μgml^{-1}) and station C at the 5 cm layer (126 μgml^{-1}). Significant differences in the phosphate concentration between stations were obscured by the wide variability in the replicate samples. Peak concentrations of phosphate were recorded at station A at the 3 cm layer (32.9 μgml^{-1}), station B at the 4 cm layer (46.1 μgml^{-1}) and station C at the 3 cm layer (20.8 μgml^{-1}).

4.3.6 Benthic Community Structure

A total of 33 macrofaunal species were identified at this site, comprising 951 individuals (complete species/abundance matrix is presented in Appendix 3 - Site B). The five most abundant species at each station are presented in Table 4.10, together with the percentage of the total number of individuals they represent.

Table 4.10 : Top five ranked species (abundance), numbers and percentage of total across stations at Site B.

		#	%			#	%
A	*Ophryotrocha hartmanni*	295	62.9	B	Gammaridae spp.	113	41.3
	Aphelochaeta vivipara	40	8.5		*Ophryotrocha hartmanni*	30	10.9
	Nematode spp.	27	5.7		*Nephtys hombergii*	19	6.9
	Tharyx killariensis	20	4.2		*Aphelochaeta vivipara*	15	5.4
	Chaetozone setosa	15	3.2		*Abra alba*	9	3.3
		Total	84.6			Total	68.1

		#	%
C	Gammaridae spp	89	42.5
	Melinna palmata	16	7.6
	Abra alba	16	7.6
	Tanaidae spp.	12	5.7
	Protodorvillea kefersteini	7	3.3
		Total	66.9

The dominant species at station A were the polychaetes *Ophryotrocha marioni* (Huth, 1993), *Aphelochaeta vivipera* (Christie, 1984) and *Tharyx killariensis* (Southern, 1914). At stations B and C, the dominant species were gammarid amphipods, highly abundant in the surficial layer of sediment. The pollution indicating polychaete *Capitella capitata* (Fabricius, 1780) occurred at stations A and B, however in very low numbers.

4.3.6.1 Univariate Analysis of Community Structure

Similarities between the stations, in the number, type and distribution of animals recorded, were observed. Analysis of the indices derived from the species/abundance data matrix revealed that the faunal community at station A was significantly different compared to those at stations B and C as measured by the Shannon-Wiener index (*H'* $\log_e$), Margalef's species richness (d) and Pielou's evenness index (*J'*) (Table 4.11). Shannon-Wiener values close to the farm (Station A, H' = 1.5) increased dramatically with distance (Station B, H' = 2.2; Station C, H' = 2.3).

Table 4.11 : Univariate analysis of the benthic community structure at Site B.

Univariate measure/index	Sampling Station		
	A	B	C
Number of Individuals	469	273	209
Number of Species	19	22	25
H' $\log_e$	1.568	2.259	2.321
J'	0.5327	0.7308	0.721
d	2.927	3.744	4.492

4.3.6.2 Multivariate Analysis of Community Structure

The complete species matrices were used for multivariate analyses (Appendix 3 - Site B). The dendrograms produced by hierarchical agglomerative clustering, together with the 2-dimensional ordination plots produced by non-metric MDS of the resulting community are presented in Figures 4.37 and 4.38. The stress value associated with these MDS ordination was 0.11. This plot indicates a strong trend in community composition with distance from the farm site. At station A, the community was impoverished and dominated by deposit feeding polychaetes. This fauna was replaced by a more diverse

community at station B, leading to a community typical of background conditions at station C. These distinctions can be seen in the dendrogram (Figure 4.37) where the different stations are generally separated into distance from site groups. A line has been superimposed onto the MDS separating the sampling stations into three distinct groups. These were statistically analysed by One-way ANOSIM tests. Significant differences in the community structure were recorded between each of the sampling stations.

4.3.6.3 Infaunal Trophic Index Analysis

A reduced species/abundance matrix was used for ITI analysis containing 891 individuals. This was because some of the species identified were not benthic polychaetes and therefore not included in the calculations. The ITI scores for each station are presented in Table 4.12.

Table 4.12 : Number of individuals in each of the trophic groups and the resultant ITI score at each station at Site B.

	Station		
Trophic Group	A	B	C
1	0	0	0
2	93	157	128
3	24	48	39
4	338	49	15
ITI	15.47	47.56	54.08

Relating the ITI scores to benthic classification, each of the three sampling stations are within different categories. Station A was 'degraded', Station B was 'enriched' whilst Station C was 'little effect'. However, the scores at Stations B and C are very similar and bridge the borderline between the two categories. The low ITI score recorded at Station A indicates that significant alterations to the benthic community had occurred very close to the farm site.

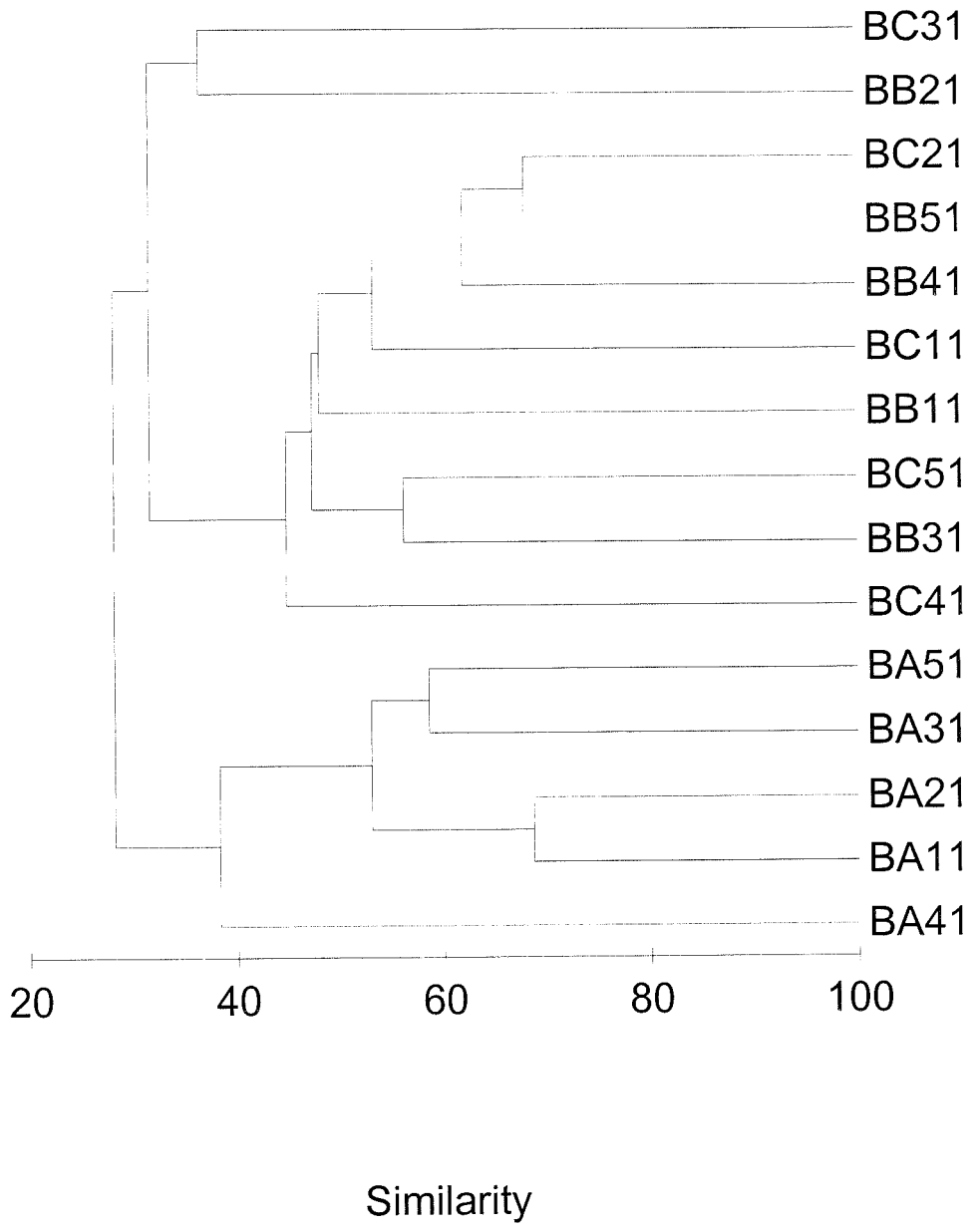

Figure 4.37 Dendrogram of all replicates at each station at Site B, using group-averaged clustering from Bray Curtis similarities on root-transformed abundances.

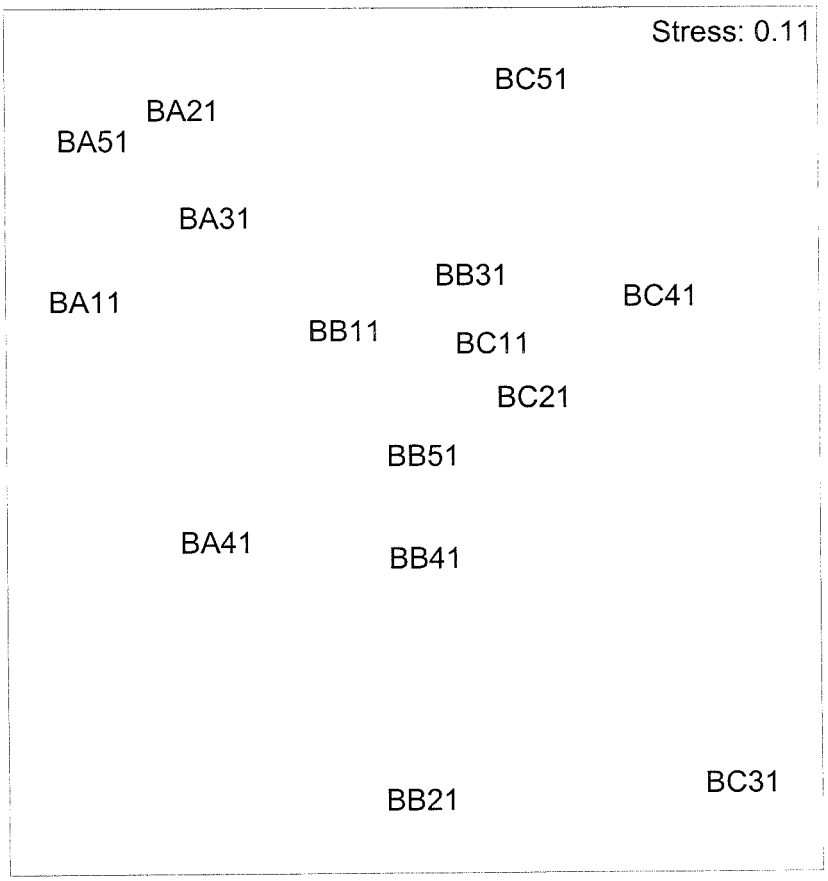

Figure 4.38 Two-dimensional ordination plot of all replicates at each station at Site B.

5 Field Studies of the Impact of Mussel Farming - Discussion

5.1 Site S

The dominance of polychaetes (e.g. *Prionospio fallax*, *Sphaerosyllis erinaceus* and *Tharyx killariensis*) at stations near the farm and bivalves only occurring further away from the site may indicate some degree of disturbance from (organic) sedimentation. The Shannon Wiener index was not significantly different ($p>0.05$) between stations, however this index is mostly useful for indicating marked changes in diversity such as in areas of high disturbance.

The redox profiles for the 5 stations were not significantly different indicating that there is similar input of organic matter and biological activity at all stations. In addition, *Beggiatoa* sp. were not present on the sediment surface, as reported in some studies (e.g. Dahlback and Gunnarson, 1981), which would have indicated the presence of anoxic sediment and oxic bottom-water.

The increased percentage carbon content of the sediment at the 1cm level between stations A, B and C and Station D could indicate increased sedimentation due to biodeposition by the mussels. However, it would be expected that difference would have been found between the reference station E and the other stations for other parameters, such as the percentage fraction of sediment <63 um and <20um, if the sediment had contained a high proportion of biodeposits.

With the slight differences in the benthic infauna between the raft stations and the control, the effect of the farm on the benthos may possibly be described as intermediate disturbance. This is consistent with the small size of the farm and the low biomass. Despite the apparently depositional nature of the site and low current velocities, the quantity of faeces and pseudofaeces available for deposition would only be small.

Most forms of aquaculture contribute to enhanced sedimentation of organic material in the vicinity of culture units (Hall et al., 1990; Jaramillo et al., 1992). Previous *in*

situ observations at the study site indicated that the surface of the sediment was fine grey flocculent material, which Holmer (1991) attributed to mussel faecal matter. However, the current results at Site S suggest that the impact of the mussel farm on the surrounding environment is minimal with only slight (ecologically insignificant) alterations to the benthic community and physico-chemical structure of the surficial sediment. The observed changes cannot be attributed to the farm and could be as a result of natural variations in the environment.

An interesting feature of the benthic faunal data is the uniformly low ITI values (16 – 26). These values would normally be understood as indicating degraded or enriched conditions. However, this is apparently not consistent with the moderate organic carbon concentrations in the sediment (~3%) and the positive redox potentials. In a review of Scottish Sea Lochs, Tett (1986) found that small lochs, such as the one studied, contained enhanced chlorophyll concentrations, which suggested substantial excess of phytoplankton growth over losses within the loch. Thus it is possible that the area surrounding the farm is subject to a high rate of natural sedimentation, to which the mussel biodeposits provide only a small further addition of material to the seabed. This could provide a possible explanation for the similar results between the raft stations and the control located away from the farm site, but within the same embayment. Grenz *et al.* (1990) suggested that a possible reason for not observing any effect of a mussel farm on the benthos below was that the deposition of bloom phytoplankton might confound the effects of biodeposits on the sediment organic matter.

5.2 Site A

At site A, the seabed sediment was characterised by soft glutinous mud with *Nephrops* burrows and (possibly) *Maximullaria* casts (Nickell, pers.comm.). The characteristic grey flocculent faecal matter commonly reported at mussel farm sites was not seen at this Site. Benthic conditions at Site A appeared unimpacted.

The benthic infauna at Site A showed ITI values around 50 at all sampling stations, and the dominant species did not change with distance from the farm. Sediment

characteristics did not change between stations, showing a high proportion of fine-grained material at all stations. Organic carbon concentrations were ~3% and did not change between stations.

Similar lack of impact on the seabed was reported by Baudinet *et al.* (1990) and Grant *et al.* (1995). Both studies concluded that biodeposits from the respective mussel farms had little impact on the benthos. The alterations observed by Grant *et al.* (1995) were attributed to fall-off from the mussel lines, but changes caused by organic enrichment were considered minimal.

5.3 Site B

In contrast to Sites S and A, the fauna at Site B showed marked changes with distance from the farm. The community was degraded beneath the farm (ITI value 15) but was relatively healthy 20m from the farm (ITI value 47). At the station furthest from the farm, the ITI value was 54. Beneath the cages, the dominant species were surface and sub-surface deposit feeders such as *Ophryotrocha*, *Aphelochaeta*, and *Tharyx* sp. At stations further from the farm, the dominant species were Gammarid amphipods. These changes are consistent with the effects of high rates of faeces and pseudofaeces sedimentation beneath the mussel lines and extending ~15m away from the ropes.

The percentage of fine-grained material in the sediment also decreased significantly with distance from the ropes, as did the organic carbon concentration in the sediment (to a lesser degree). Sediment redox values were positive at Station C, but were negative at more than 1 cm depth at Stations A and B.

The results for Site B are broadly comparable to those obtained in previous studies of benthic effects of suspended mussel culture, which generally demonstrate a reduction in macrofaunal diversity beneath mussel farms (Tenore *et al.*, 1982, Mattson and Linden, 1984; Kaspar *et al.*, 1985; Jaramillo *et al.*, 1992).

Dahlback and Gunnarson (1981) and Tenore *et al.* (1982, 1984) showed high rates of faeces and pseudofaeces sedimentation beneath mussel lines, which are consistent

with the observations at Site B. Increased sedimentation through biodeposition increased surficial sediment organic matter (Kaspar et al., 1985) leading to an impoverished benthic community around the culture site in a sediment consisting of organically enriched fine grey flocculent material.

5.4 Discussion

Alteration of macrofaunal community structure by organic enrichment has been a keystone of benthic environmental studies (Findlay et al., 1995) since the seminal review of Pearson and Rosenberg (1978). Biodeposits from mussel farms were shown to affect the benthic infaunal community of the surficial sediment at one of the three sites studied, where the benthos was clearly subjected to elevated levels of sedimentation and organic enrichment. The effects were localised and the community was similar to communities typical of unaffected conditions beyond a 40-m radius of the farm site.

Conversely, at the remaining sites, no alterations of the community structure were observed and an infaunal community typical of background conditions appeared to persist under the farms.

It is clear that the degree and extent of effects from mussel cultures differs considerably between locations. A number of factors have been suggested for explaining these differences including age of farm, stocking densities on ropes, physical structure of farm (density and orientation of ropes, distance from the bottom, hydrodynamics, sediment adsorption, etc.

Published literature on the benthic effects of mussel farms fall into three categories:

- those which identify a significant alteration in the bio-physicochemical structure of the surficial sediment surrounding the farm sites;

- those that do not observe any change in the environment that can be attributed to the mussel farms; and

- those that identify some changes in the near field environment. However, such alterations are not significant and whether they are a result of the mussel farm or natural variability is questionable.

Therefore, the results of the present surveys cover the range of previous observations, since the different sites showed differing degrees of impact from grossly affected (bullet 1) to no observable effect (bullet 3).

Probably the most important factor affecting the benthic infauna and the sediment characteristics is the intensity of deposition of particulate waste from the farm, and its magnitude relative to natural fluxes. The final depositional fate of faecal matter, and any subsequent impact, is the degree of dispersion of biodeposits from the farm site arising from tidal and other water movements. Information on current speed and direction, water depth and settling velocities of biodeposits are all required to examine this aspect, in accordance with the model proposed by Gowen *et al.* (1988) to simulate benthic impacts at mariculture sites. Additional factors that we considered important were the production tonnage of the farm and the food availability to the mussels (i.e. suspended particulate matter) prior to the time of sampling.

It is possible that resuspension of material could also affect the area over which the biodeposits finally settle. However, because of the low current velocities around the farms investigated, resuspension was probably not an important factor. Still, slight variations in current velocity and direction and water depth around the farm could have a great effect on the dispersion of biodeposits and thus on the rate of organic enrichment within the dispersion area.

Chapter 7 presents the validation of a simulation model developed from a model of salmon farming impact, DEPOMOD (Cromey *et al.*, 1998, 2000 a&b, 2002 a&b), which can be used to predict the benthic impact of mussel farms. It will also have the potential for separating sites on a quantitative basis, with respect to input to the sediment and response by the benthic community. The model will provide a useful

management tool to aid in the establishment of appropriate biomass limits for culture units and in site selection, monitoring and management of mussel farming.

6 Settling rate characteristics of mussel faeces and pseudofaeces

6.1 Introduction

The modelling of the dispersion and dilution of particulate waste from aquaculture units requires knowledge of the settling velocity of the ejected material. As discussed in Chapter 2, rapidly settling material will impact the seabed close to the farm, whereas slowly settling material will have a longer residence time in the water column and will be dispersed over greater distances.

The importance of settling velocity in this context was identified in classic papers by Gowen *et al.* (1988), who listed the three primary parameters of dispersion as settling velocity, current velocity and depth of the water column.

Published data on settling velocities of waste at fin fish farms are surprisingly scarce (examples of such publications are Chen *et al.* 1999 a&b and Cromey *et al.*, 2000a). The significance of this deficiency is discussed by Chen *et al.* (1999 a&b), in which they identify the need to update frequently the information in response to changes in the technology of feed production, and the composition of feed pellets.

A literature search early in this project failed to find any useful information on settling velocities of waste from cultivated bivalves that could be used in the context of the models discussed in Chapter 2. In order to adapt the models to mussel cultivation it was therefore necessary to make measurements of the settling velocities of particulate waste products from mussels.

As discussed in Chapter 1, mussels extract a mixture of living and non-living particles from the suspended material in the water column. Seawater is drawn through the gills where food particles are 'actively' selected and carried into the digestive system while unwanted material is bound with mucus, discarded and ejected from the shell (Bayne, 1976) as pseudofaeces. Waste material emerging from the end of the alimentary canal is voided as faeces.

The net result of these processes is that natural suspended matter is repackaged in large units (faeces and pseudofaeces) which will tend to have a lower organic content (and therefore higher density) than the original material. Both of these factors will increase the settling velocity above that of the original suspended matter (Simpson, 1982).

An experiment was therefore designed to measure the settling velocities of waste pellets derived from mussels feeding on measured concentrations of a unicellular alga. The experiment was carried out in the presence of different concentrations of inorganic silt-sized material in order to mimic possible field conditions and to encourage the production of pseudofaeces.

6.2 Materials and methods

Mussels were obtained from a mussel farm in Loch Etive, Argyll. Fine grained, largely inorganic material was obtained by seiving muddy sediment from Loch Etive through a 63 μm sieve. A stock algal culture (*Nannochloris atomus*) was supplied by Seafish Laboratory, Ardtoe, together with nutrient solution to allow the production of sufficient numbers of cells for the subsequent experiments.

6.2.1 Algal culture

The stock solution was sub-cultured into two 10 litre glass containers (fish tanks) and was kept at 15°C under continuous illumination for 6 days. The concentrations of algal cells were monitored by counting by microscope using a standard haemocytometer. At the end of the 6 day cultivation period, the cell concentration had attained 450,000 cells l^{-1}.

6.2.2 Experimental arrangement

The mussels were acclimatised to the laboratory for a week prior to the experiments, during which time they were not fed. Experimental batches of mussels were suspended on plastic mesh in the upper parts of 500 litre glass aquaria, containing 70

cm depth of water (Figure 6.1 a and b) in a constant temperature environment at 8°C (± 1 °C). A measuring scale was supported vertically in the centre of the tank in such a way that subsequent measurements would not be distorted by refraction of light. Observations of settling were made over the middle of the tank to avoid possible drag effects from the sides, shear effects from the bottom, and to allow time for the pellets to attain constant velocities (Chen, 1999a).

The mussels were continuously observed for periods of up to 20 hours by a time-lapse camera (one frame per second) and video recording system. The recording used a CCTV camera (Panasonic WV-CL350 CCTV camera) with a close-up lens (Panasonic WV-LA6A 1:1.4 auto iris). This was connected to an on screen timer (Horita II TG-50) and monitor and the output was recorded onto video format (Panasonic AG-6720A SVHS) (Figure 6.2 a and b).

The tank was illuminated by a high-powered light source from the side of the tank and a reflective light board was placed behind the tank to increase luminescence. This set-up was found to produce the greatest contrast between the water and the faecal material being ejected from the mussels.

Trials were conducted at the FRS fish behaviour unit in Aberdeen.

6.2.3 Experimental procedure

Approximately 20 mussels (mean shell length 41.5 mm) were initially placed into empty aquaria. Aliquots of suspensions of algae (and sediment, as necessary) were added to the tank, and then clean seawater was added to give the appropriate dilution factors (Table 6.1). The tanks were aerated to keep the particulate matter in suspension, and the mussels were allowed to feed for 2 hours. After this time, aeration was discontinued and video observation began. Experiments were terminated when production of faeces had declined to low levels due to the reduction in the food concentration in the aquaria and passage of material through the gut of the mussels.

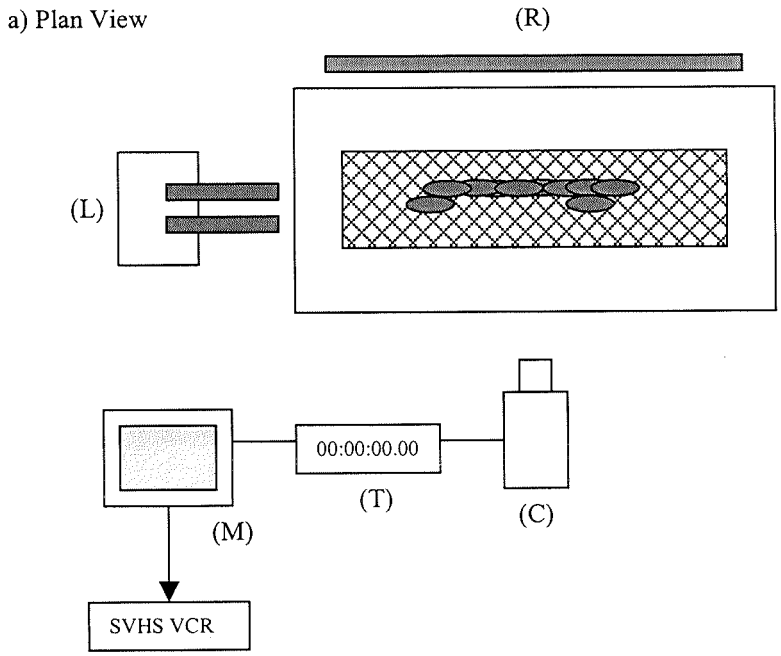

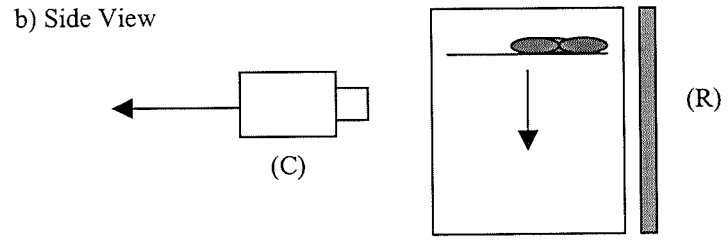

Figure 6.1 (a and b) : Schematic diagram of the experimental set-up. (Not to scale)
Key – (C) CCTV camera, (T)Timer, (M) Monitor, (L) High powered light source and (R) Reflective lightboard.

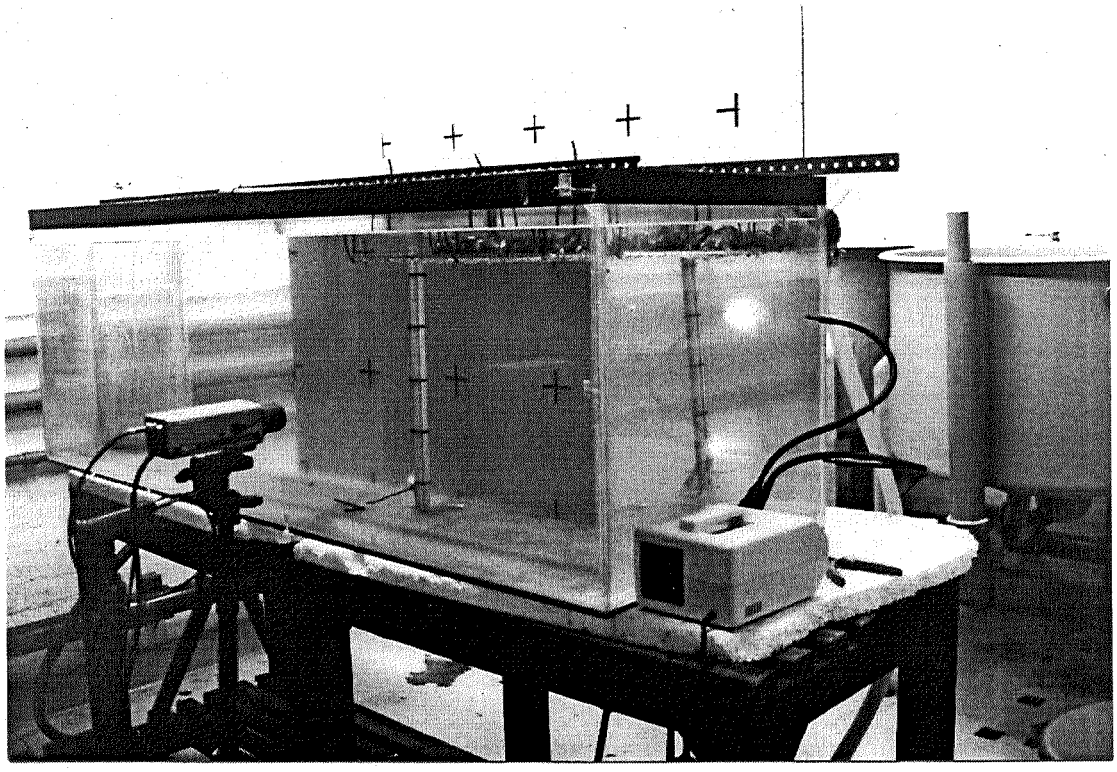

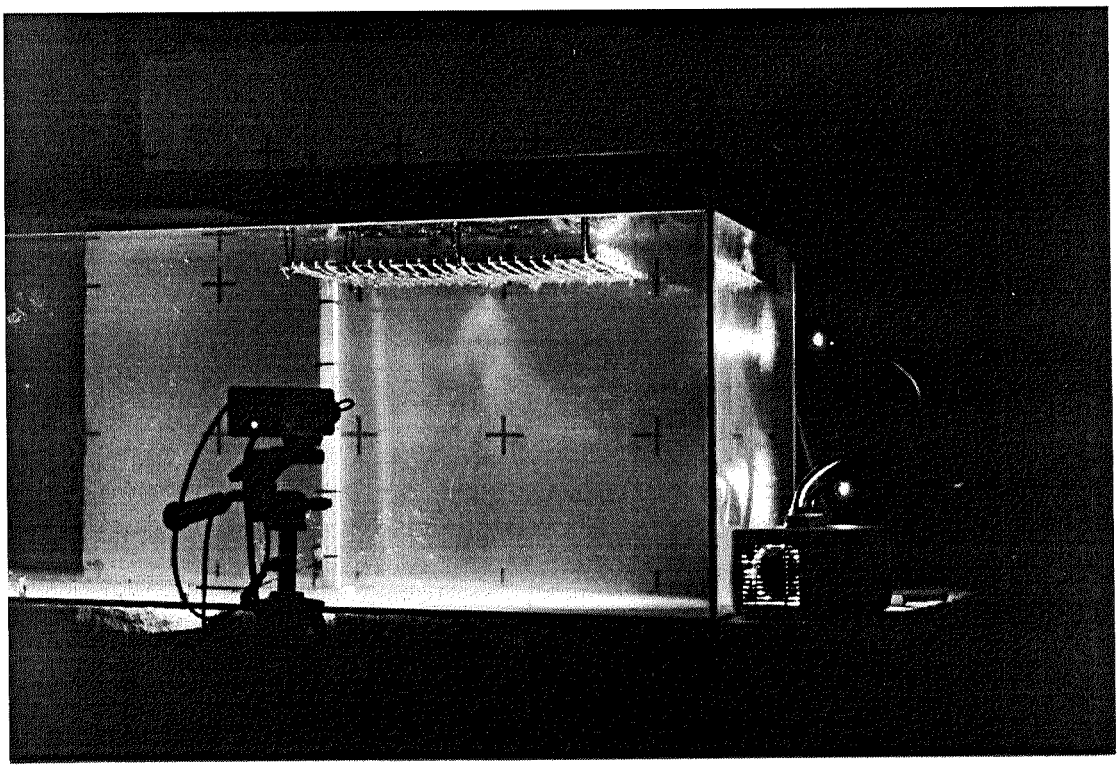

Figure 6.2 (a and b) : Photographs of the experimental set-up. a) prior to start of experimental run and b) during the experiment.

A number of experiments were conducted at different concentrations of algal cells and silt covering a wide range of conditions. Additionally, a number of test runs were also conducted to ensure that the experimental design was set-up correctly. The results from four experiments are presented, covering two concentrations of algal cells and three levels of silt (Table 6.1). The concentrations of algae and silt were similar to those used by Kiorboe *et al.* (1980) to examine the feeding, particle selection and carbon absorption of mussels, and were reported to be sufficient to induce a feeding response and thus excretory products.

Table 6.1 : Concentrations of algae and silt in the suspensions presented to the experimental mussels in each run.

Video tape reference	Concentration of algae (cells ml^{-1})	Concentration of silt (mg l^{-1})
Run 2.2	20000	0
Run 2.3	10000	50
Run 2.5	10000	25
Run 2.7	10000	10

6.2.4 Interpretation of Recorded Results

After the experiments had run to completion (no further production of faecal material), the video recordings were examined. Each recording was found to contain records of hundreds of particles settling through the water column past the measuring scale. Timings were automatically recorded on the video frames. It was therefore necessary to select particles for measurement, and to take particular care to avoid bias in the sampling, for example selection of large, bright particles. Criteria were established as follows:

1. Select every fifth particle entering the measuring zone.
2. Discard particles that did not clearly leave the 20 cm deep measuring zone.
3. Discard particles that appeared to be affected by turbulence (rare).
4. Discard particles that appeared to interact with other particles, e.g. a rapidly moving particle might collide with a more slowly settling particle.
5. Discard particles that had air bubbles entrained on their surfaces.

Typical settling times over the 20 cm measuring zone varied from 20 – 200 seconds. These settling times were then converted to settling velocities (cm s^{-1}) using the following formula:

$$Settling\ Velocity\ (cm\,s^{-1}) = \frac{20}{Settling\ Time\ over\ 20\ cm\ (s)}$$

6.3 Results

The raw settling velocity data (cm s^{-1}) are summarised in Table 6.2.

Table 6.2 : Summary statistics of particle settling velocity data (cm s^{-1}) for each experimental 'run'. (Note: For experiment 'run 2.3' there are two modal values reported, as there was a bi-modal distribution of settling velocities)

	Run 2.2	Run 2.3	Run 2.5	Run 2.7
Mean	0.27	0.64	0.34	0.29
Standard Error of mean	0.01	0.02	0.02	0.02
Median	0.24	0.59	0.27	0.22
Mode (from histograms)	0.2-0.3	0.5 - 0.6 1.0 - 1.1	0.2-0.3	0.2-0.3

These data were subsequently classified into velocity ranges at 0.1 cm s^{-1} intervals (Table 6.3). These are also presented as percentages of particles showing settling velocities within each 0.1 cm s^{-1} bin size in Figures 6.3 – 6.6.

In the four experimental runs, settling velocities of individual particles varied from <0.1 cm s^{-1} to 1.8 cm s^{-1}. In all experimental runs, most of the particles settled at <1.0 cm s^{-1}. The mean and median velocities in experiments 'run 2.2' (algae) and 'run 2.7' (algae plus 10 mg l^{-1} silt) were not significantly different. The mean and median velocities in experiment 'run 2.3' (algae plus 50 mg l^{-1} silt) were greater than in the other experiments. The results from this experiment also showed a clear bimodal distribution of velocities, with one mode at 0.5 – 0.6 cm s^{-1} and another at 1.0-1.1 cm s^{-1}.

Table 6.3 : Frequency analysis (counts and percentages) of the particle settling velocity data classed into 0.1 cm s^{-1} bin sizes.

	Run 2.2		Run 2.3		Run 2.5		Run 2.7	
Bin	Frequency	Percentage frequency (%)	Frequency	Percentage frequency (%)	Frequency	Percentage frequency (%)	Frequency	Percentage frequency (%)
0.0	0	0.00	0	0.00	0	0.00	0	0.00
0.1	15	11.36	2	1.19	13	7.65	9	6.82
0.2	37	28.03	2	1.19	47	27.65	54	40.91
0.3	32	24.24	15	8.93	38	22.38	20	15.15
0.4	26	19.70	21	12.50	24	14.12	28	21.21
0.5	17	12.88	25	14.88	16	9.41	8	6.06
0.6	1	0.76	22	13.10	13	7.65	2	1.52
0.7	0	0.00	17	10.12	1	0.59	2	1.52
0.8	2	1.52	13	7.74	10	5.88	3	2.27
0.9	1	0.76	9	5.36	4	2.35	0	0.00
1.0	0	0.00	30	17.86	0	0.00	6	4.55
1.1	0	0.00	0	0.00	0	0.00	0	0.00
1.2	1	0.76	4	2.38	2	1.18	0	0.00
1.3	0	0.00	3	1.79	0	0.00	0	0.00
1.4	0	0.00	0	0.00	0	0.00	0	0.00
1.5	0	0.00	3	1.79	0	0.00	0	0.00
1.6	0	0.00	0	0.00	0	0.00	0	0.00
1.7	0	0.00	2	1.19	2	1.18	0	0.00
1.8	0	0.00	0	0.00	0	0.00	0	0.00
1.9	0	0.00	0	0.00	0	0.00	0	0.00
2.0	0	0.00	0	0.00	0	0.00	0	0.00
2+	0	0.00	0	0.00	0	0.00	0	0.00
Total	132	100	168	100	170	100	132	100

6.4 Discussion

The settling velocities experiment 'run 2.2' can be assumed to represent the settling of 'true' faeces derived from organic material (i.e. the feed algae). The concentration of algal cells was not high and would not be expected to give rise to substantial amounts of pseudofaeces, particularly following a period of starvation (Bayne, 1976). The mean settling velocity observed in experiment 'run 2.2' (0.27 cm s^{-1}) is very similar to that for experiment 'run 2.7' (0.29 cm s^{-1}). It may be concluded that either the

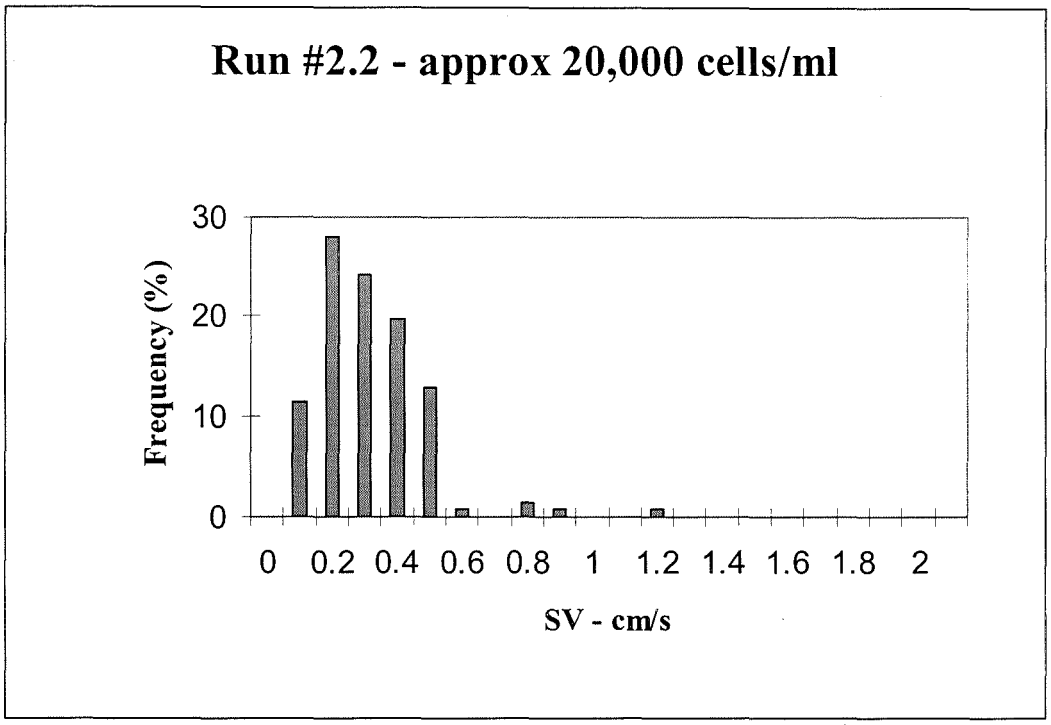

Figure 6.3 : Percentage frequency histogram of distribution of settling velocities for experiment 'run 2.2'.

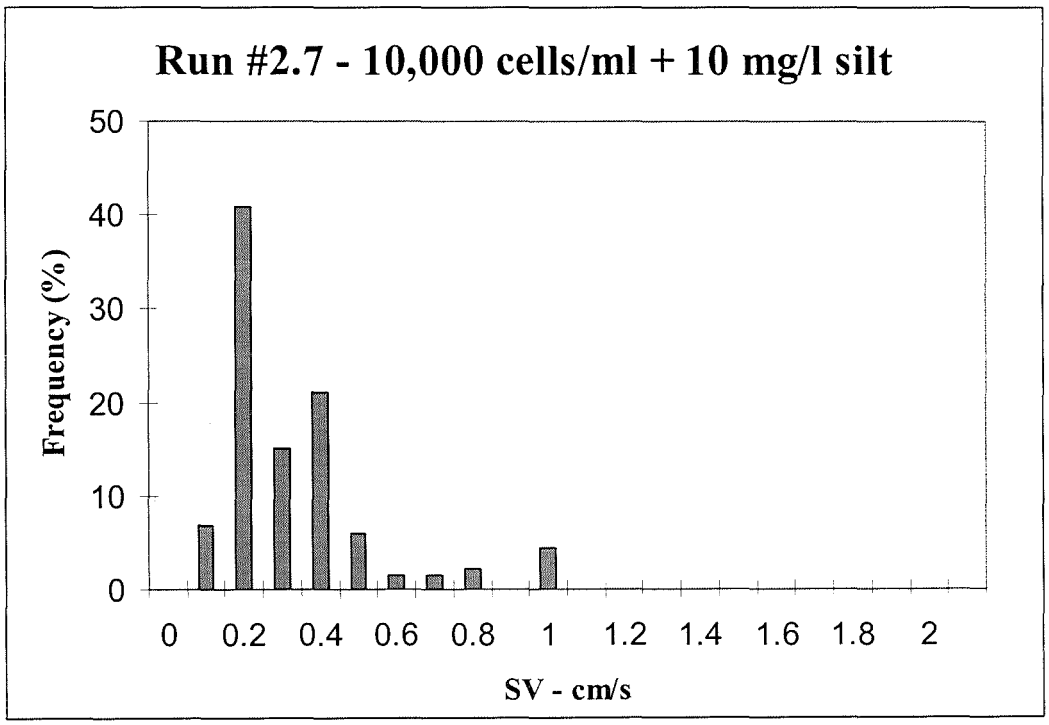

Figure 6.4 : Percentage frequency histogram of distribution of settling velocities for experiment 'run 2.7'.

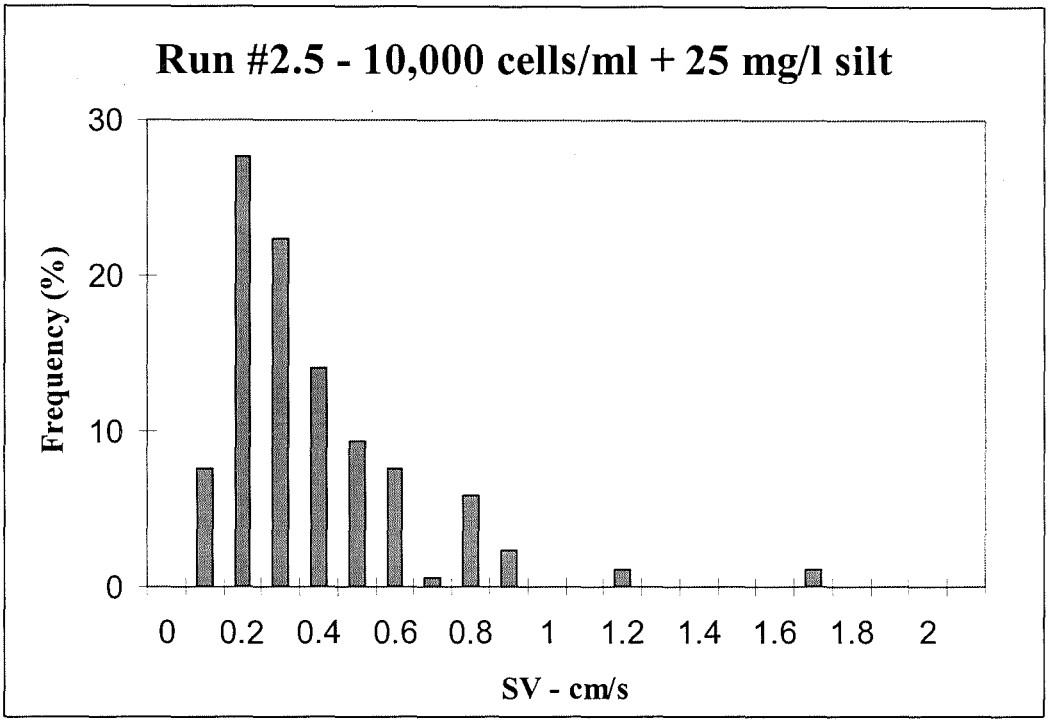

Figure 6.5 : Percentage frequency histogram of distribution of settling velocities for experiment 'run 2.5'.

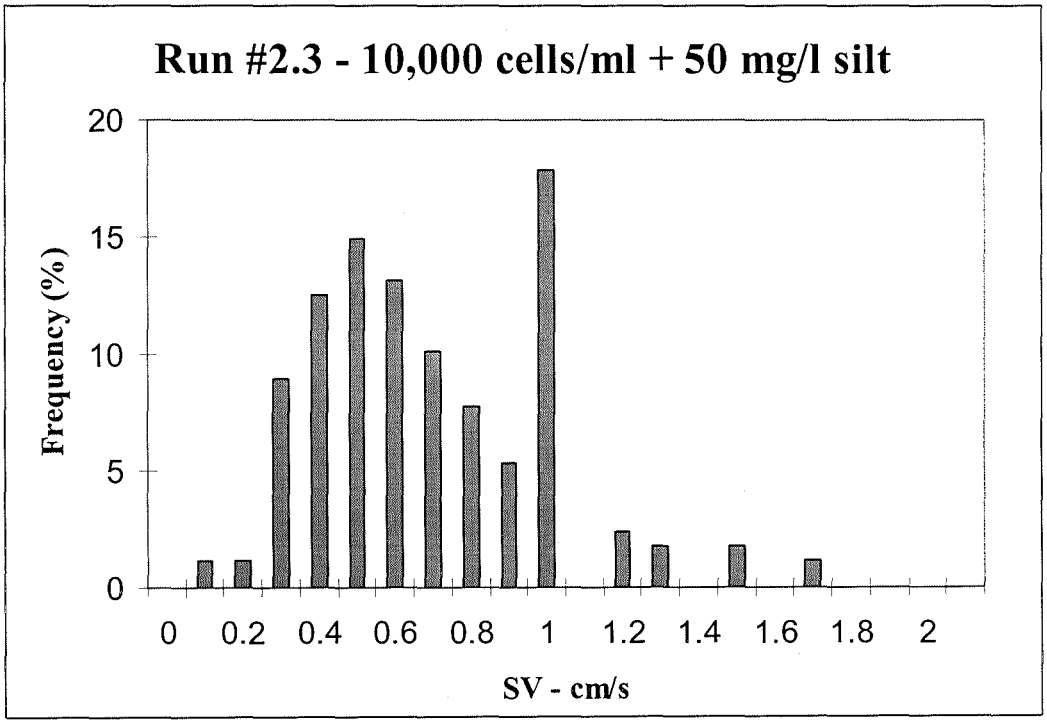

Figure 6.6 : Percentage frequency histogram of distribution of settling velocities for experiment 'run 2.3'.

faeces in experiment 'run 2.7' were predominantly organic, or that the presence of 10 mg/l^{-1} inorganic silt made little difference to the settling characteristics of the waste.

In contrast, the data for experiment 'run 2.3' (50 mg l^{-1} silt) show two modal values of settling velocities at 0.5 – 0.6 cm s^{-1} and 1.0 – 1.1 cm s^{-1}. Pseudofaeces, which are generally larger particles than faeces (Bayne, 1976), comprise of large and non-digestible material that tend to be excluded from the digestive system through particle selection in the gills. The accumulation of this material in pseudofaeces could lead to large, dense particles of higher settling velocity. It can therefore be suggested that the mode at 1.0 - 1.1 cm s^{-1} represents pseudofaeces. The higher quantity of silt in this experiment would be expected to promote the formation of pseudofaeces (Bayne, 1976).

The lower mode in experiment 'run 2.3' (0.5 – 0.6 cm s^{-1}) is considerably higher than the modes attributed to faeces in experiments 'run 2.2' and 'run 2.7' (and 'run 2.5'). It is likely that this material is also faeces, and that the increase in settling velocity is due to incomplete separation of organic and inorganic material by the gills, and the subsequent incorporation of silt in the faeces. This will increase the density of the faeces, and increase the settling velocity, in accordance with Stoke's Law.

The above settling velocities will be used in the adaptation of the DEPOMOD model to mussel farms (Chapter 7). Comparisons may be made between the settling of mussel waste and that of waste at fish farms. As would be expected, the settling rates of salmon feed pellets (5 – 15 cm s^{-1}; Chen *et al.*, 1999a) are substantially greater than those of mussel waste recorded in this experiment. Mean settling velocities of salmon faecal pellets (5.3 – 6.6 cm s^{-1}; Chen *et al.* 1999b) are also much greater than those of mussel waste. It can therefore be predicted that waste from mussel farms will be dispersed over a much greater area than waste from salmon farms.

In developing the experiments described in this chapter, no attempt was made to make direct use of Stoke's Law to predict or analyse settling velocities.

Stoke's Law:

$$u = \frac{1}{18} \frac{g(\rho_p - \rho_f)d^2}{\eta}$$

[i.e. the settling velocity is proportional to the difference in density between the particle and the fluid, and to the square of the particle diameter]

where u is the velocity of fall (cm s^{-1}), g is the acceleration of gravity (cm s^{-2}), d is the diameter of the particle (mm), p_p and p_f are the densities of the particle and medium respectively and n is the viscosity of the medium.

Theoretical considerations of the likely variability in the shape, composition and degree of aggregation of faecal material, and the difficulties involved in making appropriate measurements of these parameters argued against such approaches. Other practical studies have found that Stoke's Law gave large over-estimates of the settling velocity of faecal pellets from small freshwater invertebrates (amphipod, dipteran larvae; Ladle *et al.*, 1987). Hawley (1982) noted that Stoke's Law was directly applicable only to slowly falling impermeable spheres. Natural particles, and aggregations of particles, often deviated greatly from these characteristics. As a consequence, whereas Stoke's Law indicates that settling velocity is a function of the square of the particle diameter, measurements on oceanic aggregates had found that the data were best fitted by a wide range of exponents from 0.6 – 1.2. Mud aggregates show exponents in the range 0.4 – 1.0 (ten Brinke, 1994). It was therefore concluded that it would not be productive to attempt to utilise Stoke's Law and that subsequent modelling would be based upon direct empirical measurements.

7 Modelling of Benthic Impacts

7.1 Introduction

The theory and assumptions of simulation models forecasting the impact of fin fish farms on the benthic environment were introduced in Chapter 2. As discussed, the majority of these models are based on the concept of (Lagrangian) particle tracking, plotting the fate of simulated particles released into the water column and influenced by a number of parameters, including the depth of water, current speed and direction and settling velocity of the particles.

For the purpose of the work undertaken in this research, the fish farm impact model 'DEPOMOD' (v.2.1) (A model for predicting the effects of solids deposition from mariculture to the benthos) developed by Cromey *et al.* (1998, 2000 a&b, 2002 a&b) was used as a platform from which to develop a predictive model of the impacts from mussel farms. DEPOMOD is a fully validated particle tracking model with resuspension and benthic component. DEPOMOD's original specification was to predict the solids deposition on the seabed arising from fish farms. DEPOMOD was developed at the Dunstaffnage Marine Laboratory and is currently used by the Scottish Environment Protection Agency for setting the discharge consent limits on in-feed anti-parasitic chemotherapeutants at marine cage fish farms.

The model simplifies and unifies hydrography, sediment dynamics and benthic impact so that it may be used as a management or regulatory tool. Additionally, and more importantly for this current project, both the input and output parameters of the model may be manipulated to allow the adaptation of the model. Irrespective of the source of particles to the water column, the initial deposition of particles on the seabed is predicted using a Lagrangian particle tracking model. Subsequently, a resuspension model is utilised to redistribute particles across the model grid according to the near – bed current flows to predict the net solids accumulated on the seabed within the grid area. Thus, DEPOMOD was a suitable base from which to develop methods for modelling the benthic impacts of mussel farms.

DEPOMOD was developed from the model BENOSS (Cromey *et al.*, 1997) which forecast the deposition of solids and biological effects of excess carbon from sewage discharges. Although this type of discharge may seem very different to that from mussel farming, the processes are subject to the same hydrographic and modelling principles. Particles are released into the water column and the model tracks each particle in relation to the applied current regime over a defined number of time steps.

The purpose of this chapter is to describe the processes involved in the adaptation of DEPOMOD for the prediction of benthic impacts of mussel farming. Initially, a description of the structure and functionality of DEPOMOD as configured for fish farming is presented. A series of necessary adaptations for mussel farming are identified and the processes behind these modifications are described. The assumptions and associated errors involved in these modifications are discussed. These modifications are incorporated into the model, which is then run for each of the field survey locations under different scenario conditions and comparisons are made between the simulations and the field data.

7.1.1 General modular structure

The overall structure of DEPOMOD is made up of four separate modules, all of which were retained in the modified version for mussel farming:

- Grid Generation, which generates a grid for the area of interest
- Particle Tracking, which simulates the deposition of the faecal particles
- Resuspension and Carbon Degradation, which resuspends and degrades the carbon (or other factor of the particles)
- Benthic Processes, which relates a general benthic community structure to the carbon available

These modules stand alone and operate as separate entities. Each module has a series of configuration files that contain the input data conditions and variable settings

specified by the user for the module run, together with general files that contain data required for the complete model.

Each module produces data that are used by following modules, files containing the set up information for a particular model run and general files (e.g. files for contouring).

This type of modular structure has the advantage of avoiding the need for having one large input data configuration file containing all the information for each process (module). In addition, the modules may be run in sequence, or a single module may be run several times with different input parameters before proceeding to the next process. It also allows the user to check information after a run to confirm that the desired input conditions have been used before proceeding to the next module. On a technical level, each module is a separate executable file. Therefore, all available memory can be allocated to each module, decreasing the time required for the models to run to completion (Cromey *et al.*, 2000a).

7.1.2 Model output and contouring

DEPOMOD does not generate contour plots of results as there are many commercial applications that can be used to produce these. It is important to choose the correct contouring algorithm and spacing of nodes in the contouring scheme. The *Kriging* algorithm has been found to consistently produce satisfactory results for DEPOMOD grids. Cromey *et al.* (2000a) suggest that satisfactory results are obtained when the spacing of grid nodes in the scheme are half that of the DEPOMOD grid resolution (e.g. DEPOMOD grid resolution = 25 m, contour grid node spacing = 12.5 m). In addition, it is useful to set the limits of the contour grid so that it starts at (0,0) rather than (12.5,12.5), as will be the case with a DEPOMOD grid of 25 m resolution if default values in the contour grid limits are accepted.

By using the minor grid *x, y, z* file produced in the grid generation module, a post map can be generated and overlaid onto the contour plot so that farm positions and sampling station positions can be seen on the contour plot. The user should select contour levels with caution, ensuring that unnecessary contours are not included, e.g.

for ITI calculation contours of 1, 10, 30 and 55 are suitable. For solids accumulation, the minimum contour level used may be 1 g m^{-2} yr^{-1}, but the user may prefer to eliminate this contour due to the high level of intricate (and probably not meaningful) detail generated by the contouring package at this level.

Additional features of contouring packages may also be useful in the analysis of the results. Many packages include a tool for analysing the grid volume and surface area of the results. This can be used for determining the mass or surface area of material between 2 contour levels or for the whole grid.

7.2 Grid Generation

The objectives of this module are:

- to create a major grid containing bathymetry, farm site and sampling station location and any additional information
- to create a major grid depth array and input data files
- to generate a minor grid which is used in subsequent modules

The grid generation module takes user defined input data of bathymetry, farm and sampling station positions and generates a sea bed depth array which is used by the particle tracking and resuspension modules. A major grid is first created covering the overall area of interest. With experience, a reasonable estimation of the potential area of impact can be deduced through examination of the site hydrographic and bathymetric data. A minor grid with finer resolution nodes is then defined on areas where deposition is likely to occur. It is possible that the major and minor grids are virtually the same size (the major grid by default has to be larger than the minor grid). Once a major grid has been created, the minor grid can be generated in different areas if required.

The horizontal and vertical minor grid dimensions can be set to different lengths allowing the grid to be elongated along the main axis of flow and eliminating largely unused areas that would be present in a square grid.

Cromey *et al.* (2000a) suggest that fine resolution of the minor grid (e.g. 5 metre cell dimensions) is desirable where the majority of the predicted sphere of influence is expected to be less than 100m away from the farm and the spacing of sampling stations is small. If a predicted sphere of influence is expected to be large, minor grid cell resolution can be increased (e.g. 20 metre cell dimension).

The algorithm in the grid generation model interpolates linearly between master grid nodes to determine the depth at each minor grid node in the area of interest (the interpolation methodology is described later in this section). Some inaccuracies will occur in areas of unusual or dramatic bathymetry and the spatial scales on both the major and minor grids should be small in these cases.

In addition to water depths, land cells are also defined in the major and minor grids. In the particle tracking module, when a particle enters a land cell, the particle is moved back to its last position in the particle sequence.

7.2.1 Major and minor grid cell resolution

It is practical to generate a major grid that contains a large proportion of the predicted footprint without the need for extension once initial runs have been undertaken. Although some estimate of the size of the grid necessary may be estimated from settling velocity, depth and maximum current speed, the bathymetry at the site will often indicate the grid size necessary. Cromey *et al.* (2000a) suggest that at most sites a cell resolution of 10 or 25 m is adequate. When using fine cell resolution (e.g. 5 m), often the total number of particles used in the particle tracking model needs to be increased to prevent unrealistic patchiness occurring in the grid.

7.2.2 Modelling Procedures

A major grid is created in the area surrounding the fish farm and the depths and positions on the grid are determined. The following data are required for a major grid:

- major grid dimensions (grid cell sizes and number of cells along each axis)
- bathymetry of the maximum area of interest including any land points
- all pen positions or the positions of end pens in a line or group
- sampling station positions

It should be noted that the grid orientation, which is true north, is orientated towards the top of the output. The coordinate system is in metres in the user interface, but is converted into special grid coordinates by the model. This grid coordinate system is used throughout all modules and the particle positions are tracked in these special grid coordinates to save time in processing.

7.2.3 Generation of Major and Minor Grid arrays from Admiralty Chart Bathymetry

A suitably sized area surrounding the farm site is identified (in most cases, the farm being at the centre of a 1 km^2 square will be sufficient depending on the expected sphere of influence from the farm). A grid (orientated with the vertical axis on a north-south axis and the horizontal axis on an east-west axis) is then overlaid on the area and the iso-baths and spot depths in the grid are recorded. Land boundaries are assigned a value of '4 m' (this value exceeds the height of mean sea level above chart datum throughout Scotland). Latitude and Longitude positions should be converted into Eastings and Northings using suitable software for the area. The x and y distances of these points from the origin (in metres) are then calculated and transferred to a spreadsheet format (e.g. *Excel*) to create a comma delimited file of all the x, y and z points.

These data are then converted into a grid format using the mapping package '*Surfer*' (Golden Software) and employing the '*Kriging*' method of interpolation. The grid line geometry is set to half the desired major grid array spacing (typically 12.5 m to produce a 25 m grid). The grid node editor function in *Surfer* is then be used to examine the interpolation grid. Interpolated values are assigned to nodes that correspond to distances from the origin. However, the DEPOMOD major grid array requires these values to reside in the centre of the i and j cells. These points can be determined as the bathymetric data was contoured at twice the desired major grid spacing. Using the '*Extract*' function in *Surfer*, the point in the centre of the first grid can be identified and every second node selected.

7.2.4 Interpolation method for depths from major to minor grids

The algorithm in the grid generation interpolates linearly between major grid nodes to determine the depth at minor grid nodes, as detailed below. This algorithm is also the most accurate for minor grid dimensions smaller or equal to major grid dimensions.

7.2.4.1 Grid generation interpolation

The depth at x_i y_i for the minor grid is interpolated from the four nearest major grid points to it (Figure 7.1).

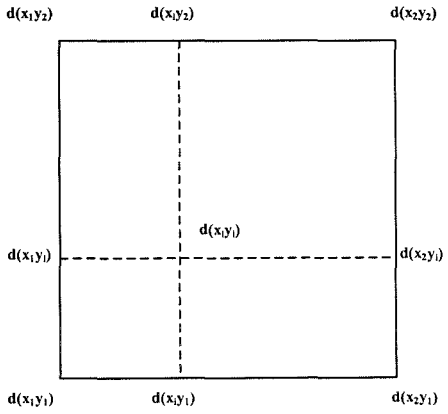

Figure 7.1 : Schematic diagram illustrating depths (d) at coordinate points x and y which are used in the interpolation algorithm

A weighting along both the x and y direction is calculated as follows:

$$gradx = \frac{(x_i - x_1)}{(x_2 - x_1)} \qquad \text{Eq. 7.1}$$

where $gradx$ = weighting of point x_i between two points x_1 and x_2 and

$$grady = \frac{(y_i - y_1)}{(y_2 - y_1)} \qquad \text{Eq. 7.2}$$

where $grady$ = weighting of point y_i between two points y_1 and y_2

Therefore, to determine a depth (d) at a coordinate specified:

$$d(x_i y_2) = d(x_1 y_2) + gradx \qquad \text{Eq. 7.3}$$

Between these two points $d(x_i y_2)$ and $d(x_i y_1)$ the point $d(x_i y_i)$ can be determined

$$d(x_i y_i) = d(x_i y_1) + grady(d(x_i y_2) - d(x_i y_1)) \qquad \text{Eq. 7.4}$$

7.2.4.2 Grid Generation Module Output

This module produces a grid of the bathymetric conditions (including land boundaries) around the farm site for use in the Particle tracking and Resuspension modules. In addition the location of the farm site (the source) and sampling stations are also plotted onto the grid for use in the subsequent modules and overlaying on the final output plot.

7.3 Particle Tracking

The objectives of this module are to:

- read in a minor grid generated from the grid generation module
- simulate release of particles from the farm to the water column

- simulate differential settling and advection of particles using applied hydrographic data and turbulence via a random walk model
- deposit particles on the sea bed and pass information on particle distributions to the next module

A Lagrangian particle tracking method is used to simulate the settling of particles and their movement through the water column. The processes involved are summarised below:

- Differential settling of particles of different sizes and settling velocities
- Advection of particles in water currents in two horizontal dimensions
- Simulation of turbulence in three dimensions via a random walk process (see Chapter 2 and Random walk Section 7.3.1.4)
- Deposition of particles on the sea bed

For a successful model run to be completed, the particle tracking module requires hydrographic data, representative of the site, and waste allocation data defining the release of material from the farm site.

A large number of particles are used to simulate the waste material and requires information on the feed input, conversion factors and relative excretion values. The particles are then assigned settling velocities depending on the type of waste material and are subject to settlement through the water column. The particles' start position is randomly defined within the cage or farm structure after which they are advected in two dimensions by the water current. Particles are subject to random walk in a horizontal and vertical direction as a representation of turbulence (described in Section 7.3.1.4). Particle trajectories are evaluated either every 600, 60 or 6 seconds (user defined) allowing regular checking of the particles' positions both horizontally and vertically. Particles can pass into a different grid square or into a different current layer, thereby allowing a change in trajectories as particles pass into different current regimes. The particles are then deposited onto the seabed and information on particle distribution on the bottom is passed to the resuspension module.

The settling velocities used in the model were taken from the values measured in the experiment described in Chapter 6. A mean value with standard deviation limits was defined and each time a new particle was assigned in the model, a settling velocity was taken from this distribution. This approach is advantageous over using a single settling velocity as it represents more accurately the range of settling velocities associated with different shape and diameter faecal particles Cromey *et al.* (1999).

A mean tidal height is added to the charted depths in the grids. No changes in elevation are modelled in DEPOMOD as mean sea level is used. The model is generally insensitive to elevation changes caused by the settling velocities used and in particular, where the depth of water column is large in proportion to the tidal range (Cromey *et al.*, 1999).

7.3.1 Modelling Procedure

7.3.1.1 Current Advection

If the current regime is reasonably homogenous with depth then one velocity data set representative of the grid area may be sufficient. However, if the current regime is not homogenous then more than one data set will be necessary as current profiles in stratified waters can be extremely complex. Particles settling through the layers are subject to differential settling, turbulence and the shear of the current, leading to spatial sorting of particles of different settling rates. Generally, Cromey *et al.* (2000) found the use of hourly data from at least one spring-neap cycle to be practical in terms of availability and incorporation into the model. Current velocity data are implemented into the model as a number of layers. Each data set represents a layer that may have different current amplitude and direction to other layers. The resuspension model uses critical speeds measured between 2 and 4 metres above the bed (SCCWRP, 1992). If depth averaged speeds are to be used at a particular site, it should be determined whether they differ significantly from the current regime at this depth. Often, the use of observed data is a more accurate method of describing the water column than fitting an elaborate profile (e.g. logarithmic) to a single point data set. Additionally, many of these profiles are unsuitable for use in areas around mariculture operations where shear and stratification in the water column are high.

The hydrographic data can either be in easting and northing vector components (m s^{-1}) or speed (m s^{-1}) and direction (degrees, true or magnetic). However, the model calculates particle trajectories using vector components, so speed and direction data are converted. In addition, the model requires the mean tidal height, the magnetic variation of the area and the depth of water and the depths of each individual meter. Cromey *et al.* (1999) warn that, although collection and examination of 24 hour record of a site might give some general characteristics and qualitative information on a site, such a record can be merely a snap shot of conditions at the site and is inadequate for modelling purposes. For this reason, the authors recommend that a minimum record length of 1 spring-neap cycle (≈ 15 days) be obtained for DEPOMOD modelling studies.

7.3.1.2 Particle Tracking

In modelling the horizontal trajectory of a particle it is convenient to consider the current as a sum of two parts: a slowly varying component relating to tidal or wind forcing plus a more rapidly varying component relating to turbulence with a mean of zero. Given a time step (t) and a position of a particle defined as $P_{(x,y,t)}$ and velocity components u and v, then transport can be defined as:

$$P_{(x,y,t+1)} = P_{(x,y,t)} + transport\ in\ x\ direction + transport\ in\ y\ direction \quad \text{Eq. 7.5}$$

or alternatively

$$P_{(x,y,t+1)} = P_{(x,y,t)} + u_{(z,t+1)}\delta\ t + rw_{step(x)} + v_{(z,t+1)}\delta\ t + rw_{step(y)} \quad \text{Eq. 7.6}$$

In the vertical direction for a settling velocity of vs, the vertical step can be defined as:

$$P_{(z,t+1)} = P_{(z,t)} + vs\delta\ t + rw_{step(z)} \quad \text{Eq. 7.7}$$

Typically, δt is assigned a value of 60 seconds which is suitable for the settling velocities of the waste materials modelled. The model allows the user to specify as many particles as possible to represent the waste material. Generally the larger the number of particles used, the better representation of the cumulative particle

trajectories. Sensitivity analysis has shown that beyond a certain threshold further increases in particle numbers will result in an insignificant change in particle distribution as described below.

7.3.1.3 Particle numbers and particle trajectory evaluation

The use of the correct number of particles in a modelling run is important, as use of too few particles will result in unrealistic predictions and too many particles will increase the computation time. At the particle tracking stage it is necessary to determine the optimum number of particles so that the subsequent resuspension stage performs optimally. The resuspension model tends to increase the overall numbers of particles in the model run, as when erosion takes place it will be necessary to create resuspended particles that have similar properties to the bed particles from which they have been resuspended. For example, for a patch of bed particles of mass m^1, a resuspension event may cause resuspension of particles of mass m^2, in which case the bed particles are reduced by $m^1 - m^2$ so that mass balances are correct. Thus, particles have been created by resuspension, but are also lost when passing outside the limits of the grid. At sites where there is some resuspension, computational times may be long, as resuspension can create large numbers of particles in the model grid. For these sites, particle numbers in the particle tracking stage may be reduced to speed computation.

In general, it is useful to test the effect of increasing particle numbers, particularly if resuspension is expected to be low at the site. Undertaking runs at different particle numbers can test this. As a guide, developers have found the following formula to be useful:

$$No.\ particle\ types * No.\ time\ steps * No.\ cages * N_p = 5*10^4\ to\ 1*10^6 \qquad \text{Eq. 7.8}$$

Where *No. particle types* is the number of particle groups defined in the settling velocity dialog (e.g. faeces and pseudofaeces), *No. timesteps* is the number of time steps in the current velocity record (e.g. 360 for 15 days of hourly data) and N_p is the number of particles setting in the particle tracking input data dialog.

For most applications, it is necessary to evaluate a particle trajectory every 60 seconds in the trajectory model, and this has been set as default. This variable can be changed if necessary in the particle tracking main input dialog and can be simply explained by examining the settling velocity of the waste material. If a particle sinks through the entire water column in one step, then any change of current speed and direction with depth implemented in the model will not be applied to the particle as it moves from surface to the seabed in one vertical step. The effect of this time step is increased on coarse particles and so it is necessary to use 60 second time step to eliminate this effect. For these types of particles, the use of a 6 second time step was found to increase the computational time and, through sensitivity analysis, make no difference to the model predictions.

7.3.1.4 Turbulence

Random walk has been implemented into the model as a representation of turbulence. Important factors involved in determining the effects of this process on particle trajectory are (Allen, 1982)

- Size/direction of the random excursion
- Settling speed of the particle and thus the time in the turbulent field

$$rw_{step}(x) = rw_{dir}\sqrt{(2\,k\,dt)} \qquad \text{Eq. 7.9}$$

where:

rw_{step}	=	size of step (length)
rw_{dir}	=	step direction + or – (determined from a random number generator)
k	=	dispersion coefficient (length^2 time^{-1})
dt	=	time in turbulent field (time)

The direction of the random excursion is derived from a random number generator. The computer can generate the same sequence of random numbers for each subsequent run of the model. This allows the same results to be obtained after each run so that no variation occurs during model development due to randomness.

7.3.1.5 Shoreline and boundary effects

In the model, when a particle intersects a land point during the particle tracking stage, it is displaced back to its previous position in the grid (e.g. back 60 seconds of transport depending on the trajectory model time step). In the resuspension model, resuspended particles that are treated in the same way may also intersect shorelines and accumulate in these areas. Generally, accumulation on the shoreline is a result of the lack of accurate representation of spatially varying currents within the grid. In grids where there are headlands in the direction of residual current, accumulation of particles may occur. These are artefacts of the model, as in reality, flows around the headland would transport the particles around these features. However, in some cases, in the absence of protruding topography, particles may be found to deposit on shorelines. Cromey *et al.* (2000a) advise that it is up to the user to determine the accuracy of the model in these areas, taking into account the distance from the farm, the likelihood of spatially varying currents and the increasing potential for dispersion at greater distances from the farm.

A sensitivity analysis of the particle tracking module by Cromey *et al.* (2000a) identified that the model results were sensitive to the following variables (in order of priority):

- Particle starting position within farm structure
- Horizontal dispersion coefficient increase
- Inaccurate current meter readings
- Use of one settling velocity only

Particle starting positions in DEPOMOD are therefore random within the farm structure.

The computational run time for this module depends entirely on the number of particles being used and the computer numeric processor. It may take from 5 minutes

to 24 hours to run. If the module takes an excessive time to run, one or more of the following changes can be investigated:

- decrease the number of particles in the simulation
- generate another minor grid decreasing the minor grid size
- generate another minor grid increasing the minor grid cell dimensions
- use hourly averages for velocity data if not already in use
- change the setting of Particle Trajectory Evaluation to the default if not already set

7.4 Resuspension

The objectives of this module are to:

- Accept data from the particle tracking module on the deposition of particles on the bed from the source
- Calculate periods of resuspension from the hydrographic data record (when critical resuspension speed is exceeded).
- Simulate the resuspension, movement and redeposition of particles in the model grid.
- Calculate location and mass of redeposited particles
- calculate the distribution of the total deposition (g m^{-2} bed) or flux (g m^{-2} yr^{-1}) of material on the seabed.

The importance of resuspension will be dependent on a number of variables, in particular, near bed current speed, waste particle size, seabed cohesiveness, sediment type, and benthic community. In the resuspension module, a number of these variables are represented by the critical resuspension speed. Resuspension occurs when the near bed current velocities exceed this threshold. Resuspension events result in the transport and redeposition of material originating from underneath the

farm (i.e. the main area of deposition) to areas outwith the model grid or to locations at a greater distance from the source.

The model is run until a steady state occurs whereby solids accumulation (S_{avail}) in the following mass balance becomes constant:

$$S_{avail} = S_{depo} + M_d - M_e \qquad \text{Eq. 7.10.}$$

where S_{avail} is the flux of solids from the discharge available to the benthic community, S_{depo} is the flux of solids deposited directly from the fish farm (e.g. from sea surface to benthos), M_d is the flux of redeposited material which has been resuspended from elsewhere in the model grid and M_e is the flux resuspended. Thus, S_{avail} represents material available to the benthic community and is referred to as solids accumulation through subsequent sections.

The resuspension model (and all of DEPOMOD) has been validated as far as possible by DML – for validation techniques and results refer to Cromey et al. (2000 a&b, 2002 a&b).

7.4.1 Modelling Theory

Resuspension models typically consist of four components: erosion, transport, deposition and consolidation. The erosion function used in DEPOMOD is:

$$M_e = M(\tfrac{\tau b}{\tau ce} - 1) \qquad \text{Eq. 7.11}$$

where M_e is the mass resuspended (mass area^{-1} time^{-1}) when the bed shear stress τ_b exceeds the critical shear stress for erosion τ_{ce}. M is the erodibility constant with units of kg m^{-2} s^{-1} by convention used to validate the erosion function against field data sets. A variation of this formula substitutes bed shear stress for current speed given the relationship between τ and U_b^2, the current velocity at the bed.

To allow calculation of the bed shear stress from the measured current velocity near the bed, bed shear velocity U_* (m s^{-1}) is used in the following relationship (Bowden, 1983):

$$\tau_b = \rho U_*^2 \qquad \text{Eq. 7.12}$$

where ρ is the density of seawater (≈ 1025 kg m^{-3}). There is both theoretical and experimental evidence that a logarithmic profile exists in the boundary layer (Bowden, 1983; McLellan, 1965; Neumann and Pierson, 1966) which can be used to calculate U^*. Hethershaw (1988) reported a range of hydraulic bottom roughness lengths (z_o) of 2-7*10^{-4} m. Using a z_o of 2*10^{-4} m for a muddy bottom (Soulsby, 1983), data from the instrument deployed close to the bed (i.e. z = 2 m) can be used to define a logarithmic profile from this point to the bed by the following relationship (Dyer, 1979):

$$U_* = \frac{\kappa\, U_{(z)}}{\ln(z / z_0)} \qquad \text{Eq. 7.13}$$

where κ is the von Kàrmàn constant (= 0.4). A variation of equation (7.11) substitutes bed shear stress for current speed given the relationship between κ and U_b^2, the current velocity at the bed. Thus, this equation in its current velocity form is (Uncles *et al.*, 1985):

$$M_e = M\left(\left(\frac{U_{(z)}}{vr}\right)^2 - 1\right) \qquad \text{Eq. 7.14}$$

where *U(z)* is the current velocity at some reference height above the bed typically 2 metres and *vr* is the critical speed for resuspension. Some measurements of this threshold have been made for organic wastes associated with sewage outfalls with a value of 9.0 cm s^{-1} being used by a Californian group (SCCWRP, 1992) and a value of 15.0 cm s^{-1} being used by Burt and Turner (1984). Critical resuspension speed is likely to vary with particle size, cohesiveness and bed sediment type. Few measured

data exist in the literature relating to the variation of critical resuspension speed with these environmental variables for organic wastes.

Typically, *vr* is varied at the validation stage within bounds to obtain best fit to field data and then set as a parameter in the model. More data exist on critical resuspension speeds for erosion of bed load sediments in estuarine transport models with values as high as 50 cm s^{-1} not uncommon (Harris *et al.*, 1993).

In the resuspension model shown in equation 7.11, once the critical resuspension speed is exceeded a resuspension event occurs resulting in an amount of solids being resuspended from the bed. This can be imagined to be a patch of particles that are eroded from the bed and transported in the water column until redeposition occurs when the current speed falls below a critical deposition speed. Typical values for critical deposition speed (*vd*) for organic solids are 4.5 cm s^{-1} (SCCWRP, 1992) and 6.5 cm s^{-1} (Cromey *et al.*, 1997) where the deposition equation is:

$$M_d = (vs * pe)(1 - (\frac{U(z)}{vd})^2) \qquad \text{Eq.7.15}$$

where M_d is the rate of deposition and *vs* and *pe* are settling velocity and particle concentration respectively.

For shellfish farm sites similar to those described in this study, the main area of initial deposition is estimated to be at most 150 m from the farm structure. This value was calculated using the model:

$$D_Z(S) = VZ / S$$

with *V* (mean current velocity (cm s^{-1})) set to 3 cm s^{-1}, Z (depth (m)) set to 15 m and S (settling velocity of particle (cm s^{-1})) set at 0.3 cm s^{-1} (these values describe the site being more energetic than the low dispersion sites actually studied). In the resuspension model, if a critical resuspension speed of 9.0 cm s^{-1} is used and the hourly average current speed is 10.4 cm s^{-1}, a patch of particles will be resuspended and transported for 60 minutes at this speed. This will result in advective transport of

374m of this patch and deposition will occur if the current speed falls below the critical speed for deposition. Where a shorter time step is used, there will be slight variation in the mass resuspended and net transport for individual resuspension events depending on current speeds of the shorter time intervals in relation to the critical resuspension speed. However, over a fifteen day record, the resuspension model predictions are generally insensitive to the time step of current velocity data used (Cromey *et al.*, 2000a).

7.4.2 Quantitative comparisons of resuspension between sites

Following a resuspension event, should no redeposition occur in the immediate area around the fish farm site according to equation (7.11), such that M_d is zero in equation (7.15), then Cromey *et al.* (2000a) suggest the following methodology can be used to estimate the quantitative resuspension for different sites (M_e) to obtain S_{avail}. The use of mean current speed, or the percentage of current speeds above a threshold in a record, allows general site comparisons but gives no quantitative information on the effect a resuspension model would have.

The constant (α) for each resuspension event (i) of length (t_r) dependent on $U(z)$ and vr is given by:

$$\alpha(i) = \left(\frac{U(z)}{vr}\right)^2 - 1 \qquad \text{Eq.7.16}$$

Given n resuspension events in a record and the scaling of M (kg m^{-2} s^{-1}) to m (g m^{-2} d^{-1}), the amount resuspended m_e (g m^{-2}) for the record can be expressed as:

$$m_e = \sum_{i=1}^{n} m t_r \alpha(i) \qquad \text{Eq.7.17}$$

which rearranges to:

$$m_e = m t_r \sum_{i=1}^{n} \alpha(i) \qquad \text{Eq.7.18}$$

If the current record is taken as representative of typical conditions and is to be used in DEPOMOD for prediction of steady state conditions, then this value of m_e can be scaled up to a yearly value by the following:

$$M_e = m_e \frac{365.25 T_r}{t_{record}} \qquad \text{Eq.7.19}$$

where T_r is the total time of resuspension events (nt_r) and has unit of days, t_{record} is the total length of the current record (days), m_e has units g m^{-2} and M_e is the amount resuspended (g m^{-2} yr^{-1}) comparable with the initial deposition predictions from DEPOMOD (i.e. S_{depo}).

By combining these two equations, to compare the relative differences between sites in relation to the potential for resuspension, the critical resuspension speed *vr* defines the differences between sites independent of *m*:

$$M_e = m t_r \sum_{i=1}^{n} \alpha(i) \frac{365.25 T_r}{t_{record}} \qquad \text{Eq.7.20}$$

For site comparison, the value β is used, as this is dependent on *vr*:

$$M_e = m\beta \qquad \text{Eq.7.21}$$

To calculate the actual amount resuspended from a site (M_e), the constant *m* needs to be defined as a result of validation studies either with a tracer study or with comparisons of benthic fauna at sampling stations.

7.4.3 Resuspension Module Settings

The current setting of critical resuspension speed is 9.0 cm s^{-1} and critical deposition speed is 4.5 cm s^{-1}, as used in the configuration for fish farms.

The parameters of the resuspension model are:

- Critical shear stress for resuspension - 0.0179 N m^{-2} (approximately 9.5 cm s^{-1} near bed current speed)
- Critical shear stress for deposition - 0.004 N m^{-2} (approximately 4.5 cm s^{-1} near bed current speed)
- Erodibility constant - $7*10^{-7}$ kg m^{-2} s^{-1}
- Consolidation time - 4 days (period of time a particle spends on the bed before it is removed from the resuspension model processes)

These model parameters have been validated using a tracer study and using benthic data from several fish farm sites (Cromey *et al.,* 2000a). The only resuspension parameter that can be varied by the user is the consolidation time of a particle, the benthic data sets were validated using a consolidation time of 4 days.

7.5 Benthic module

The objectives of this module are to:

- read in predictions of solids accumulation (S_{avail}) from resuspension model output files
- generate predictions of the Infaunal Trophic Index and Total Abundance for the grid area and for sampling station positions; predictions of solids (or chemical) accumulation/deposition are also given for sampling station positions
- provide Envelopes of Acceptable Precision with these predictions which give an indication of the confidence of the predictions

The Benthic Module relates the predicted solids accumulation on the seabed, derived from the preceding modules, to changes in the benthic fauna, parameterised as changes in the Infaunal Trophic Index (described in Chapter 3 Section 3.3.5). The initial stage is to consider the solids accumulation mass balance

$$S_{avail} = Me + Md - Mr \qquad \text{Eq. 7.22}$$

where S_{avail} is the flux of solids arising from the farm site to the benthic community, Me is the deposition flux from the farm site, Md is deposition flux arising from resuspended material inside the grid area originating from the farm, and Mr is the resuspension flux. Units are g solids m^{-2} yr^{-1}. However, S_{avail} in equation 7.22 does not include carbon from primary production nor carbon degraded by the G-model (Westrich and Berner, 1984). To obtain a more realistic value for the flux of material to the seabed, it is necessary to take into account an estimate of natural background sedimentation. In this module, DEPOMOD assumes that the rate of natural sedimentation is constant (k) such that equation 7.22 can be modified to:

$$S_{avail} = Me + Md - Mr + k \qquad \text{Eq.7.23}$$

A figure of 750 g solids m^{-2} yr^{-1} was used – adjusted from an estimate of 250 g carbon m^{-2} yr^{-1} for coastal and sea loch areas (Cromey *et al.*, 2000a). It is obvious that the rate of natural sedimentation will fluctuate over numerous timescales; however, the model developers felt that the above figure was not an unreasonable estimate. They add that the influence of this additional input on the model predictions will be dependent on the quantity of material being discharged from the farm site. The original purpose of this module was to position the reference and far field stations in low dispersive sites in a more realistic position on the solids accumulation scale. At these stations, the natural background sedimentation is deemed to be the main input of material to the benthic community.

7.6 Development of DEPOMOD for mussel farms

Many aspects of fish farm modelling are also pertinent to modelling of mussel farms. As described above, DEPOMOD was originally developed from another model, BenOss, that was used to model deposition and biological effects of excess carbon from sewage discharges. A method for the determination and regulation of the impacts of fish farms on the surrounding environment has been developed by the author for the Scottish Environment Protection Agency (Chamberlain, unpub.). The methods used in the general set-up of the model are similar to those used for fish farms. The parameters that require modification are:

- Alteration of farm structure to represent mussel raft and lines
- Differences in the settling characteristics of faeces and the inclusion of pseudofaeces
- Differences in the quantity and quality of feed provided to the farmed animal (and the associated excretion rates).

7.6.1 Farm structure

To set up the model for a mussel farm scenario, a mussel raft or batch of lines is considered analogous to a single fish cage. The size and shape of the cage was defined as the dimensions of the mussel farm (this process is described in more detail in section 7.7.1.2). Particles of waste are then modelled as being ejected from the 'cage' at randomly assigned *x, y, z* co-ordinates. This is not strictly realistic, as faecal and pseudofaecal particles from the mussels are actually ejected from discrete locations within the farm (i.e. the 'droppers'). However, it is considered that the significance of this effect on the footprint of the overall farm structure will be minimal. As the particles are transported away from the farm site, they will form a large homogenous patch rather than separate smaller individual patches representing each mussel line.

7.6.2 Settling velocity

The settling velocity of mussel faeces and pseudofaeces were determined in Chapter 6, and the values derived in that Chapter were integrated into the model.

7.6.3 Food loading/excretion rate

The use of realistic feed/excretion values within the model was considered using two different approaches. Both methods involved modifying the 'fish farm' set-up such that the model used values more relevant to mussel farms.

a) Provide values for the feed load to the farm structure

This method involves providing the farm with a quantity of food (per time step) which could fluctuate over the annual cycle. Food conversion parameters would then be used to determine the quantity of faecal and pseudofaecal material being ejected from the farm structure per time step. This approach has an intuitive appeal, as it is very similar to the 'fish' modelling approach in providing the farm site with known food quantities. However, difficulties were encountered in identifying suitable values due to the sparse nature of data on mussel feeding and excretion under natural (and farmed) conditions. Mussel feeding and excretion data has been collected in many studies (e.g. Bayne et al., 1998). However, these are mainly derived from individual (or very small numbers) in laboratory studies. At a mussel farm, differences in the quantity of food available, water movement and environmental conditions will result in a broad range of values. Mussels will filter out a high proportion of the suspended particulate matter and will then select portions of the consumed material to ingest (Navarro *et al.*, 1991). The rest will be excreted as pseudofaeces (see Chapter 1).

b) Provide values of excretion rate

This method involves defining the quantity of material being ejected from the farm site and the relative proportions of faeces and pseudofaeces. This approach involved modifying the DEPOMOD set-up such that all the 'food' provided to the cages would immediately be excreted (i.e. zero food consumption). This method

allows the characteristics of the 'excreted' particles to be predetermined. This negates the requirement for calculations involving mussel physiology (feeding/excretion rates etc.) and allows the quantity released over the growth cycle (or specified period) to be defined. This results in both the growth of the mussels and seasonal fluctuations in the food availability to be set, or a mean value over the modelled period to be defined. The model can incorporate more than one type of 'feed', thus allowing quantities and characteristics of both the faecal and pseudofaecal particles to be defined.

An extensive series of test model runs were conducted to assess the suitability of the two methods described above. Good correlation was attained between providing values for feed loading with conversion factors, and values for excretion rate. The area and extent of impact were broadly similar as would be expected as the same hydrographic processes were applied in all cases.

Difficulties were encountered when attempting to apply a feed load and conversion factor that were environmentally realistic and also produced results that were representative of the field data. It quickly became apparent that there were processes involved that were not being taken into account. Model results generally over-estimated the extent of impact when the input values were from processes measured on individual specimens and scaled up to a whole farm scenario. Conversely, when values were used from estimates of the food load applied to a whole farm, the model results tended to under-estimate the degree of impact.

Applying a correction factor to the input values could alter model output such that they were similar to the field data measurements. However, it was considered that such an approach would be applying too many assumptions to the input data and invalidating any further model outputs.

Consequently, the approach described above whereby values for rate and quantity of excretion for the whole farm site are applied within the model, was selected as the most suitable method to compare model and field data results.

7.7 Model Specification

7.7.1 Modelling approach

A scenario-based assessment was considered to be an appropriate method of assessing the model and testing the approach described above. Initially, this involved producing a model grid for each of the three field sites. The model was then run for a large number of scenarios applying different excretion loads and varying the proportion of faeces and pseudofaeces. The resultant model outputs were then examined and compared with the field data.

7.7.1.1 Grid Generation Module

Admiralty charts (paper and electronic) were used to extract the topographic features of the sea bed surrounding each of the farm sites examined. This information was then used to produce major and minor grid files as described in section 7.2. The resulting grid plots, overlaid with cage and sampling locations, are presented in Figures 7.2 (Site S), 7.3 (Site A) and 7.4 (Site B).

7.7.1.2 Particle Tracking Module

Hourly averaged hydrographic data, collected from each site, were applied to the respective model simulations. The dimensions of the farms within the model were defined according to Table 7.1.

	Length (m)	Width (m)	Depth (m)
Site S	25	25	8
Site A	100	100	10
Site B	100	100	10

Table 7.1 Farm dimensions as defined in the Particle Tracking module

The dimensions used in the model for the farm structure at Site S were an accurate representation of the actual farm on site. However, the dimensions used at Sites A and B were nominal values as the actual farm sites were spread across a wide area covering a large proportion of the model grid. The positioning and size of the farm structure within these models was defined such that a representative depositional area

would arise within the vicinity of the sampling stations. This was considered a satisfactory approach for comparison of gradients of deposition within a small area.

The excretion load at each farm site was defined within the model as an applied food load with zero digestibility. This resulted in the mass of faeces being excreted from the farm site as being equivalent to the applied food loading. The settling velocity of the excreted material was then defined. DEPOMOD has the capability to simulate particles of differing settling velocities - therefore the relative proportion of faeces and pseudofaeces (with their associated settling velocities) could also be defined.

A total of 42 different scenarios, involving varying excretion rates and proportions of faecal and pseudofaecal material were run for each farm site. The values used in these scenarios are outlined in Table 7.2.

Excretion rate (kg farm^{-1} day^{-1})		Proportion of excreted material (%)	
1		Faeces	Pseudofaeces
5		100	0
10		90	10
15		80	20
20		70	30
25		60	40
50		50	50

Table 7.2 Excretion rate loadings and proportion of faecal material as defined within the particle tracking module at all farm sites

For each different loading, models were run for all of the faecal distribution scenarios. This resulted in a broad range of material being deposited within the model grid surrounding the farm sites.

The values used within the turbulence model were defined as 0.1 m^2s^{-1} in the horizontal x and y direction and 0.001 m^2s^{-1} in the vertical z direction (after Gillibrand and Turrell, 1997).

Within the particle trajectory model, 10 particles were released per time step and were evaluated every 60 seconds. These were selected following scoping runs to determine

the optimum values for model accuracy whilst avoiding excessive computational time in determining outputs.

7.7.1.3 Resuspension Module

The values used within this module were primarily the DEPOMOD default values, as defined for fish farming. Data on the resuspension characteristics of mussel faeces and pseudofaeces were not available. It was considered that the default values would provide a reasonable estimate of resuspension at the farm sites.

The model output was parameterised as 'flux of material' (mass $m^{-2}yr^{-1}$) with the output units measured in g $m^{-2}yr^{-1}$. The output of this model was the predicted flux of material to the seabed (g solids $m^{-2}yr^{-1}$) within each minor grid cell.

7.7.1.4 Benthic Module

The values from the Resuspension Module were used as input data for this module. Calculations were undertaken to produce predictions of the Infaunal Trophic Index status within each minor grid cell.

7.8 Modelling Outputs

In common with other studies utilising particle tracking models, the model output is in the form of a 'footprint of deposition' upon the seabed. This patch can then be parameterised in terms of area and the concentration of material be calculated. The actual size of patch does not tend to vary dramatically with alterations to the applied loading as equivalent processes occur with each model run. Consequently, the overall effect of increasing the quantity of material being ejected from a source will be to increase the concentration of material within the patch and have little effect on the area coverage on the seabed. This effect may be countered by increasing the number of particles used within the model. However, earlier sensitivity analysis in the scoping runs of the model identified that any increases in the number of particles used in the model runs did not result in significant changes in the size of patch and merely increased the computational time to unacceptable levels.

The results from the model runs for each of the farm sites are discussed below.

7.8.1 Site S

There was a discrete patch of deposition around the farm site for all the model scenarios tested. This was considered to be an effect of the low current velocities recorded at the site and applied to the model. This resulted in the particles being transported a short distance before settling on the sea bed. Resuspension was not a significant factor at this site due to the low near bed current velocities throughout the hydrographic data set.

The farm structure illustrated in Figure 7.2 has been removed to allow examination of the contours of the depositional patch. Figure 7.5 illustrates the model output (g m^{-2} yr^{-1}) for an applied load of 10 kg farm-$unit^{-1}$ day^{-1} with 100% faeces content. Figure 7.6 shows a more detailed illustration of the area of deposition. It can be seen that the footprint was centred around the centre of the cage with a gradient of deposition along the line of the sample station transect. A similar footprint is shown in Figure 7.7 for an applied load of 50 kg $cage^{-1}$ day^{-1} with a similar distribution and increased concentrations of deposited material.

The resulting ITI plots for the two loadings above are presented respectively in Figures 7.8 and 7.9. From these plots it can be seen that the model predictions indicate that the area shown as 'impacted' conditions (ITI < 20) is enlarged as the feed/excretion loading is increased. However, the overall size of the impact patch does not increase dramatically between the two plots. For both scenarios, there is a gradient of ITI values along the sample station transect.

The effect of altering the proportions of faecal and pseudofaecal material is illustrated in Figure 7.10. This plot illustrates the model output (ITI) for an applied load of 10 kg $cage^{-1}$ day^{-1} with 50% faeces and 50% pseudofaeces content. It can be seen that there is little difference between the plots within the 'impacted' area. The footprint for the 100% faeces model output appears larger than the 50% faeces 50% pseudofaeces plot. However, this was not considered a significant factor and was possibly due to randomness in the model runs. The effect of incorporating both faecal

and pseudofaecal particles in the model runs at this site was considered negligible, as particle transport and advection was minimal due to the low current velocities.

7.8.2 Site A

The larger farm site at Site A resulted in a more dispersed and larger footprint over the farm area. However, the depositional patch was again centred over the farm site. The model output for a loading of 10 kg farm-unit^{-1} day^{-1} resulted in a maximum value of 250 g m^{-2} d^{-1} and was poorly defined due to the dispersed nature of the deposited material.

Figure 7.11 illustrates the model output (g m^{-2} yr^{-1}) for an applied load of 50 kg cage^{-1} day^{-1} with 100% faeces content. To aid interpretation of the figure, the bathymetry has been removed to show extent of dispersion. It can be seen that the patch is an elliptical shape with a major axis along a NE-SW direction. This indicates that the current regime is having a greater effect on the settling particles during the simulation. There is a gradient of deposition along the sample station transect from an area of high deposition to medium deposition.

The resulting ITI plot for this loading is presented in Figure 7.12. From this plot it is apparent that there is a predicted area of impact (ITI < 20) extending well beyond the farm limits. The gradient of ITI scores runs parallel to the sample station transect although it can be seen that there are predicted impacts beyond the extent of the transect.

A similar ITI plot for a reduced loading of 20 kg farm-unit^{-1} day^{-1} with 100% faeces content is presented in Figure 7.13. The area of deposition is slightly reduced at this loading, however, more significantly, there are no areas with a predicted ITI score of less than 25. The material being ejected from the farm site at this loading is predicted to be dispersed sufficiently such that there will be little alteration to the benthic fauna in the surrounding area.

Applying a scenario of 50% faeces and 50% pseudofaeces to the same loading results in the plot shown in Figure 7.14. Again, the separation of particles into two settling

velocities has little effect on the overall area of deposition. The area of deposition appears to be slightly smaller, as would be expected through applying particles with greater settling velocity. However, despite the currents appearing to have a greater effect on the spread of particles on the seabed, as seen by the larger footprint compared to Site S, the effect of the more rapidly sedimenting particles appears to be minimal.

7.8.3 Site B

The depositional area at Site B is directly beneath the farm site and extending around the periphery of the site. Figure 7.15 shows the model output for a loading of 50 kg $cage^{-1}$ day^{-1} with 100% faeces. The maximum deposition value for this loading is 1760 g m^{-2} yr^{-1} which occurs directly beneath the farm site. The same plot is shown in more detail in Figure 7.16. The sampling station transect can be seen to cover a gradient of deposition from a high to medium level of sedimentation.

The ITI plot for the same loading is presented in Figure 7.17. From this output it can be seen that at this loading, the impacted area (ITI < 20) extends beyond the limits of the sample station transect. There is no obvious elliptical effect from the currents dispersing the ejected material. The low current velocities measured at this site concur with this result. At a reduced loading of 20 kg $cage^{-1}$ day^{-1} the impacted area is much reduced and the sample station transects appears to coincide with a sharp increase in the ITI score (Figure 7.18).

Applying a scenario of 50% faeces and 50% pseudofaeces to this same loading results in the plot shown in Figure 7.19 again results in a smaller area of impact from the faster settling particles. However, a distinct gradient in the ITI score along the sample station transect is still observed.

7.9 Analysis of Results

Overall, the model outputs described above predict that the majority of material being excreted from the farms will be deposited in close proximity to each site. The main

functions within the model that determined this outcome were the settling characteristics of the particles (as calculated in Chapter 6) and the low current velocities at each site. The particles were not in suspension for sufficient time and the applied currents not strong enough for the particles to be advected any great distance from the farm site.

Analysis of the influence of varying the feed/excretion load permitted comparisons of the extent and degree of impact under different conditions. The predictions of the concentration of material on the seabed were then used to determine the degree of impact on the benthic infauna as measured by the ITI.

The effect of incorporating both faecal and pseudofaecal particles did not have a great effect on the model outputs. As expected, the application of a proportion of more rapidly sedimenting 'pseudofaecal' particles had the effect of slightly reducing the area of impact and increasing the concentration of material beneath the farm sites.

At a constant feed/excretion load, the degree and extent of impact at each site was different at each of the modelled sites. Such variations can be attributed to differences in the hydrographic regime and the bathymetry at each farm site.

7.9.1 Site S

The model outputs from this site predicted a footprint of deposition surrounding the farm site at all feed/excretion loadings. The small size and low production at the site would suggest that the higher loading values used in the model would be unrepresentative of the actual situation at the farm site. The footprints produced by the model suggest that the sampling station transect was well placed to detect a gradient of deposition from the farm site. However, the field survey data reported that low ITI scores were recorded at all stations around this site irrespective of distance from the farm. Additionally, there was no gradient of deposition observed in the biological or physico-chemical characteristics measured at this site. Consequently, the model results are not a good representation of the field data. Additional factors that may have caused the disparity between model and field results are discussed below.

7.9.2 Site A

A marked elliptical patch of deposition was observed in the modelling outputs from this site. This was apparent at all feed/excretion loadings and was in the direction of the major current flow in the area. There was a gradient of deposition along the sample site transect. The feed/excretion loading of 20 kg farm-unit^{-1} day^{-1} resulted in similar ITI scores along the transect as was identified in the field data results. At higher loadings, the extent of impact was greater than observed at the site and the concentrations within the patch (and consequent ITI score) were an overestimate of the actual field data. This feed/excretion loading is not considered a sufficient quantity to be ejected from a 100 tonne mussel farm each day. Consequently, for the model and field data to concur at this level, the model appears to be over-estimating the impact of the farm site on the benthic community.

7.9.3 Site B

There was a tight depositional footprint around the farm structure at Site B. The very low current velocities resulted in the model predicting that most material would settle out before being advected away from the site. Consequently, there were very high concentrations of deposited material on the seabed beneath the farm. The ITI scores from both 50 kg farm-unit^{-1} day^{-1} and 20 kg farm-unit^{-1} day^{-1} indicated that the sample station transect was well placed overlapping a gradient of deposition moving away from the farm site. The ITI scores from the 20 kg farm-unit^{-1} day^{-1} model runs compared favourably with the data collected from the farm site at all the sampling stations. However, as discussed for Site A – this feed/excretion loading is considered low for the size of farm and the model appears to be over-estimating any impacts on the benthic community.

7.10 Discussion of modelling results

The outputs for Sites A and B showed that the model produced a realistic distribution of material on the seabed that was comparable to the field data observations.

However, in both cases, it was considered that the model would over-estimate the degree of impact on the benthic environment. The quantity of material that would be ejected from the farm site is considered to be greater than the values used within the model to produce comparable results.

Conversely, the outputs for Site S were less clear with the predicted area of deposition not being observed in the field data results. All stations at Site S had low ITI values irrespective of distance from farm site. Factors that could have caused this situation to arise were discussed in Chapter 5. The effect of faecal and pseudofaecal material being deposited on the sea bed was considered to have been obscured by a high quantity of naturally sedimenting material.

The over-estimation of deposition and consequent benthic impact could be a result of a number of factors. The parameters used within the model contain many assumptions about the processes involved. These values could affect the model outputs and account for the overestimation of impact. Possible parameters that would require further investigation to validate the model further are discussed below.

Feed/Excretion Load

The models were set up to discharge a fixed quantity of material over a set time period. The quantity of food available to the farm site, quantity consumed and excreted were variable and possibly unpredictable. Estimates of these values resulted in either over- or under-estimation of a realistic value for use within the model. Additionally, these values would be highly site specific and not amenable to a generalised model of impact.

Feed/Excretion Rate

The model runs used in this study used a constant excretion rate with time. In reality, there would be fluctuations in the feeding rate and food availability over the annual cycle. The importance of this effect on determining benthic impacts is unclear as consolidation time for particles and biological uptake of deposited material is currently unknown.

Consolidation Time

The time period that the particles remain on the sea bed before being incorporated into the benthos is currently set at the DEPOMOD default value of 4 days. Additional information specifically for mussel faeces and pseudofaeces was unavailable.

Coprophagy

One factor that could account for the over-estimate of benthic impact is the re-ingestion of previously excreted material within the farm structure. This would have the effect of reducing the final quantity of material being ejected from the farm site as a proportion of the excreted material would not actually deposit on the seabed.

Overall, the model presented in this chapter provided a useful indication of the potential benthic impacts at Sites A and B. The model outputs for Site S indicate that caution should be used when applying the model results as additional factors may have a greater effect on the system and confound any predictions that are made.

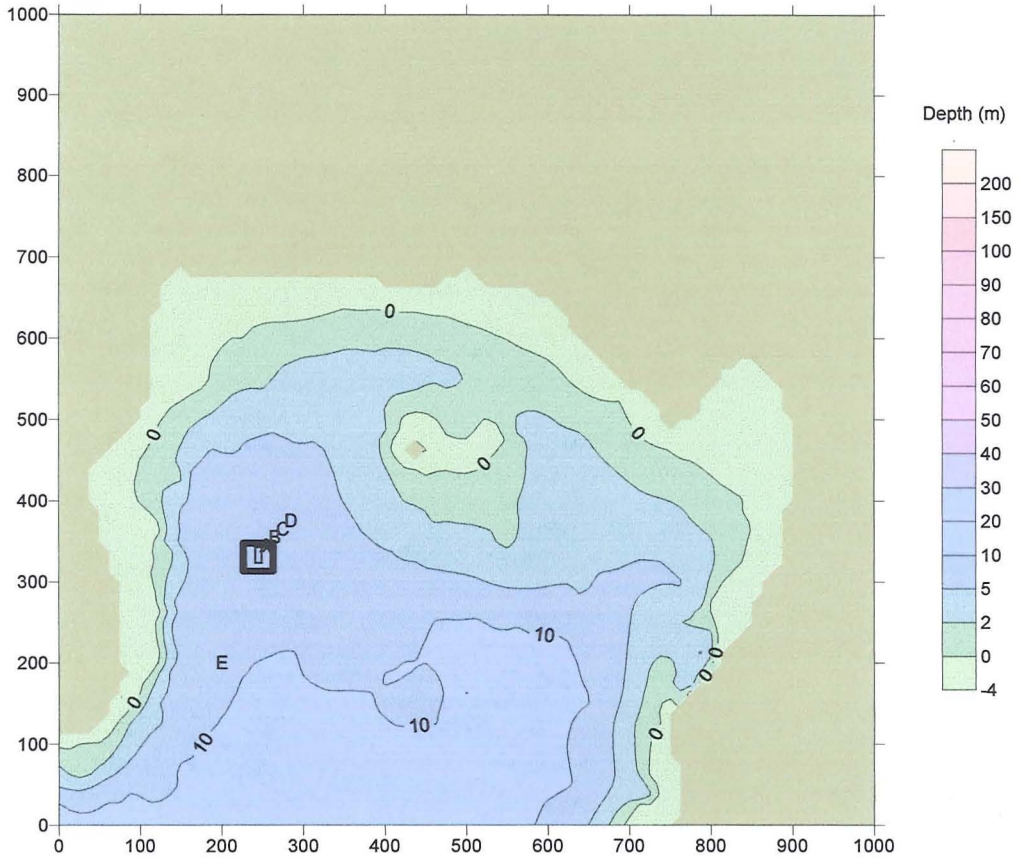

Figure 7.2 Site S – Grid layout with farm structure and sampling stations

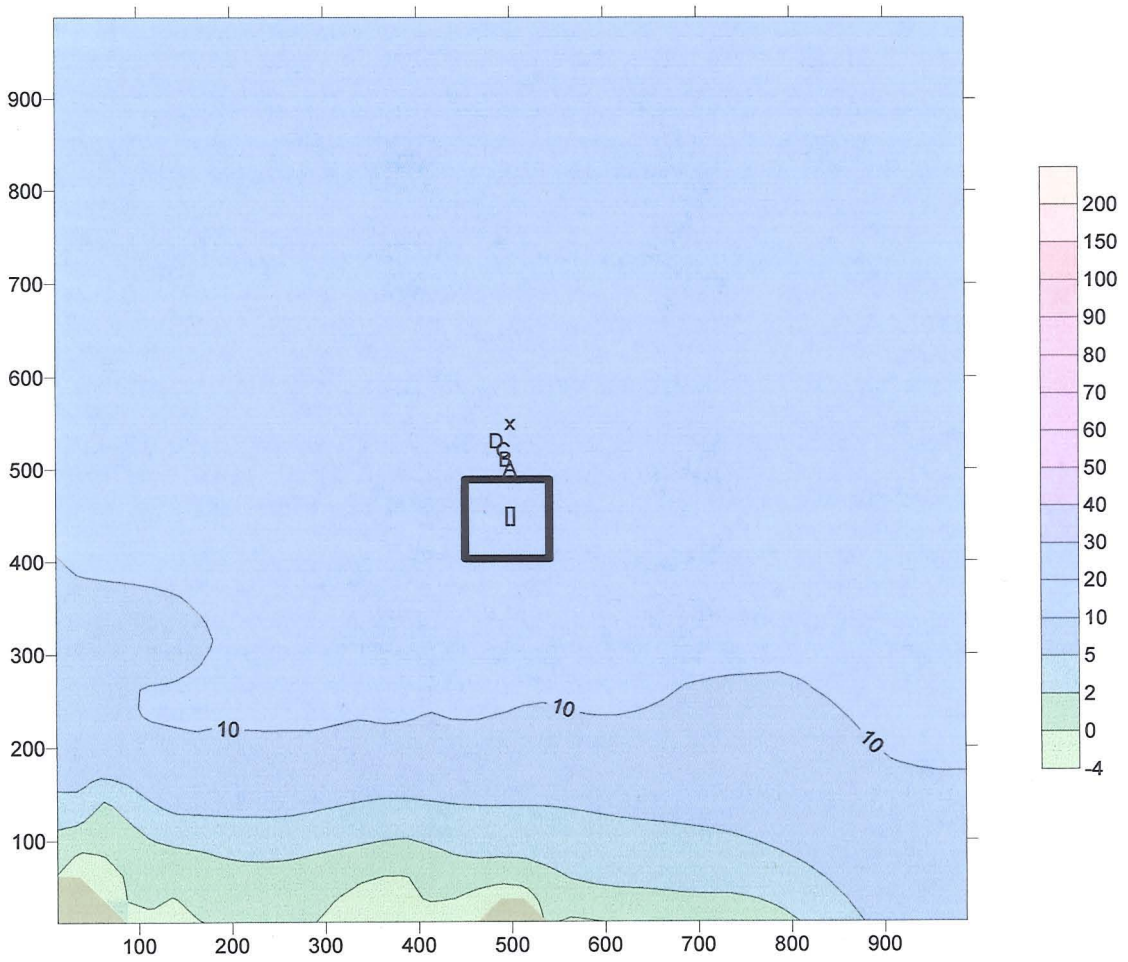

Figure 7.3 Site A – Grid layout with farm structure and sampling stations

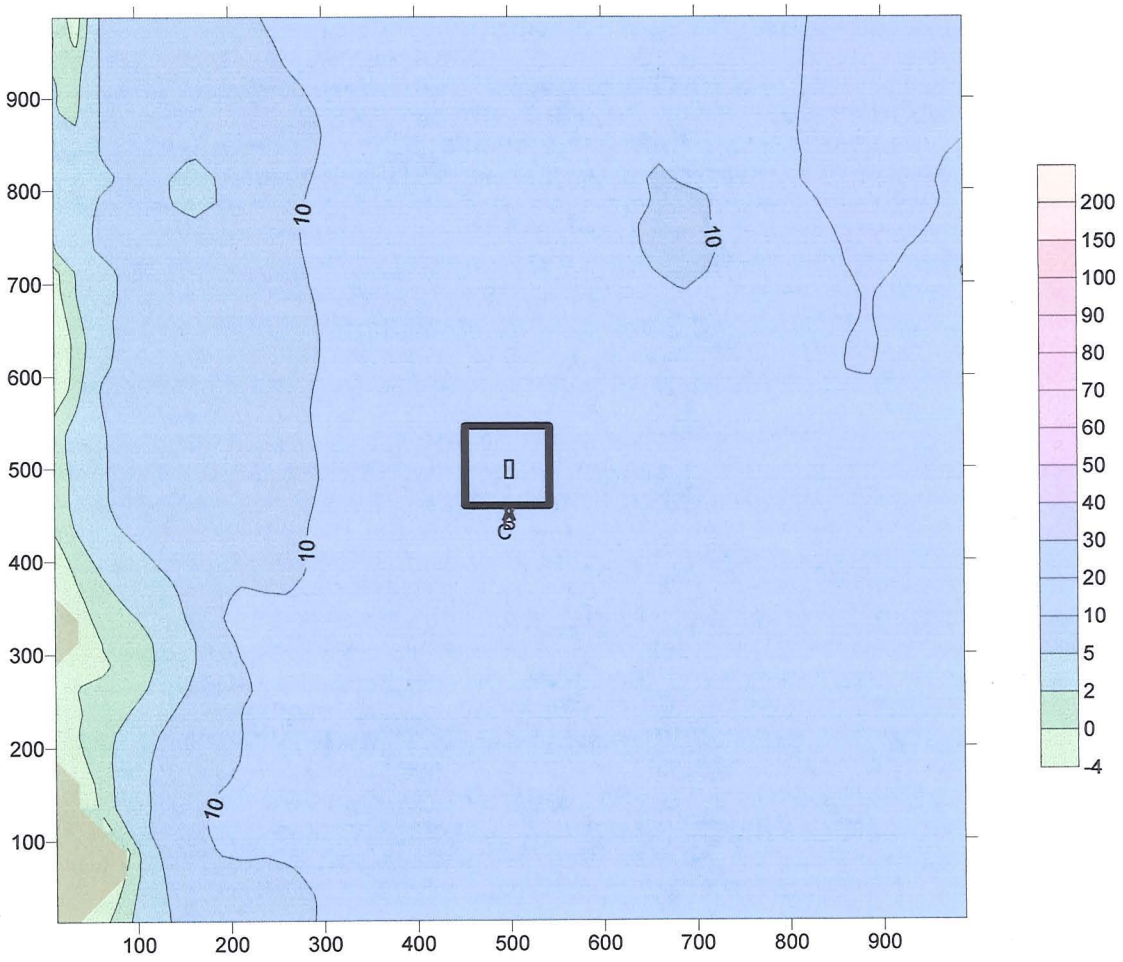

Figure 7.4 Site B – Grid layout with farm structure and sampling stations

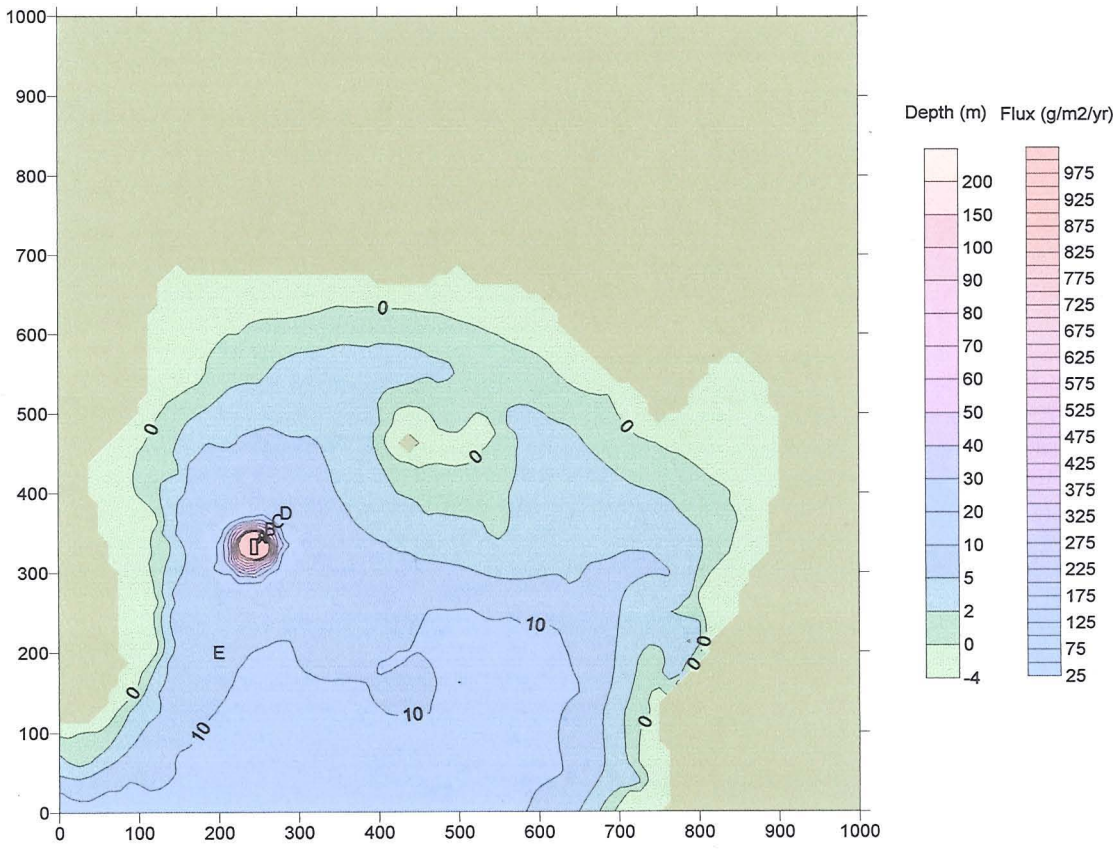

Figure 7.5 Site S – 10 kg cage^{-1} day^{-1} with 100% faeces

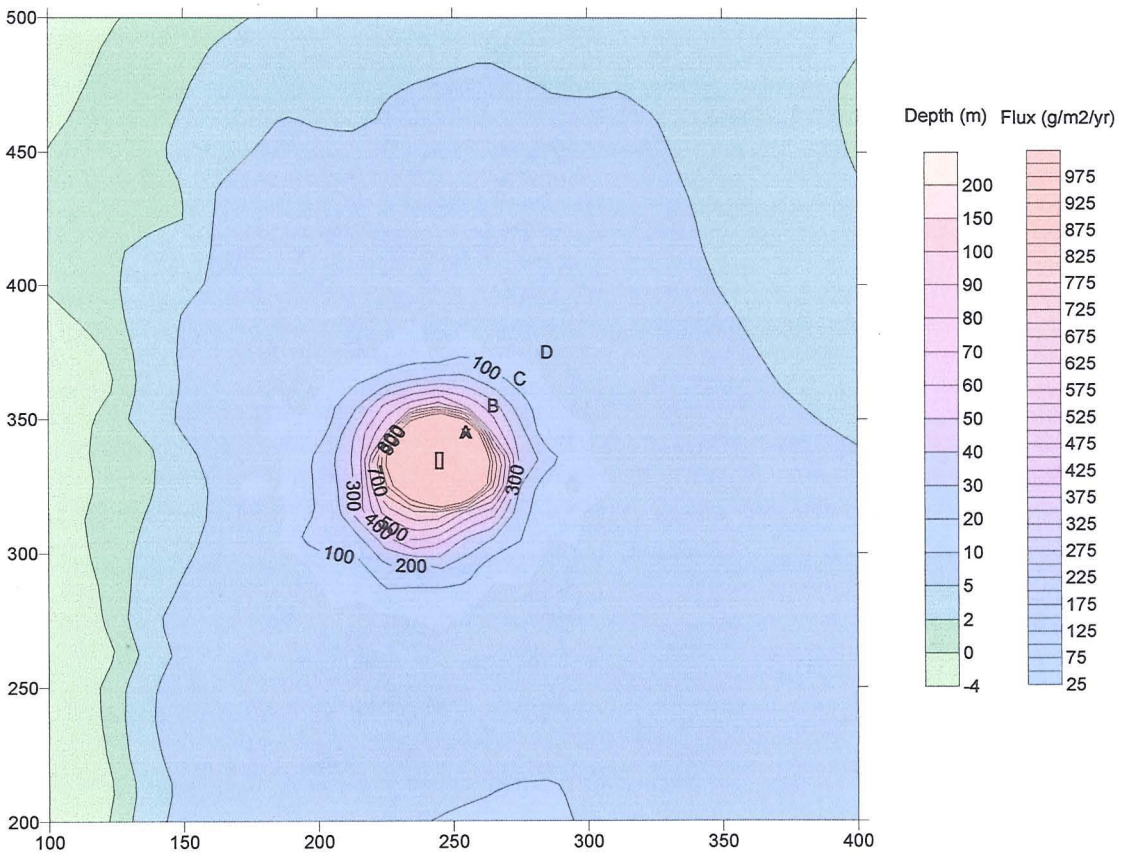

Figure 7.6 Site S – 10 kg cage^{-1} day^{-1} with 100% faeces – close detail

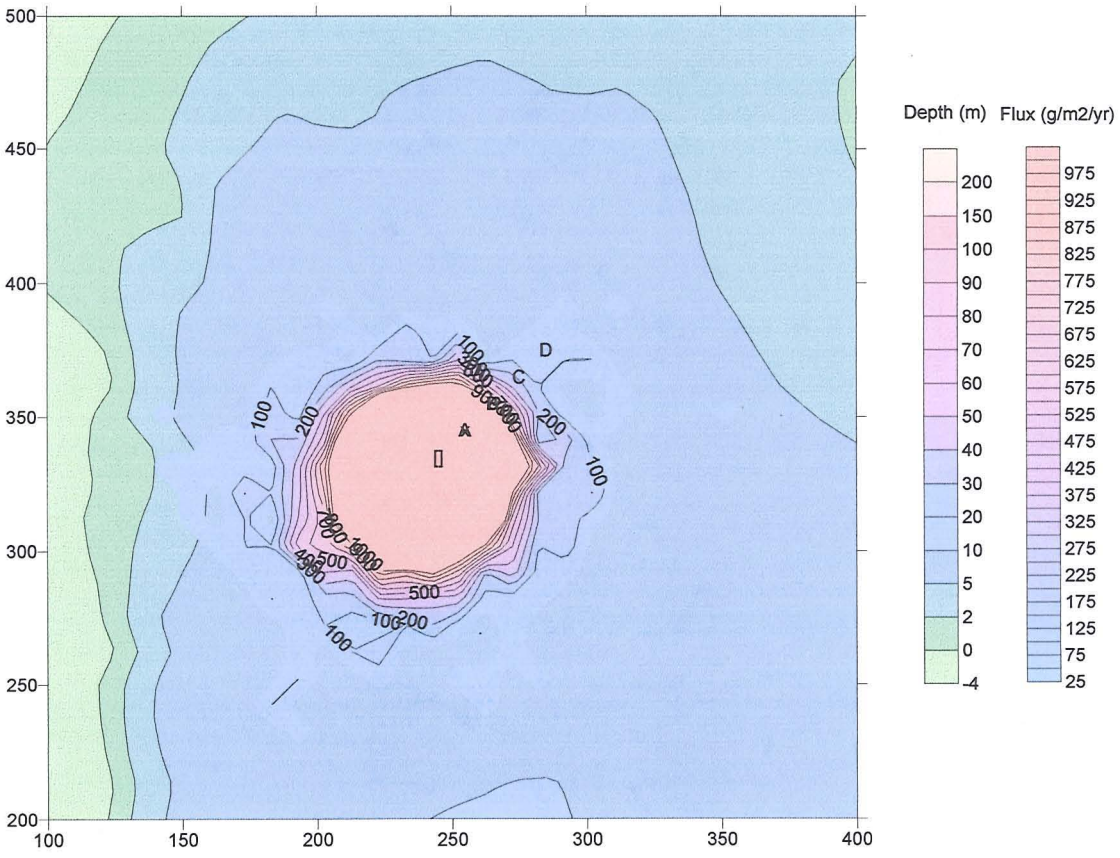

Figure 7.7 Site S – 50 kg cage^{-1} day^{-1} with 100% faeces – close detail

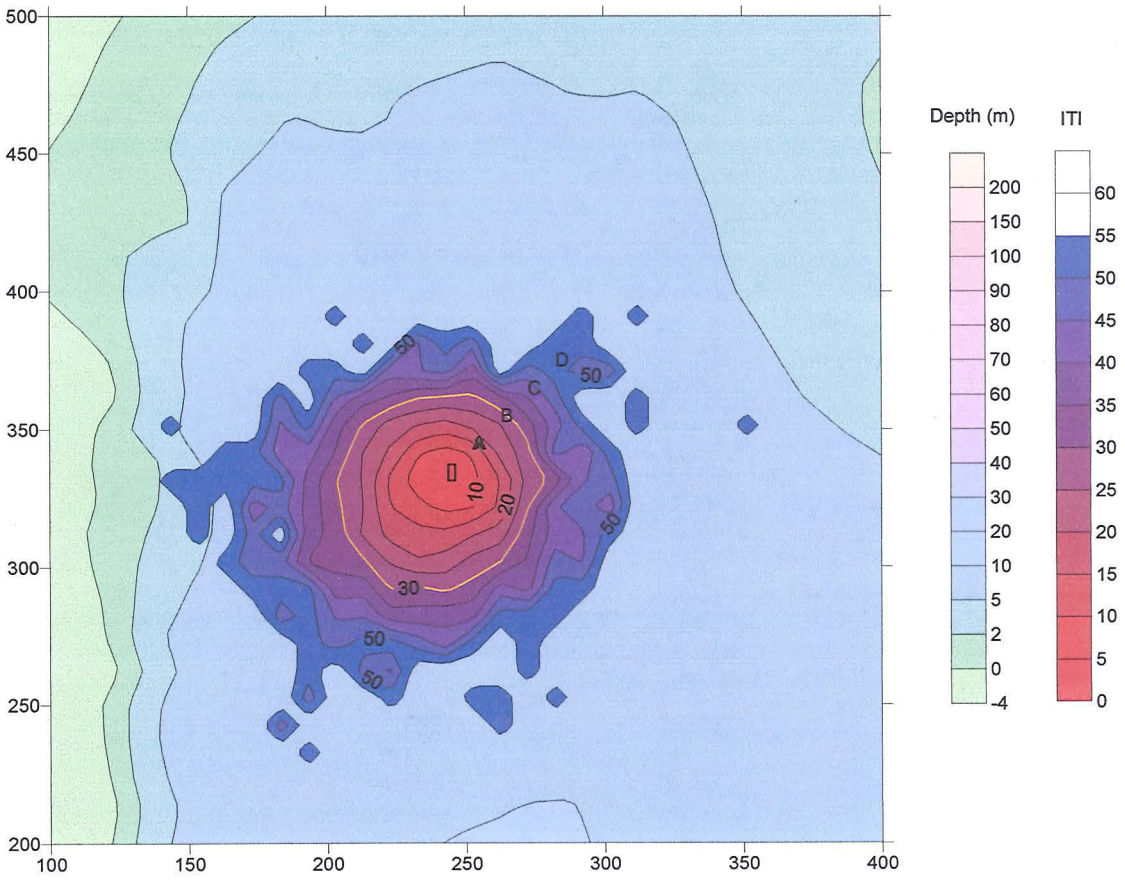

Figure 7.8 Site S – 10 kg cage^{-1} day^{-1} with 100% faeces – close detail

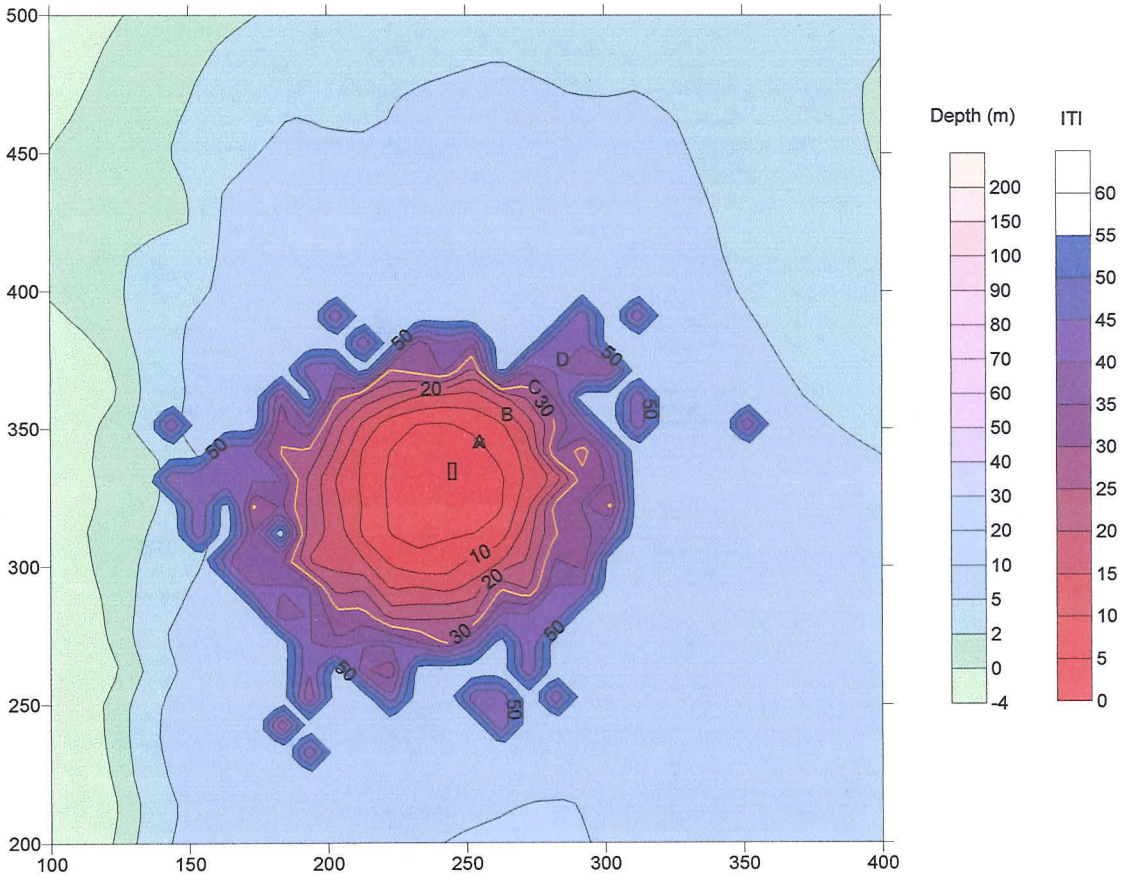

Figure 7.9 Site S – 50 kg cage^{-1} day^{-1} with 100% faeces – close detail

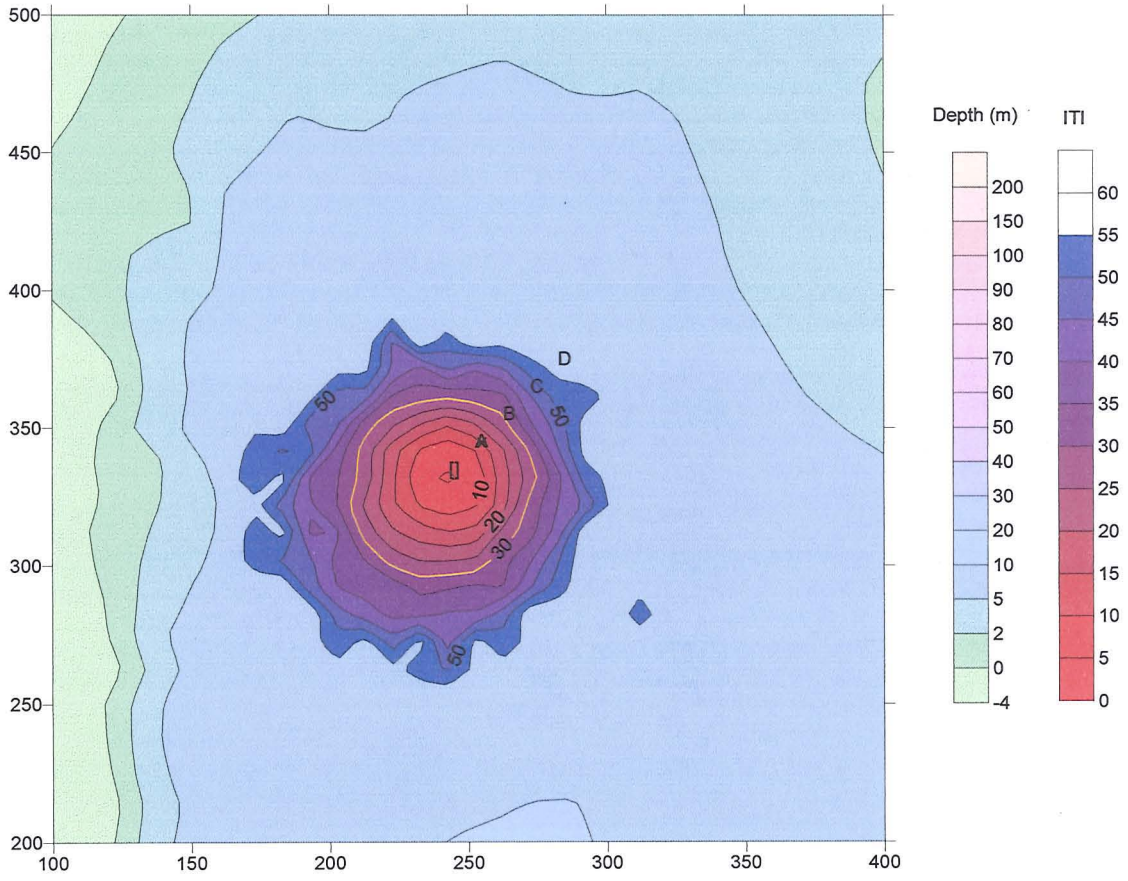

Figure 7.10 Site S – 10 kg cage^{-1} day^{-1} with 50% faeces and 50% pseudofaeces – close detail

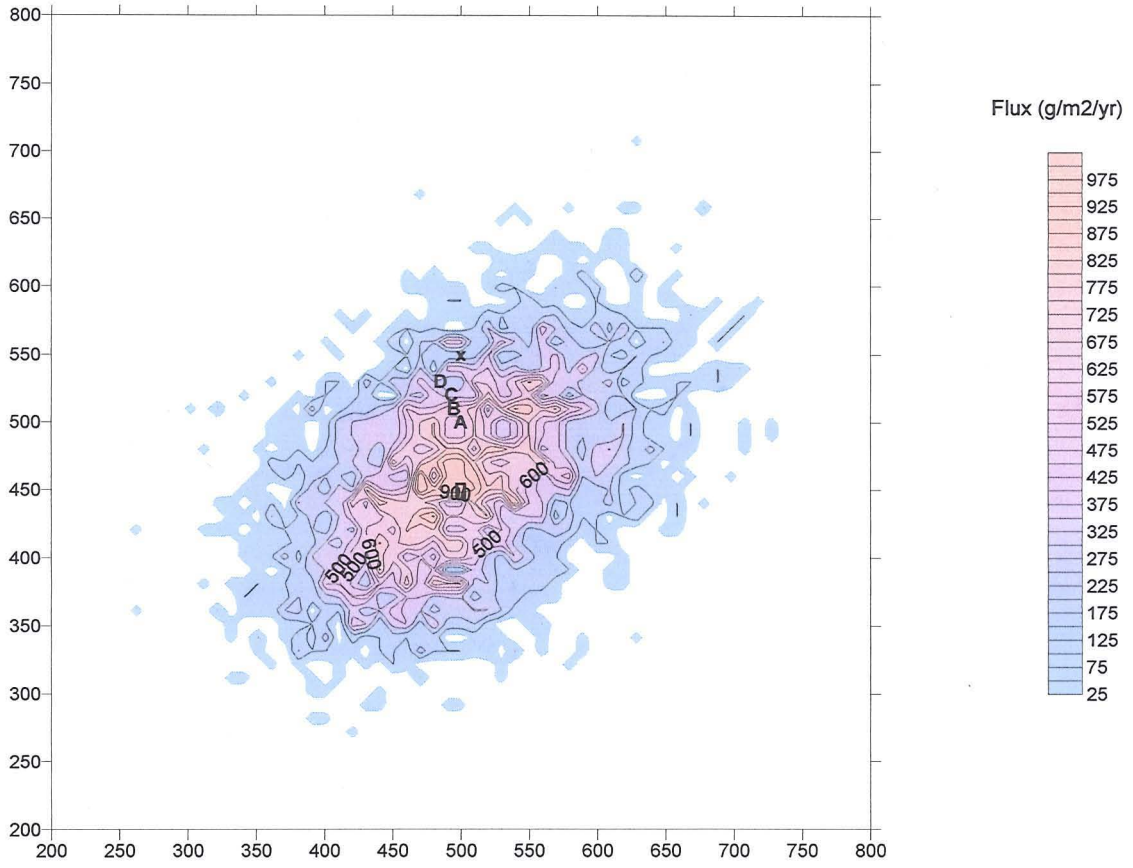

Figure 7.11 Site A – 50 kg cage^{-1} day^{-1} with 100% faeces – close detail (Bathymetry removed to aid interpretation)

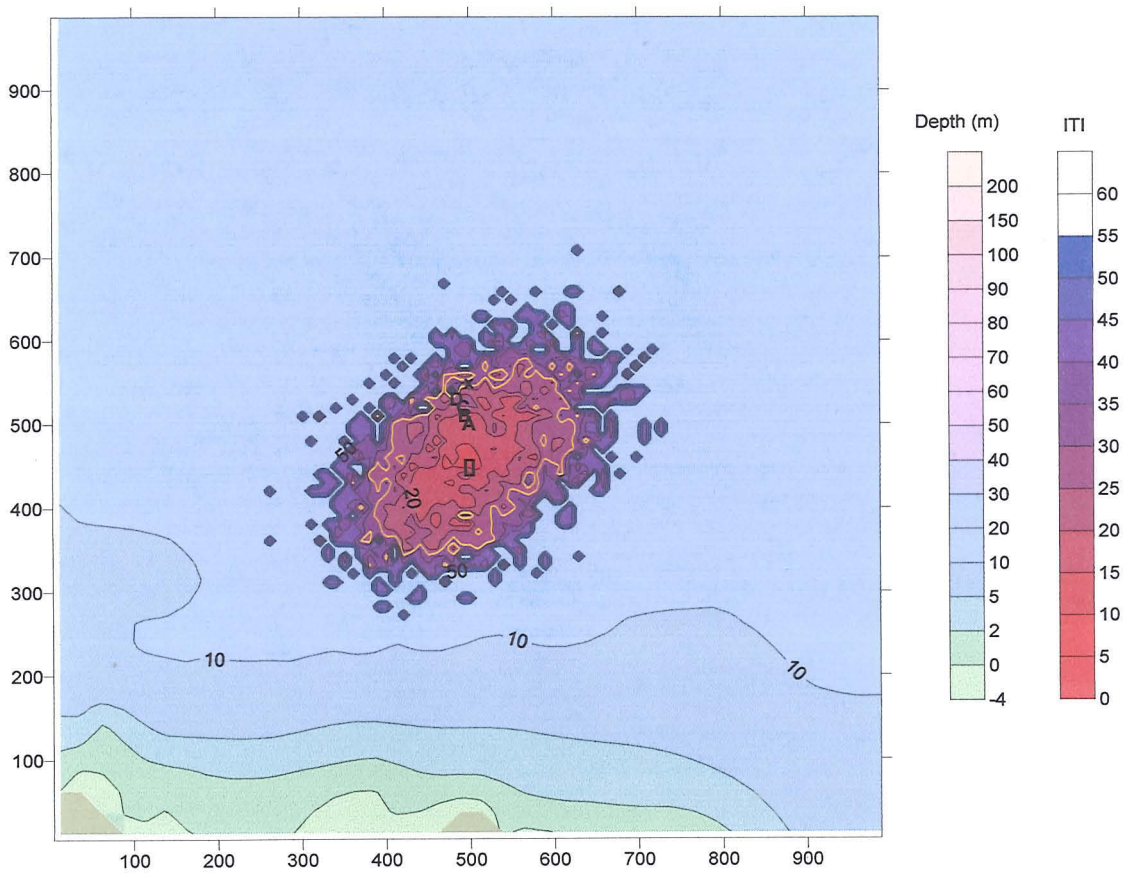

Figure 7.12 Site A – 50 kg cage^{-1} day^{-1} with 100% faeces – close detail

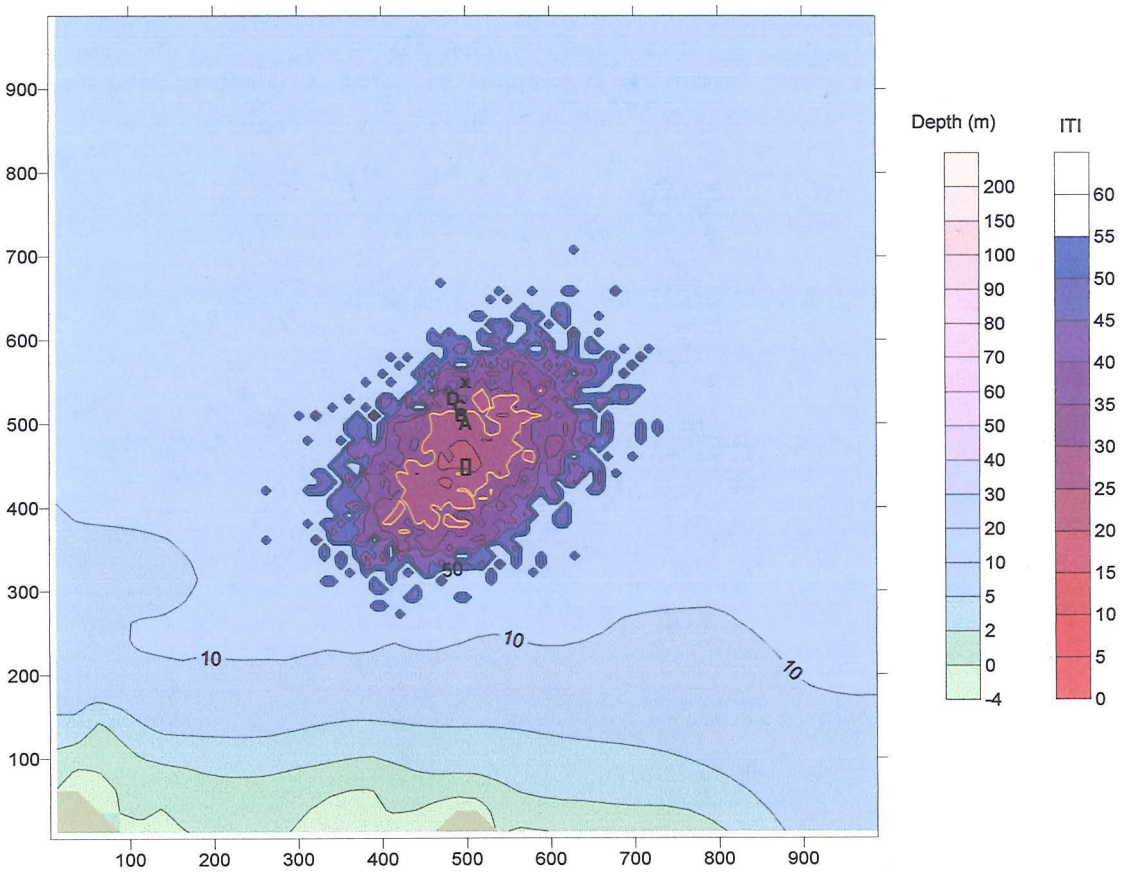

Figure 7.13 Site A – 20 kg cage^{-1} day^{-1} with 100% faeces – close detail

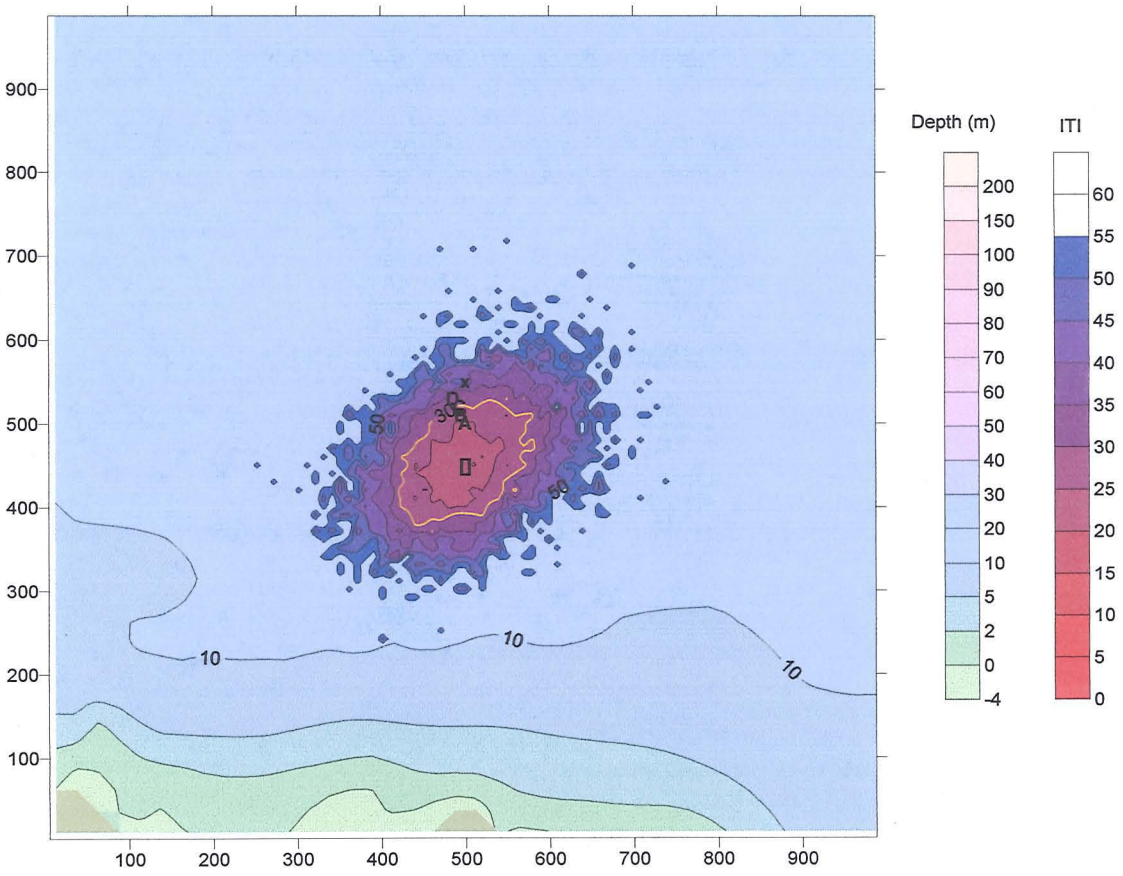

Figure 7.14 Site A – 20 kg cage^{-1} day^{-1} with 5% faeces and 50% pseudofaeces – close detail

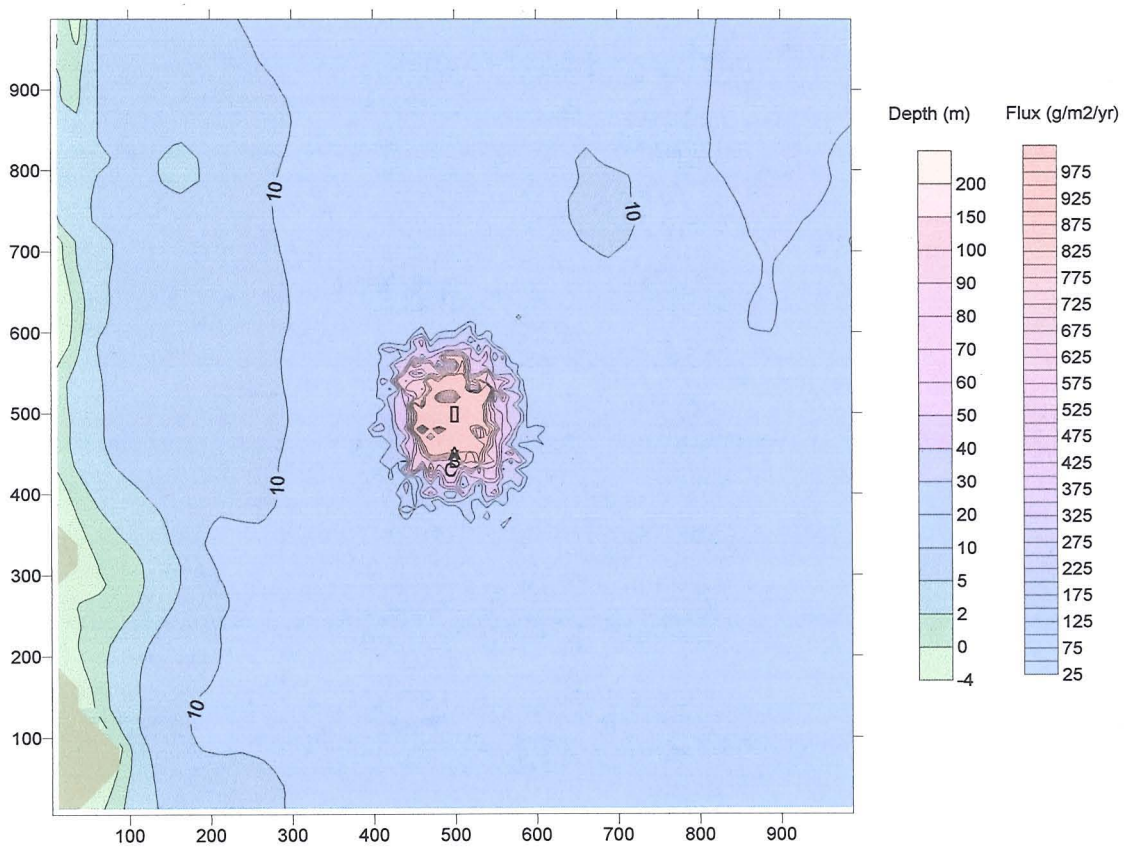

Figure 7.15 Site B – 50 kg cage^{-1} day^{-1} with 100% faeces

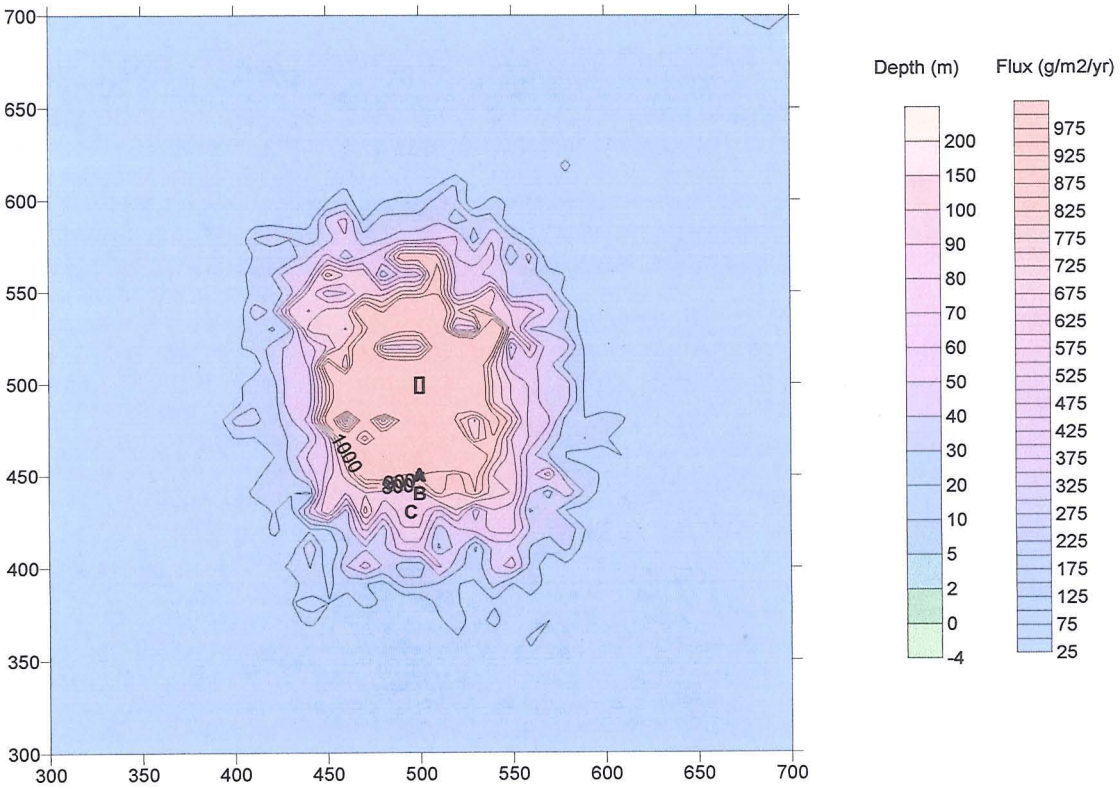

Figure 7.16 Site B – 50 kg cage^{-1} day^{-1} with 100% faeces – close detail

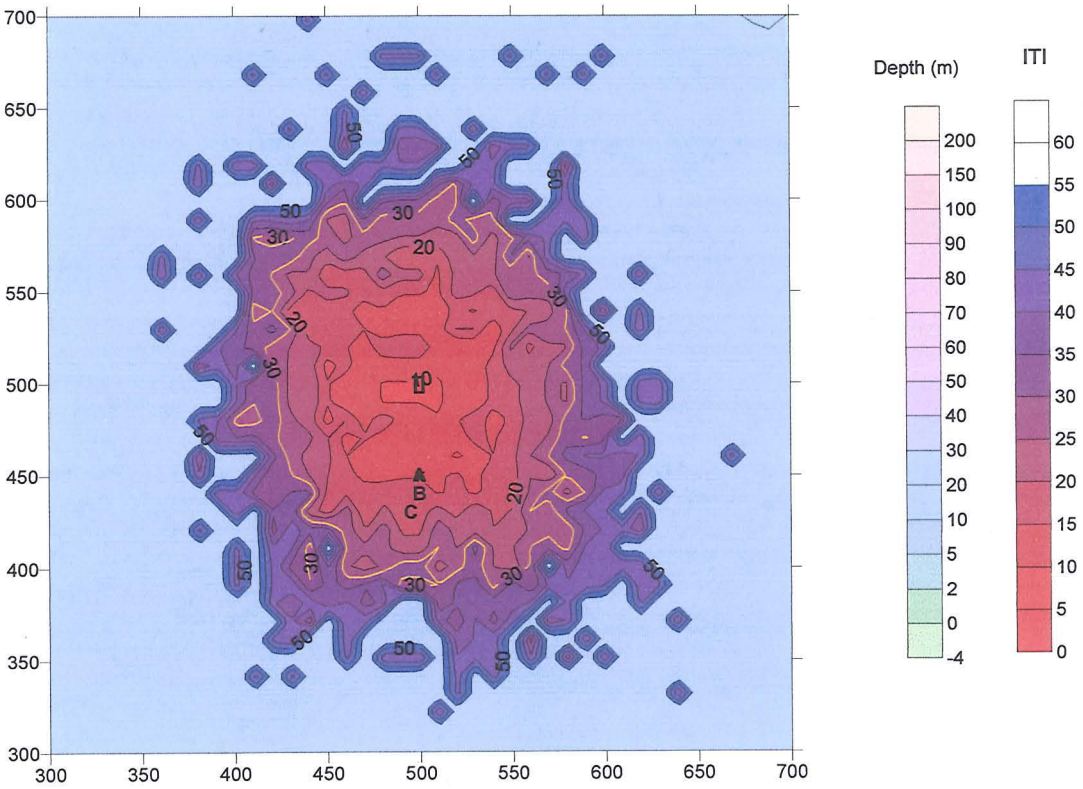

Figure 7.17 Site B - 50 kg cage^{-1} day^{-1} with 100% faeces – close detail

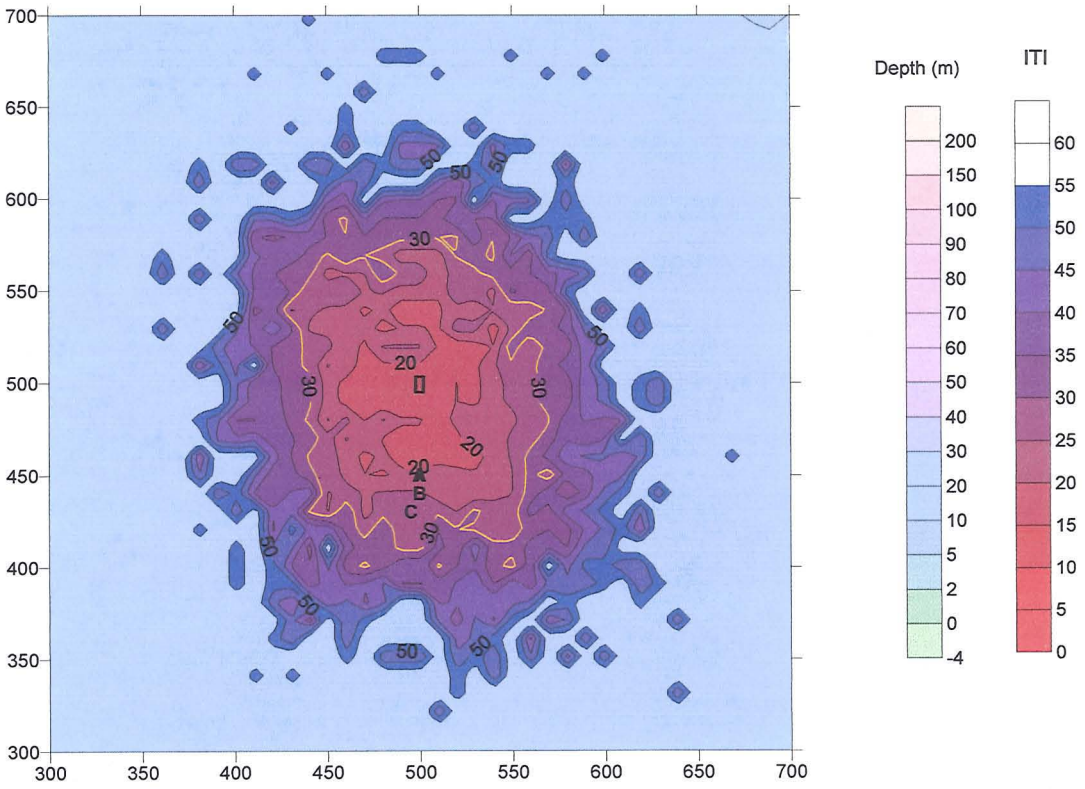

Figure 7.18 Site B – 20 kg cage^{-1} day^{-1} with 100% faeces – close detail

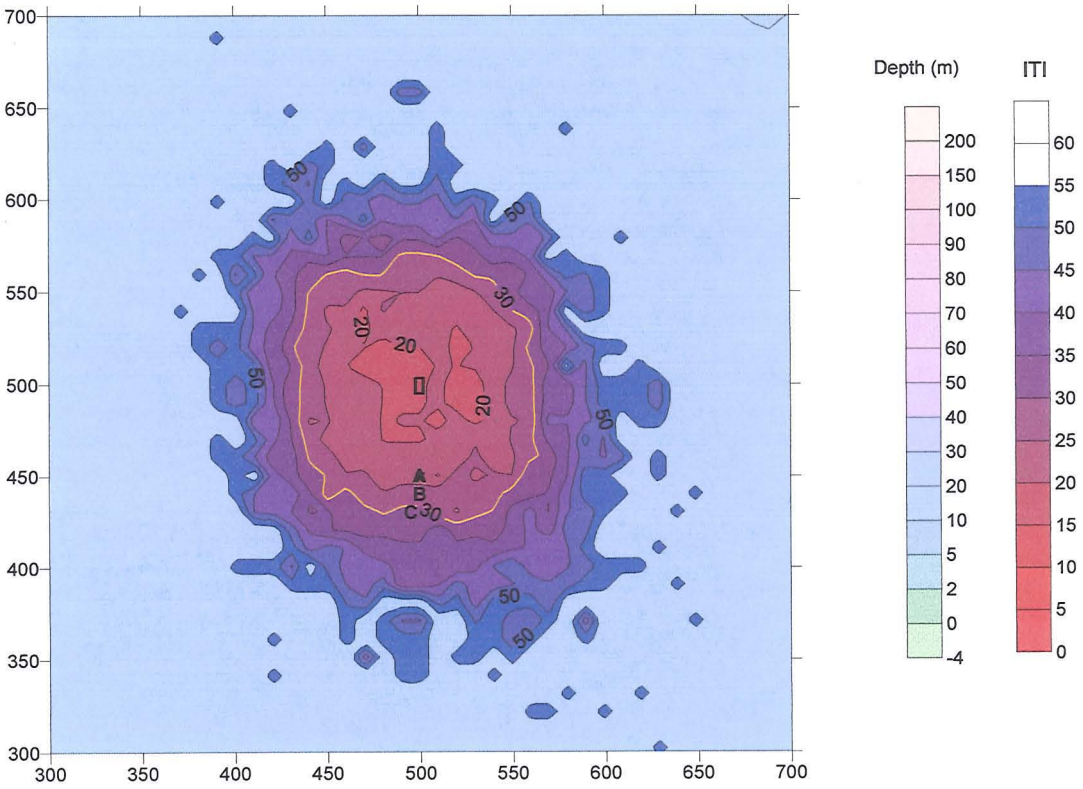

Figure 7.19 Site B – 20 kg cage^{-1} day^{-1} with 50% faeces and 50% pseudofaeces – close detail

8 Discussion

8.1 Achievement of aims and objectives of the thesis

The overall aim of this thesis was to develop mathematical models of the impact on the seabed of suspended culture of mussels (*Mytilus edulis*). To address this aim, a series of objectives was established, namely:

- to describe the benthic impacts of mussel farming at sites typical of those used in Scotland and Ireland;

- to development a conceptual framework of the impacts of mussel farming and their causes and to assess the suitability of existing models of the dispersion and effects of waste from fish farms for application to mussel farms;

- to develop and validate a management model of the effects of suspended mussel cultivation on the seabed in sheltered coastal waters.

A series of field studies were carried out at three very different mussel cultivation sites in Scotland and Ireland. The sites were selected to cover a range of environmental settings and scales of operation. Consequently, the intensity of benthic impact of the farming operations was found to differ considerably between sites. The most impacted site, Site B, had the highest biomass and had been established for the longest period (over 13 years). The benthic community and the physico-chemical characteristics of the sediment were significantly different from the conditions at local reference stations. Details are given in Chapters 4 and 5.

By contrast, there were no detectable benthic impacts attributable to the mussel farms at Sites S and A. The benthic communities at Site S showed indications of degradation, but stressed conditions were apparent at all sampling stations and it appears that this may be a natural feature of the loch system. Conversely, the benthic communities at Site A

showed no such characteristics, and had ITI values indicating "little effect" of benthic enrichment. The field studies of the biology and chemistry of the benthic environments were supported by hydrographic records of water currents at 2 or 3 depths at each field Site.

A review of the mathematical modelling approaches available for potential application to the particulate wastes from mussel farms indicated that the most developed and comprehensive models utilise particle tracking methods. In these models, the waste is simulated as a large number of discrete particles that settle through the water column and are influenced by the hydrographic processes in the water column. The most useful model was found to be DEPOMOD, which is used in relation to wastes from fish farming. DEPOMOD links the physics of particle settlement with hydrography, sediment dynamics and impact on the benthic infaunal community. Details of the functionality and configuration of DEPOMOD were examined (Chapter 7). The model was amended to simulate shellfish farming. The main areas of adaptation were in the parameterisation of the mussel lines in place of cages of fish, the settling characteristics of the waste, and the feeding and excretion rates of mussels.

Good information on the statistical distribution of settling rates of the mussel faeces and pseudofaeces was found to be both critical to the application of the model, and unavailable in the literature. Laboratory experiments were therefore carried out to determine values for these parameters (Chapter 6).

The amended version of DEPOMOD was applied to the field sites, and the output was compared with field data on the infaunal community structures. It was found that the model could produce realistic predictions of the distribution of wastes on the seabed, and also the general nature of the changes in the benthic fauna. However, the model tended to over-estimate the severity of the benthic impact in terms of the infaunal trophic index (ITI). It was not possible to make reliable comparisons between carbon flux to the seabed and organic carbon in the sediments.

It was possible to adjust the parameters of the model, and the relationship between carbon flux and ITI values to match the field data. However, it was not clear whether such adjustments would be equally applicable in other field locations. Further field studies are required for full validation of the model. This is equally applicable to the parent DEPOMOD model with both versions (Finfish and mussel impact) requiring validation across a range of field sites.

The overall objectives of the programme were therefore broadly achieved.

8.2 Does the model work?

It is clear that the physical processes affecting the deposition of particulate waste are effectively parameterised in the model. The model works reliably for fish farms, and is now used in the prediction of impact, and the regulation of fish farms in Scotland. The relationship between carbon deposition and biological response has been validated for fish farms (and in a previous version of the model, for sewage discharges).

The current project has shown that the model can also work for mussel farms. However, the applicability of the model is currently limited by inadequate knowledge in some critical areas.

a) By far the most important area of uncertainty is the feed load and excretion rate. This is critical to the model as it determines the quantity of waste material that is released from the mussel farm. It also influences the ratio between faeces and pseudofaeces released. In fish farms, these parameters are reasonably well defined by the knowledge of the amount of feed offered to the fish, and the feed conversion efficiency of the fish. In shellfish farms, however, the farm operator does not control the quantity of material presented to the stock. The shellfish rely upon the natural resources of food available to them in the water column. The variability in this is not well known, and is likely to be site-specific. In addition, there is some uncertainty in the proportion of the suspended matter that is filtered from the water column by the

stock. It will be important for further development of the model to find an appropriate strategy to account for these uncertainties, such as routine monitoring for suspended solids and phytoplankton concentrations on a seasonal basis.

b) The relationship between carbon deposition and benthic response, as measured by ITI, has been shown to be predictable between fish farm sites within envelopes of acceptable precision. The relationship at mussel sites appears to differ from that at fish farms, and may differ between sites. The underlying reasons for these differences may be related to the nature of the waste material being deposited. At fish farms, this is predominantly organic matter (excess feed pellets, and faeces). At shellfish farms, the faeces, and particularly the pseudofaeces will contain inorganic as well as organic material, i.e. will resemble the composition of the natural seston. This is reflected in carbon concentrations in seabed sediments, which can reach high values (>15%) at fish farms, but only a maximum of 6% at the most impacted shellfish site in this study. The benthic infauna at shellfish sites is subject to greatly increased deposition of material, but not the heavy organic enrichment encountered at fish farm sites. Therefore the model requires further adaptation with adjustments to the ITI curves from more empirical data.

c) Resuspension of deposited sediment is important in the maintenance of good benthic conditions at relatively energetic aquaculture sites. The critical erosion and deposition velocities used in the model were those used in relation to fish farm waste. It is not clear how different the true values for shellfish farm waste would be. The current velocities measured at the study sites were very low, well below the critical erosion velocity in DEPOMOD. Therefore, it may be that resuspension is not an important factor in the model as presented in this study. It may be that if the critical erosion velocity for mussel waste is similar to that for fish waste, then the lower settling velocities of mussel waste would result in wide dispersion of the waste prior to settlement on the sea bed.

d) A related factor is the parameter known as "consolidation time", which is the time after deposition of waste at which the waste is considered permanently incorporated into the seabed and not available for resuspension. This is unknown for mussel wastes and the value used in the model is as used for fish waste.

e) The model does not take into account the possible effect of turbulence on the structure of the particles. Break-up of the particles would decrease their settling velocity and alter the final distribution on the seabed. Broken particles are also more likely to become assimilated into the natural particulate matter, and potentially taken up by other shellfish, altering the flow of material through the farm.

f) No account has been taken of the potential of the mussel farm to alter the local hydrographic regime. The "barrier" to flow through the farm presented by the mussel lines will increase as the mussels grow. Conversely, current speeds will be increased around the side and beneath the mussel farm as a result of this baffle effect. The effect of this 'increased' water movement on the stability and deposition of the faecal matter is unclear. This factor could be measured in field studies using current meters positioned in and around the farm.

8.3 Regulatory application of the model

A declared objective of this work is the development of a management model for the assessment and control of shellfish (mussel) farm developments. There are two primary environmental factors that control the ability of an area to support shellfish cultivation. The first is the magnitude of the available food resource. This comprises particulate organic matter advected into the farming area by tidal and other currents. This has been studied in various areas, and a number of models of varying complexity are available for assessing the maximum amount of shellfish that can be successfully cultivated in a body of water (Smaal *et al.*, 1986)

The second is the environmental consequences of the shellfish cultivation. The most comprehensive studies in this area have been carried out in the rias of NW Spain (Tenore *et al.*, 1984), where very large scale farming was shown to have altered the structure of the pelagic and benthic communities. The current project has addressed the benthic impact of mussel farming on much smaller scales. Impact has been shown to occur and has been shown to be amenable to assessment through modelling.

Currently, few, if any, European Union countries require impact assessment of shellfish cultivation projects, or monitoring of the environmental consequences. Shellfish farming is not explicitly covered by the EU Environmental Impact Assessment Directive 85/337/EEC. However, there is pressure for an increased degree of monitoring and assessment of shellfish farming, eg as discussed in the reports of the EU MARAQUA project (Fernandes *et al.*, 2000). Modelling, as presented in this thesis, can provide a valuable framework within which to structure environmental assessments and monitoring programmes.

8.4 Future work

The above discussion has identified as series of topics that need to be addressed in the further development and utilisation of models of benthic impact of shellfish farming. These can be summarised as:

- Improved parameterisation of the input function of food and associated inorganic suspended matter, and the subsequent excretion of waste.

- Improved definition of the relationship between benthic biological response (ITI) and input to the seabed of organic matter or total solids from shellfish farms.

- Improved information on the settling rates of faeces and pseudofaeces from the range of shellfish species grown in suspended culture.

- Parameterisation of consolidation and resuspension of waste from shellfish farms.

- Definition of procedures and scope of impact assessments for shellfish sites.

- Development of procedures linking modelling of shellfish farm sites with subsequent monitoring programmes.

REFERENCES

Allen, C.M. 1982. Numerical simulation of contaminant dispersion in estuarine flow. *Proceedings of the Royal Society of London - A* **381**, 179-194.

Aller, R. C. 1978. Experimental studies of changes produced by deposit feeders on pore water, sediment and overlying water chemistry. *American Journal of Science* **28,** 1185-1234.

Aller, R. C. 1982. The effects of macrobenthos on chemical properties of marine sediment and overlaying water. In: *Animal sediment relations. The biogenic alteration of sediments.* (ed. P. L. McCall & M. J. S. Tevesz). New York: Plenum Press. pp. 53-102.

Baudinet, D., Alliot, E., Berland, B., Grenz, C., Plante-Cuny, M. R., Plante, R. & Salen-Picard, C. 1990. Incidence of a mussel culture on biogeochemical fluxes at the sediment water interface. *Hydrobiologia* **207,** 187-196.

Bayne, B. L. 1976. Marine mussels: their ecology and physiology. Cambridge University Press. pp. 411.

Bayne, B. 1998. The physiology of suspension feeding by bivalve molluscs: an introduction to the Plymouth "TROPHEE" workshop. *Journal of Experimental Marine Biology and Ecology* **219,** 1-19.

Black, K., Kiemer, M.C.B. & Ezzi, I. 1995. The relationships between hydrodynamics, the concentration of hydrogen sulphide produced by polluted sediments and fish health at several marine cage farms in Scotland and Ireland. *Journal of Applied Ichthyology* **12**, 15-20.

Bowden, K.F. 1983. Physical Oceanography of coastal waters. Ellis Horwood Limited, Chichester, UK. pp. 26-32.

Brown, J.R., Gowen, R.J. & McLusky D.S. 1987. The effect of salmon farming on the benthos of a Scottish sea loch. *Journal of Experimental Marine Biology and Ecology* **109,** 39-51.

Burt, T.N. & Turner, K.A. 1983. Deposition of sewage sludge on a rippled sand bed. Hydraulics Research Report IT248. Wallingford, Oxon, U.K.

C.S.T.T. 1994. MPMMG Comprehensive studies for the purpose of Article 6 of DIR 91/271 EEC. The Urban Waste Water Treatment Directive. Forth River Purification Board, Edinburgh. pp. 42 + figs.

Chen, Y.S., Beveridge, M.C.M. & Telfor, T.C. 1999a. Physical characteristics of commercial pelleted Atlantic salmon feeds and consideration of implications for modelling of waste dispersion through sedimentation. *Aquaculture International* **7**, 89-100.

Chen, Y.S., Beveridge, M.C.M. & Telfor, T.C. 1999b. Settling rate characteristics and nutrient content of the faeces of Atlantic salmon, *Salmo salar* L., and the implications for modelling of solid waste dispersion. *Aquaculture Research* **30**, 395-398.

Clarke, K.R. 1993. Non-parametric multivariate analyses of changes in community structure. *Austalian Journal of Ecology* **18**, 117-143.

Cornel, G.E & Whoriskey, F.G. 1993. The effect of rainbow trout (*Oncorhynchus mykiss*) cage culture on the water quality, zooplankon, benthos and sediments of Lac du Passage, Quebec. *Aquaculture* **109,** 101-117

Cromey, C.J., Black, K.D., Edwards, A.E. Jack, I.A. 1997. BenOss version 2 software - Biological effects and organic solids sedimentation. CCMS Dunstaffnage Marine Laboratory, P.O. Box 3, Oban, Argyll, PA34 4AD.

Cromey, C. J., Black, K. D., Edwards, A. & Jack, I. A. 1998. Modelling the Deposition and Biological Effects of Organic Carbon from Marine Sewage Discharges. *Estuarine, Coastal and Shelf Sciences* **47,** 295-308.

Cromey, C.J, Nickell, T.D. & Black, K.D. 2000a. DEPOMOD (v1.5) software: a model for predicting the effects of solids deposition to the benthos from mariculture. CCMS Dunstaffnage Marine Laboratory, P.O. Box 3, Oban, Argyll, UK, PA34 4AD.

Cromey, C.J., Nickell, T.D., Black, K.D., Provost, P.G. & Griffiths, C.R. 2000b. Observations and modelling of the resuspension of a particulate tracer from a point source for impact predictions. In: *Proceedings of Oceanology International 2000*, Brighton, UK, 7th - 10th March 2000.

Cromey, C.J., Nickell, T.D., Black, K.D., Provost, P.G. & Griffiths, C.R. 2002a. Validation of a fish farm waste resuspension model by use of a tracer discharged from a point source in a coastal environment. *Estuaries* **25**, 946-929.

Cromey, C.J., Nickell, T.D. & Black, K.D. 2002b. DEPOMOD: Modelling the deposition and biological effects of waste solids from marine cage farms. *Aquaculture* **214**, 211-239.

Dahlback, B. & Gunnarson, L. A. H. 1981. Sedimentation and sulfate reduction under a mussel culture. *Marine Biology* **63,** 269-275.

Dame, R. F. 1989. Ecosystem dynamics and bivalve culture. *Journal of Shellfish Research* **8**(2), 471.

Drinkwater, J. 1987. Shellfish cultivation in Scotland. Department of Agriculture and Fisheries for Scotland, Marine Laboratory. Report number 13. pp.20.

Dyer, K.R. 1979. Estuarine hydrology and sedimentation. Cambridge University Press, Cambridge, UK.

Edwards, A. & Sharples, F. 1985. Scottish Sea Lochs: a catalogue. Oban: Scottish Marine Biological Association.

Ervik, A., Kupka Hansen, P., Aure, J., Stigebrandt, A., Johannessen, P. & Jahnsen, T. 1997. Regulating the local environmental impacts of intensive marine fish farming. I. The concept of the MOM system (Modelling - Ongrowing fish - Monitoring). *Aquaculture* **158**, 85-94.

F.R.S. 2002. Scottish Shellfish Farm Production Survey 2001. Fisheries Research Services Report. FRS Marine Laboratory, P.O. Box 101, Victoria Road, Aberdeen, AB11 9DB, UK.

Fernandes, T.F.M., Miller, K.L. & Read P.A. 2000. Monitoring and regulation of marine aquaculture in Europe. *Journal of Applied Ichthyology* **16** (4-5), 138-143.

Field, J.G., Clarke, K.R. & Warwick, R.M. 1982. A practical strategy for analysing multispecies distribution patterns. *Marine Ecology Progress Series* **8**, 37-52.

Findlay, R. H. & Watling, L. 1994. Toward a process level model to predict the effects of salmon-pen aquaculture on the benthos. In: *Modelling benthic impacts of organic enrichment from marine aquaculture.*, vol. 1949 (ed. B. T. Hargrave.), pp. 47-77: Canadian Technical Report of Fisheries and Aquatic Sciences.

Findlay, R. H. & Watling, L. 1997. Prediction of benthic impact for salmon net-pens based on the balance of benthic oxygen supply and demand. *Marine Ecology Progress Series* **155**: 147-157.

Findlay, R. H., Watling, L. & Mayer, L. M. 1995. Environmental Impact of Salmon Net-Pen Culture on Marine Benthic Communities in Maine: A case study. *Estuaries* **18,** 145-179.

Folke, C. & Kautsky, N. 1989. The role of ecosystems for a sustainable development of aquaculture. *Ambio* **18,** 234-243.

Froelich, P.N., Klinkhammer, G.P., Bender, M.L., Luedtke, N.A., Heath, G.R., Cullen, D., Dauphin, P., Hammond, D., Hartman, B. & Maynard V. 1979. Early oxidation of organic matter in pelagic sediments of the eastern equatorial Atlantic: sub-oxic diagenesis. *Geochemica et Cosmochimica Acta*, **43**, 1075-1090.

GESAMP (IMO/FAO/UNECO-IOC/WMO/IAEA/UN/UNEP Joint Group of Experts on the Scientific Aspects of Marine Environmental Protection) 1991. Reducing environmental impacts of coastal aquaculture. *Rep. Stud. GESAMP* **47** pp. 35.

GESAMP (IMO/FAO/UNECO-IOC/WMO/IAEA/UN/UNEP Joint Group of Experts on the Scientific Aspects of Marine Environmental Protection) 1996. Monitoring the ecological effects of coastal aquaculture wastes. *Rep. Stud. GESAMP* **57** pp. 38.

Gillibrand, P.A. & Turrell, W.R. 1997. The use of simple models in the regulation of the impact of fish farms on water quality in Scottish sea lochs. *Aquaculture* **159**, 33-46.

Gowen, R. J. & Bradbury, N. B. 1987. The ecological impact of salmonid farming in coastal waters: A Review. *Oceanography and Marine Biology Annual Review* **25,** 563-575.

Gowen, R. J., Brown, J. R., Bradbury, N. B. & McLusky, D. S. 1988. Investigation into benthic enrichment, hypernutrification and eutrophication associated with mariculture in Scottish coastal waters (1984-1988). Department of Biological Sciences, University of Stirling, Stirling.

Gowen, R. J., Bradbury, N. B. & Brown, J. R. 1989. The use of simple models in assessing two of the interactions between fish farming and the marine environment. In: *Aquaculture - a biotechnology in progress.* (ed. E. J. a. N. W. N. De Paux), Bredene, Belgium: European Aquaculture Society. pp. 1071 - 1080.

Gowen, R. J., Smyth, D. and Silvert, W. 1994. Modelling the spatial distribution and loading of organic fish farm waste to the seabed. In *Modelling Benthic Impacts of Organic Enrichment from Marine Aquaculture* (ed. B. T. Hargrave). Vol. 1949 pp. 19-30: Canadian Technical Report of Fisheries and Aquatic Sciences. 1949.

Grant, J. 1996. The relationship of bioenergetics and the environment to the field growth of cultured bivalves. *Journal of Experimental Marine Biology and Ecology* **200,** 239-256.

Grant, J., Hatcher, A., Scott, D. B., Pocklington, P., Schafer, C. T. & Winter, G. 1995. A multidisciplinary approach to evaluating benthic impacts of shellfish aquaculture. *Estuaries* **18,** 124-144.

Grenz, C. 1989. Quantification et destinee de la biodeposition en zones de production conchylicole intensive en Mediterranee. In: *Centre d'Oceanologie de Marseille*, pp. 144. France: Universite d'Aix- Marseille II.

Grenz, C., Hermin, D., Baudinet, D. & Daumus, R. 1990. In situ biochemical and bacterial variation of sediments enriched with mussel biodeposits. *Hydrobiologia* **207,** 153-160.

Grenz, C., Plante-Cuny, M., Plante, R., Alliot, E., Baudinet, D. & Berland, B. 1991. Measurement of benthic nutrient fluxes in Mediterranean shellfish farms: A methodological approach. *Oceanological Acta* **14,** 195-201.

Hagino, S. 1977. Physical properties of the pollutants, In: *Senkai Yoshoko to Jika Osen (Shallow-sea aquaculture and self pollution)* pp. 31-41. (Ed. Japanese Society of Scientific Fisheries. Suisdangaku Shirizu) **21** (Fish Ser 21). Published by Koseisha Koseikaku. pp. 134.

Hall, P. O. J., Anderson, L. G., Holby, O., Kollberg, S. & Samuelsson, M. O. 1990. Chemical fluxes and mass balances in a marine fish cage farm. I. Carbon. *Marine Ecology Progress Series* **61,** 61-73.

Hansen, P.K., Lunestad, B.T. & Samuelson, O.B., 1992. Ecological effects of antibiotics and chemotherapeutants from fish farming. In: *Chemotherapy in aquaculture: from theory to reality.* (eds. Michel, C. & Alderman, D.J.) 1992. Office International Des Epizooites Symposium, Paris, 12-15 March 1991. pp. 174-178.

Hansen, P.K., Pittman, K. & Ervik, A., 1990. Effects of organic waste from marine fish farms on the sea bottom beneath cages. *ICES*, CM-1990/F:34: 1-14.

Hargrave, B. T. (1994). Modelling benthic impacts of organic enrichment from marine aquaculture. In: *Canadian Technical Report on Fisheries and Aquatic Sciences.*, vol. 1949, pp. xi + 125 p.

Harris, J.R.W., Gorley, R.N. & Bartrett, C.A. 1993. EcoS Version 2 - a user manual. Plymouth Marine Laboratory, Prospect Place, Plymouth, PL1 3DH, UK. pp. 101-102.

Hatcher, A., Grant, J. & Schofield, B. 1994. Effects of suspended mussel culture (Mytilus spp.) on sedimentation, benthic respiration and sediment nutrient dynamics in a

coastal bay. *Marine Ecology Progress Series* **115,** 219-235.

Haven, D. S. & Morales-Alamo, R. 1966. Aspects of biodeposition by oyster and other invertebrate filter feeders. *Limnology and Oceanography* **11,** 487-498.

Hawley, N. 1982. Settling velocity distribution of natural aggregates. *Journal of Geophysical Research* **87,** 9489-9498.

Henderson, A. & Davies, I.M. 2001. Review of the regulation and monitoring of aquaculture in Scotland, with emphasis on environment and consumer protection. MLA Report, 01/01. pp. 28.

Henderson, A., Gamito, S., Karkassis, I., Pederson, P. & Smaal, A. 2001. Use of hydrodynamic and benthic models for managing the environmental impacts of marine aquaculture. *Journal of Applied Ichthyology* **17**, 163-172.

Hethershaw, A.D. 1988. Sediment transport in the sea, on beaches and in rivers; Part 1 - Fundamental principles. *J. Nav. Res.* **14**, 154-170.

Hevia, M., Rosenthal, H. & Gowen, R.J. 1996. Modelling benthic deposition under fish cages. *Journal of Applied Ichthyology* **12**, 71-74.

Holmer, J. 1991. Impacts of aquaculture on surrounding sediments: generation of organic-rich sediments. In: *Aquaculture and the Environment*, vol. 16 (ed. N. De Paux and J. Joyce), pp. 155-175.

Jaramillo, E., Bertran, C. & Bravo, A. 1992. Mussel biodeposition in an estuary in southern Chile. *Marine Ecology Progress Series* **82,** 85-94.

Jorgensen, B. B. 1982. Mineralization of organic matter in the sea bed - the role of sulphate reduction. *Nature* **296,** 643-645.

Jorgensen, C.B. 1990. *Bivalve Filter Feeding.* Olson and Olson.

Kaiser, M. J., Laing, I., Utting, S. D. & Burnell, G. M. 1998. Environmental impacts of bivalve culture. *Journal of Shellfish Research* **17,** 59-66.

Kaspar, H. F., Gillespie, P. A., Boyer, I. C. & MacKenzie, A. L. 1985. Effects of mussel aquaculture on the nitrogen cycle and benthic communities in Kenepru Sound, Marlborough Sounds, New Zealand. *Marine Biology* **85,** 127-136.

Kaspar, H.F., Hall, G.H. & Holland, A.J., 1988. Effects of sea cage salmon farming on sediment nitrification and dissimilatory nitrate reduction. *Aquaculture* **70,** 333-344.

Kautsky, N. & Evans, S. 1987. Role of biodeposition by *M. edulis* L. in the circulation of matter and nutrients in a Baltic coastal system. *Marine Ecology Progress Series* **38,** 201-212.

Kiorboe, T., Mohlenberg, F. & Nohr, O. 1980. Feeding, particle selection and carbon absorption in *Mytilus edulis* in different mixtures of algae and resuspended bottom materials. *Ophelia* **19,** 193-205.

Ladle, M., Welton, J. S. & Bell, M. C. 1987. Sinking rates and physical properties of faecal pellets of freshwater invertebrates of the genera *Simulium* and *Gammarus*. *Arch. Hydrobiol.* **108,** 411-424.

Lefley, J. W. & MacDougall, N. 1991. The Dunstaffnage sedimentation trap and its moorings. Dunstaffnage Marine Laboratory Internal Report No. 174. March 1991 pp. 8.

Loo, L. O. & Rosenberg, R. 1983. *Mytilus edulis*, culture, growth and production in Western Sweden. *Aquaculture* **35,** 137-150.

Mardia, K.V., Kent, J.T. & Bibby, J.M. 1979. *Multivariate Analysis*. Academic Press. London.

Mason, J. & Drinkwater, J. 1981. Experiments on suspended cultivation of mussels in Scotland.: Department of Agriculture and Fisheries for Scotland, Marine Laboratory. Report number 4. 15pp.

Mattson, J. & Linden, O. 1984. Impact from cultures of *Mytilus edulis* on the benthic ecosystem in a narrow sound on the Swedish West coast. *Vatten* **40,** 151-163.

McLellan, H.J. 1965. *Elements of Physical Oceanography*. Permagon Press, Oxford, UK.

McLusky, D.S. 1990. The Estuarine Ecosystem 2nd edition. Blackie and Son, Glasgow UK. pp. 215.

Mearns, A.J. & Word, J.Q. 1982. Forecasting effects of sewage solids on marine benthic communities. In: *Ecological Stress and the New York Bight: Science and Management*. (ed. Mayer) G.F. Columbia S Carolina Estuarine Research Federation. pp. 495-512.

Morris, A.W. 1983. *Practical procedures for estuarine studies*. Handbook prepared by the Estuarine Ecology Group of the Institute for Marine Environmental Research. Natural Environment Research Council.

Nature Conservancy Council 1989. *Fish farming and the safeguard of the natural marine environment*. Nature Conservancy Council Scottish Headquarters, Edinburgh. 136 pp.

Nature Conservancy Council 1990. Fish farming and the Scottish freshwater environment. Report to the Nature Conservancy Council, Scottish Natural Heritage,

Edinburgh, UK. Contract No. HF3-03-450. pp. 285.

Navarro E, Iglesias J. I. P., Pérez-Camacho A., Labarta U. & Beiras R.. 1991. The physiological energetics of mussel (*Mytilus galloprovincialis* Lmk) from different cultivation rafts in the Ria de Arosa (Galicia, NW Spain). Aquaculture, 94: 197-212

Neiland, S. & McMahon, T. 1999. A benthic survey of Inner Bantry Bay. Fisheries Bulletin No. 18 - 1999. Marine Institute. Dublin.

Neumann, G. & W. J. Pierson jr. 1966. *Principles of Physical Oceanography.* Prentice-Hall, Englewood Cliffs.

Odum, W. E. 1974. Potential effects of aquaculture on inshore coastal waters. *Environmental Conservation* **1,** 225-230.

Pearson, T.H., 1987. Benthic ecology in an accumulating sludge disposal site. In: *Oceanic processes in marine pollution. Vol 1. Biological processes and wastes in the ocean.* (eds. Capuzzo, J.M. & Kester, D.R.) R.E. Krieger Publishing Co., Malabar, USA. pp. 195-200.

Pearson, T.H. & Black, K.D. 2001. The environmental impacts of marine fish cage culture. In: *Environmental Impacts of Aquaculture* (ed. Black, K.D.), Sheffield Academic Press, Sheffield, UK. ISBN 0-8493-0501-2. pp. 1-31.

Pearson, T. H. & Rosenberg, R. 1978. Macrobenthic succession in relation to organic enrichment and pollution of the marine environment. *Oceanography and Marine Biology Annual Review* **16,** 229-311.

Pearson, T. H. & Stanley, S. O. 1979. Comparative measurement of the redox potential of marine sediments as a rapid means of assessing the effect of organic pollution. *Marine Biology* **53,** 371-379.

Pereira, P.M.F. 1997. Macrobenthic succession and changes in sediment biogeochemistry following marine fish farming. PhD Thesis. University of Stirling. 220 pp.

Pielou, E.C. (1966). The measurement of diversity in different types of biological collections. *Journal of Theoretical Biology* **13,** 131-144.

Rhoads, D.C. & Boyer, L.F., 1982. The effect of marine benthos on physical properties of sediments. A successional perspective. In: McCall, P.L. & Tevesz, M.J.S. (eds.), 1982. *Animal sediment relations. The biogenic alteration of sediments.* Plenum Press, New York. PP.3-57.

Ritz, D.A., Lewis, M.E. & Shen, M., 1989. Response to organic enrichment of infaunal macrobenthic communities under salmonid seacages. *Marine Biology*, **109**: 211-214.

Rodhouse, P. G., Roden, C. M., Hensey, M. P. and Ryan, T. H. (1985). Production of mussels, *Mytilus edulis*, in suspended culture and estimates of carbon and nitrogen flow: Killary Harbour, Ireland. *Journal of the Marine Biological Association of the U.K.* **65,** 55-68.

S.C.C.W.R.P. 1992. Modification and verification of sediment deposition models. Southern Californian Coastal Waters Research Project Authority. California. USA, Final Report Sep. 1992, 331 pp.

S.E.P.A. 1998. Regulation and monitoring of marine cage fish farming in Scotland: a manual of procedures. Scottish Environment Protection Agency, Erskine Court, Castle Business Park, Stirling, U.K. FK9 4TR. 71 pp.

Samuelson, O.B., Ervick, A. & Solheim, E., 1988. A qualitative and quantitative analysis of the sediment gas and diethylether extract of the sediment from salmon farms.

Aquaculture, **74**: 277-285.

Shannon, C.E. & Weaver, W. 1949. The mathematical theory of communication. Urbana: University of Illinois Press. pp. 117

Silvert, W. 1992. Assessing environmental impacts of finfish aquaculture in marine waters. *Aquaculture* **107,** 67 - 79.

Silvert, W. 1994. Modelling benthic deposition and impacts of organic matter loading. In *Modelling Benthic Impacts of Organic Enrichment from Marine Aquaculture.* (ed. B. T. Hargrave) **Vol. 1949** pp. 1-18: Canadian Technical Report of Fisheries and Aquatic Sciences. 1949.

Silvert, W. & Cromey, C.J. 2001. Modelling Impacts. In: Black, K.D. (ed.) *Environmental Impacts of Aquaculture*, Sheffield Academic Press, Sheffield, UK. ISBN 0-8493-0501-2, pp. 154-181.

Silvert, W. & Sowles, J. W. 1996. Modelling environmental impacts of marine finfish aquaculture. *Journal of Applied Ichthyology* **12,** 75-81.

Simpson, W. R. 1982. Particulate matter in the oceans - sampling methods, concentration, size distribution and particle dynamics. *Oceanographic Marine Biological Annual Review* **20,** 119-172.

Soulsby, R. 1983. The bottom boundary layer of shelf seas. In: Johns, B. (ed). *Physical Oceanography of Coastal and Shelf Seas*. Elsevier, Amsterdam. pp. 189-266

Smaal, A. C., Verhagen, J. H. G., Coosen, J. & Haas, H. A. 1986. Interaction between seston quantity and quality, and benthic suspension feeders on Oosterschelde, The Netherlands. *Ophelia* **26,** 385-399.

Smaal, A.C. & Heral, M. 1998. Modelling bivalve carrying capacity. *Aquatic Ecology* **31** (4) 347-428.

Stenton-Dozey, J.M.E., Jackson, L.F. & Busby, A.J. 1999. Impact of mussel culture on macrobenthic community structure in Saldanha Bay, South Africa. *Marine Pollution Bulletin* **39** 357-366.

ten Brinke, W. B. M. 1994. Settling velocities of mud aggregates in the Oosterschelde tidal basin (The Netherlands), determined by a submersible video system. *Estuarine and Coastal Shelf Science* **39,** 549-564.

Tenore, K. R. & Dunstan, W. M. 1973a. Comparison of feeding and biodeposition of three bivalves at different food levels. *Marine Biology* **21,** 190-195.

Tenore, K. R. & Dunstan, W. M. 1973b. Comparison of rates of feeding and biodeposition of the American oyster, *Crassostrea virginica* Gmelin, fed different species of phytoplankton. *Journal of Experimental Marine Biology and Ecology* **12,** 19-26.

Tenore, K. R., Boyer, L. F., Cal, R. M., Corral, J., Garcia-Ferdandez, C., Gonzalez, N., Gonzalez-Gurmaran, E., Hanson, R. B., Iglesias, J., Krom, M., Lopez-Jamar, E., McClain, J., Pamatmat, M. M., Perez, A., Rhoads, D. C., de Santiago, G., Tietjen, J., Westrich, J. & Windom, H. L. 1982. Coastal upwelling in the Rias Bajos, N.W. Spain, contrasting benthic regimes of the Rias de Arosa and de Muros. *Journal of Marine Research* **40,** 701-772.

Tenore, K. R., Cal, R. M., Hanson, R. B., Lopez-Jamar, E., Santiago, G. & Tiejen, J. H. 1984. Coastal upwelling off the Rias Bajas, Galicia, Northwest Spain II. Benthic studies. I*CES, The Biological Productivity of the North Atlantic Shelf Areas* **183,** 91-100.

Tenore, K. R., Corral, J. & Gonzalez, N. 1985. Effects of intense mussel culture on food

chain patterns and production in coastal Galicia, NW Spain. *ICES CM* **F:62**.

Tett, P. B. 1986. Physical exchange and the dynamics of phytoplankton in Scottish sea-lochs. In *Proceedings of a NATO advanced study workshop on the role of freshwater outflow in coastal marine ecosystems.* (ed. S. Skreslet and K. Drinkwater), pp. 205-218. Berlin, Germany. Springer-Verlag.

Tsutsumi, H. & Kikuchi, T., 1983. Benthic ecology of a small cove with seasonal oxygen depletion caused by organic pollution. *Publications from the Amakusa Marine Biological Laboratory Kyushu University*, **7**: 17-40

Uncles, R.J., Elliott, R.C.A. & Weston, S.A. 1985. Observed fluxes of water, salt and suspended sediment in a partly mixed estuary. *Estuarine, Coastal and Shelf Sciences* **20** 147-167,

Warwick, R. M. & Clarke, K. R. 1991. A comparison of some methods for analysing changes in benthic community structure. *Journal of the Marine Biological Association of the United Kingdom* **71,** 225-244.

Warwick, R.M. & Clarke, K.R. 1994. *Changes in marine communities: An approach to statistical analysis and interpretation.* Natural Environment Research Council, U.K., 144 pp.

Weston, D. P. 1990. Quantitative examination of macrobenthic community changes along an organic enrichment gradient. *Marine Ecology Progress Series* **61,** 233-244.

Westrich, J.T. & Berner, R.A. 1984. The role of sedimentary organic matter in bacterial sulphate reduction: The G-model tested. *Limnology and Oceanography*. **29**: 236-249.

Word, J.Q. 1978. The Infaunal Trophic Index. In: Annual Report 1978. Coastal Water Research Project, El Segundo, California, USA. pp. 19-39.

Word, J.Q. 1980. Classification of benthic invertebrates into Infaunal Trophic Index feeding groups. In: Coastal Waters Research Project Biennial Report 1979-1980. SCCWRP, Long Beach, California, USA. pp. 103-121.

WRc Plc.1992. Development of a biotic index for the assessment of the pollution status of marine benthic communities. Final Report NR 3102/1. pp. 78.

Zar, J.H., 1984. *Biostatistical Analysis* (2nd edition). Prentice Hall Inc, USA. 718 pp.

Zobell, C. E. 1946. Studies on redox potential of marine sediments. *Bulletin of the American Association of Petroleum Geologists* **30,** 477-511.

APPENDIX 1.

1. **Introduction and Scope**

This method describes the procedure to determine ammonia in estuarine and sea waters. Concentration range from 0.1 - 12.0 µM ammonia.

2. **Principles of the Method**

In the presence of a catalyst and excess chlorine, ammonia reacts with phenol to form indophenol blue. The intensity of the blue colour is proportional to the concentration of the ammonia, the absorbance is determined at 630 nm.

3. **Reference Materials**

At present there is no Certificated Reference Material (CRM) for ammonia. With each set of analysis a LRM is randomly analysed. The results are used to maintain shewart control charts. LRM stock Sol^N 0.539 g (± 1 mg) NH_4Cl make up to 1000 ml with deionised water in a volumetric flask. 0.1 ml LRM stock contains 10 µg NH_4-N. eg 20 µl stock standard made up to 100 ml with low nutrient sea water (LNSW) in a volumetric flask = 2 µm.

4. **Reagents**

All chemicals are of Analar grade unless otherwise stated.

4.1 **2% Hydrochloric acid wash**

hydrochloric acid	(sp.gr.1.18)20 ml (± 2 ml)
deionised water	1,000 ml (± 100 ml)

In a fume cupboard, using a dispenser, carefully add the hydrochloric acid to the deionised water in a beaker.

4.2 **Reagent 1 (buffer)**

tri-sodium citrate	15.6 g (± 2 g)
sodium hydroxide	0.9 g (± 10 mg)
deionised water	100 ml (± 10 ml)

Weigh tri-sodium citrate and sodium hydroxide in weighing cups. Rinse a beaker with approx 50 ml hydrochloric acid wash followed by a rinse with deionised water. Add the deionised water and weighed chemicals to the washed beaker and dissolve (prepared on day of use).

4.3 **Reagent 2 (phenol-catalyst)**

phenol (A.R. grade)	3.5 g (± 0.4 gl)
potassium ferrocyanide (A.R grade)	0.4 g (± 10 mgl)
deionised water	100 ml (± 10 ml)

Weigh phenol and potassium ferrocyanide in weighing cups. Rinse a beaker with at least 50 ml hydrochloric acid wash followed by a rinse with deionised water. Add the deionised water and weighed chemicals to the washed beaker and dissolve (prepared on day of use).

4.4 **Reagent 3 (oxidising solution)**

dichloro-s-triazine-2,4,6-trione (A.R grade)	0.2 g (± 10 mg)
deionised water	100 ml (± 10 ml)

Weigh dichloro-s-tiazine-2,4,6-trione into a weighing cup. Rinse a beaker with at least 50 ml hydrochloric acid wash followed by a rinse with deionised water. Add the deionised water and weighed chemical into the washed beaker and dissolve (prepared on day of use).

4.5 **Standards**

Prepared fresh on day of use by pipetting predetermined volumes of concentrated stock solution containing a known amount of ammonia into standard volumes of Low Nutrient Seawater (LNSW). LNSW from each new carboy must be checked for excessive (not more than 0.5 µM) ammonia blank by analysis before use. Standards must be prepared in "B" grade volumetric flasks. Once opened the stock solution is stable for six months.

Stock ammonium standard solution is purchased from Aldrich chemical company. The standard contains a nominal 1.0 mg NH_4/ml. NB: this concentration requires to be checked on the label of each new bottle since they are individually calibrated and there will be variations between batches. If this is the case the concentrations in the example below will be amended accordingly and used in the calculation of results. Dividing by 18 and multiplying by 1,000 converts mg of NH_4/ml to µmoles NH_4/ml. This is achieved by dividing the given mg/ml by 18. Typical supplied level is 0.975mg NH_4/ml. This converts to 54.17µmoles NH_4-N/ml.

Standards need to be prepared in the appropriate analysis range eg. open sea 0.1-6.0 µM NH_4-N, estuarine samples 1.0-12µM NH4-N.

A suitable set of calibration standards for normal open sea samples is prepared as follows using the Aldrich stock standard solution.

2 µl stock solution made up to 100 ml with LNSW = 1.08 µM
5 µl stock solution made up to 100 ml with LNSW = 2.7 µM
10 µl stock solution made up to 100 ml with LNSW = 5.4 µM
15 µl stock solution made up to 100 ml with LNSW = 8.1 µM
A LNSW blank and reagent blank will also be prepared (see section 9).

5. **Equipment**

25 ml Nunc vials
100 ml beakers (3)
weighing cups
top pan balance (2 decimal places)
top pan balance (4 decimal places)
100 ml measuring cylinder

1 ml calibrated Oxford dispenser (marked 1 and 2)
1 ml calibrated Oxford dispenser (marked 3)
10-100 µl calibrated pipettes
100 ml volumetric standard flasks (4)
Phillips pu8675 visible spectrophotometer
UV light box
Nunc vial racks

6. **Environmental Control**

Ammonia analysis requires a stable temperature, avoiding contamination of samples and reagents eg contact with fingers, dirty equipment etc.

7. **Interferences**

Samples that are likely to contain high particulates eg water from around fish farms or estuarine water (these must be filtered by the Client before accepted for analysis), air bubbles in the cell (ensure cell does not dry out when not in use), carry over from high concentration samples (check blank).

8. **Sampling and Sample Preparation**

Samples are logged into the laboratory according to SOP 60.
Avoid contamination: the samples must be stored in a clean freezer used only for the storage of nutrient samples, always wear gloves when handling samples, use fresh deionised water, anticipate when samples will be required for analysis and remove from the freezer the night before to thaw and analyse immediately. Samples are disposed of according to SOP 60.

9. **Analytical Procedure**

Set up racks of Nunc vials and mark with sample identifications. Also mark vials for sets of standards (1 set per 50 samples) including LNSW blanks and reverse (reagent) blanks. A reverse blank is required as deionised water may contain high levels of ammonia. This is prepared by adding the reagents to an empty Nunc vial, incubating with the samples, and diluting with 20 ml (± 2 ml) LNSW (measured in a Nunc vial) immediately prior to analysis.

Remove the lids.

Pour samples into the relevant NUNC vials up to the 20 ml mark.

As for the samples, add each standard up to the 20 ml mark in identified vials including 20 ml of LNSW in the vials marked "blank sea water".

Make up reagents immediately before addition to samples.

Acid wash and deionised water rinse the Oxford dispensers.

Add 1 ml (± 0.1 ml) of each reagent in order(from the relevant Oxford dispenser) to each sample, standard and blank.

NB: Reagents 1 and 2 are added from the dispenser marked "1 and 2" separately, carefully acid washing and rinsing with deionised water between reagents. Reagent 3 is added from dispenser marked "3".

Cover the vials with cling film.

Incubate in the UV box (DO NOT switch on the bulbs when the lid is open as UV is harmful to the eyes) for a minimum of 40 minutes and up to 2 hours.

Remove and allow to cool.

Use the spectrophotometer (SOP 795) to record the absorbencies (Record Sheet B54). Record the blank corrected absorbance of the 8.1 µM standard on Record Sheet B156. If lower than 600 with blank correction consult the Technical Manager.

10. **Calculation of Results**

Mean standard and blank absorbance readings. Subtract the Reverse blank reading from all the sample readings. Subtract the LNSW blank from the standard readings. Plot standard concentration v absorbance readings and calculate an analysis factor (conc/absorbance). Multiply all the corrected sample readings by the slope to produce results in µM

11. Precision, Bias and Limit of Detection

PERFORMANCE CRITERIA								
Low std replicate (0.5 uM (within batch)								
0.35	0.43	0.41	0.41	0.44	0.41	0.44	0.43	Mean 0.41 SD 0.03 uM CV 7.49%
Std replicates (5.4 uM) (within batch)								
5.4	5.5	5.5	5.4	5.5				mean 5.5 uM SD 0.05 CV 100%
LRM replicates (2.0uM) (within batch)								
2.2	2.2	2.3	2.3	2.4				mean 2.3 uM SD 0.1 CV 4.25% recovery 115%
Sea water replicates (within batch)								
0.04	0.05	0.06	0.07	0.05	0.09			Mean 0.06 SD 0.017889 CV 29.81424 LOD 0.1 uM
6.3	6.5	6.4	6.5	6.4	6.4			mean 6.4 uM SD 0.06 CV 0.93%

Ammonia

Quasimeme Nutrient Data

Mat Gr Id Mat Gr Name

1 Standard solution
2 Seawater
3 Sediment
4 Estuarine water
5 Biota
6 Sediment extract

Lab Code	Ex No Recovery	Anal Unit	Mean	Z	Det Name	Mat Gr Id	Mat Name
Q152A	60 66.7	umol/l	370	-5.5555555556	Ammonia	1	QNU013SS
Q152A	90 70.3	umol/l	300.3	-4.9453551913	Ammonia	1	QNU020SS
Q152A	60 84.4	umol/l	4.1	-2.6063100137	Ammonia	2	QNU007SW
Q152A	90 89.4	umol/l	2.35	-1.7743979721	Ammonia	2	QNU019SW
Q152A	120 85.2	umol/l	2.6	-2.4590163934	Ammonia	2	QNU024SW
Q152A	60 92.6	umol/l	4.5	-1.2345679012	Ammonia	2	QNU030SW
Q152A	60 87.4	umol/l	1.6	-2.0947176685	Ammonia	2	QNU031SW
Q152A	160 117.9	umol/l	3.3	2.97619047619	Ammonia	2	QNU035SW
Q152A	200 85.8	umol/l	2.6	-2.3652365237	Ammonia	2	QNU039SW
Q152A	260 119.8	umol/l	1.9	3.30261136713	Ammonia	2	QNU041SW
Q152A	305 89.7	umol/l	19.4	-1.7154748008	Ammonia	2	QNU044SW
Q152A	305 88.7	umol/l	9.4	-1.8888065879	Ammonia	2	QNU045SW
Q152A	324 101.9	umol/l	1.3	0.31688828135	Ammonia	2	QNU048SW
Q152A	324 93.2	umol/l	5.25	-1.1286383737	Ammonia	2	QNU049SW
Q152A	341 98.5	umol/l	2.6	-0.2481492355	Ammonia	2	QNU052SW

Q152A 341 umol/l 4.6 0.02284495888 Ammonia 2 QNU053SW 100.1

Estimation of uncertainty

General sources of error:
Sampling: Not currently covered in scope of accreditation – samples analysed as received;

Weight: Tolerance of balance/decimal places - balances check weight tolerance generally <1%,
Volume: Pipettes and dispensers used in preparation of reagents – reagents prepared are to excess, error associated not critical.
Pipettes used for calibration standards ±1%
Time: Not applicable

Analysis
Calibration standards prepared using plastic volumetrics – error 3% max
Maximum typical variance associated with standards = 7.5% (0.5µM)
Typical r asssociated with standard curve: (Batch 935): 0.9994

Validation data:
Coefficient of variance:
Blank: 29.8%
Low Standard (0.9µM): 7.5%
High Standard (10µM): 1.0%
Precision of LRM: 4.3%
Recovery of Sagami Certified Reference Material: 115%
Variance from Shewart Chart: (Std Dev: 0.172/Mean: 2.07): 8.3%

Combined uncertainty:

Systematic component (Recovery on CRM): 15.0/2%
Random Component (Shewart chart S.D.): 8.3%

Assume linear summation and a value of k=2:

Combined standard uncertainty = $2*(7.5^2 + 8.3^2)^{0.5}$ µM = 22.4%

(Following procedure M3003, p20-23.)

12. **Reports**

Record the concentration results of LRM on sheet B102. Reports are issued according to section 10.6 of the Quality Manual.

13. **Safety**

Wear laboratory protective clothing and gloves when dispensing chemicals.

COSHH assessments required:
050 Preparation of nutrient standard solutions
053 Preparation of reagents for ammonia analysis by the manual procedure
064 Manual Ammonia method
Weighing of phenol must be carried out in a fume hood or cupboard.
Dilution of concentrated hydrochloric acid must be carried out inside a fume cupboard.
UV is harmful to the eyes do not switch on the lights in the UV light box until the lid is closed.

14. **Literature References** - Not relevant.

1. **Introduction and Scope**

This method describes the colorimetric determination of o-phosphate in estuarine and sea waters. Working range: 0.02-5 µM [=µmol/l] phosphate

2. **Principle of the Method**

Ortho-phosphate forms a yellow complex with molybdate ions in strongly acid solutions. The phosphomolybdate complex is reduced in the presence of trivalent antimony by ascorbic acid to molybdenum blue.

The intensity of the blue colour is proportional to the phosphate concentration and determined by colorimetric measurement.

3. **Reference materials**

A laboratory reference material (LRM) is routinely randomly analysed with each batch of analysis and the results used to maintain Shewart control charts and cusum plots.

This is a stock phosphate standard diluted with LNSW stock. Dissolve 0.2722 g KH_2PO_4 in 1000 ml deionised water using a volumetric flask (stable for six months). 1 ml stock contains 2 µm. 20 µl stock made up to 100 ml with deionised water in a volumetric flask = 0.4µM.

4. **Reagents and Standards**

All chemicals used are Analar grade unless otherwise stated.

4.1 **Reagents**

a) 2.5 M SULPHURIC ACID is purchased from Merck. Alternatively using a measuring cylinder carefully add 70 ml concentrated sulphuric acid to approximately 400 ml distilled water, then make up to 500 ml (± 50 ml) with deionised water. Use safety gloves to carry out the dilution of sulphuric acid and work in a fume cupboard. 2.5 M sulphuric acid may alternatively be purchased from MERCK.

b) AMMONIUM MOLYBDATE. Weigh 20 g (± 2 g) ammonium molybdate in a beaker, add 500 ml (50 ml) deionised water and dissolve. Store solution in Pyrex glass and discard if white precipitate forms. Use within six months.

c) POTASSIUM ANTIMONYL TARTRATE. Weigh 0.274 g (± 0.01 g) potassium antimonyl tartrate in a beaker, add 100 ml (± 10 ml) deionised water and dissolve. Stable for one month.

d) ASCORBIC ACID. Weigh 1.58 g (± 0.2 g) ascorbic acid in a beaker, add 90 ml (± 9 ml) deionised water and dissolve. This must be done fresh on each day of use.

e) Mixed Reagent. Mix 150 ml (± 15 ml) 2.5 M sulphuric acid (reagent a), 45 ml (± 5 ml) ammonium molybdate solution (reagent b), 15 ml (± 2 ml) potassium antimonyl tartrate solution (reagent c) and 90 ml (± 9 ml) ascorbic acid solution (reagent d).

f) Turbidity reagent. Mix 150 ml (± 15 ml) sulphuric acid (reagent a), 45 ml (± 0.5 ml) deionised water, 15 ml (± 2 ml) potassium antimonyl tartrate solution (reagent c) and 90 ml (± 9 ml) ascorbic acid solution (reagent d).

4.2 **Standards**

Prepare fresh each day of use by accurately pipetting set volumes (see later in this section) of concentrated stock solution containing a known amount of phosphate into standard volumes of Low Nutrient Sea Water (LNSW).

Standards must be prepared in "B" grade volumetric flasks.

A standard stock solution is purchased. Typically the stock solution may have a nominal concentration of 0.522 mg PO4/l (Aldrich Company). This value is used for calculations set out below although it may vary and has to checked to be identical if following calculations are referred to. If stock phosphate concentrations are differing from 0.522 mg/l PO4. Standards of different concentrations may be prepared to avoid the use of unwieldly alliquots of stock.

The equivalent expression in molarity is obtained by dividing 0.522 mg/l PO4 by the molecular weight 95 g/mol converting the concentration to 5.49 mM. Once opened the stock solution is stable for six months.

Standards need to be prepared in the appropriate analysis range, eg open sea water samples 0.2-1.0 µM PO4, estuarine samples 0.2-5.0 µM PO4.

A suitable set of calibration standards for open sea samples are prepared as follows using Aldrich stock standard:

5 µl stock solution made up to 100 ml with LNSW = 0.27 µM
10 µl stock solution made up to 100 ml with LNSW = 0.55 µM
15 µl stock solution made up to 100 ml with LNSW = 0.82 µM
20 µl stock solution made up to 100 ml with LNSW = 1.10 µM

In case the phosphate concentration of the stock solution differed from 5.49 mM the resulting concentrations from the above dilution scheme have to be recalculated.

5. **Equipment**

Philips PU 8675 VIS Spectrophotometer. Path length of cell 8 cm.
100 ml volumetric flasks (4)

5 µl calibrated pipette
10-100 µl calibrated pipette
Nunc vials 25 ml, graduated. One vial from each batch is tested (SOP 270/280).
100 ml measuring cylinder
500 ml measuring cylinder
Top pan balance (3 decimal placed)
250 ml plastic reagent bottle (2)
500 ml plastic reagent bottle (4)
Calibrated oxford dispenser marked P04 analysis set at 4 ml.

5.1 **Apparatus**

Philips PU 8675 VIS Spectrophotometer. Path length 8 cm; Wavelength 882 nm.

6. **Environmental Control**

Phosphate analysis requires a stable environment, avoiding contamination of samples and reagents eg contact with fingers, dirty equipment, smoking, etc.

Dilution of sulphuric acid must be carried out in a fume cupboard wearing protective clothing.

7. **Interferences**

Turbidity interferences are eliminated by filtration and/or turbidity correction (see 8). Interferences due to the sea water matrix in the analysis of estuarine and marine waters are negligible. Colour development in sea water is reduced by less than 1% compared to fresh water.

Interference from several ions, which are known to interfere in molybdenum blue methods for the determination of phosphate, can be expected to be negligible at the natural concentrations of the interfering ions. This is valid for copper, iron, silicate and arsenate.

Interference from phosphate released by easily hydrolysable organic compounds is low, but can be expected to increase with time delay in colour measurement. Therefore colour measurement is preferably done between 10 min and 2 h colour development time although the molybdenum blue complex is stable for 24 h (see 11).

8. **Sampling and Sample Preparation**

Analysis is preferably done immediately after sampling. If storage of samples is necessary, store frozen in a clean freezer used only for the storage of nutrient samples. Anticipate when samples will be required for analysis and remove from the freezer the night before to thaw.

9. **Analytical Procedure**

Allow samples to warm to room temperature. Pour samples up to the 20 ml mark into a Nunc vial and add 4 ml (± 0.4 ml) mixed reagent (reagent e) from the Oxford dispenser. Close vial and mix well. Let colour develop for a minimum of 10 min. Adjust the wavelength to 882 nm and zero the spectrophotometer using distilled water. Transfer solutions into the cell and measure the extinction. Once the analysis of a batch of samples has commenced it should be completed within two hours.

Sample turbidity and background absorption is measured by treating samples as above with the turbidity reagent (reagent f) replacing the colour reagent (reagent e).

Three replicate measurements of all blanks and standards are carried out.

Quality control: A LRM is randomly analysed with each batch of samples. A CRM is randomly analysed when parts of the instrumentation are exchanged or analysis has not been carried out for several weeks. Record the blank corrected absorbance of the 1.10 µM standard on B156. If lower than 100 contact the Technical Manager. Record all analysis on B54.

10. **Calculation of Results**

Take the mean of replicate blank and standard measurements.

Manipulation of sample absorbances: abs(sample, turbidity and blank corrected) = abs(sample reading) - abs(sample turbidity) - abs(distilled water blank)

Manipulation of standard absorbances: abs(standard, blank corrected) = abs(standard) - abs(calibration blank)

abs(calibration blank) denotes the mean absorbance of three replicate measurements on LNSW in case of sea water and estuarine water analysis or the mean absorbance of three replicate measurements on distilled water in case of fresh water analysis. Thus it reflects the matrix of standards.

The calibration line has the form: abs(standard, blank corrected)*Factor = conc(PO4) and the phosphate concentration of the sample is calculated by

conc(PO4 in µM) = abs(sample, turbidity and blank corrected)*Factor

11. **Precision, Bias and Limit of Detection**

Seawater replicates µM (within batch)							
0.14	0.14	0.13	0.12	0.14	0.14	0.13	LOD 0.03µM
Standard replicates (0.33µM) (within batch)							
0.35	0.35	0.35	0.36	0.35	0.37	0.35	Mean 0.3524 µM SD 0.00729 CV 2.07%
Standard replicates (0.99) (within batch)							
0.99	1.01	1.01	0.99	1.01	0.99	1.00	Mean 1.0012 µM SD 0.011771 CV1.176%
LRM replicates (0.40 µM) (within batch)							
0.37	0.37	0.37	0.39	0.39	0.39	0.39	Mean 0.3806 µM SD 0.00924 DV 2.428%
Spiked LRM recovery (0.4 µM spike) (within batch)							
0.82	0.80	0.78	0.82	0.81	0.82	0.83	Mean 0.812 µM recovery 107.35%

12. **Reports**

Record all LRM and CRM concentrations on Sheet B102. Reports are issued according to Section 10.6 of the Quality Manual.

13. **Safety**

Wear laboratory protective clothing. Wear gloves when handling chemicals. Use of concentrated acids must be carried out in a fume cupboard.

COSHH assessments required:
050 Preparation of nutrient standard solutions
090 Manual determination of orthophosphate

14. **Literature References**

Skalar Manual Sans Plus Analyser.
Skalar Manual Datasystem.
Chemistry Section Laboratory Manual.

1. **Introduction and Scope**

The method is used to determine particle size distributions of marine sediments in the range 0.1-600 microns.

2. **Principle of the Method**

The Mastersizer is a light-scattering based particle sizer comprised of an optical measurement unit and computer. The angle through which light is scattered by a particle is proportional to the particle's size, and this property is used to determine the size distribution of the sample.

3. **Reference Materials**

Glass beads are used as an LRM. The glass beads, trade name "Vaquashene C100", are supplied by Abrasive Development Ltd. The machine is validated each year by Malvern instruments using a reticle, and the LRM run immediately after.
Glass beads are also used as an LRM for the 500 micron sieve which is used to determine the > 500micron portion (see section 9.6). The beads used are "Vaquashene glass beads S90-840) and are run using the 500 micron and 710 micron sieves with each batch. The result for the 500 – 710 micron portion is recorded on Form B106 and used for Shewart chart update.

4. **Reagents**

No reagents are required for marine sediments, as the sample is added directly into a water bath.

5. **Equipment**

Optical measurement unit - Malvern Mastersizer/E EN 82
Computer
Printer
45 mm, 300 mm lenses
500 micron sieve
Spatula
Tapwater wash bottle
Lens cleaning tissues
Small plastic top
Paint brush tray
Paint brush
Calibrated balance

6. **Environmental Control**

The Mastersizer laser mechanism is sited on an optical bench to reduce interference due to vibration. Sites experiencing extremes of light and heat should be avoided.

7. **Interferences**

The production of bubbles is limited by the use of ultrasonic treatment as the sample is introduced into the water bath.

It is essential that the water bath is rinsed out at least twice after each analysis to avoid carry over of sediment from the previous sample.

Dust or smears on the lenses or cell windows should be removed by following the procedure outlined on p3.7 in the maintenance section of the manual.

8. **Sampling and Sample Preparation**

The samples may be introduced either as a wet slurry or as a freeze-dried powder (see SOPs 110 and 120). Breaking up of the sample, eg by pressing sample firmly through sieve apertures, should be avoided.

9. **Analytical Procedure**

The proportion of sediment >500 Φm is measured for each sample (see 9.6). If there is >5% in the >500 Φm fraction, and the client requests, more detailed analysis of the >50Φm faction is carried out (see SOP 855). Sieving must be carried out AFTER automated analysis

9.1 **Switching on**: Masterizer is normally kept switched on and warmed up. If for any reason it has been switched off follow the following;

Ensure Mastersizer is switched **off** at the rear left of the unit. Switch mains power on - then switch on at rear of unit. Allow at least five minutes for the laser to warm up. Switch on computer, and type "win" to enter Windows. Click on sizer icon to start.

9.2 **Sample logging:** Each batch of samples, should be saved in a separate sample file. Each "record" within a "sample file" corresponds to a "sample" in the Laboratory sense. From the various menus at the top of the screen, select File, then Open Sample. Select the file you wish your data to be saved to, then click "OK". If you wish to create a new file, type in "filename.sam", "OK" - the computer prompts that no such file exists, do you want to create a new one? - "Yes".

9.3 **Default settings:** The Mastersizer has been set up so that the default settings are those which are most commonly used in routine analyses. These are described below.

The data output is in the form of %age amounts by volume of the sample lying within specified size bands. The default size bands are based on a "PHI" units scale, commonly used within Geological literature.

Statistical descriptors such as mean, median %<20 micron are also displayed.

9.4 **Software setup:** Setup the lens configuration: each is used to analyse a different size range: 45 mm, 0.1-80 µm; 300 mm, 1.2-600 µm. Samples are normally analysed first using the 300 mm lens. If there is greater than 4% material within the 1.381 µm size band, the analysis is repeated using the 45 mm lens and the results blended. Setup, Hardware, select Range - 45 or 300 mm, click on "OK". All other parameters should remain unchanged.
Check View Result 2 is ticked and check extend high box in set up, result modification is unchecked.

Setup the presentation required for analysis: Setup, Presentation. For sediment samples, use 2OHD; glass bead reference 2ODD. Click on "OK" twice.

Setup Analysis: For sediment samples "Polydisperse", for glass beads "monomodal".

Align the lens system. Ensure the correct lens is fitted (printed on lens casing), and that the detector (underneath right-hand flap on instrument) is in the correct position - far left for 45 mm lens and far right for 300 mm lens (see manual - Installation 2.4-2.5). Click on Measure, Align - the Measurement Window appears. Disable the auto-scaling by clicking on the auto-scale box, and select a scale of 100 divisions. If some of the detectors appear not to be working (zero readings on parts of the display), click on Close, then click on Control, Run program; Load "lin.bsc", and Run. Re-enter Measure Align. Adjust the X and Y alignments using the adjusters on the unit until the system is aligned (see page 2.9-2.12 of manual). A laser power reading in the green on the bar on the left, and detector readings of <50 (biased higher to the left of the display), is normal. If laser reading <65%, check alignment of optics; if detector reading >100, clean lens and cell windows (see Manual: Maintenance 3.7). Once system is aligned, click on Close.

9.5 **Sample measurement:** To regulate the water level in the chamber, use the control switch on the front of the unit - "Drain" and the fill hose connected to the mains. Before the first run, flush the system three times, or until all traces of "Decon" have been removed (no frothing). Fill the sample chamber. By visual inspection, ensure that the chamber is clear of any sediments or particulates - if any are found, drain, flush chamber with wash bottle, and fill again.

9.5.1 Daily Calibration: Run the LRM at the start of each day, following the procedure detailed below - the mean diameter (D(4,3)) should lie within the limits determined by the control chart. Save the data under "refer.sam", with that day's date as the Sample name. Mean diameter for the day should be recorded on Form B103. After analysis change the "presentation" back to 20HD, and "analysis" to Polydisperse.

9.5.2 Sample Details: Enter the sample details - click on Measure, Document. Enter the sample name, and any relevant Notes in the appropriate boxes. Click "OK".

9.5.3 Background Measurement: A measurement of the background interference must be made before the sample is analysed. This should be done each time a sample is to be analysed. Switch on the pump and tank stirrer at setting 10. Click Measure, Background - a stable display should appear. If the display is unstable (peaks >30 appearing at intervals on the display), flush out the system again and refill. If display is stable, but with readings >100, clean lens and cell windows (Manual : Maintenance 3.7). Press space bar to start. Once background measurement is complete, the display "freezes".

Background levels tend to be slightly higher with the 45 mm lens than the 300 mm lens.

9.5.4 Sample Inspection: Once the background has been measured, press space bar twice. Ensure the sample has been well mixed, and remove a subsample, place a small amount on the end of a spatula from the sample. Silty samples will require significantly less sample than sandy ones. Place the 500 µm sieve over the chamber, and sieve the sample through it. Wash any remaining sample through using the wash bottle filled with tap water.

Switch on the ultrasonic at setting 10 for at least 30 seconds, or until the obscuration stabilises ± 2%. Keep adding sample until the obscuration is between 10 and 30%. If it goes over 30%, add more water. There is now sufficient sample for a measurement to be made. Obscurations of <5% or >30% are too unreliable to be used. Between 5 and 10% is undesirable, but in the absence of sufficient sample can be tolerated.

9.5.5 Sample Measurement: Press the space bar to begin the measurement - this takes about four seconds. Once measurement is complete, press space bar again to begin analysis. After iteration (approximately 20 seconds), the screen will then show a tabular and graphical representation of the results. Double click on either side of the window to view table or graph details full screen. Note on form B64 the record number for lens and whether 45 mm is to be run.

9.5.6 Saving: Save the sample details - File, Save Sample, or Save Sample As, and if required print out the tabulated results. Select, File, Print, a list of options comes up. By clicking on the appropriate box (becomes marked by a cross) you can select the desired printout. In most cases a report is printed. The correct report is obtained by selecting Setup, Report and highlighting reshist3.rep, then click on "OK".

Drain the sample chamber, flush with tap water using wash bottle, and refill at least twice, or until no particulates remain in the chamber. Repeat from "Sample Details" until all the samples have been analysed.

9.5.7 Switch Off Procedure: When finished, double click on the "-" icon at the top left or File, Exit; the computer will ask you if you wish to save the configuration - click on "No". The PC is normally kept switched on; to switch off; exit from Windows. Switch off the computer, the optical unit at the rear, and ensure the water tap is

switched off. Once analysis is complete fill the chamber with decon until next use.

9.6 **Measurement of the >500 micron fraction**. Place the 500 Φm sieve(EN276) on a plastic tray. Transfer to the balance and tare. Add a suitably sized weight of sample. Record this total weight on Form B65. Lightly brush the sample through using the paint brush until no further sample passes through. Remove the <500Φm fraction from the tray then record the >500 Φm weight (sieve, contents of sieve, plastic tray) on Form B65. Ensure all sample is removed from the sieve before analysing the next sample.

9.7 **Blending results:** In order to measure a sample over more than one lens range, the data from these two ranges must be blended. Open the 300 mm sample record. Select Setup, Result Modification. In the "blend" box, enter the record number of the sample to be blended (the 45 mm record), and check the "modify" box. Also check the ACurrent Result modify" box. Click "OK". The blended result should now appear on the screen. Change Measure, Document if required, and save sample as usual. When using both the 45 and 300 mm lenses the size ranges need to be increased to account for the smaller size ranges. To do this enter Edit, Input, Sizes click on Load and select phi3.siz, then click on "OK".

The original 45 and 300 mm lens recorded must remain in the same record numbers and must not be deleted - the blended results will also be altered.

Where data from outwith the size range (eg sieved sample above 500 µm) is to be blended, first alter the size range, using Edit, Input, Sizes. Add the size ranges to those already present, or Load a previously created size range. The various options are detailed below:

300 mm lens, no sieving: phi.siz
300 mm lens, + 1 mm, 2 mm, 4 mm sieves: phi2.siz
45 + 300 mm lens, no sieving: phi3.siz
45 + 300 mm lens, + 1 mm, 2 mm, 4 mm sieves phi4.siz

Then, using Edit, Input, Extended Result, Insert the %age below each specified size range - [1] should be 600, [2] should be eg 600 or 1,000 etc. Click on "OK". In Setup, Result Modification, check the Extend "high" box, and ACurrent Result modify" box, then click on "OK" - the graph and results should now show the extended results. Remember to View Histogram sizes, rather than Measure sizes. For sediments sieved through a 500 µm sieve (see 9.6), the %age below 500 µm can be entered and 600 µm set as an arbitrary 100%.

9.8 **Transferring data to spreadsheets:** Program "phtran.bsc" has been written to transfer phi histogram data to a text file in order to be statistically analysed - if any other data is to be transferred, the file should be modified, using Control, Edit program. phtran.Bsc has been adapted for data that has been through the 300 mm lens, Phtran3.bsc has been adapted for blended results (ie sediments through 45 and 300 mm lenses (no sieving) and phtran4.bsc for 45 + 300 mm lens data sieved through 0.5, 1, 2 and 4 mm.

The files to be transferred should be in consecutive order, and the relevant "phi" size range should be loaded. Click on Control, Run program, Load, "phtranx.bsc", Run. The program prompts for the sample filename, ie the file containing the records to be transferred. Enter the filename without the ".sam" extension. Click "OK". Enter the text file name at the prompt, without the .txt extension. The program prompts for the first record number, enter it, click "OK", and repeat for the final record number. The phi data for each record will then be transferred to a ".txt" file - the program runs as an icon at the foot of the page while this is done.

Save the "txt" file to disk (the file will be found in C:\sizer\data*txt) and then import it into a spreadsheet. The customer is given a paper and electronic copy of this plus print outs of the data and graphs from the mastersizer.
All .SAM and .TXT files should be transferred to CHEMDAT/ BATCHxxx. The .SAM files contain detector data which cannot be reproduced if the file(s) are deleted.

10. **Calculation of Results** - See above.

11. **Precision, Bias and Limit of Detection**

Accuracy: ±2% on volume mean diameter
Dynamic range: 800 : 1 max on single measurement
Analytical range: 0.1-600 µm
Background correction: Background scattered light and electrical background is measured automatically.

Particle size LRM (glass beads) using 300 mm lens.

Date	Size (µm)							
	22.097	31.250	44.194	62.50	88.388	125.00	176.77	Mean
25/6/98	0.00	0.81	24.98	59.27	14.98	0.07	0.00	72.94
26/6/98	0.00	0.81	25.02	59.24	14.87	0.07	0.00	72.93
3/8/98.1	0.00	0.81	27.98	59.23	14.91	0.07	0.00	72.95
3/8/98.2	0.00	0.79	24.71	59.39	15.05	0.07	0.00	73.06
3/8/98.3	0.00	0.80	24.82	59.29	15.03	0.07	0.00	73.03
3/8/98.4	0.00	0.80	24.91	59.26	14.96	0.07	0.00	72.98
4/8/98	0.00	0.80	24.84	59.36	14.94	0.07	0.00	72.99
10/8/98	0.00	0.78	24.63	59.47	15.05	0.07	0.00	73.08
12/8/98	0.00	0.78	24.68	59.57	14.91	0.06	0.00	73.02
13/8/98	0.00	0.76	24.57	59.73	14.87	0.06	0.00	73.05
Mean%	0.00	0.794	25.111	59.38	14.96	0.068	0.00	73.003
S.D.	0.00	0.0156	0.966	0.156	0.065	0.004	0.00	0.050
Coeff Var	0.00	1.967	3.845	0.263	0.438	5.88	0.00	0.069

Detection Limits %

Based on 22.097 - 31.250 Φm: 0.073%
Based on 125.0 - 176.77 Φm sizeband: 0.019%

12. **Reports** - Not relevant.

13. **Safety**

Refer to COSHH Assessments
008 Automated Particle Size Analysis

The sizer has an electrically operated safety shutter fitted to the optics within the transmitter module - this is failsafe in the closed position and will not allow laser light to emit.

14. **Literature References**

Mastersizer Operating Manual.

1. **Introduction and Scope**

The method describes the determination of total carbon and nitrogen in sediment samples using a Perkin Elmer CHN 2400 elemental analyser.

The working range for carbon is 1.5 µg - 13 mg per sample.
The working range for nitrogen is 7 µg - 2.4 mg per sample.

2. **Principle of the Method**

The CHN analyser uses a combustion method to convert the sample elements to simple gases (CO_2, H_2O and N_2). The sample is first oxidised in a pure oxygen environment; the resulting gases are then controlled at exact conditions of pressure, temperature and volume. Finally, the product gases are separated. Then, under steady state conditions, the gases are measured as a function of thermal conductivity.

3. **Reference Materials**

Acetanilide is used to calibrate the machine on startup. Mess -2 and Tibet Soil are used as system suitability checks for C and N respectively. "Clean" homogenised sediment from Raasay Sound is used as an LRM. Values are given below:

	Total C%	Total N%
Raasay*	4.12 ± 0.04	0.27 ± 0.3
Mess -2	2.14 ± 0.03	
Tibet Soil		0.128 ± 0.005

*Typical values; LRM data should be checked against Shewart charts.

Reference materials are prepared in the same manner as samples. However, acetanilide weights should be in the range 1-2.5 mg.

4. **Reagents**

Helium Prepurified 99.995 mole % minimum
Oxygen (Research Grade) 99.995 mole % minimum
Acetanilide Standard

5. **Equipment**

Perkin Elmer CHN 2400 Elemental Analyser
Perkin Elmer AD-4 Autobalance
Okidata Microline 320 Printer

Regulators: Helium: dual stage with stainless steel diaphragm, 5-60 psi (35-415 kPa) outlet pressure. Oxygen: single stage with stainless steel diaphragm, 5-60 psi outlet pressure.
Pressed tin capsules 8 x 5 mm
Microforceps (2)
Microspatula
Sample trays

6. **Environmental Control** - Not relevant.

7. **Interferences**

Samples must be completely freeze-dried and ground (see SOP 110 and 120). Excess moisture within the sample affects the sample weight and hence the analysis results.

Care should be taken when preparing samples that no foreign material (dust, excess sample, etc) is collected on the outside of the sample cups, as this will affect the weight and hence the sample results. Any cups suspected of being contaminated should be discarded.

8. **Sampling and Sample Preparation**

The samples must be freeze-dried and ground (see SOPs 110 and 120) prior to analysis. The spatula, forceps and sample preparation tray used must be kept scrupulously clean to prevent contamination of the sample during preparation.

Using the forceps place an empty capsule in the pedestal on the sample side of the balance, this is counterbalanced with another empty capsule (this is folded) on the reference side. Close the doors, lower the pan arrests, and then press the **Autotare** key. Once integration is complete raise the pan rests and place the capsule from the sample side on a clean surface. Carefully place the sample (using a metal spatula) in the vial. Tap the vial lightly to ensure all the sample particles have reached the bottom of the capsule. Return the capsule to the pedestal and lower the pan arrests to weigh the sample. When the weight has stabilised, note the weight. Remove the capsule and place on a clean surface. Then, with the forceps, pinch the center of the capsule and fold it in half and flatten. Then fold in half again and make sure the there are no jagged edges. Reweigh the capsule to ensure no sample has been lost in folding.

For total Carbon results, tin capsules are used, and the sample can be run without further treatment. Record the weight of each sample and LRM on Form B 68.

The sample weight taken for sediments is typically 10-30 mg. The Perkin-Elmer AD-4 Autobalance is calibrated prior to sample weighings as stated in the Quick Reference Guide 0993-7138. To prevent moisture ingress to the samples, they should be stored in a desiccator cabinet prior to analysis.

9. **Analytical Procedure**

9.1 **Setting up**

The analyser is normally kept switched on and at operating temperature. However if the analyser has been switched off, refer to section 5A, "Automatic Startup Procedure" in the manual.

The following steps should be carried out at the start of each analysis day.

Adjust the helium regulator to 20 psig ± 5 and the oxygen regulator to 15 psig ± 5. Adjust the pneumatic gas (normally Nitrogen, any grade, or compressed air) to 50 psig ± 10.

On the analyser keyboard, press "Monitor"; "Y". The temperature readings are printed out - check that the combustion temperature is 925° ± 2°C, and the reduction temperature is 640° ± 2°C. If they are not, enter the correct values, and wait for the temperature to be reached (see manual page 6-12). If the combustion or reduction temperature is around 100°C, and entering the correct temperature makes no change, check that the furnace is on (Parameters 12) - if it is, the furnace element is likely to have blown - consult the Technical Manager.

Perform a Combustion Zone Leak Test as stated in the Manual (page 5-3)

Purge the analyser with helium (see manual p.5-2) for at least 120 secs. The analyser is NOT purged with oxygen as this reduces the life of the reduction tube. (If the oxygen cylinder has been changed disconnect the Swagelock quick-release gas fitting situated behind and to the left of the auto-injector mechanism. Set to purge with oxygen for 30-60 seconds (see manual page 5-2) to ensure there is no air lock between cylinder and analyser. Reconnect the Swagelock fitting.)

a) Blanks: A series of blanks should be run after instrument startup and at start of analysis day. Blanks should be reproducible to within the following values:

Carbon ± 30; Hydrogen ± 100; Nitrogen ± 16

If the results are not within acceptable values, run several more blanks. NB: The actual values may vary depending on reagents, glassware or gas supplies. It is the reproducibility between successive blanks that is important, not the actual values. However, if the blank values for nitrogen are greater than 300 and consistently within limits, this indicates that a high level of impurity exists in the oxygen supply. Although the analyser can operate in this condition it is recommended that a purer supply of oxygen is obtained. Rapidly increasing nitrogen >>500 indicates the reduction tube needs replacing (see Manual pp 4-6 et seq). When all blanks are consistently outwith expected limits and the combustion tube has done more than 800 runs, the combustion tube should be changed. (See manual pp 4-6 et seq). If <800 runs have been performed, check that the temperatures and pressures are within expected limits. If these are found to be satisfactory, consult the Technical Manager.

When carbon blank readings are high (>20 units above previous blanks) immediately after running samples, and then fall back to within expected limits, the vial receptacle in the combustion tube needs to be emptied - see manual page 4-8. It should also preferably be emptied whenever the reduction or combustion tubes are changed.

When changing either tube, check the condition of the small filters at the bottom left and top right of the furnace/tube structure and change if they are fouled. Change them regardless of condition after new combustion tubes.

If new tube(s) have been installed, or the vial receptacle emptied, calibrate the instrument as described in the following section. Otherwise, run a tin LRM, and if this is within expected limits (see above, section 3), the samples may be run (see manual section 6F "Performing a series of Auto Runs") a list of character codes is included in Appendix 4.. Tin capsules should be run with the combustion temperature set at 925° ± 2°C. A typical run sequence is 10-15 samples, two blanks, and an LRM.

9.2 **Calibration and quality control**: The analyser is calibrated using Acetanilide. A bottle of this is kept in the desiccator cabinet. See manual page 5-12 for details of how to calibrate the instrument. Weigh out 2 mg ± 0.2 mg acetanilide. Repeat twice and run as detailed in 5-12 of the manual. If the K values lie within limits (see manual), run Mess -2 and Tibet Soil samples consecutively. If the percentage values lie within the specified range (see table, page 1), calibration is complete and the samples may be run. If the percentage values are outwith limits, prepare more acetanilides and repeat procedure. Record all calibration results on Form B67.

An LRM (Raasay sediment) is prepared in the same manner as samples (see above, section 8). They should also be run after calibration and during sample runs, typically every 10-15 samples (more often if desired). The values for Total Carbon and Nitrogen for Raasay, Mess -2 and Tibet Soil are entered in Shewart charts updated by the QC Chart Manager. Record the values on Form B105.

10. **Calculation of Results**

Details of carbon and nitrogen percentages are printed out after each run, and no further calculations are required. For details of how such values are obtained, see section 10, "Calculations", in the manual. Record all sample results on Form B68.

When using the autosampler, samples can occasionally get "stuck", or the autosampler may jump. If a 0% reading is obtained at a position, and the sample is still at that position, simply rerun the sample. If a 0% reading is obtained, and no sample is present, then a double drop may have occurred, and both the presumed missing and immediate next sample should be repeated as a check. If the autosampler position is one in advance of where it should be after completion of the run, it has jumped forward one position, and the samples analysed after the jump will need to be recalculated - see Technical manager.

11. **Precision, Bias and Limit of Detection**

Precision
Carbon - 1.39%
Nitrogen - 7.11%
Calculated with reference to Shewart charts.

Bias
Carbon 101%
Nitrogen 84%

Limit of Detection
Carbon - 1.5 µg
Nitrogen - 7.0 µg
The Limit of Detection was determined as follows according to SOP 1310

Calculate the standard deviation of 5-10 blanks x 4.65 / k factor.

12. **Reports**

A hard copy of all data should be archived with analysis documentation as a control document (SOP 1350). All hard copies should include the date of analysis and the signature of the analyst.

13. **Safety**

Labcoat, safety specs and gloves should be worn in the laboratory and when handling samples.
See also COSHH Assessments 003, 070, 077.

14. **Literature Reference**

Perkin Elmer 2400 CHN Elemental Analyser Instructions. Instruction Manual 0993-7147,0 revised October 1988.

Sample	Raasay mg Actual C mg	Acet mg % Recovery	Total mg	%C Result	%N Result	Expt C Raasay mg	Expt C Acet mg	Expected C mg
C1	11.51	0.000 11.51	4.031	0.258	0.473	0.473	0.464	
C2	10.04	0.000 10.04	4.031	0.259	0.412	0.412	0.405	
C3	9.46	0.000 9.46	4.064	0.246	0.388	0.388	0.384	
C4	10.55	0.000 10.55	3.982	0.242	0.433	0.433	0.420	

Sample	Expc N Raasay	Expec N Acet	Expected N mg	Actual mg N	% Recovery
C1	0.029	0.000	0.029	0.030	
C2	0.025	0.000	0.025	0.026	
C3	0.024	0.000	0.024	0.023	
C4	0.026	0.000	0.026	0.026	
C5	0.026	0.000	0.026	0.026	
C6	0.044	0.212	0.256	0.290	115.9
C7	0.059	0.208	0.267	0.300	115.8
C8	0.048	0.246	0.293	0.334	116.7
C9	0.046	0.219	0.264	0.301	116.6
C10	0.046	0.224	0.269	0.308	117.1
C11	0.021	0.115	0.136	0.152	113.2
C12	0.021	0.095	0.117	0.130	113.4
C13	0.022	0.096	0.118	0.130	112.7
C14	0.022	0.111	0.133	0.144	110.0
C15	0.022	0.103	0.124	0.140	115.1
			Mean N recovery		**114.7**
			STD		**2.1**
			RSD		**1.9**

Fisheries Research Services LABORATORY MANUAL	M860	Page 8 of 8
	Issue No	5.00
Determination of Total Carbon and Nitrogen in Sediments	Issued By	Lynda Webster
	Date of this Issue:	30/10/2000

Carbon Range

% C	Mass sed	Mass of C in sed	%N	Mass Sed	Mass N in sed
70.8	1.80	1.274	10.22	1.8	0.18
71.7	2.79	2	10.50	2.79	0.29
71.955	3.81	2.741	10.55	3.81	0.40
72.096	5.03	3.626	10.71	5.03	0.54
72.085	6.14	4.426	10.76	6.14	0.66
72.026	6.60	4.754	10.80	6.6	0.71
71.984	7.36	5.298	10.81	7.36	0.80
71.668	8.53	6.113	10.83	8.53	0.92
71.714	9.68	6.942	10.92	9.68	1.06
71.557	10.68	7.642	10.97	10.68	1.17
71.577	11.58	8.289	11.03	11.58	1.28
71.308	12.85	9.163	11.04	12.85	1.42
71.082	13.90	9.88	11.08	13.9	1.54
71.028	14.94	10.612	11.13	14.94	1.66
70.901	15.90	11.273	11.16	15.9	1.78
70.716	16.82	11.894	11.20	16.82	1.88
70.636	18.47	13.046	11.27	18.47	2.08
70.398	19.45	13.692	11.31	19.45	2.20
70.253	20.94	14.711	11.37	20.94	2.38

Mean C 71.34
s.d. (from shewart) 0.726
+2*s.d. 72.37739
-2*s.d. 70.30513

Mean N 10.9300526316
s.d. (from Shewart) 1.518
+ 2*s.d 12.44268
- 2*s.d 9.417423

1. **Introduction and Scope**

The procedure describes the method for removing carbonate from dried sediments using 15% hydrochloric acid. The sample can then be analysed for organic carbon content using the Perkin Elmer CHN 2400.

2. **Principle of the Method**

HCl reacts with carbonate in the sample to produce CO_2 and water, leaving only organic carbon to be analysed. The sample is dried to remove excess HCl which may interfere with the CHN analyser when the sample is analysed.

3. **Reference Material**

An LRM, Raasay sediment, is analysed after every 10-15 samples.

4. **Reagents**

Hydrochloric Acid 15% v/v (approx)

Using a measuring cylinder, measure out 85 ml ± 5 ml of distilled water and pour into a beaker. In a fume cupboard, carefully dispense 15 ± 2 ml HCl (37%, AR grade, BDH) into the distilled water and gently mix.

5. **Equipment**

200 ml glass beaker
100 ml measuring cylinder
20 µl and 30 µl calibrated pipettes
Aluminium sample tray
Teflon sample tray
Hot plate EN69
Silver cups 12.5 x 5 mm
Forceps
Plastic Sample Tray

6. **Environmental Control**

The acidification and drying should be carried out in a fume cupboard.

7. **Interferences**

Not relevant.

8. **Sampling and Sample Preparation**

Samples are received in a prepared (dry, ground) condition.

9. **Analytical Procedure**

Carefully weigh out sample into a silver cup as described in CHN2400 Manual 5D.

9.1 Switch on the hot plate in the fume cupboard checking it is set for at least 120°C. (Mark 65).

9.2 Make up 15% HCl and pipette 20 µl to each of the samples standing in the plastic tray.

9.3 Depending on how vigorous the reaction with the first 20 µl of acid, after at least five minutes pipette a further 20 µl of acid and transfer the cups to the Teflon tray. Dry samples for at least 15 minutes and transfer cups back to the plastic tray.

9.4 Repeat the addition of acid as in 9.2 and 9.3 above.

9.5 Pipette 30 µl of acid to each sample and transfer samples to the Teflon tray to dry for at least 15 minutes. Remove cups back to the plastic tray.

9.6 Repeat 9.5 a further three times until 200 µl (total) has been added to each sample.

On transferring the samples to the Teflon tray for the last time, leave the samples to dry for at least 30 minutes, then transfer to the aluminium tray and leave to dry for at least one hour.

9.7 Return samples to a plastic tray and place in a desiccator until ready for analysis, (Method M885).

10. **Calculation of Results**

Not relevant.

11. **Precision, Bias and Limit of Detection**

Not relevant.

12. **Reports**

Not relevant.

13. **Safety**

Disposable gloves should be worn when handling silver cups, and all digestion should take place inside a fume cupboard. Acid is added to distilled water using an automatic dispenser.

14. Literature References

Not relevant.

1. **Introduction and Scope**

This procedure describes the preparation of samples into a homogeneous condition.

2. **Principle of Method**

Sediments are sieved to remove the coarse fraction and then ground to homogenise the sample for further chemical analysis.

3. **Reference Materials**

NA

4. **Reagents**

Deionised water, hexane.

5. **Equipment**

Powder funnel.
Stand and clamp.
Sieve and collecting base.
Pestle and mortar.
Brush.
Aluminium foil.
Tissue.
Fume cupboard.
Sample pots/bags.
Trulla spatula.
Retsch MM2000 Grinder

6. **Environmental Controls**

All sieving and grinding is to be undertaken in a fume cupboard to prevent contamination, and inhalation of the sediment.

7. **Interferences**

Not relevant.

8. **Sampling and Sample Preparation**

The sediment is freeze dried prior to sieving SOP 110.

9. **Analytical Procedure**

The extent of the sample preparation is dependent on the analysis to be undertaken (see request form B21). 2 mm fraction is removed prior to PSA for some clients. For some chemical analyses, a proportion of the <2 mm is ground to a fine powder.

9.1 **Particle Size Analysis**

Attach the funnel to the clamp and place the 2mm sieve inside the funnel.
Locate one of the mortars beneath the funnel.
Transfer the sample to a mortar and gently dissociate the sediment with a pestle into its constituent grains. It is essential not to damage the sediment grains so that the sample integrity is maintained.
Place a labelled pot below this sieve.
Pour the dissociate sample into the sieve, using the brush to remove any fine material adhered to the mortars surface.
Assist the sieving using a brush gently.
Clean the funnel, pestle and mortars between samples with a damp tissue or brush, ensuring all equipment is dry before preparing the next sample.

9.2 CHN Analysis/Metal Analysis

9.2.1 Manual Method (CHN /Metal analysis)
Using a clean mortar and pestle, a proportion of the sieved material is ground into a fine homogenous mixture and then transferred to a second labelled sample pot/bag.

9.2.2 Automated Method (CHN analysis only)
Place a proortion (up to 1/3 of the cup volume) of the sample in the cup. Place one 20 mm ball within the cup. Close the cup and mount it on the grinder as described in p 13 of MM2000 manual. Set the running time to 8 minutes, and the amplitude to 100 as described in page 14 of the MM2000 manual. After grinding cycle is complete, visually inspect the ground sample. If it does not appear homogenous, regrind for further 8 minute periods, repeating until homogeneity is achieved. Empty the ground sample into a labelled pot/bag. Clean the grinding cup with a tissue, ensuring the cup is completely dry before further samples are ground. Switch the instrument off after use.

9.3 **Fish Farm Chemical, OCP and CB Analysis**

Transfer the freeze dried sediment into the 2 mm sieve, with the collecting base attached. Gently break up the sediment, using the back of a Trulla spatula, and allow it to pass though the 2 mm mesh. Transfer the sieved sediment to a mortar and grind to a powder with a pestle. Transfer the powder onto aluminium foil and then back into the original container. The use of the powder funnel is permitted for sample transfer, if required. Clean the sieve, pestle and mortars between samples with a tissue moistened with hexane. Ensure all equipment is dry before preparing the next sample.

10. **Calculation of Results**

Not relevant.

11. **Precision, Bias and Limits of Detection**

Not relevant.

12. **Reports**

Not relevant.

13. **Safety**

See COSHH assessments no 005, 010 and 105. Gloves and dust mask are required.

14. **Literature References**

Not relevant.

APPENDIX 2.

Site S – Faunal Data (Raw)

		Station				
		A	B	C	D	E
Anth sp.		1	0	0	0	0
Nerm sp.		3	0	0	0	0
Nema sp.		89	72	180	42	32
Sipu sp.		2	0	0	0	0
Phol inor		1	1	4	1	3
Poly sp.		0	0	0	0	0
Eteo long		2	2	1	0	0
Glyc alba		2	3	0	1	0
Goni sp.		1	0	0	1	1
Exog hebe		0	1	3	4	0
Spha erin		7	15	24	6	0
Neph Homb		0	2	1	0	1
Neph inci		1	0	0	0	0
Ophy hart		12	0	0	0	0
Prot kefe		4	3	1	2	2
Scol armi		0	2	1	1	0
Prio fall		20	49	33	22	31
Prio sp.		1	0	13	0	0
Aphe mari		1	1	0	1	0
Aphe vivi		0	0	0	1	0
Caur zetl		0	1	0	0	0
Chae seto		9	4	0	0	0
Cirr cirr		0	2	1	0	0
Thar kill		20	10	0	2	0
Cirr sp.		4	4	3	1	0
Coss sp.		1	2	0	0	0
Capi capi		13	0	0	0	0
Mald sp.		0	0	0	1	0
Ophe acum		0	1	0	0	0
Scal infl		2	0	0	0	0
Owen fusi		0	0	0	0	0
Meli palm		6	3	8	13	4
Meli juv.		0	1	0	0	0
Tere stro		0	0	0	0	0
Mega sp.		0	0	0	0	0
Olig sp.		4	3	0	1	0
Cope sp.		0	1	1	0	17
Olig sp.		0	0	0	0	0
Biva Sp.A		5	5	2	1	9
Biva Sp.B		0	1	17	8	19
Biva Sp.C		0	1	1	0	0
Phor muel		0	0	0	1	0
Labi busk		0	1	0	1	0
Ophi sp.		0	0	2	3	1

Site A – Faunal Data (Raw)

		Station			
		A	B	C	D
Anth sp.		0	4	5	3
Nerm sp.		0	0	2	2
Nema sp.		2	0	2	0
Sipu sp.		5	0	0	0
Eteo long		0	0	1	0
Glyc alba		0	0	0	2
Spha erin		0	0	1	0
Neph inci		0	2	1	3
Ophy hart		0	3	1	9
Prot kefe		8	8	12	8
Scol armi		6	12	2	8
Prio fall		16	0	1	0
Aphe mari		81	12	11	1
Aphe vivi		1	0	0	0
Aphe mult		6	0	0	0
Caur zetl		15	1	6	3
Chae seto		1	3	0	0
Cirr cirr		28	0	6	6
Thar kill		3	0	0	1
Cirr sp.		2	0	0	0
Coss sp.		23	9	14	23
Scal infl		0	2	2	2
Meli palm		3	2	0	0
Tere stro		1	0	0	0
Olig sp.		1	3	3	8
Biva Sp.A		3	4	1	1
Biva Sp.B		1	0	0	0
Ophi sp.		2	3	1	2
Gypt cape		27	16	18	6
Tana sp.		11	27	19	21
Gamm sp.		5	11	10	7
Bodo sp.		0	2	1	0
Pseu limb		0	3	6	7
Noot late		0	0	0	2

Site B – Faunal Data (Raw)

		Station		
		A	B	C
Ophi hart		295	30	4
Holo sp.		1	0	1
Phol inor		4	12	4
Capi capi		8	9	0
Mald sp.		1	0	7
Neph homb		6	19	5
Cope sp.		0	10	8
Prio mult		4	5	4
Exog hebe		1	0	0
Sten zetl		0	0	1
Nere long		0	0	1
Nerm sp.		0	1	6
Nema sp.		27	1	1
Eteo flav		0	4	0
Eteo long		2	0	0
Glyc alba		0	1	0
Prot kefe		8	8	7
Prio fall		0	5	6
Aphe mari		0	0	0
Aphe vivi		40	15	6
Aphe mult		0	3	1
Caul zetl		5	0	1
Chae seto		15	8	0
Cirr cirr		7	7	3
Thar kill		20	4	2
Meli palm		12	6	16
Tere stro		0	2	0
Biva Sp.A		10	9	16
Biva Sp.B		3	0	2
Ophi sp.		0	1	3
Tana sp.		0	0	12
Gamm sp.		0	113	89
Bodo sp.		0	0	3

APPENDIX 3.

Velocity Component Scatter Plots (All Data)

Site: Site S - Surface Current Data

SCATTER PLOT OF PARALLEL VERSUS NORMAL VELOCITY COMPONENTS

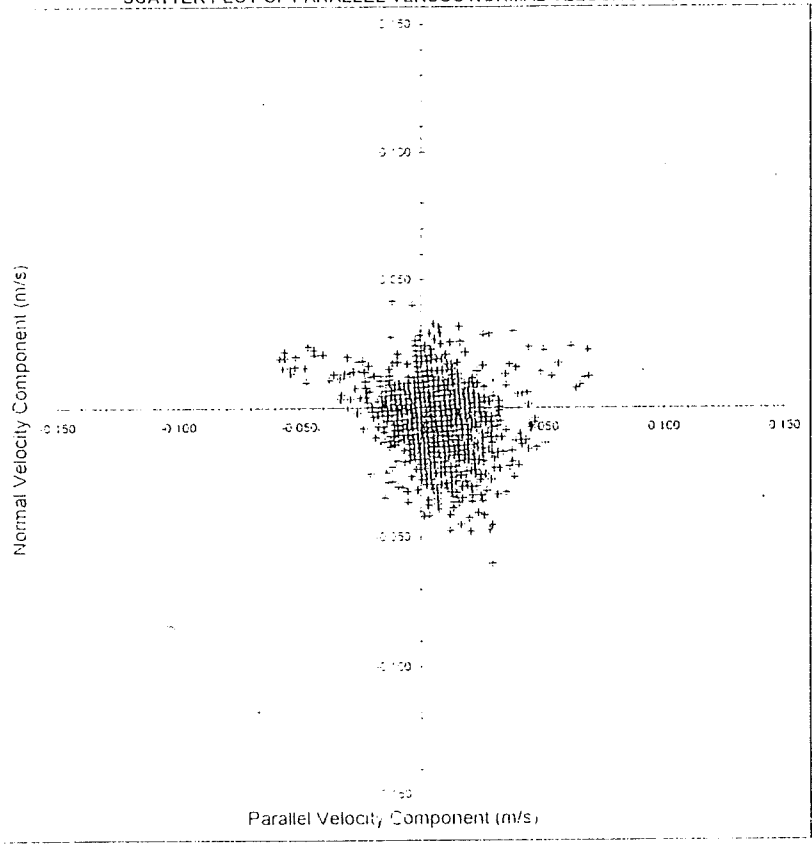

SCATTER PLOT OF EASTING VERSUS NORTHING VELOCITY COMPONENTS

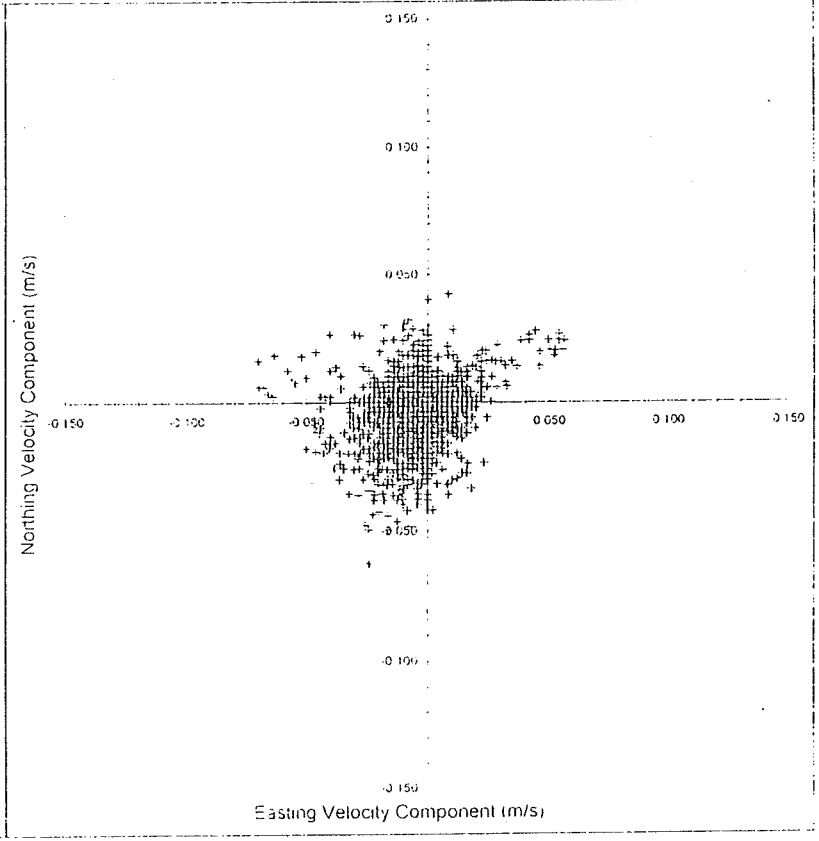

Current Meter Time Series Charts (All Data)

Site: Site S - Surface Current Data

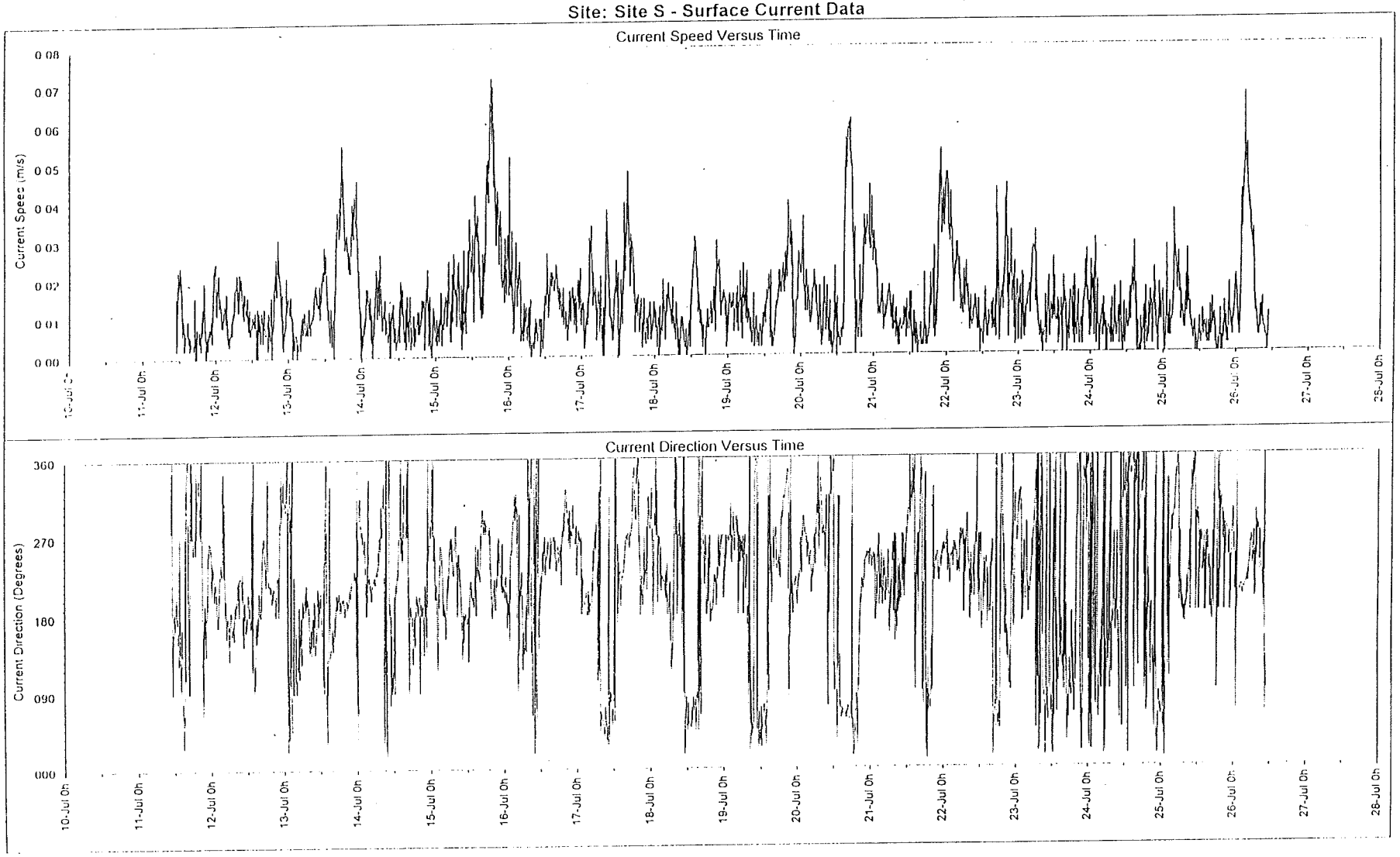

Current Meter Frequency Analysis Output (All Data)

Current Meter Data Frequency Analysis Results Table			
Site:	**Site S - Surface Current Data**		
Current Direction Frequency Bins (Degrees Magnetic)	Frequency Of Readings In Bin	Current Speed Frequency Bins (m/s)	Percentage Of Readings In Bin (%)
000 > to <=010	1	0.000> to <=0.030	91.58
010 > to <=020	24	0.030> to <=0.050	7.27
020 > to <=030	17	0.050> to <=0.075	1.16
030 > to <=040	14	0.075> to <= 0.100	0.00
040 > to <=050	34	0.100> to <=0.125	0.00
050 > to <=060	38	0.125> to <=0.150	0.00
060 > to <=070	50	> 0.150	0.00
070 > to <=080	37		
080 > to <=090	84		
090 > to <=100	8		
100 > to <=110	15		
110 > to <=120	26		
120 > to <=130	22		
130 > to <=140	38		
140 > to <=150	20		
150 > to <=160	30		
160 > to <=170	39		
170> to <=180	190		
180 > to <=190	41		
190 > to <=200	122		
200 > to <=210	100		
210 > to <=220	100		
220 > to <=230	108		
230 > to <=240	96		
240 > to <=250	99		
250 > to <=260	99		
260 > to <=270	250		
270 > to <=280	43		
280 > to <=290	47		
290 > to <=300	45		
300 > to <=310	29		
310 > to <=320	51		
320 > to <=330	25		
330 > to <=340	27		
340 > to <=350	41		
350 > to <=360	151		

CURRENT METER FREQUENCY ANALYSIS CHART OUTPUT (All Data)

Site: Site S - Surface Current Data

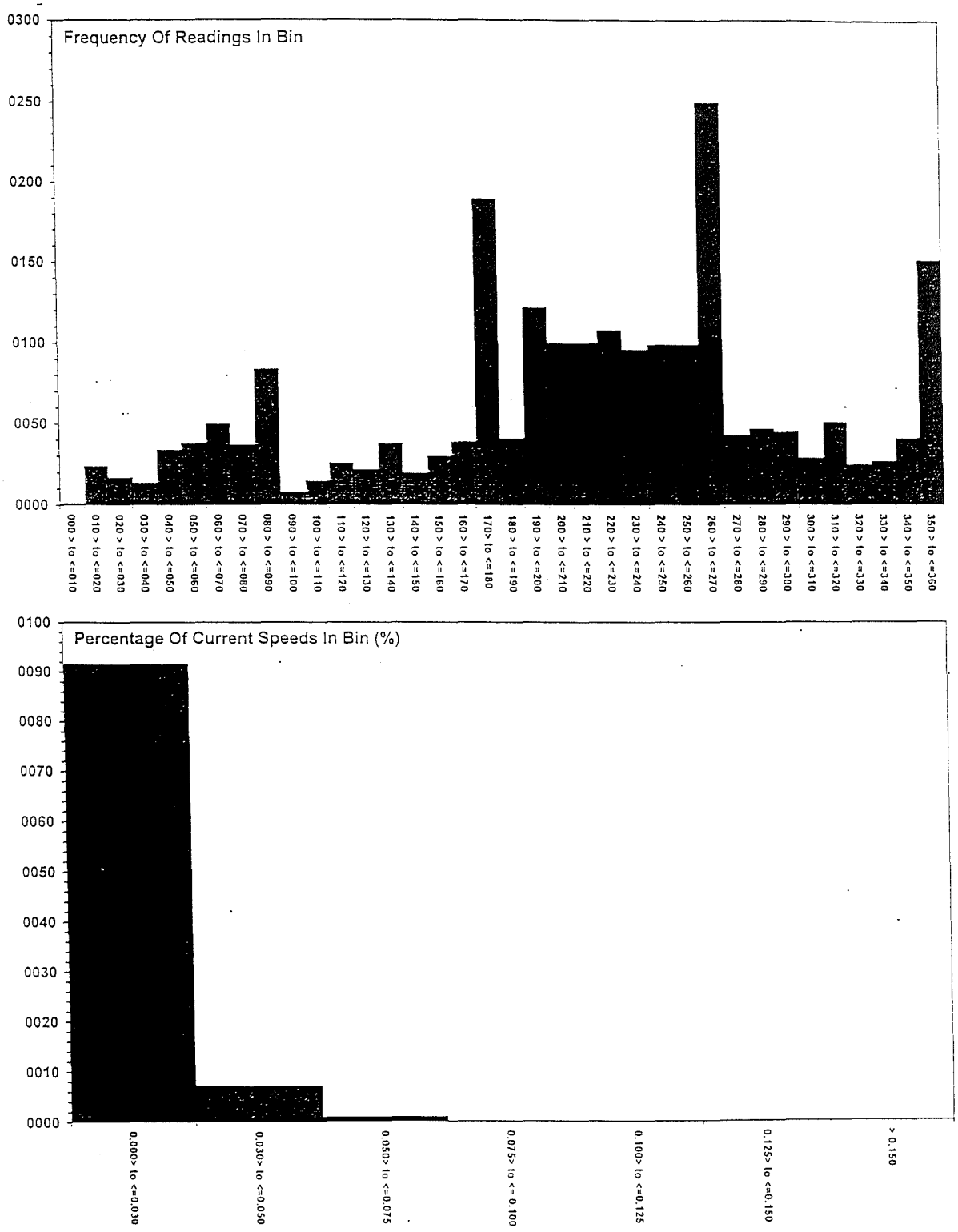

CURRENT DIRECTION AND SPEED FREQUENCY BINS

Current Meter Data Analysis

Details Of Current Meter Measurement And Analysis								
Site Details:	Enter Site Name Here ---------->	Site S - Surface Current Data			Fill in Yellow boxes only			
Measurement Details (Raw Data)								
Number Of Readings:	2161			Days:	Hours	Minutes		
Period Of Measurement:	11/07/1997 10:55:00	to	26/07/1997 10:55:00	15	0	0		
Measurement Interval (mins):	10	MEASUREMENT INTERVAL CORRECT						
Current Direction (Raw Data)								
Major Axis:(+ve)	265.00			Major Axis:(-ve)	85.00			
Minor Axis:(+ve)	355.00			Minor Axis:(-ve)	175.00			
Current Speed (m/s)	All data	Parallel Component	Normal Component	BUTTON UPDATES				
From Raw Data				Button 4:	09/08/2001 19:20:36	Button 9:	07/07/1998 12:26:38	
Mean:	0.014	0.005	-0.004	Button 6:	07/07/1998 12:25:12	Button 10:	07/07/1998 12:27:16	
Max:	0.072	0.069	0.041	Button 7:	07/07/1998 12:25:34			
Min:	0.000	-0.058	-0.060	Button 8:	09/07/1998 17:04:42			
Residual Current:	0.006	at	229.50	Degrees				
n Day Analysis (Usually 3 Days)		**Start Check:**	17/07/1997 10:55:00	**End Check:**	18/07/1997 10:55:00			
Current Speed (m/s)	**Start (dd/mm/yyyy hh:mm:ss):**		00/01/1900 00:00:00	**End:**	00/01/1900 00:00:00	Interval:		
Mean:	0.012	#DIV/0!	#DIV/0!					
Max:	0.048	0.000	0.000					
Min:	0.000	0.000	0.000					
Residual Current:	#DIV/0!	at	125.63	Degrees				
Current Direction (n Day Analysis)								
Major Axis:(+ve)				Major Axis:(-ve)	180.00			
Minor Axis:(+ve)	90.00			Minor Axis:(-ve)	270.00			
Measurement Details (n Day Analysis)								
Number Of Readings:	145			Days:	Hours	Minutes		
Period Of Measurement:	17/07/1997 10:55:00	to	18/07/1997 10:55:00	1	0	0		
Notes:		Check:		#VALUE!	#VALUE!	#VALUE!		

72hr Model Input Data	Residual	Tidal amplitude
Parallel Component U:	0.005	0.017
Normal Component V:	-0.004	0.016

Cummulative Vector Plots

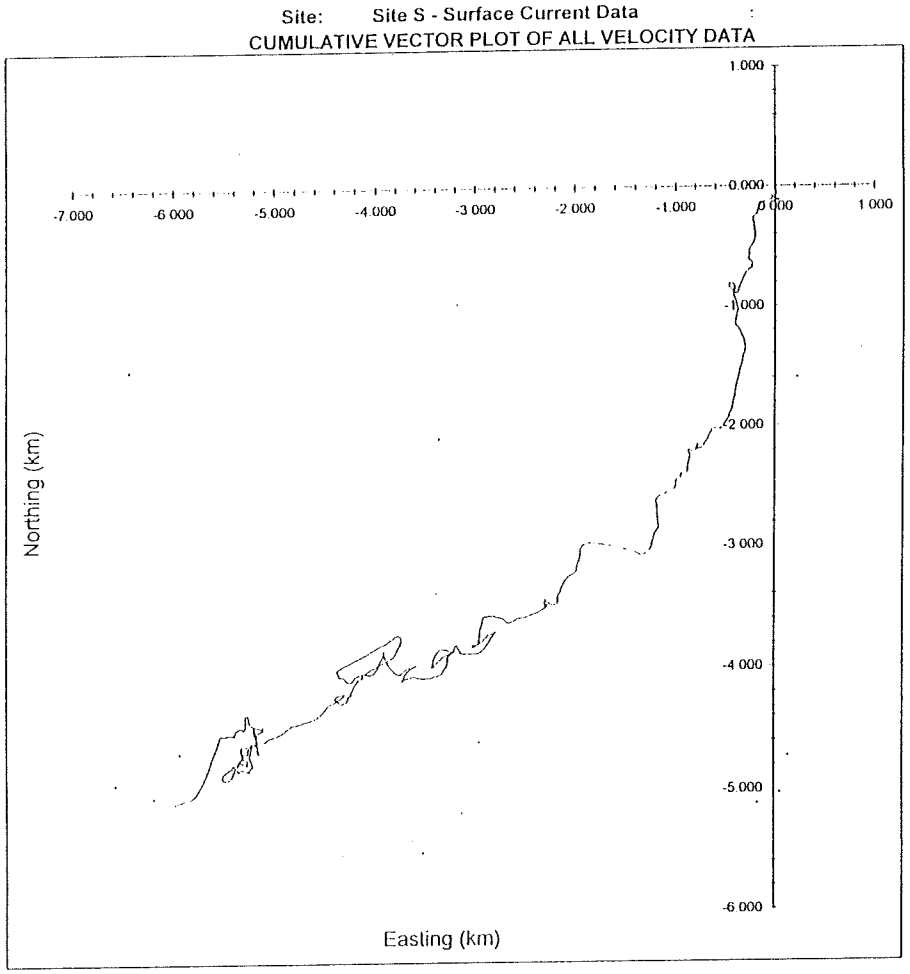

Velocity Component Scatter Plots (All Data)

Site: Site S - Midwater Current Data

SCATTER PLOT OF PARALLEL VERSUS NORMAL VELOCITY COMPONENTS

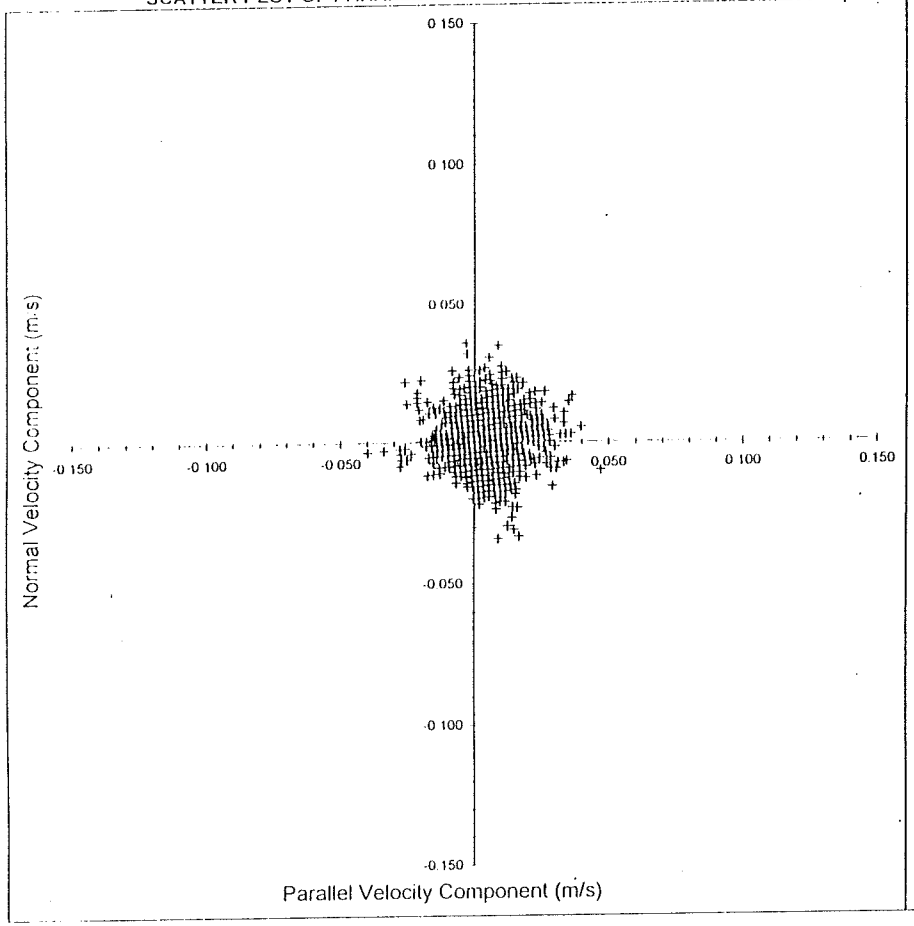

SCATTER PLOT OF EASTING VERSUS NORTHING VELOCITY COMPONENTS

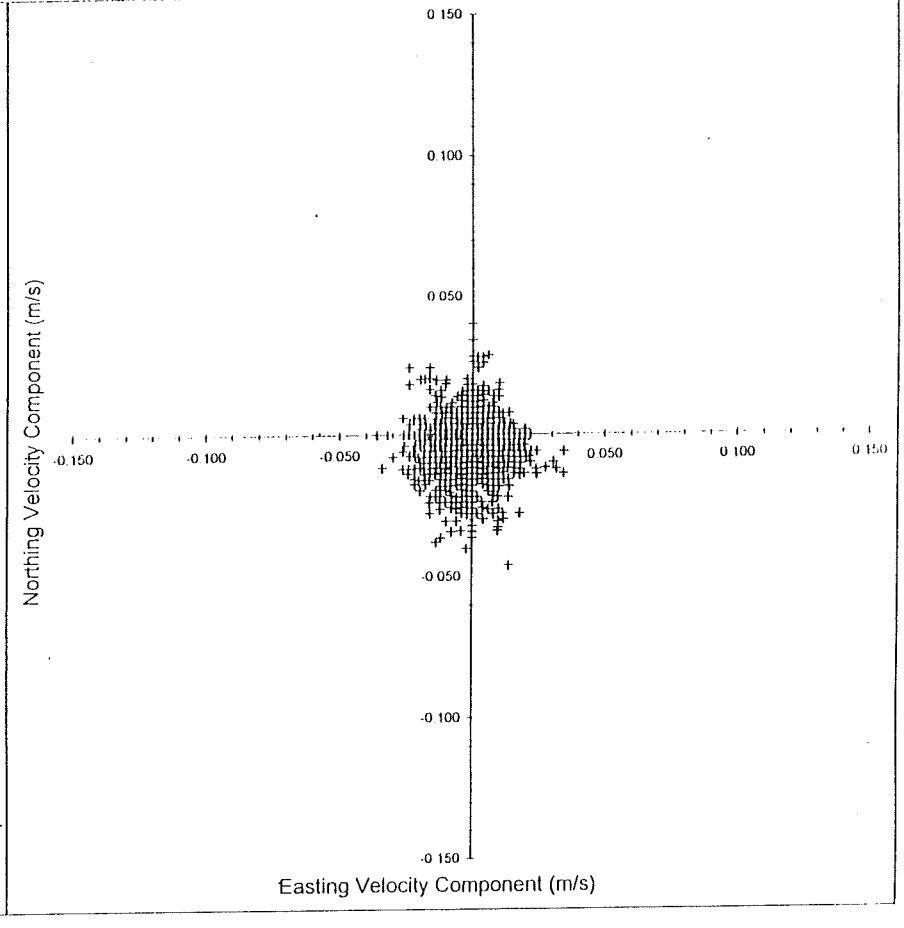

Current Meter Time Series Charts (All Data)

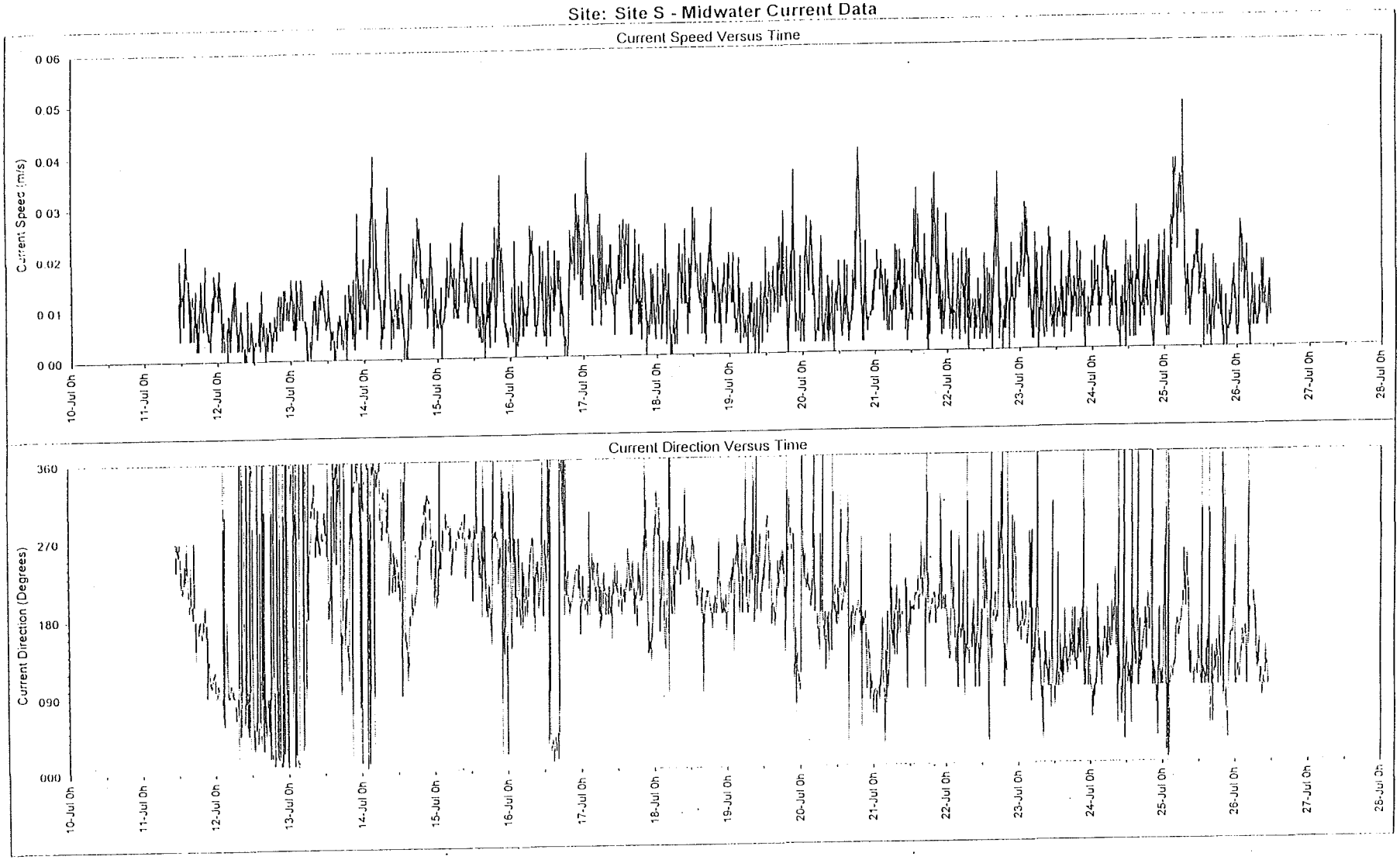

Current Meter Frequency Analysis Output (All Data)

Current Meter Data Frequency Analysis Results Table			
Site:	Site S - Midwater Current Data		
Current Direction Frequency Bins (Degrees Magnetic)	Frequency Of Readings In Bin	Current Speed Frequency Bins (m/s)	Percentage Of Readings In Bin (%)
000 > to <=010	18	0.000> to <=0.030	98.43
010 > to <=020	25	0.030> to <=0.050	1.57
020 > to <=030	27	0.050> to <=0.075	0.00
030 > to <=040	15	0.075> to <= 0.100	0.00
040 > to <=050	26	0.100> to <=0.125	0.00
050 > to <=060	13	0.125> to <=0.150	0.00
060 > to <=070	20	> 0.150	0.00
070 > to <=080	15		
080 > to <=090	146		
090 > to <=100	17		
100 > to <=110	78		
110 > to <=120	72		
120 > to <=130	70		
130 > to <=140	72		
140 > to <=150	54		
150 > to <=160	78		
160 > to <=170	78		
170> to <=180	249		
180 > to <=190	49		
190 > to <=200	113		
200 > to <=210	112		
210 > to <=220	94		
220 > to <=230	77		
230 > to <=240	71		
240 > to <=250	67		
250 > to <=260	55		
260 > to <=270	146		
270 > to <=280	15		
280 > to <=290	38		
290 > to <=300	18		
300 > to <=310	18		
310 > to <=320	24		
320 > to <=330	14		
330 > to <=340	13		
340 > to <=350	11		
350 > to <=360	153		

CURRENT METER FREQUENCY ANALYSIS CHART OUTPUT (All Data)

Site: Site S - Midwater Current Data

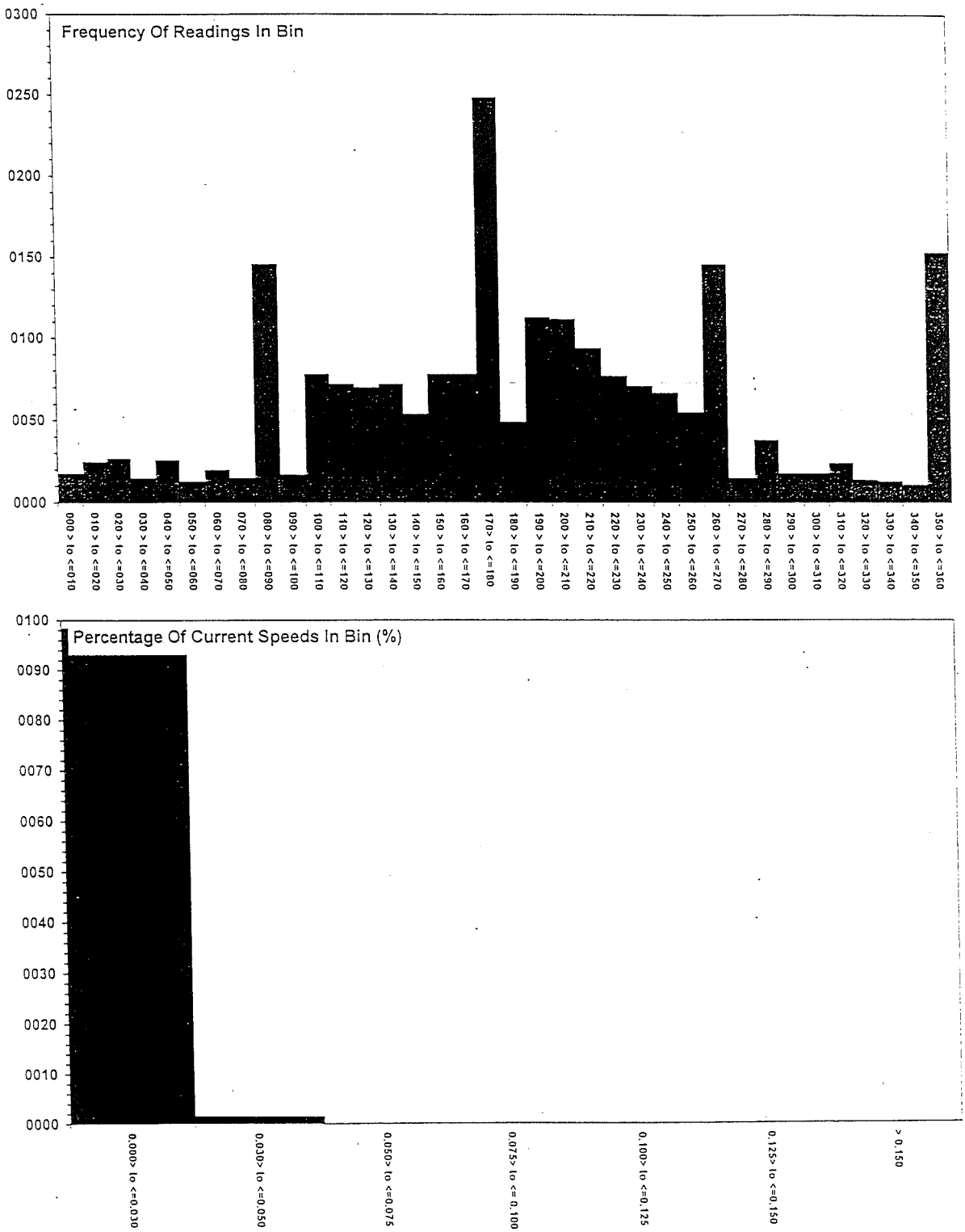

CURRENT DIRECTION AND SPEED FREQUENCY BINS

Current Meter Data Analysis

Details Of Current Meter Measurement And Analysis									
Site Details:	Enter Site Name Here ---------->	Site S - Midwater Current Data			Fill in Yellow boxes only				
Measurement Details (Raw Data)									
Number Of Readings:	2161				Days:	Hours	Minutes		
Period Of Measurement:	11/07/1997 10:55:00	to	26/07/1997 10:55:00		15	0	0		
Measurement Interval (mins):	10	MEASUREMENT INTERVAL CORRECT							
Current Direction (Raw Data)									
Major Axis:(+ve)	175.00				Major Axis:(-ve)	355.00			
Minor Axis:(+ve)	265.00				Minor Axis:(-ve)	85.00			
Current Speed (m/s)	All data	Parallel Component	Normal Component		BUTTON UPDATES				
From Raw Data					Button 4:	09/08/2001 19:23:47	Button 9:	07/07/1998 12:26:38	
Mean:	0.011	0.005	0.001		Button 6:	09/08/2001 19:24:23	Button 10:	07/07/1998 12:27:16	
Max:	0.048	0.047	0.036		Button 7:	07/07/1998 12:25:34			
Min:	0.000	-0.040	-0.034		Button 8:	09/07/1998 17:04:42			
Residual Current:	0.005	at	188.04		Degrees				
n Day Analysis (Usually 3 Days)		Start Check:	17/07/1997 10:55:00		End Check:	18/07/1997 10:55:00			
Current Speed (m/s)	Start (dd/mm/yyyy hh:mm:ss):		00/01/1900 00:00:00		End:	00/01/1900 00:00:00	Interval:		
Mean:	0.012	#DIV/0!	#DIV/0!						
Max:	0.027	0.000	0.000						
Min:	0.000	0.000	0.000						
Residual Current:	#DIV/0!	at	125.63		Degrees				
Current Direction (n Day Analysis)									
Major Axis:(+ve)					Major Axis:(-ve)	180.00			
Minor Axis:(+ve)	90.00				Minor Axis:(-ve)	270.00			
Measurement Details (n Day Analysis)									
Number Of Readings:	145				Days:	Hours	Minutes		
Period Of Measurement:	17/07/1997 10:55:00	to	18/07/1997 10:55:00		1	0	0		
Notes:			Check:		#VALUE!	#VALUE!	#VALUE!		

72hr Model Input Data	Residual	Tidal amplitude
Parallel Component U:	0.005	0.013
Normal Component V:	0.001	0.012

Cummulative Vector Plots

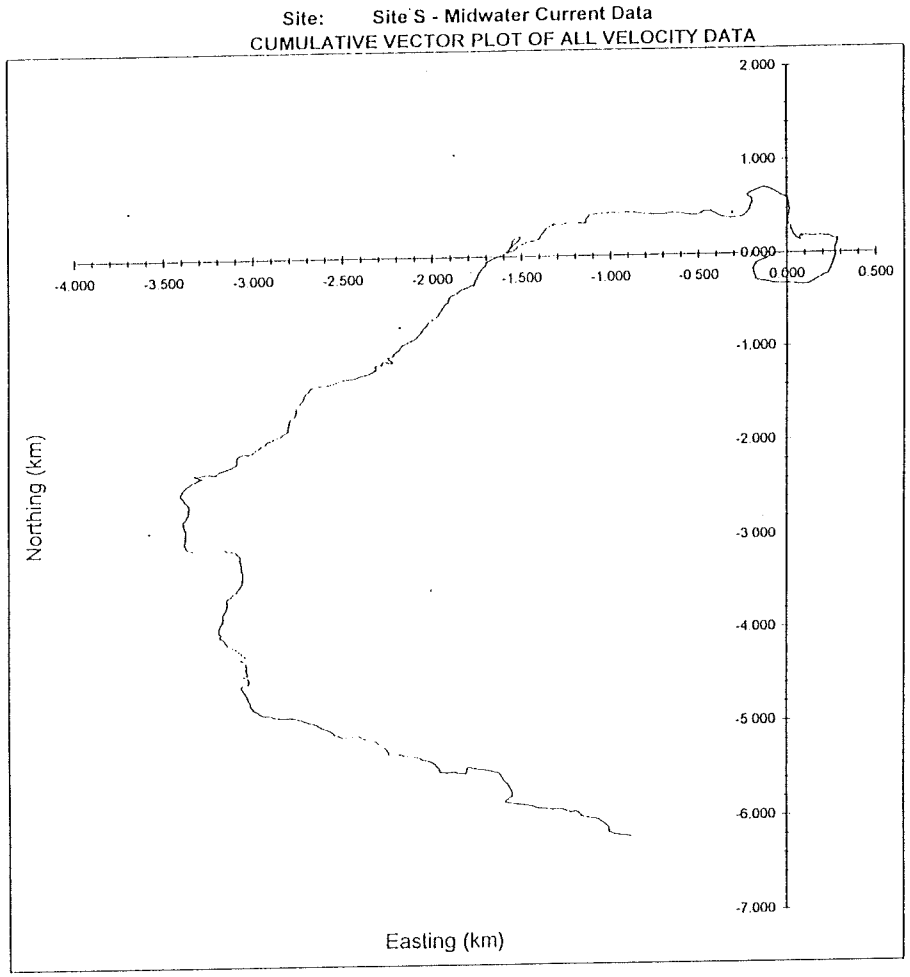

Velocity Component Scatter Plots (All Data)

Site: Site S - Bottom Current Data

SCATTER PLOT OF PARALLEL VERSUS NORMAL VELOCITY COMPONENTS

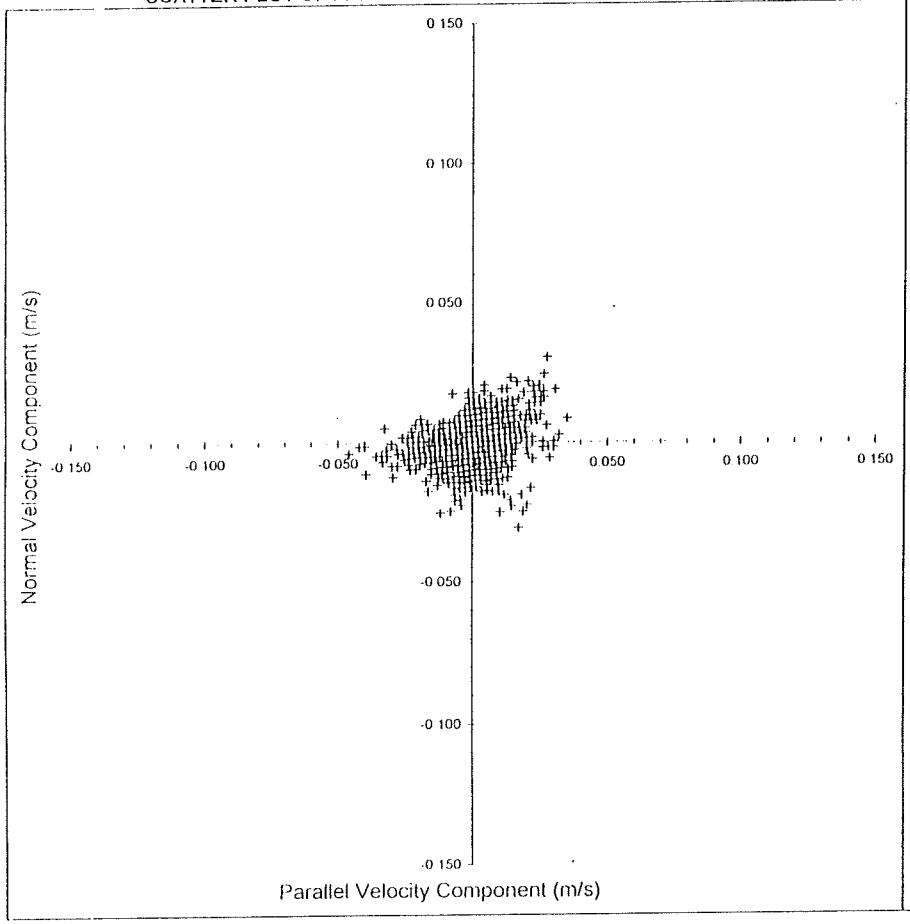

SCATTER PLOT OF EASTING VERSUS NORTHING VELOCITY COMPONENTS

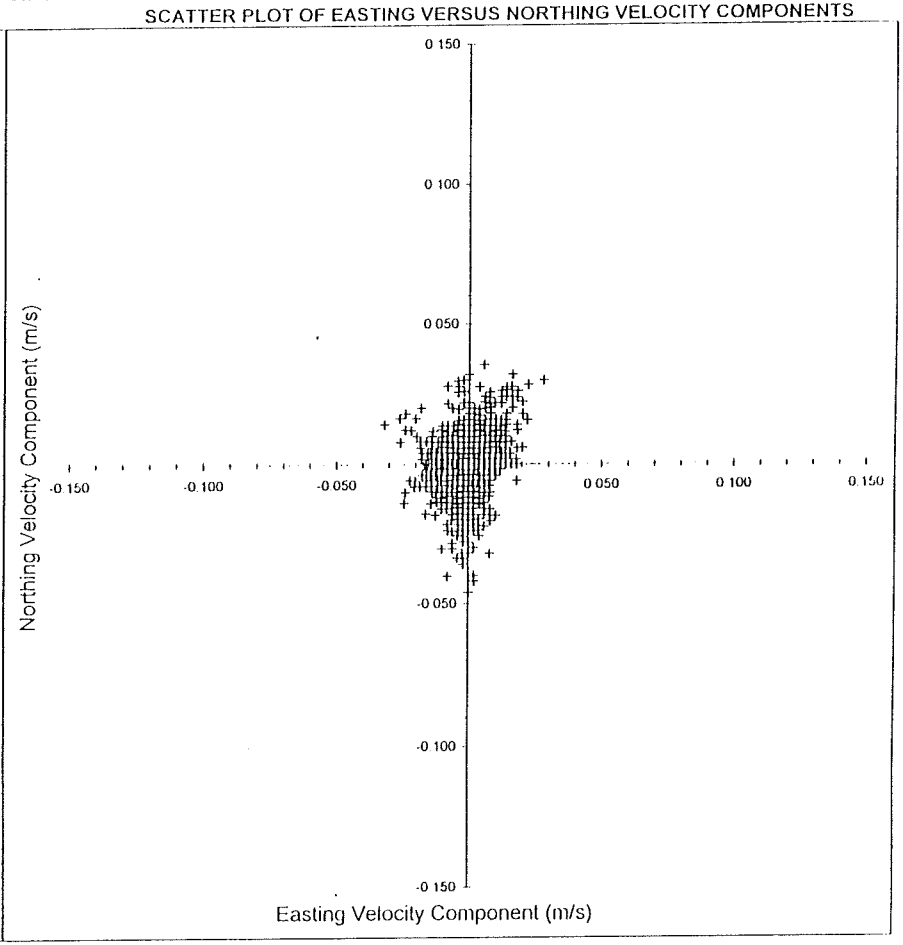

Current Meter Time Series Charts (All Data)

Site: Site S - Bottom Current Data

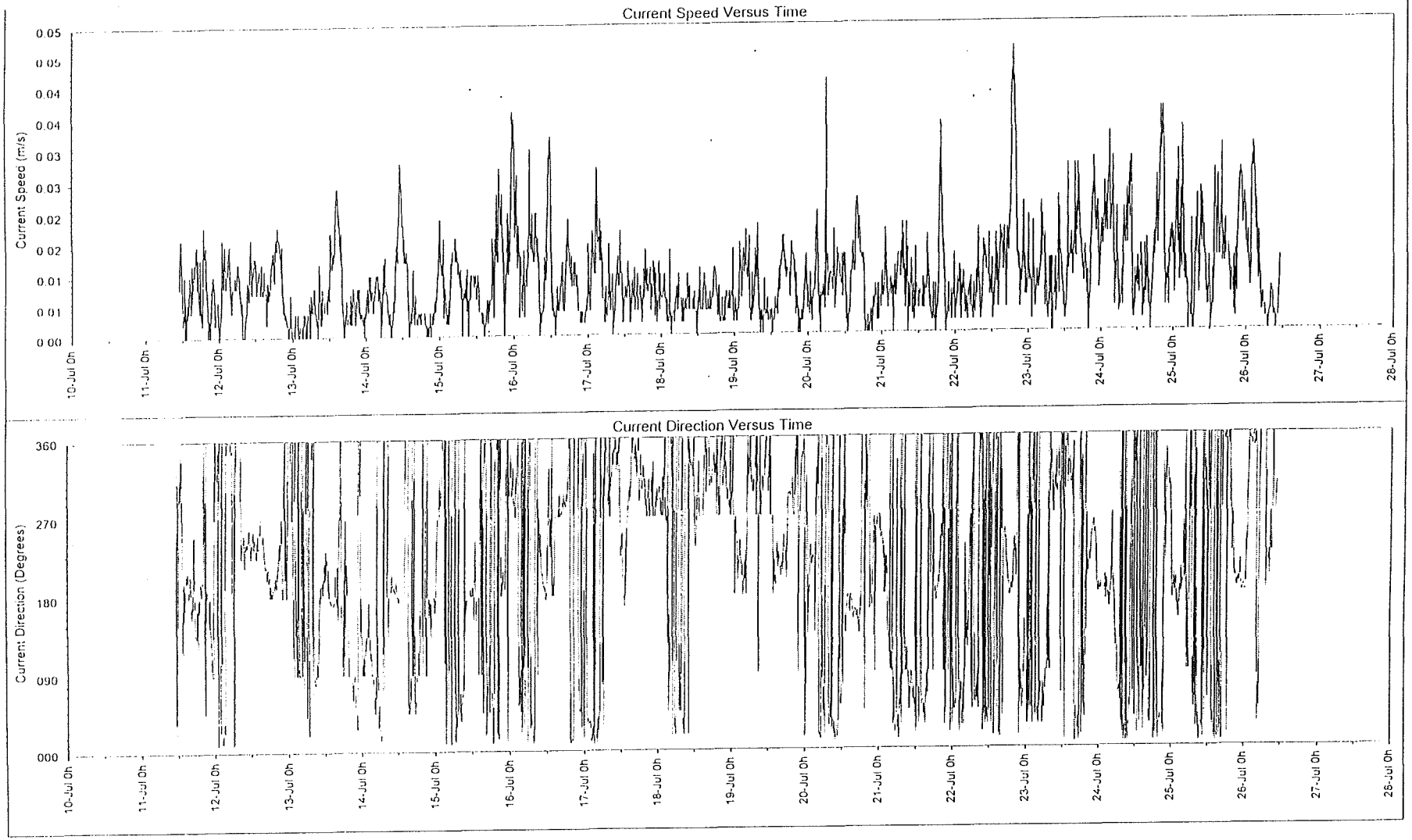

Current Meter Frequency Analysis Output (All Data)

Current Meter Data Frequency Analysis Results Table			
Site:	Site S - Bottom Current Data		
Current Direction Frequency Bins (Degrees Magnetic)	Frequency Of Readings In Bin	Current Speed Frequency Bins (m/s)	Percentage Of Readings In Bin (%)
000 > to <=010	31	0.000> to <=0.030	98.84
010 > to <=020	79	0.030> to <=0.050	1.16
020 > to <=030	86	0.050> to <=0.075	0.00
030 > to <=040	51	0.075> to <= 0.100	0.00
040 > to <=050	80	0.100> to <=0.125	0.00
050 > to <=060	46	0.125> to <=0.150	0.00
060 > to <=070	36	> 0.150	0.00
070 > to <=080	42		
080 > to <=090	120		
090 > to <=100	3		
100 > to <=110	10		
110 > to <=120	17		
120 > to <=130	4		
130 > to <=140	36		
140 > to <=150	9		
150 > to <=160	21		
160 > to <=170	30		
170> to <=180	182		
180 > to <=190	42		
190 > to <=200	77		
200 > to <=210	38		
210 > to <=220	49		
220 > to <=230	48		
230 > to <=240	39		
240 > to <=250	51		
250 > to <=260	30		
260 > to <=270	139		
270 > to <=280	8		
280 > to <=290	45		
290 > to <=300	54		
300 > to <=310	42		
310 > to <=320	66		
320 > to <=330	36		
330 > to <=340	40		
340 > to <=350	59		
350 > to <=360	415		

CURRENT METER FREQUENCY ANALYSIS CHART OUTPUT (All Data)

Site: Site S - Bottom Current Data

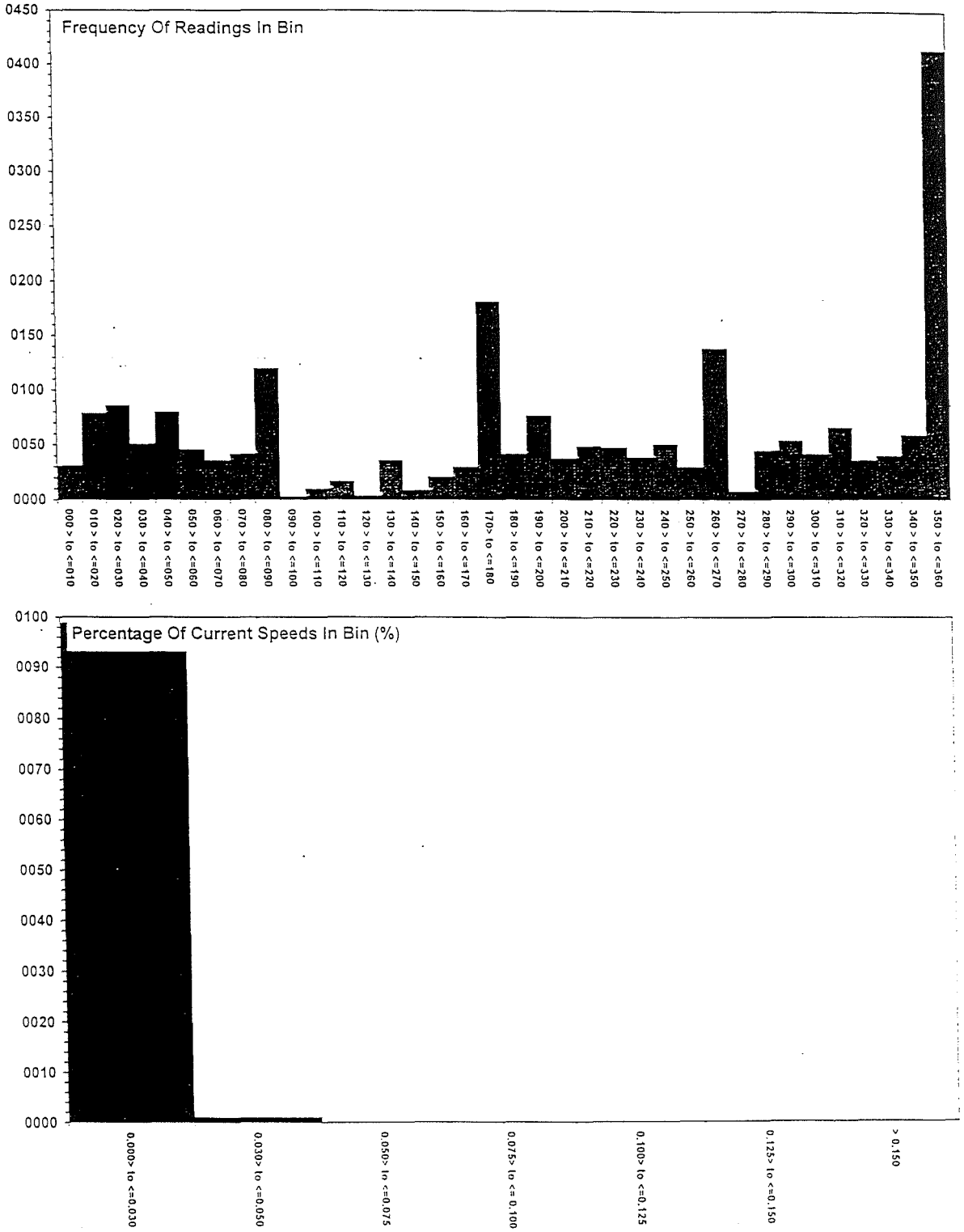

CURRENT DIRECTION AND SPEED FREQUENCY BINS

Current Meter Data Analysis

Details Of Current Meter Measurement And Analysis									
Site Details:	Enter Site Name Here ---------->	Site S - Bottom Current Data		Fill In Yellow boxes only					
Measurement Details (Raw Data)									
Number Of Readings:	2161			Days:	Hours	Minutes			
Period Of Measurement:	11/07/1997 10:55:00	to	26/07/1997 10:55:00	15	0	0			
Measurement Interval (mins):	10	MEASUREMENT INTERVAL CORRECT							
Current Direction (Raw Data)									
Major Axis:(+ve)	355.00			Major Axis:(-ve)	175.00				
Minor Axis:(+ve)	85.00			Minor Axis:(-ve)	265.00				
Current Speed (m/s)	All data	Parallel Component	Normal Component	BUTTON UPDATES					
From Raw Data				Button 4:	09/08/2001 19:25:25	Button 9:	07/07/1998 12:26:38		
Mean:	0.009	0.001	0.000	Button 6:	07/07/1998 12:25:12	Button 10:	07/07/1998 12:27:16		
Max:	0.046	0.035	0.030	Button 7:	07/07/1998 12:25:34				
Min:	0.000	-0.046	-0.031	Button 8:	09/07/1998 17:04:42				
Residual Current:	0.001	at	330.79	Degrees					
n Day Analysis (Usually 3 Days)		**Start Check:**	17/07/1997 10:55:00	**End Check:**	18/07/1997 10:55:00				
Current Speed (m/s)	**Start (dd/mm/yyyy hh:mm:ss):**		00/01/1900 00:00:00	**End:**	00/01/1900 00:00:00	Interval:			
Mean:	0.006	#DIV/0!	#DIV/0!						
Max:	0.014	0.000	0.000						
Min:	0.000	0.000	0.000						
Residual Current:	#DIV/0!	at	125.63	Degrees					
Current Direction (n Day Analysis)									
Major Axis:(+ve)				Major Axis:(-ve)	180.00				
Minor Axis:(+ve)	90.00			Minor Axis:(-ve)	270.00				
Measurement Details (n Day Analysis)									
Number Of Readings:	145			Days:	Hours	Minutes			
Period Of Measurement:	17/07/1997 10:55:00	to	18/07/1997 10:55:00	1	0	0			
Notes:			Check:	#VALUE!	#VALUE!	#VALUE!			

72hr Model Input Data	Residual	Tidal amplitude
Parallel Component U:	0.001	0.013
Normal Component V:	0.000	0.009

Cummulative Vector Plots

Site: Site S - Bottom Current Data

CUMULATIVE VECTOR PLOT OF ALL VELOCITY DATA

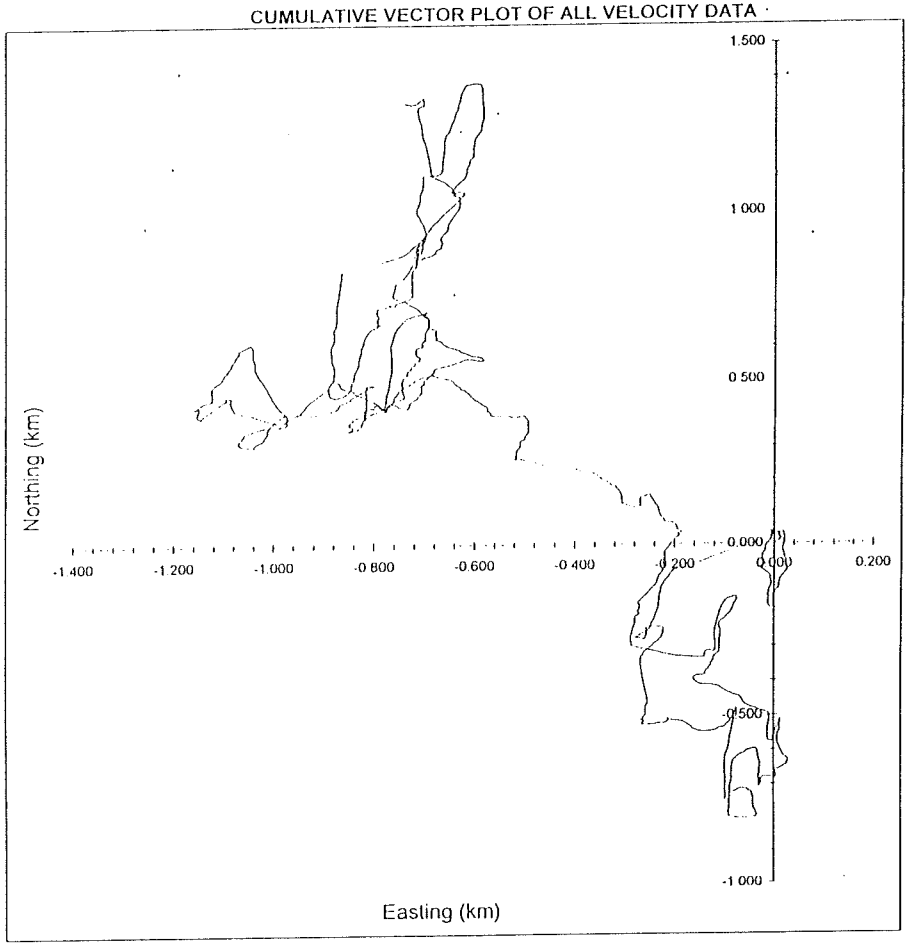

Velocity Component Scatter Plots (All Data)

Site: Site A - Surface Current Data

SCATTER PLOT OF PARALLEL VERSUS NORMAL VELOCITY COMPONENTS

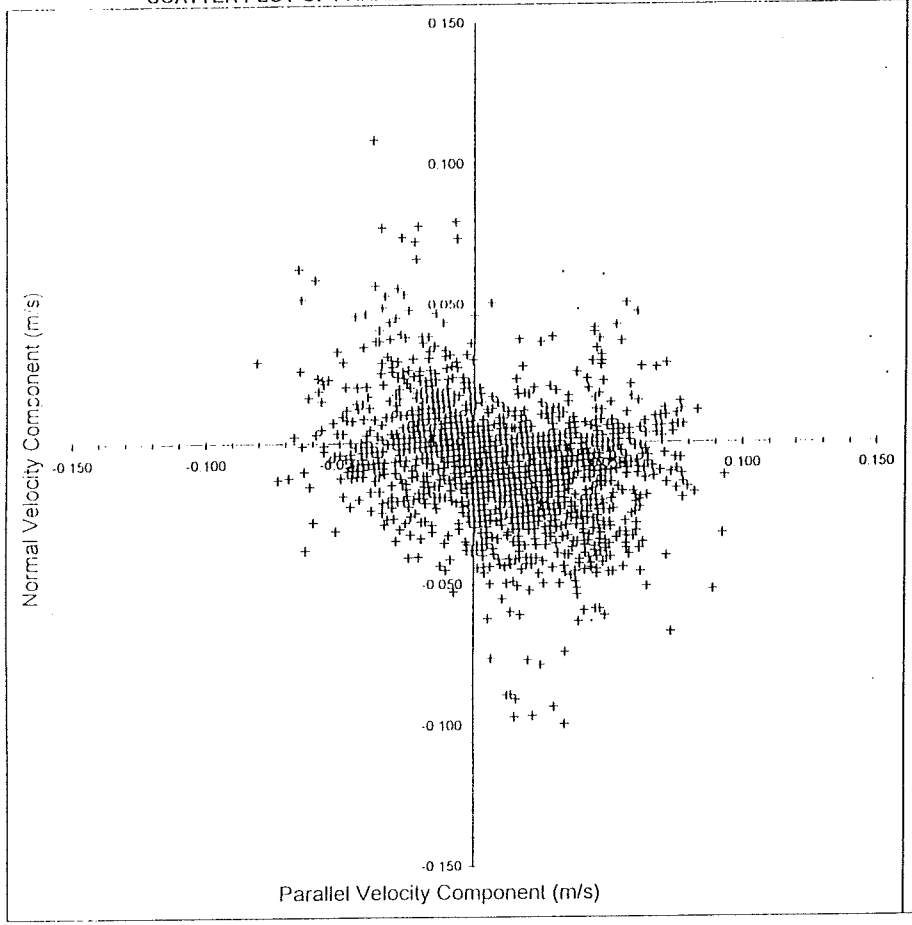

SCATTER PLOT OF EASTING VERSUS NORTHING VELOCITY COMPONENTS

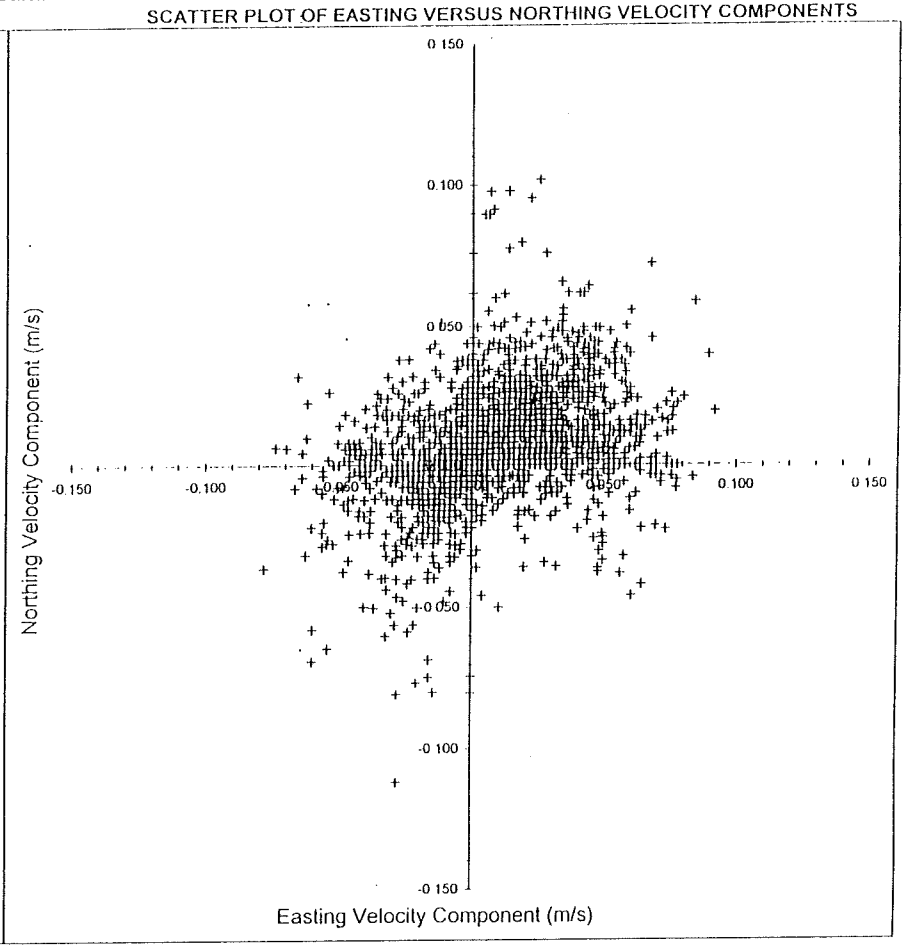

Current Meter Time Series Charts (All Data)

Site: Site A - Surface Current Data

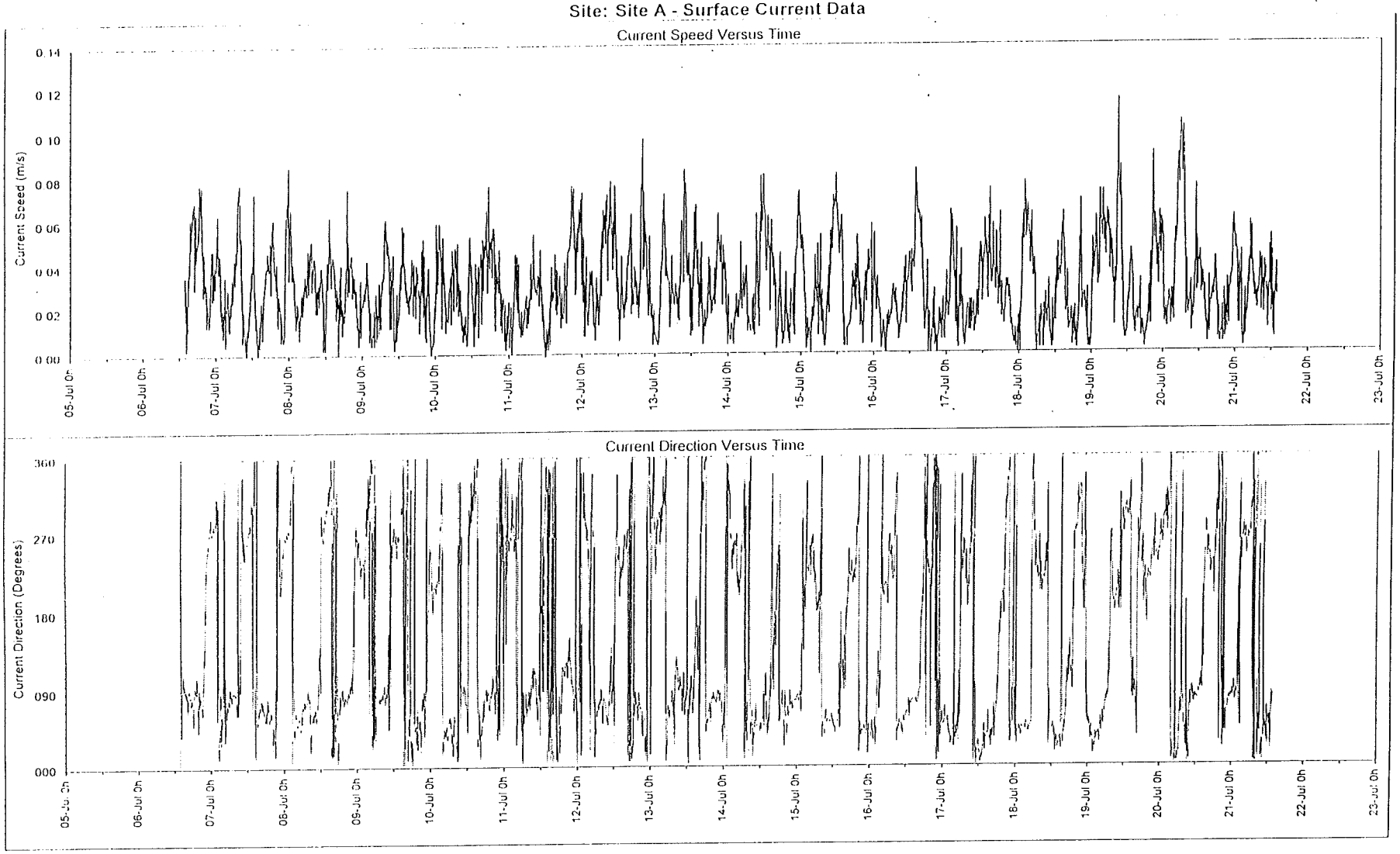

Current Meter Frequency Analysis Output (All Data)

Current Meter Data Frequency Analysis Results Table			
Site:	Site A - Surface Current Data		
Current Direction Frequency Bins (Degrees Magnetic)	Frequency Of Readings In Bin	Current Speed Frequency Bins (m/s)	Percentage Of Readings In Bin (%)
000 > to <=010	56	0.000> to <=0.030	55.53
010 > to <=020	60	0.030> to <=0.050	28.60
020 > to <=030	82	0.050> to <=0.075	13.56
030 > to <=040	119	0.075> to <= 0.100	2.17
040 > to <=050	173	0.100> to <=0.125	0.14
050 > to <=060	129	0.125> to <=0.150	0.00
060 > to <=070	126	> 0.150	0.00
070 > to <=080	170		
080 > to <=090	208		
090 > to <=100	46		
100 > to <=110	38		
110 > to <=120	22		
120 > to <=130	23		
130 > to <=140	16		
140 > to <=150	9		
150 > to <=160	6		
160 > to <=170	6		
170> to <=180	30		
180 > to <=190	13		
190 > to <=200	26		
200 > to <=210	38		
210 > to <=220	42		
220 > to <=230	50		
230 > to <=240	54		
240 > to <=250	54		
250 > to <=260	49		
260 > to <=270	128		
270 > to <=280	40		
280 > to <=290	37		
290 > to <=300	35		
300 > to <=310	34		
310 > to <=320	36		
320 > to <=330	33		
330 > to <=340	22		
340 > to <=350	33		
350 > to <=360	118		

CURRENT METER FREQUENCY ANALYSIS CHART OUTPUT (All Data)

Site: Site A - Surface Current Data

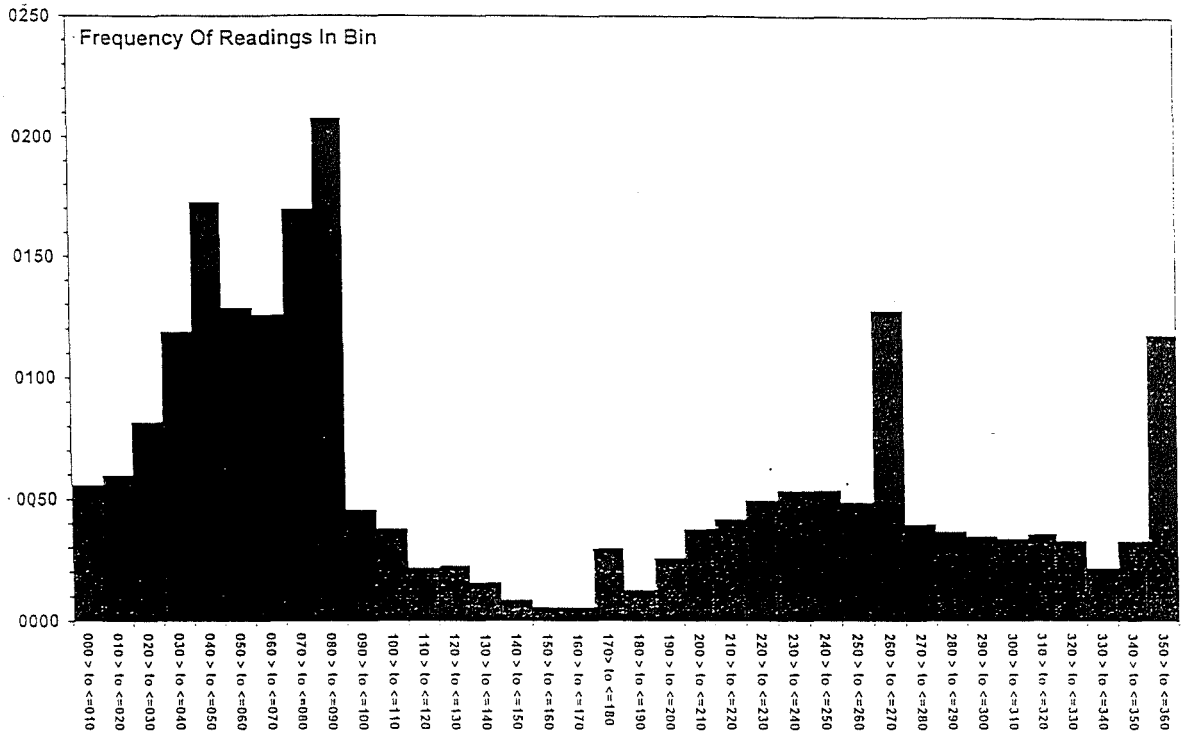

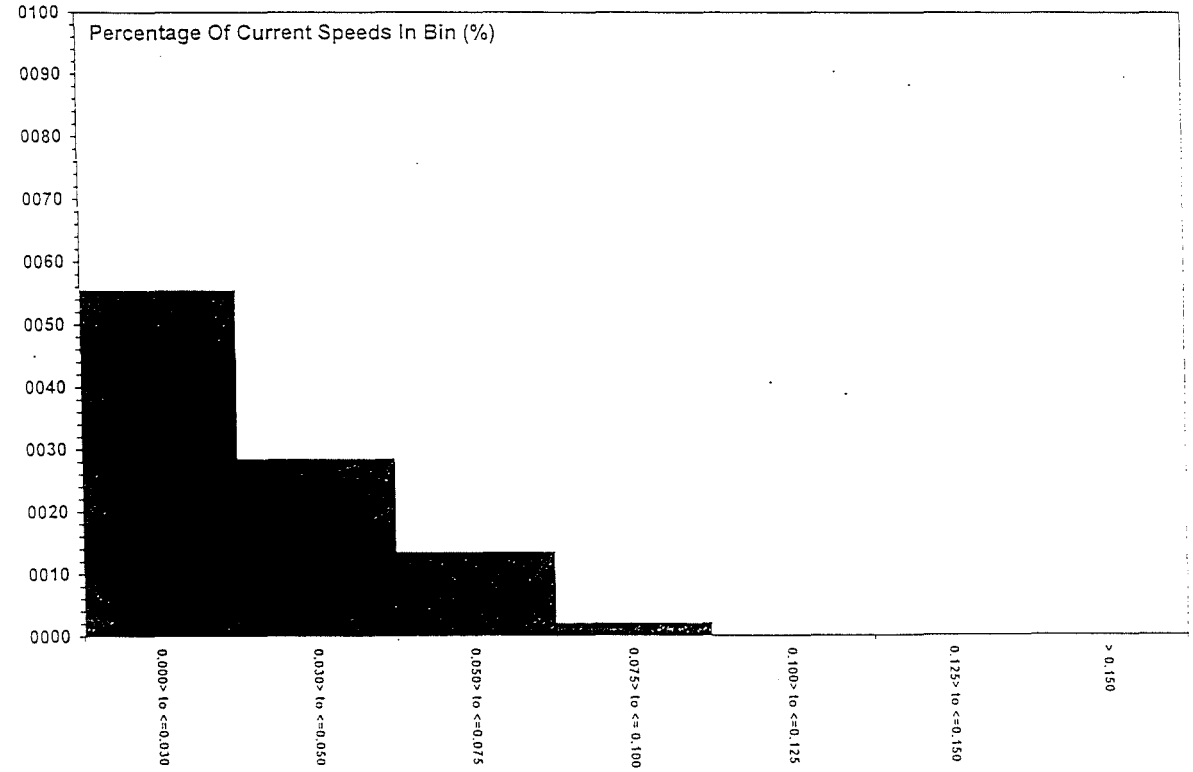

CURRENT DIRECTION AND SPEED FREQUENCY BINS

Current Meter Data Analysis

Details Of Current Meter Measurement And Analysis									
Site Details:	Enter Site Name Here ---------->	Site A - Surface Current Data			Fill in Yellow boxes only				
Measurement Details (Raw Data)									
Number Of Readings:	2161			Days:	Hours	Minutes			
Period Of Measurement:	06/07/1998 13:50:00	to	21/07/1998 13:50:00	15	0	0			
Measurement Interval (mins):	10	MEASUREMENT INTERVAL CORRECT							
Current Direction (Raw Data)									
Major Axis:(+ve)	85.00			Major Axis:(-ve)	265.00				
Minor Axis:(+ve)	175.00			Minor Axis:(-ve)	355.00				
Current Speed (m/s)	All data	Parallel Component	Normal Component	BUTTON UPDATES					
From Raw Data				Button 4:	09/08/2001 19:27:39	Button 9:	07/07/1998 12:26:38		
Mean:	0.031	0.010	-0.007	Button 6:	07/07/1998 12:25:12	Button 10:	07/07/1998 12:27:16		
Max:	0.115	0.093	0.109	Button 7:	07/07/1998 12:25:34				
Min:	0.000	-0.081	-0.099	Button 8:	09/07/1998 17:04:42				
Residual Current:	0.012	at	51.45	Degrees					
n Day Analysis (Usually 3 Days)		**Start Check:**	12/07/1998 13:50:00	**End Check:**	13/07/1998 13:50:00				
Current Speed (m/s)	**Start (dd/mm/yyyy hh:mm:ss):**		00/01/1900 00:00:00	**End:**	00/01/1900 00:00:00	Interval:			
Mean:	0.036	#DIV/0!	#DIV/0!						
Max:	0.098	0.000	0.000						
Min:	0.004	0.000	0.000						
Residual Current:	#DIV/0!	at	125.63	Degrees					
Current Direction (n Day Analysis)									
Major Axis:(+ve)				Major Axis:(-ve)	180.00				
Minor Axis:(+ve)	90.00			Minor Axis:(-ve)	270.00				
Measurement Details (n Day Analysis)									
Number Of Readings:	145			Days:	Hours	Minutes			
Period Of Measurement:	12/07/1998 13:50:00	to	13/07/1998 13:50:00	1	0	0			
Notes:		Check:		#VALUE!	#VALUE!	#VALUE!			

72hr Model Input Data	Residual	Tidal amplitude
Parallel Component U:	0.010	0.040
Normal Component V:	-0.007	0.027

Cummulative Vector Plots

Site: Site A - Surface Current Data

CUMULATIVE VECTOR PLOT OF ALL VELOCITY DATA

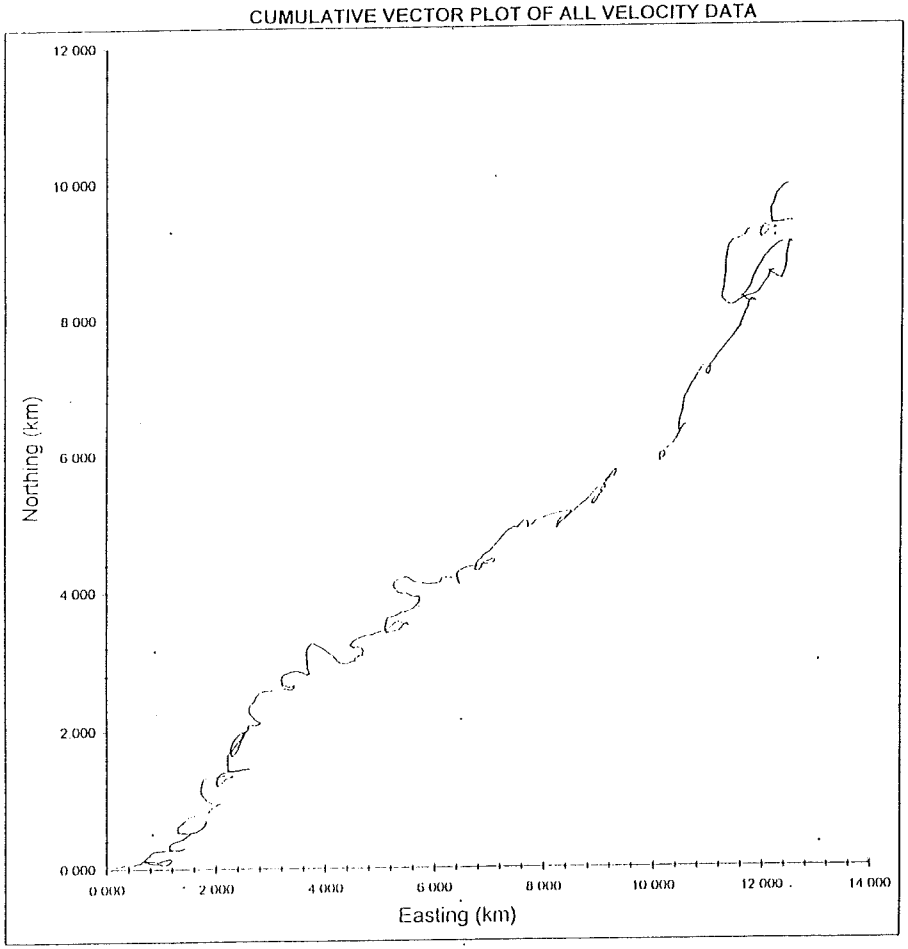

Current Meter Time Series Charts (All Data)

Site: Site A - Bottom Current Data

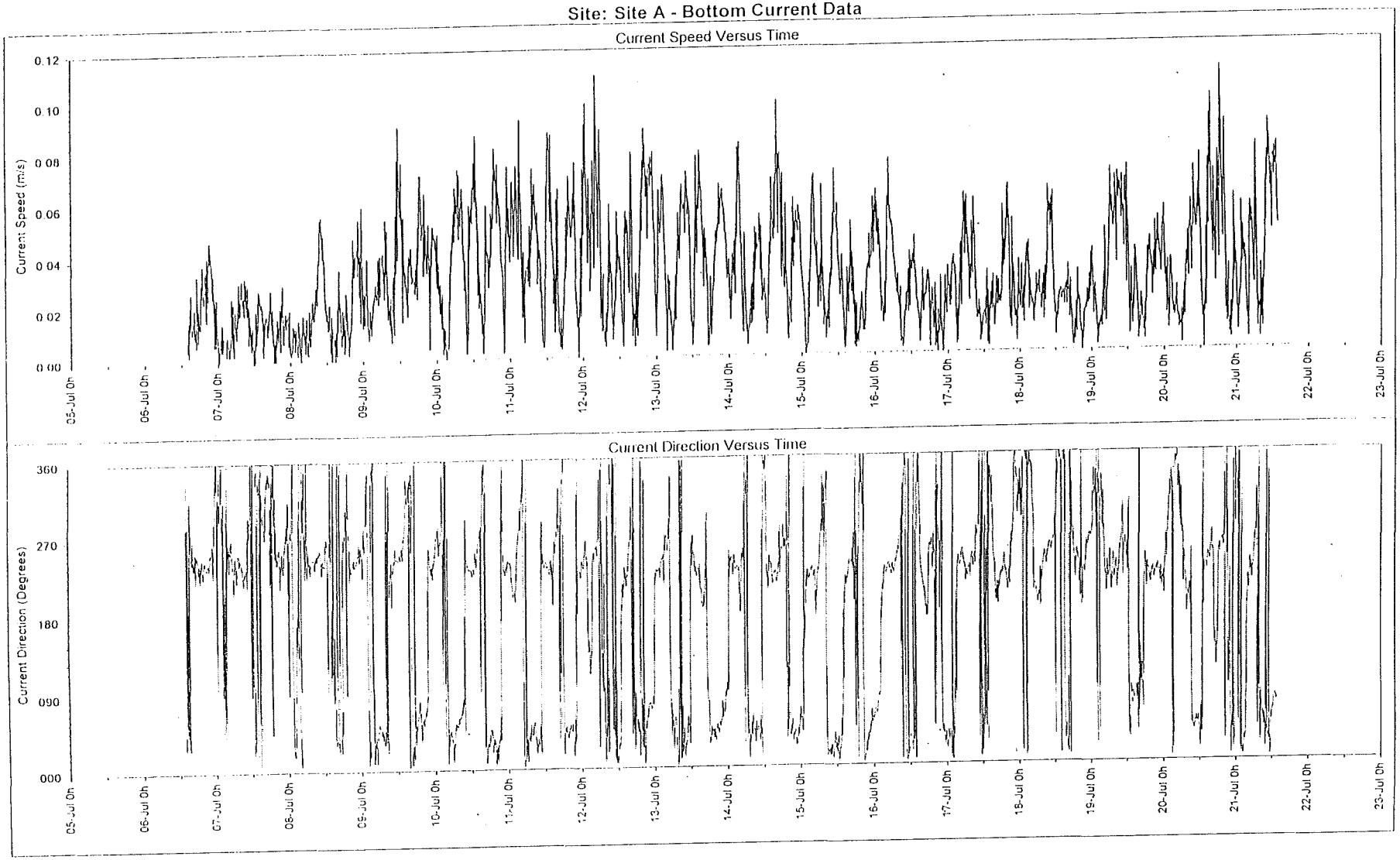

Current Meter Frequency Analysis Output (All Data)

Current Meter Data Frequency Analysis Results Table			
Site:	Site A - Bottom Current Data		
Current Direction Frequency Bins (Degrees Magnetic)	Frequency Of Readings In Bin	Current Speed Frequency Bins (m/s)	Percentage Of Readings In Bin (%)
000 > to <=010	60	0.000> to <=0.030	53.31
010 > to <=020	68	0.030> to <=0.050	25.87
020 > to <=030	107	0.050> to <=0.075	18.19
030 > to <=040	140	0.075> to <= 0.100	2.55
040 > to <=050	111	0.100> to <=0.125	0.09
050 > to <=060	78	0.125> to <=0.150	0.00
060 > to <=070	51	> 0.150	0.00
070 > to <=080	35		
080 > to <=090	54		
090 > to <=100	2		
100 > to <=110	4		
110 > to <=120	7		
120 > to <=130	1		
130 > to <=140	11		
140 > to <=150	7		
150 > to <=160	2		
160 > to <=170	1		
170> to <=180	33		
180 > to <=190	14		
190 > to <=200	40		
200 > to <=210	51		
210 > to <=220	85		
220 > to <=230	182		
230 > to <=240	205		
240 > to <=250	179		
250 > to <=260	108		
260 > to <=270	129		
270 > to <=280	20		
280 > to <=290	35		
290 > to <=300	24		
300 > to <=310	19		
310 > to <=320	39		
320 > to <=330	34		
330 > to <=340	51		
340 > to <=350	45		
350 > to <=360	129		

CURRENT METER FREQUENCY ANALYSIS CHART OUTPUT (All Data)

Site: Site A - Bottom Current Data

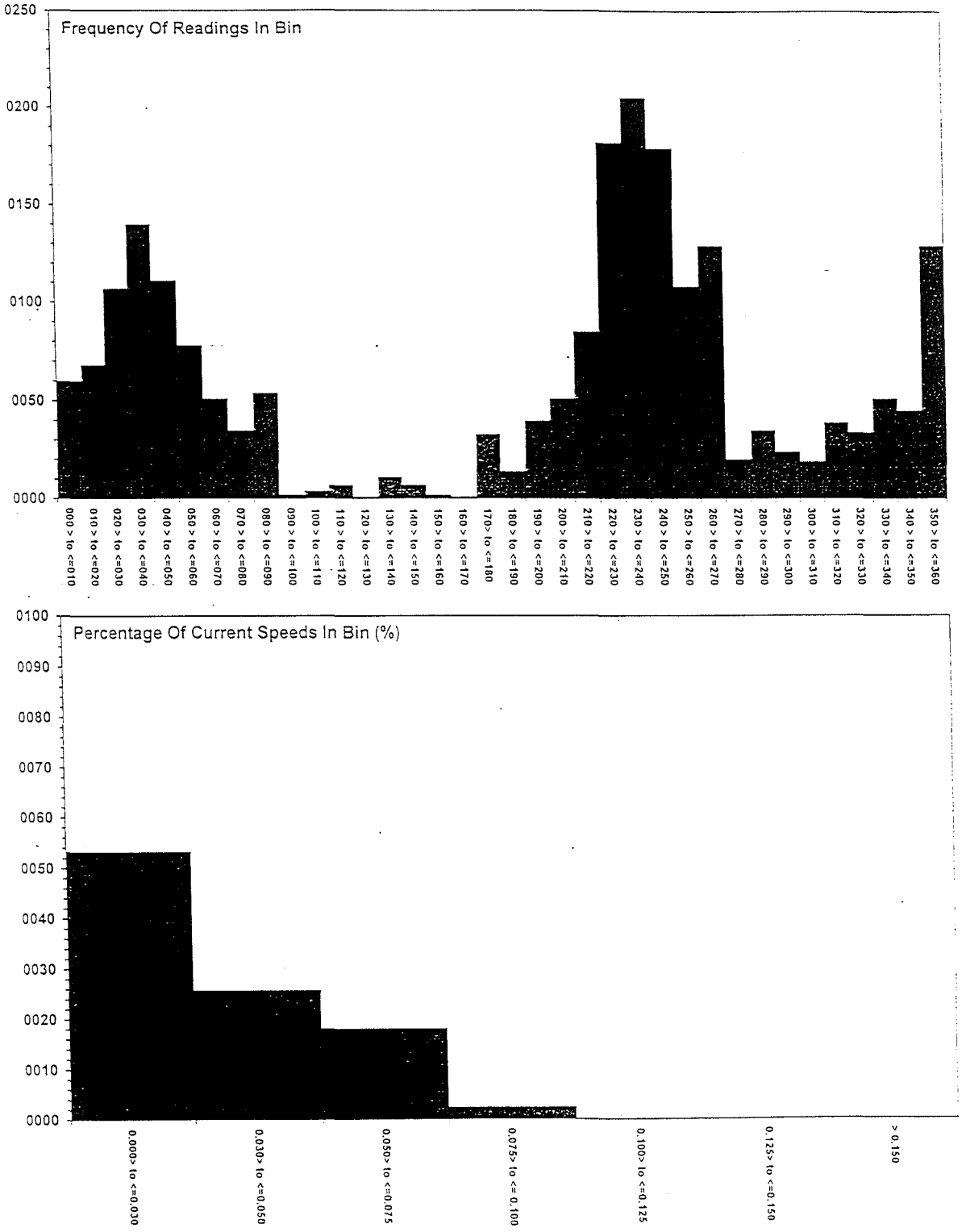

CURRENT DIRECTION AND SPEED FREQUENCY BINS

Current Meter Data Analysis

Details Of Current Meter Measurement And Analysis									
Site Details:	Enter Site Name Here ---------->	Site A - Bottom Current Data			Fill in Yellow boxes only				
Measurement Details (Raw Data)									
Number Of Readings:	2161			Days:	Hours	Minutes			
Period Of Measurement:	06/07/1998 13:50:00	to	21/07/1998 13:50:00	15	0	0			
Measurement Interval (mins):	10	MEASUREMENT INTERVAL CORRECT							
Current Direction (Raw Data)									
Major Axis:(+ve)	235.00			Major Axis:(-ve)	55.00				
Minor Axis:(+ve)	325.00			Minor Axis:(-ve)	145.00				
Current Speed (m/s)	All data	Parallel Component	Normal Component	BUTTON UPDATES					
From Raw Data				Button 4:	09/08/2001 19:31:45	Button 9:	07/07/1998 12:26:38		
Mean:	0.032	0.005	0.005	Button 6:	07/07/1998 12:25:12	Button 10:	07/07/1998 12:27:16		
Max:	0.110	0.107	0.065	Button 7:	07/07/1998 12:25:34				
Min:	0.000	-0.082	-0.064	Button 8:	09/07/1998 17:04:42				
Residual Current:	0.007	at	281.37	Degrees					
n Day Analysis (Usually 3 Days)		**Start Check:**	12/07/1998 13:50:00	**End Check:**	13/07/1998 13:50:00				
Current Speed (m/s)	**Start (dd/mm/yyyy hh:mm:ss):**		00/01/1900 00:00:00	End:	00/01/1900 00:00:00	Interval:			
Mean:	0.043	#DIV/0!	#DIV/0!						
Max:	0.089	0.000	0.000						
Min:	0.002	0.000	0.000						
Residual Current:	#DIV/0!	at	125.63	Degrees					
Current Direction (n Day Analysis)									
Major Axis:(+ve)				Major Axis:(-ve)	180.00				
Minor Axis:(+ve)	90.00			Minor Axis:(-ve)	270.00				
Measurement Details (n Day Analysis)									
Number Of Readings:	145			Days:	Hours	Minutes			
Period Of Measurement:	12/07/1998 13:50:00	to	13/07/1998 13:50:00	1	0	0			
Notes:			Check:	#VALUE!	#VALUE!	#VALUE!			

72hr Model Input Data	Residual	Tidal amplitude
Parallel Component U:	0.005	0.049
Normal Component V:	0.005	0.020

Cummulative Vector Plots

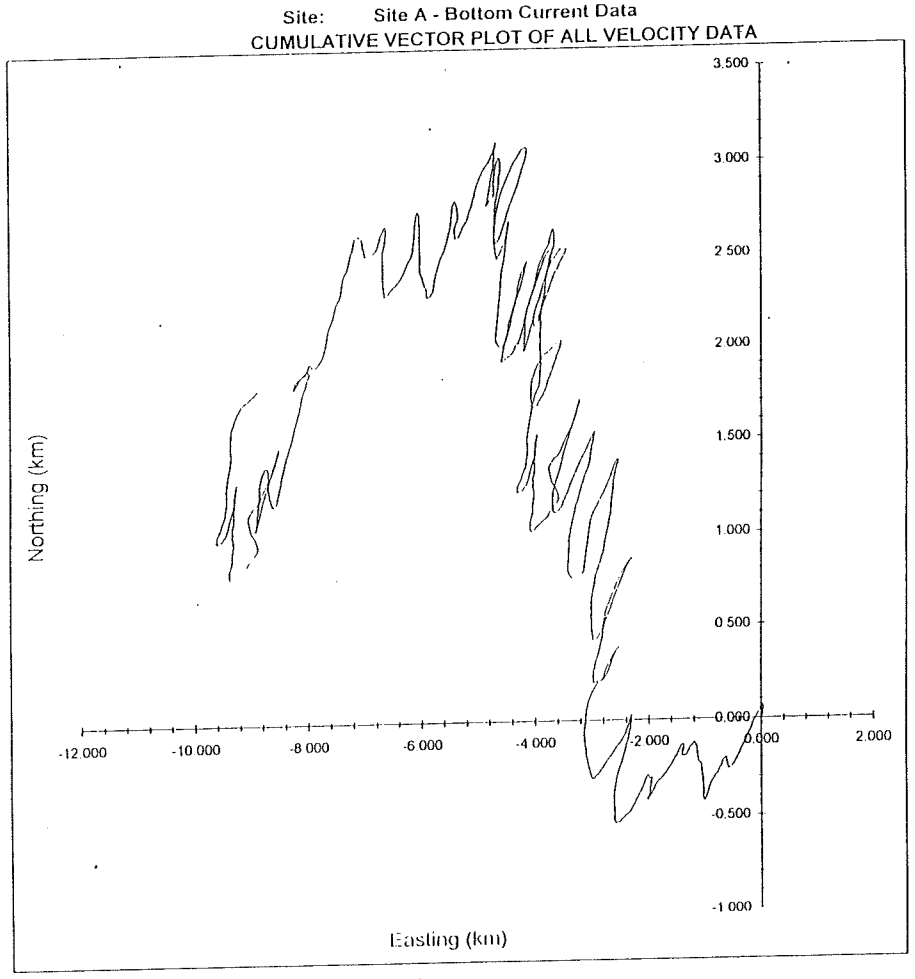

SiteA-B-Ffv4.xls

Velocity Component Scatter Plots (All Data)

Site: Site B - Surface Current Data

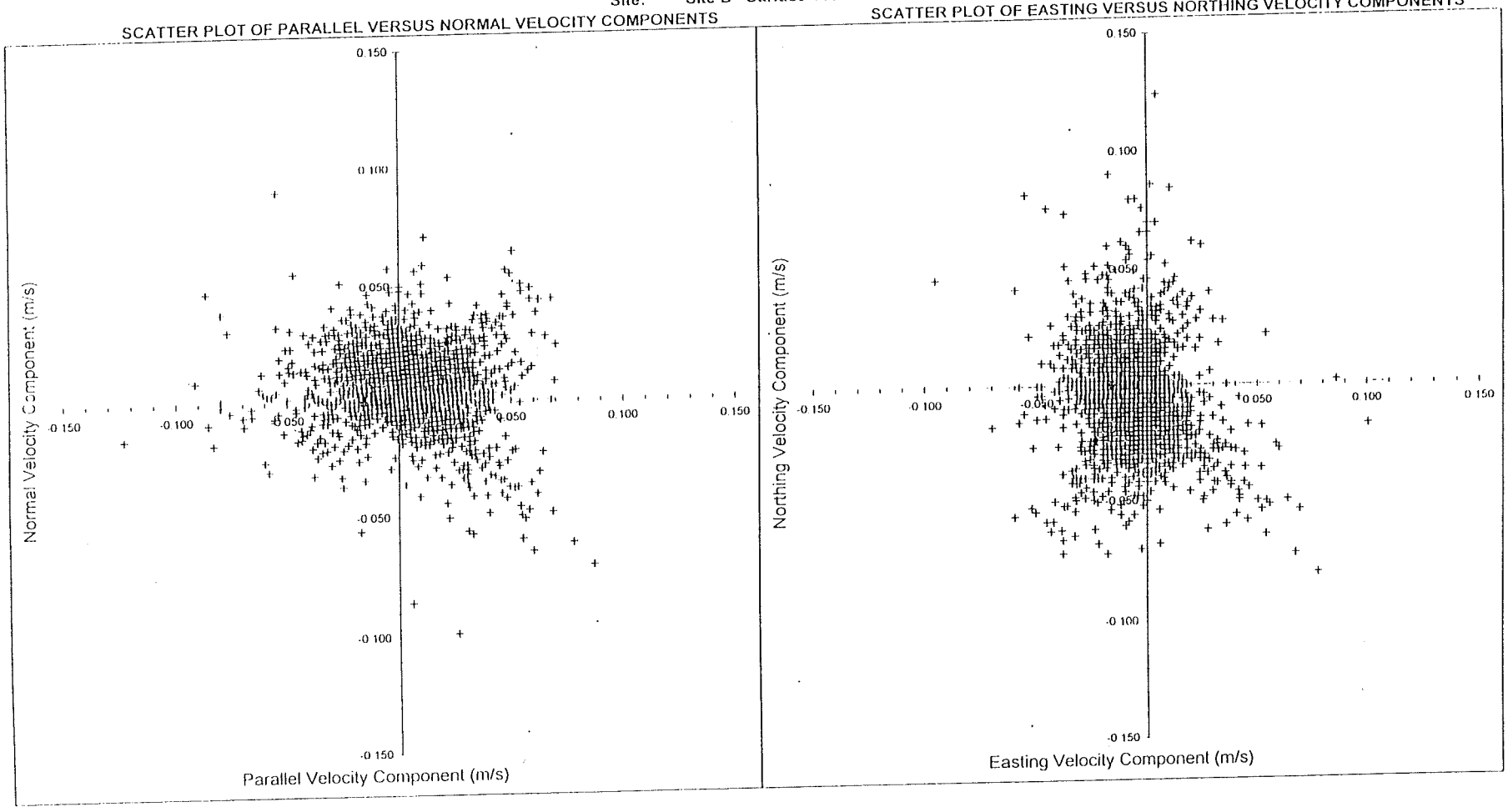

Current Meter Time Series Charts (All Data)

Site: Site B - Surface Current Data

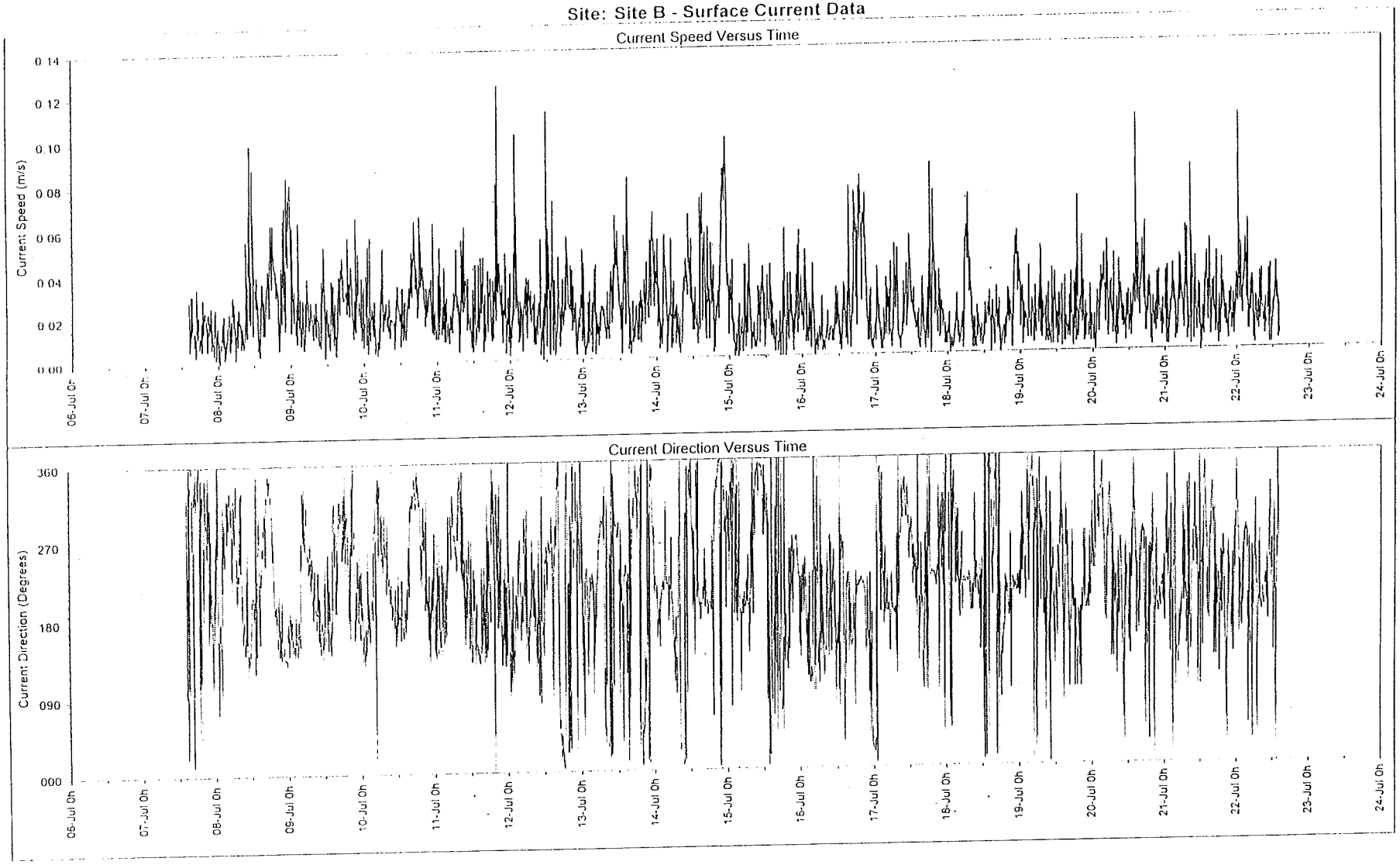

Current Meter Frequency Analysis Output (All Data)

Current Meter Data Frequency Analysis Results Table			
Site:	Site B - Surface Current Data		
Current Direction Frequency Bins (Degrees Magnetic)	Frequency Of Readings In Bin	Current Speed Frequency Bins (m/s)	Percentage Of Readings In Bin (%)
000 > to <=010	27	0.000> to <=0.030	75.57
010 > to <=020	30	0.030> to <=0.050	18.00
020 > to <=030	27	0.050> to <=0.075	5.32
030 > to <=040	12	0.075> to <= 0.100	0.88
040 > to <=050	11	0.100> to <=0.125	0.23
050 > to <=060	8	0.125> to <=0.150	0.00
060 > to <=070	5	> 0.150	0.00
070 > to <=080	8		
080 > to <=090	40		
090 > to <=100	6		
100 > to <=110	18		
110 > to <=120	21		
120 > to <=130	34		
130 > to <=140	79		
140 > to <=150	66		
150 > to <=160	63		
160 > to <=170	78		
170> to <=180	196		
180 > to <=190	72		
190 > to <=200	116		
200 > to <=210	104		
210 > to <=220	126		
220 > to <=230	118		
230 > to <=240	69		
240 > to <=250	55		
250 > to <=260	72		
260 > to <=270	165		
270 > to <=280	36		
280 > to <=290	69		
290 > to <=300	58		
300 > to <=310	41		
310 > to <=320	66		
320 > to <=330	61		
330 > to <=340	51		
340 > to <=350	37		
350 > to <=360	116		

CURRENT METER FREQUENCY ANALYSIS CHART OUTPUT (All Data)

Site: Site B - Surface Current Data

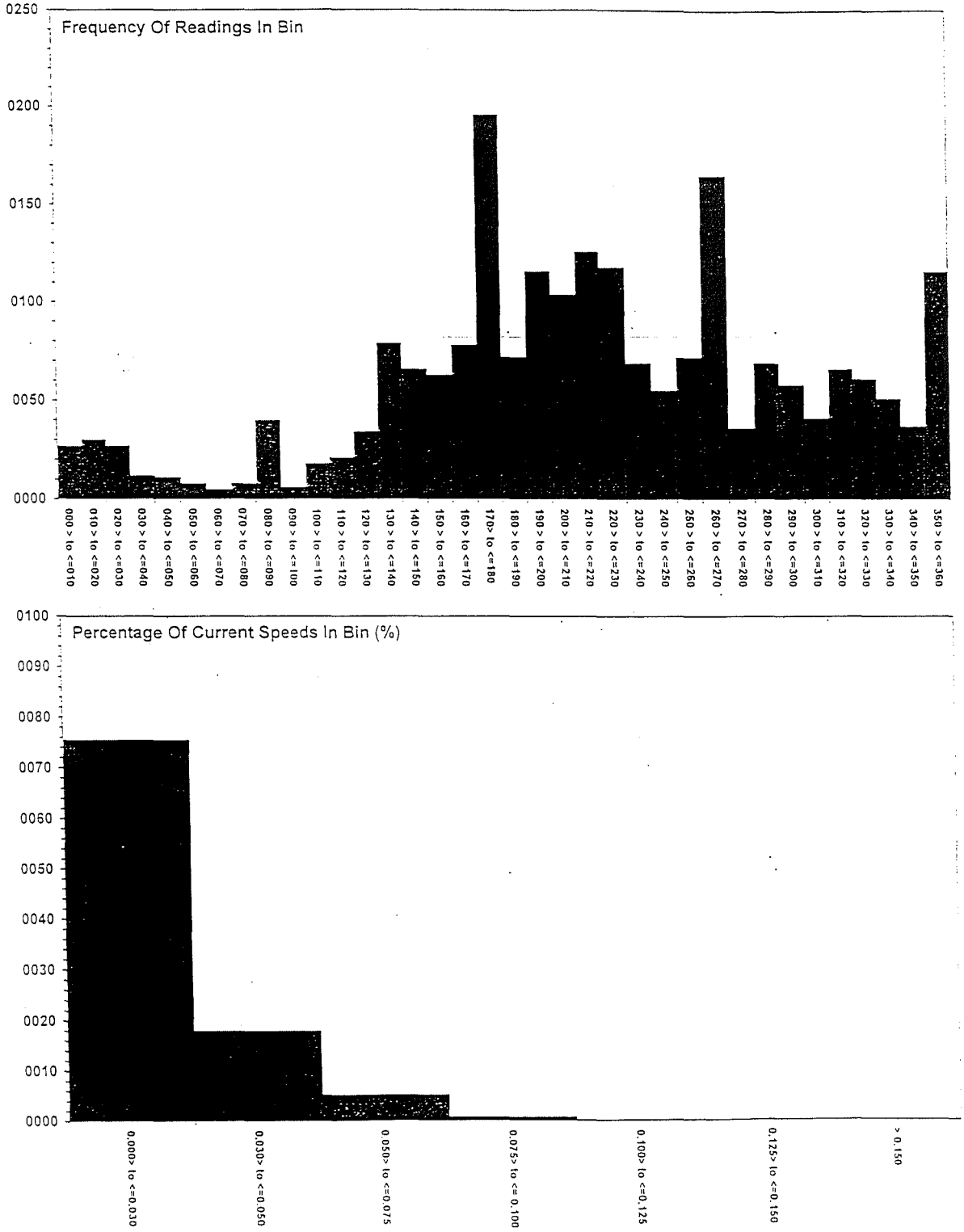

CURRENT DIRECTION AND SPEED FREQUENCY BINS

Current Meter Data Analysis

Details Of Current Meter Measurement And Analysis									
Site Details:	Enter Site Name Here ---------->	Site B - Surface Current Data			Fill in Yellow boxes only				
Measurement Details (Raw Data)									
Number Of Readings:	2161			Days:	Hours	Minutes			
Period Of Measurement:	07/07/1998 14:10:00	to	22/07/1998 14:10:00	15	0	0			
Measurement Interval (mins):	10	MEASUREMENT INTERVAL CORRECT							
Current Direction (Raw Data)									
Major Axis:(+ve)	175.00			Major Axis:(-ve)	355.00				
Minor Axis:(+ve)	265.00			Minor Axis:(-ve)	85.00				
Current Speed (m/s)	All data	Parallel Component	Normal Component	BUTTON UPDATES					
From Raw Data				Button 4:	09/08/2001 19:33:27	Button 9:	07/07/1998 12:26:38		
Mean:	0.023	0.005	0.006	Button 6:	07/07/1998 12:25:12	Button 10:	07/07/1998 12:27:16		
Max:	0.124	0.087	0.091	Button 7:	07/07/1998 12:25:34				
Min:	0.000	-0.123	-0.099	Button 8:	09/07/1998 17:04:42				
Residual Current:	0.008	at	226.71	Degrees					
n Day Analysis (Usually 3 Days)		Start Check:	13/07/1998 14:10:00	End Check:	14/07/1998 14:10:00				
Current Speed (m/s)	Start (dd/mm/yyyy hh:mm:ss):		00/01/1900 00:00:00	End:	00/01/1900 00:00:00	Interval:			
Mean:	0.025	#DIV/0!	#DIV/0!						
Max:	0.082	0.000	0.000						
Min:	0.002	0.000	0.000						
Residual Current:	#DIV/0!	at	125.63	Degrees					
Current Direction (n Day Analysis)									
Major Axis:(+ve)				Major Axis:(-ve)	180.00				
Minor Axis:(+ve)	90.00			Minor Axis:(-ve)	270.00				
Measurement Details (n Day Analysis)									
Number Of Readings:	145			Days:	Hours	Minutes			
Period Of Measurement:	13/07/1998 14:10:00	to	14/07/1998 14:10:00	1	0	0			
Notes:		Check:		#VALUE!	#VALUE!	#VALUE!			

72hr Model Input Data	Residual	Tidal amplitude
Parallel Component U:	0.005	0.030
Normal Component V:	0.006	0.023

Cummulative Vector Plots

Site: Site B - Surface Current Data

CUMULATIVE VECTOR PLOT OF ALL VELOCITY DATA

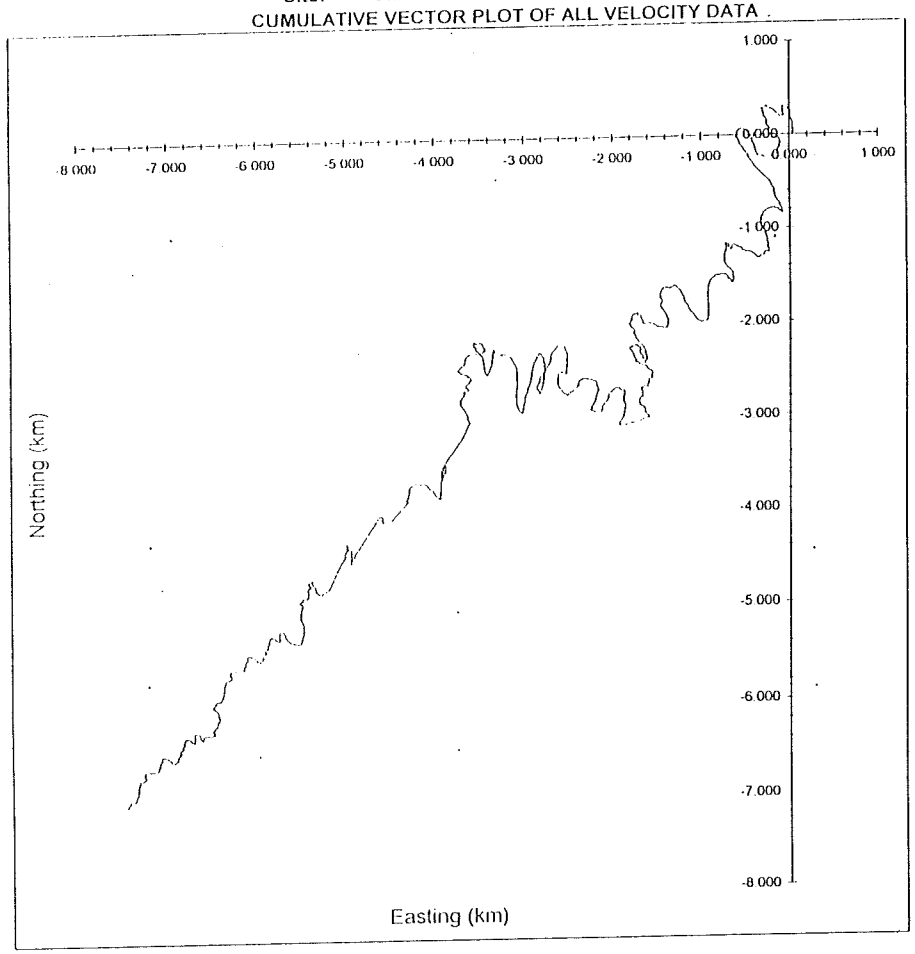

SiteB-S-Ffv4.xls

Velocity Component Scatter Plots (All Data)

Site: Site B - Bottom Current Data

SCATTER PLOT OF PARALLEL VERSUS NORMAL VELOCITY COMPONENTS

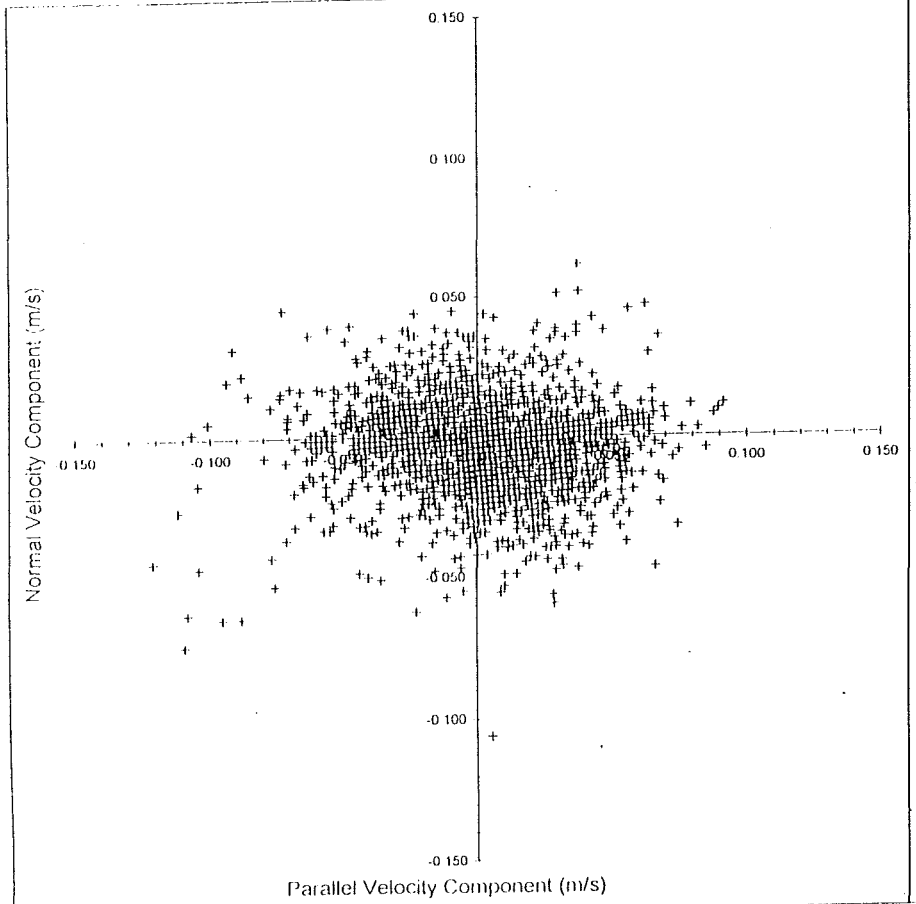

SCATTER PLOT OF EASTING VERSUS NORTHING VELOCITY COMPONENTS

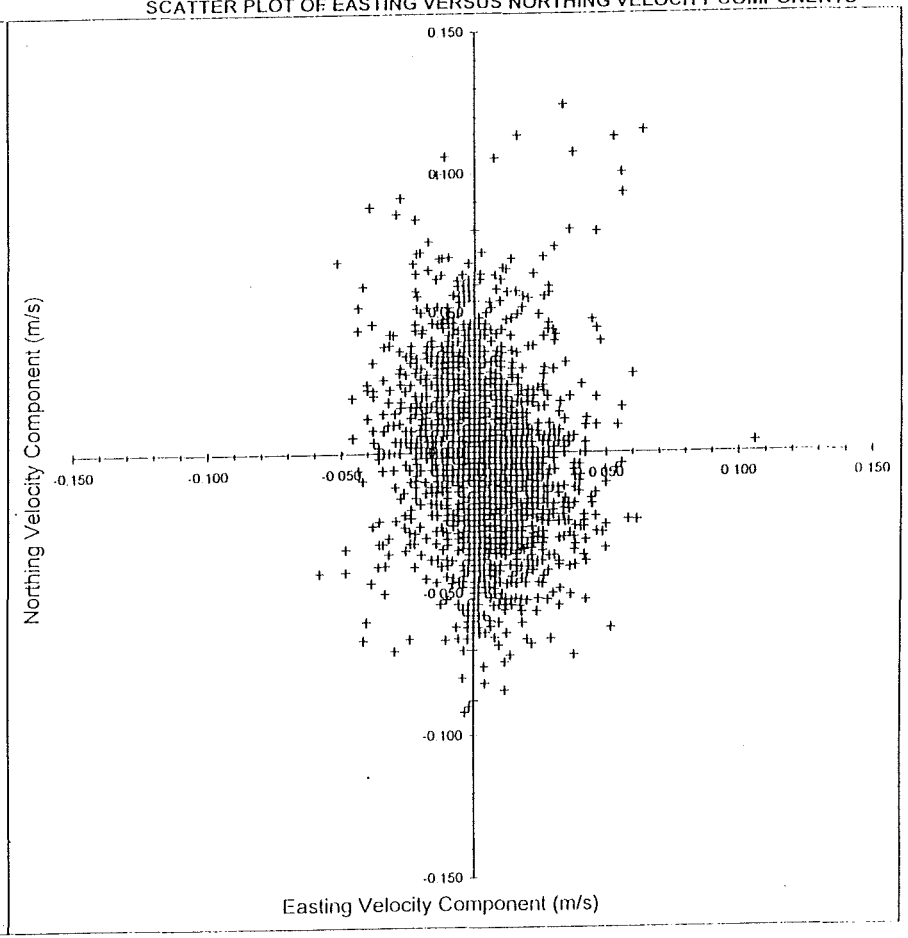

Current Meter Time Series Charts (All Data)

Site: Site B - Bottom Current Data

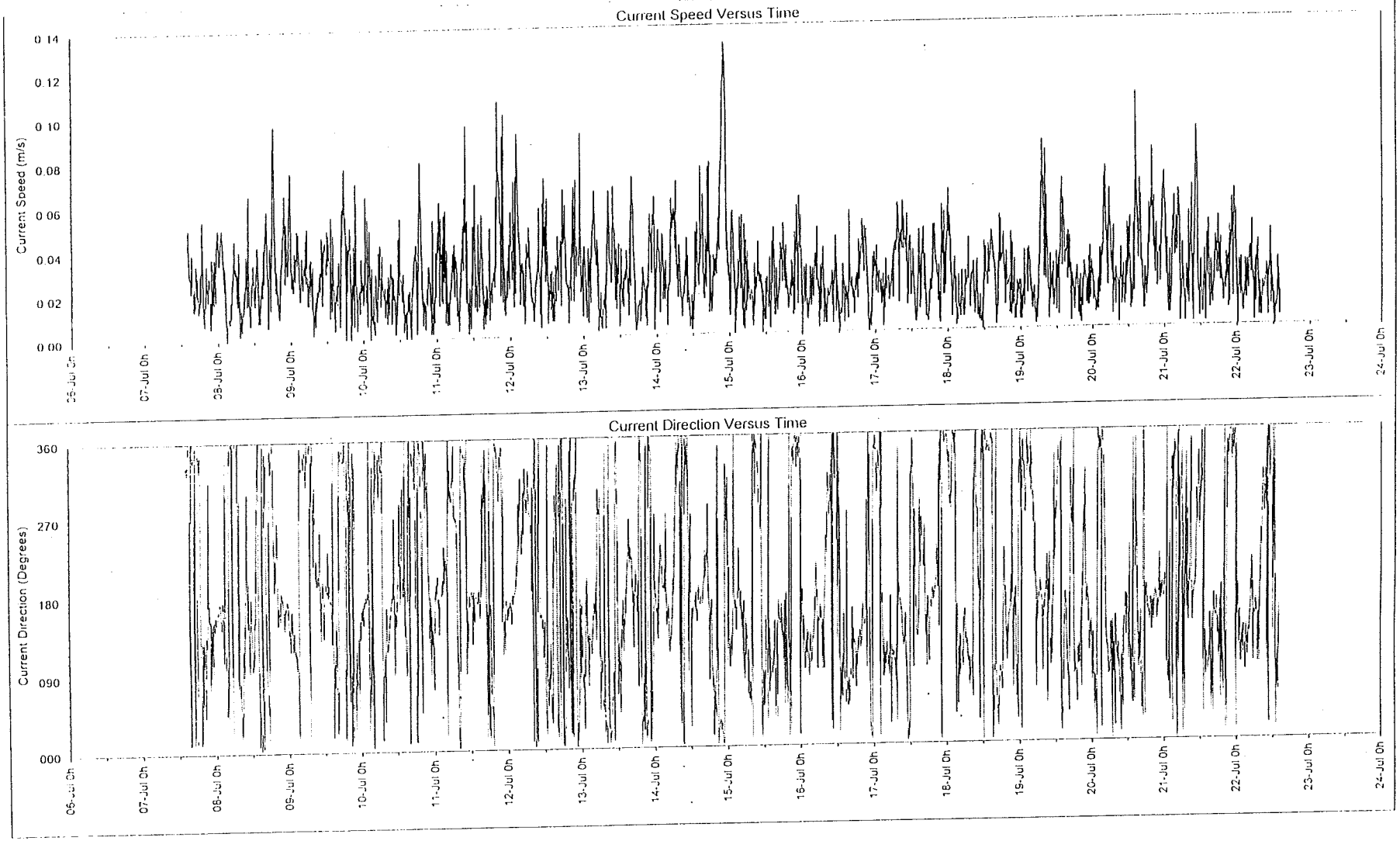

Current Meter Frequency Analysis Output (All Data)

Current Meter Data Frequency Analysis Results Table			
Site:	Site B - Bottom Current Data		
Current Direction Frequency Bins (Degrees Magnetic)	Frequency Of Readings In Bin	Current Speed Frequency Bins (m/s)	Percentage Of Readings In Bin (%)
000 > to <=010	63	0.000> to <=0.030	61.87
010 > to <=020	61	0.030> to <=0.050	27.95
020 > to <=030	51	0.050> to <=0.075	8.65
030 > to <=040	33	0.075> to <= 0.100	1.02
040 > to <=050	46	0.100> to <=0.125	0.42
050 > to <=060	26	0.125> to <=0.150	0.09
060 > to <=070	29	> 0:150	0.00
070 > to <=080	56		
080 > to <=090	111		
090 > to <=100	32		
100 > to <=110	58		
110 > to <=120	73		
120 > to <=130	84		
130 > to <=140	74		
140 > to <=150	115		
150 > to <=160	111		
160 > to <=170	106		
170> to <=180	174		
180 > to <=190	49		
190 > to <=200	44		
200 > to <=210	24		
210 > to <=220	24		
220 > to <=230	30		
230 > to <=240	21		
240 > to <=250	15		
250 > to <=260	13		
260 > to <=270	64		
270 > to <=280	16		
280 > to <=290	31		
290 > to <=300	33		
300 > to <=310	33		
310 > to <=320	37		
320 > to <=330	53		
330 > to <=340	75		
340 > to <=350	109		
350 > to <=360	187		

CURRENT METER FREQUENCY ANALYSIS CHART OUTPUT (All Data)

Site: Site B - Bottom Current Data

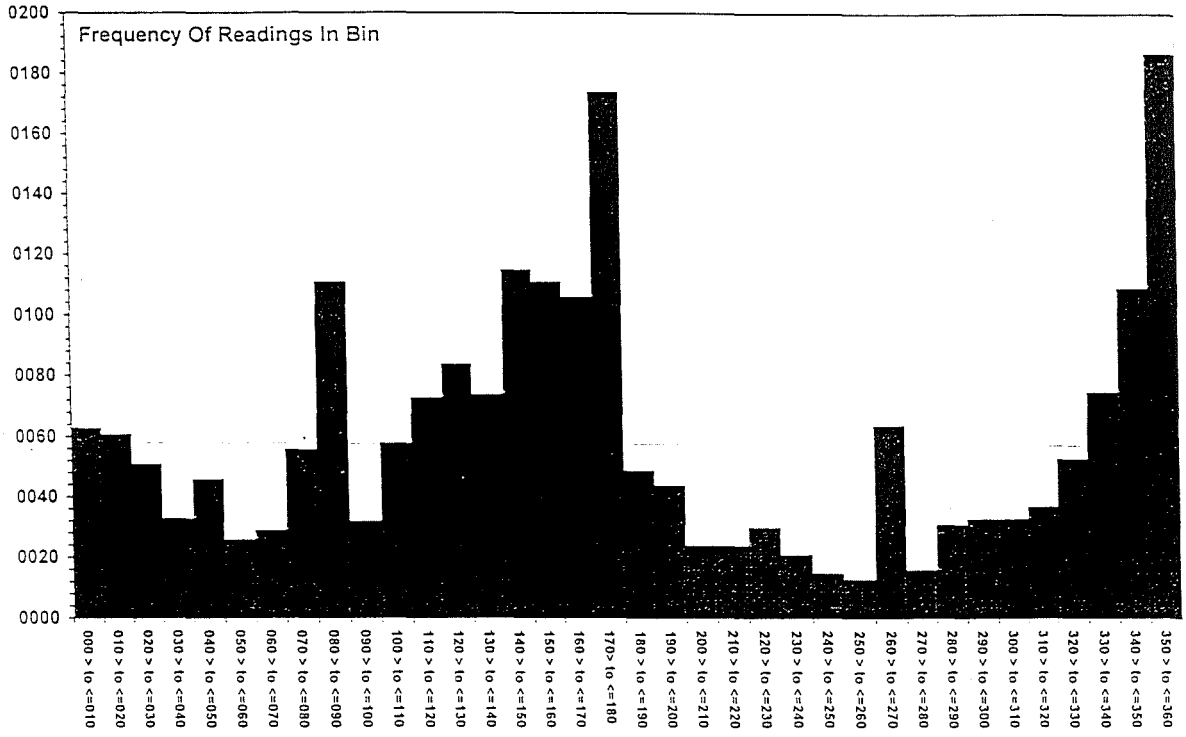

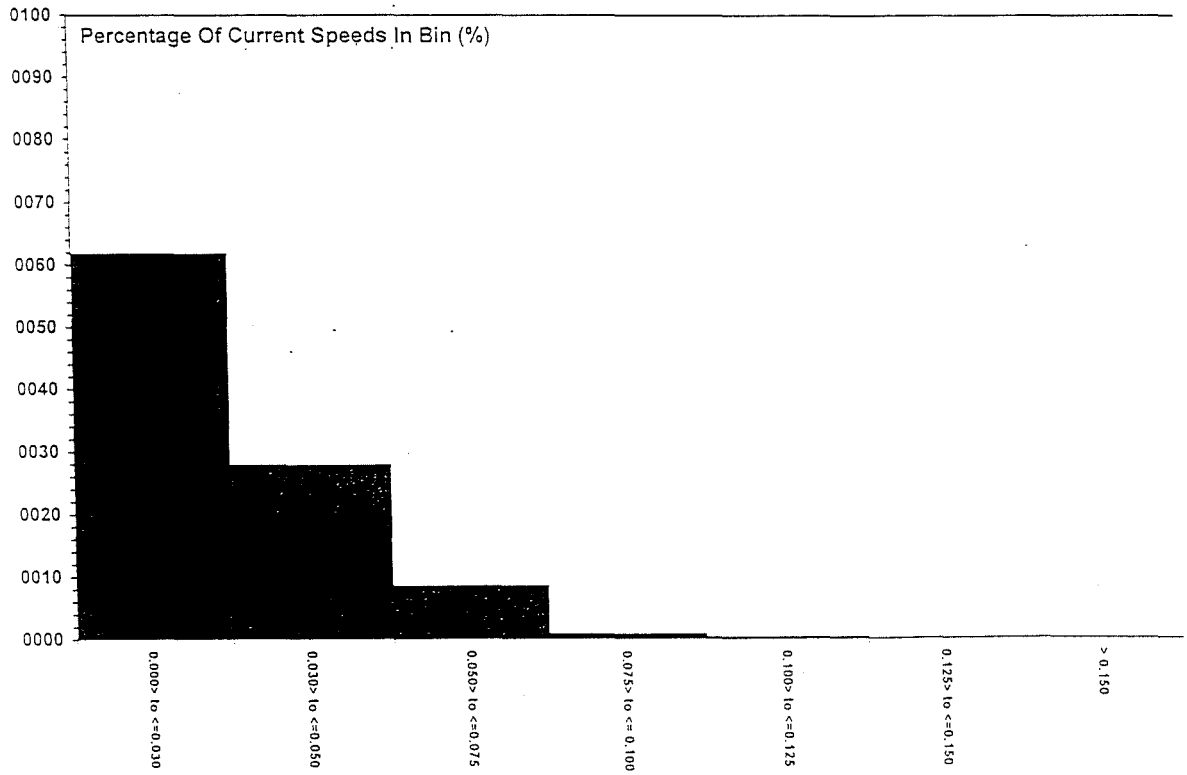

CURRENT DIRECTION AND SPEED FREQUENCY BINS

Current Meter Data Analysis

Details Of Current Meter Measurement And Analysis							
Site Details:	Enter Site Name Here ---------->	Site B - Bottom Current Data		Fill in Yellow boxes only			
Measurement Details (Raw Data)							
Number Of Readings:	2161			Days:	Hours	Minutes	
Period Of Measurement:	07/07/1998 14:10:00	to	22/07/1998 14:10:00	15	0	0	
Measurement Interval (mins):	10	MEASUREMENT INTERVAL CORRECT					
Current Direction (Raw Data)							
Major Axis:(+ve)	175.00			Major Axis:(-ve)	355.00		
Minor Axis:(+ve)	265.00			Minor Axis:(-ve)	85.00		
Current Speed (m/s)	All data	Parallel Component	Normal Component	BUTTON UPDATES			
From Raw Data				Button 4:	09/08/2001 19:35:07	Button 9:	07/07/1998 12:26:38
Mean:	0.028	0.001	-0.004	Button 6:	07/07/1998 12:25:12	Button 10:	07/07/1998 12:27:16
Max:	0.132	0.091	0.062	Button 7:	07/07/1998 12:25:34		
Min:	0.000	-0.121	-0.106	Button 8:	09/07/1998 17:04:42		
Residual Current:	0.004	at	101.80	Degrees			
n Day Analysis (Usually 3 Days)		**Start Check:**	13/07/1998 14:10:00	**End Check:**	14/07/1998 14:10:00		
Current Speed (m/s)	**Start (dd/mm/yyyy hh:mm:ss):**		00/01/1900 00:00:00	**End:**	00/01/1900 00:00:00	Interval:	
Mean:	0.029	#DIV/0!	#DIV/0!				
Max:	0.076	0.000	0.000				
Min:	0.002	0.000	0.000				
Residual Current:	#DIV/0!	at	125.63	Degrees			
Current Direction (n Day Analysis)							
Major Axis:(+ve)				Major Axis:(-ve)	180.00		
Minor Axis:(+ve)	90.00			Minor Axis:(-ve)	270.00		
Measurement Details (n Day Analysis)							
Number Of Readings:	145			Days:	Hours	Minutes	
Period Of Measurement:	13/07/1998 14:10:00	to	14/07/1998 14:10:00	1	0	0	
Notes:			Check:	#VALUE!	#VALUE!	#VALUE!	

72hr Model Input Data	Residual	Tidal amplitude
Parallel Component U:	0.001	0.041
Normal Component V:	-0.004	0.023

Cummulative Vector Plots

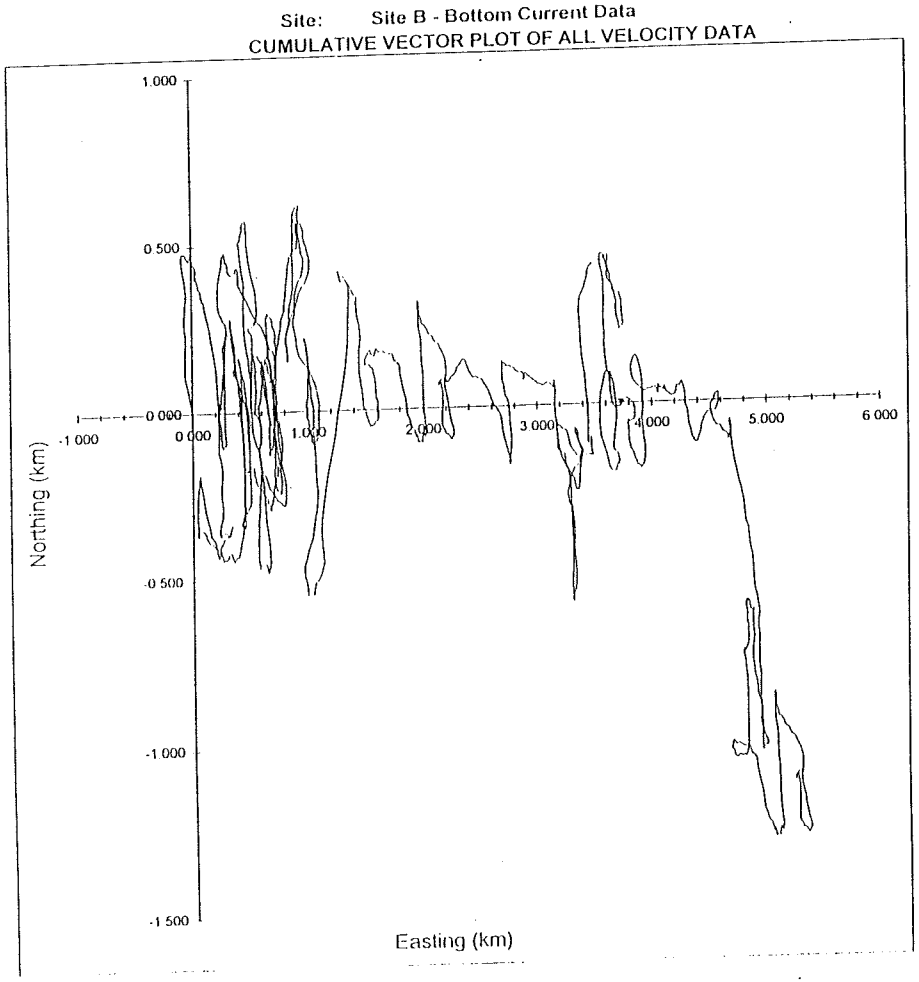

PUBLISHED PAPER NOT INCLUDED